UNIVERSITY OF MICHIGAN
NOV 19 1957
PHYSICS LIBRARY NOV 21 1957

Journal of Research

of the National Bureau of Standards

NOVEMBER 1957

VOLUME 59 NUMBER 5

U. S. DEPARTMENT OF COMMERCE
Sinclair Weeks, Secretary
NATIONAL BUREAU OF STANDARDS
A. V. Astin, Director

NOVEMBER • 1957
VOLUME • 59
NUMBER • 5

JOURNAL OF RESEARCH
of the
NATIONAL BUREAU OF STANDARDS

The National Bureau of Standards

Functions and Activities

The functions of the National Bureau of Standards are set forth in the Act of Congress, March 3, 1901, as amended by Congress in Public Law 619, 1950. These include the development and maintenance of the national standards of measurement and the provision of means and methods for making measurements consistent with these standards; the determination of physical constants and properties of materials; the development of methods and instruments for testing materials, devices, and structures; advisory services to Government Agencies on scientific and technical problems; invention and development of devices to serve special needs of the Government; and the development of standard practices, codes, and specifications. The work includes basic and applied research, development, engineering, instrumentation, testing, evaluation, calibration services, and various consultation and information services. A major portion of the Bureau's work is performed for other Government Agencies, particularly the Department of Defense and the Atomic Energy Commission. The scope of activities is suggested by the listing of divisions and sections on the inside of the back cover.

Publications

The results of the Bureau's work take the form of either actual equipment and devices or published papers. These papers appear either in the Bureau's own series of publications or in the journals of professional and scientific societies. The Bureau itself publishes three monthly periodicals, available from the Government Printing Office: The Journal of Research, which presents complete papers reporting technical investigations; the Technical News Bulletin, which presents summary and preliminary reports on work in progress; and Basic Radio Propagation Predictions, which provides data for determining the best frequencies to use for radio communications throughout the world. There are also five series of nonperiodical publications: The Applied Mathematics Series, Circulars, Handbooks, Building Materials and Structures Reports, and Miscellaneous Publications.

Information on the Bureau's publications can be found in NBS Circular 460, Publications of the National Bureau of Standards ($1.25) and its Supplement ($0.75), available from the Superintendent of Documents, Government Printing Office, Washington 25, D. C.

Order all publications from the Superintendent of Documents
U. S. Government Printing Office, Washington 25, D. C.

Use of funds for printing this publication approved by the Director of the Bureau of the Budget (May 4, 1956)

Journal of Research of the National Bureau of Standards Vol. 59, No. 5, November 1957 Research Paper 2801

A Determination of the Gamma-Ray Emission of Radium

Frank H. Attix and Victor H. Ritz

Measurements of the γ-ray emission of radium (roentgens per milligram-hour at 1 centimeter) have been made by means of a graphite cavity ionization chamber. An auxiliary experimental examination of the stopping-power correction for the non-air-equivalence of the cavity wall is also described. The resulting average value for the γ-ray emission of radium (enclosed in an 0.5-millimeter platinum capsule) is 8.26 $\pm$0.05 roentgens per milligram-hour at 1 centimeter, which is based upon the conclusion that the stopping-power data of Bakker and Segre are consistent with the results of the auxiliary experiment.

1. Introduction

Field instruments for the measurement of the exposure dose or exposure dose rate of X- or γ-radiation usually require calibration against a primary standard. In the X-ray region between 50 and 500 kv it has already been pointed out in the 1956 report of the ICRU [1]* that primary standards of the free-air chamber type can be constructed with an absolute accuracy of about $\pm$1 percent. However, the information required for the design of such instruments with this accuracy at the higher quantum energies, such as the γ-rays from Co^{60} or radium, is not yet available. Instead, the method of cavity ionization, utilizing the Bragg-Gray relation [2, 3], has generally been relied upon for measurements in this energy region.

Radium sources are frequently used for routine calibration purposes, by placing the instrument to be calibrated at a known distance from a capsule containing a known weight of radium. One must then know, from other measurements, what the exposure dose rate will be under these conditions. The ICRU report defines the specific γ-ray emission of a radioactive nuclide as "the exposure dose rate produced by the unfiltered γ-rays from a point source of that nuclide at a defined distance. The unit of specific γ-ray emission is the roentgen per millicurie-hour (r/mch) at 1 cm." For radium, the specific γ-ray emission is, instead, usually expressed in terms of the weight of radium element, i. e., roentgens per milligram-hour (r/mgh) at 1 cm. It will be convenient to refer to this quantity as K(Ra). For calibration purposes, radium sources are usually enclosed in capsules of platinum (10% iridium), having walls 0.5 mm in thickness. Thus, a more useful figure for radium is the specific γ-ray emission modified by the attenuation in such a capsule wall. This has been given several names in the literature, such as dosage constant, Q-constant, γ-ray output, and Sievert dose, the latter being the most generally accepted. For present purposes we will use the symbol k (Ra). For later reference it will be worthwhile to set down the following definition:

k (Ra) is the exposure dose rate in roentgens per hour at 1 cm from a point source of 1 mg of radium element (in equilibrium with its daughter products), enclosed in a platinum (10% iridium) capsule of 0.5-mm thickness, the surrounding air having no scattering or attenuating effect.

k (Ra) cannot, at present, be calculated theoretically with an accuracy of better than a few percent, and it must, therefore, be measured experimentally. The most common currently accepted value is 8.4 r/mgh at 1 cm,[1] which is derived as a weighted average of a number of experimental determinations over a period of many years [4 to 42]. Cavity-type ionization chambers have been most frequently employed, but some free-air chamber measurements have also been attempted [9, 17, 19, 26, 30, 42]. Even the most recent of these [42] is now known to have had substantial errors from electric field distortion and from ionization produced by scattered photons. Thus, the cavity ionization measurements appear to be the more reliable at present, and the 8.4 r/mgh figure is based principally upon these.

One of the main sources of uncertainty in cavity chamber measurements is related to the non-air-equivalence of the chamber wall material. This gives rise to a correction factor, identified by the Bragg-Gray relation [2] as the ratio of the electron stopping power in the wall material to that in air. The evaluation of this factor, usually called s, is carried out by making use of the Bethe-Bloch stopping-power formula [43], which involves a term depending on the mean excitation potential (I) for the atoms of the stopping material. It has not been adequately calculated theoretically, and must therefore be determined from experiments.

Laurence [34] computed s for a number of wall materials,[2] using the assumption that $I=13.5Z$. His results have been widely employed in the interpretation of cavity chamber measurements, and in fact the value of 8.4 r/mgh for radium is consistent with the Laurence wall corrections.[3]

Bakker and Segre [44] and Mather and Segre [45] have measured I in various materials through range measurements with fast protons. Their measurements indicate that I/Z is not a constant for different atomic numbers Z. On the other hand, a recent

*Figures in brackets indicate the literature references at the end of this paper.

[1] At the National Physical Laboratory in the United Kingdom 8.3 is the value assumed for k(Ra).

[2] Note the error existing in Laurence's eq (8), the stopping-power formula, giving rise to an underestimation of s for graphite by about 1.1 percent and an overestimation for Al by about 0.6 percent. The second term in brackets in that equation should be $\ln[(k/2^2)+k^2]$ instead of $\ln[k^2+(k/2)]$.

[3] See second footnote to table 5.

survey of existing measurements by Caldwell [46] and experiments of Bichsel and Mozley [47] show that I/Z is approximately constant with Z, at least for $Z \geq 13$. An even more recent paper by Brandt [48] tends again to confirm the Bakker and Segre results. This difference will only be resolved by further experimental measurements of I, and at present brings about an uncertainty of the order of 1 percent in the interpretation of cavity ionization measurements.

The present experiment was initially undertaken with two purposes in mind:

(1) To provide a relatively precise determination of k(Ra) by the cavity chamber method.

(2) To compare the abilities of the variously computed stopping-power corrections to reduce the experimental data for cavity chambers of differing wall materials (carbon and aluminum) to give a common value for the radium gamma-ray emission.

The experimental work was originally done in two parts. The first was the absolute measurement of the ionization produced in a graphite and an aluminum chamber at approximately 1-atm air pressure, at several measured distances from a known radium source. The second part was a study of the pressure dependence of the ionization in the same chambers, from 0.1 to 1 atm, to determine the degree to which the cavity ionization was under the influence of the electrons originating in the chamber walls. The results of these two experiments were then combined to give the absolute ionization in each chamber as a function of air pressure.

Two unforeseen difficulties were encountered which rendered these results indeterminate. The first was that the ionization in the cavity chambers did not strictly obey the inverse square law as a function of distance between centers of source and chamber. This was found to be true after taking into account the air attenuation, scattering from the floor and other objects, and the size of the chamber and source. The most startling feature of this behavior was the fact that the Al chamber showed a greater divergence from inverse-square-law behavior than did the graphite. Thus, the ratio of ionizations in the two chambers (aluminum to carbon, of the same dimensions) was found to decrease with increasing distance from the source. The explanation of this effect will be discussed in the next section.

The other difficulty arose when the Al/C ionization ratio was measured with several different radium sources, all having 0.5 mm Pt capsule walls, but varying diameters. This ratio was found gradually to increase by 1 percent as the inside diameter of the source was decreased from 5.5 to 0.7 mm. This effect may be the result of photoelectric interactions in the Al chamber wall by the bremsstrahlung produced within the source by β-rays, a point to be investigated further. It does, however, make the measurement of the Al/C ionization ratio indefinite for radium. Moreover, it raises the question of whether the bremsstrahlung is to be included with the γ-radiation in the definition of k(Ra). From practical considerations one concludes that it should be included, because it will always be present for radium sources enclosed in platinum capsules. Variations in the bremsstrahlung output with different source diameters will be taken into account approximately by the correction for attenuation in the radium salt, as measured by Whyte [51].

In view of the difficulties described above, it was decided to revise the approach to the measurement of k(Ra) in three respects:

(A) The "distance effect" (nonobeying of inverse square law) was to be investigated with the object of eliminating the uncertainty resulting from it.

(B) Measurements with radium γ-rays were to be confined to the graphite chamber (eliminating the aluminum chamber for the reason outlined in the previous paragraph), using the information found in (A) to avoid the distance effect.

(C) Cobalt-60 γ-rays were to be used in place of radium γ-rays for the study of the stopping-power corrections for the non-air-equivalence of the chamber walls, to avoid the photoelectric effect. An additional chamber of copper, nearly identical in size to the graphite and aluminum chambers, was also constructed for inclusion in this study.

The results of this modified version of the experiment will be presented in the following sections. However, the original setup will first be described briefly to show how the distance effect entered the picture.

2. Preliminary Measurements and the Distance Effect

2.1. Setup Initially Used for Radium Measurements

Figure 1 is a photograph of the over-all arrangement. The cylindrical cavity chamber (graphite or aluminum), shown in figure 2, was located at the end of a rigid, evacuated coaxial connector 2 m in length, which was connected to the input head of a vibrating reed electrometer. This head was enclosed in a 15-cm-thick lead housing which was supported by an electric lift truck, capable of raising the chamber to a height of 3 m above the floor. The radium source was supported at 2-m height by a paper stand, so constructed to contribute a minimum of γ-ray scattering. The chamber was located directly above the source so that the chamber axis was at right angles to a line joining their centers. The distance between centers (15 to 100 cm) was determined by adding half the source and chamber diameters to the distance between their surfaces as measured by a cathetometer. An area of the concrete floor, 2.4 by 3.5 m in extent, was covered with a thickness of 6 mm of lead, to reduce the scattered radiation. Further details about the chambers, the radium source, and the corrections for scattering and attenuation will be given in section 3.

2.2. Initial Results

Figure 3 is a graph of iD^2 as a function of D, where i is the ionization in the cavity chamber, and D is the center-to-center distance from source to chamber. Two corrections have been applied to these curves, accounting for attenuation by the air and scattering

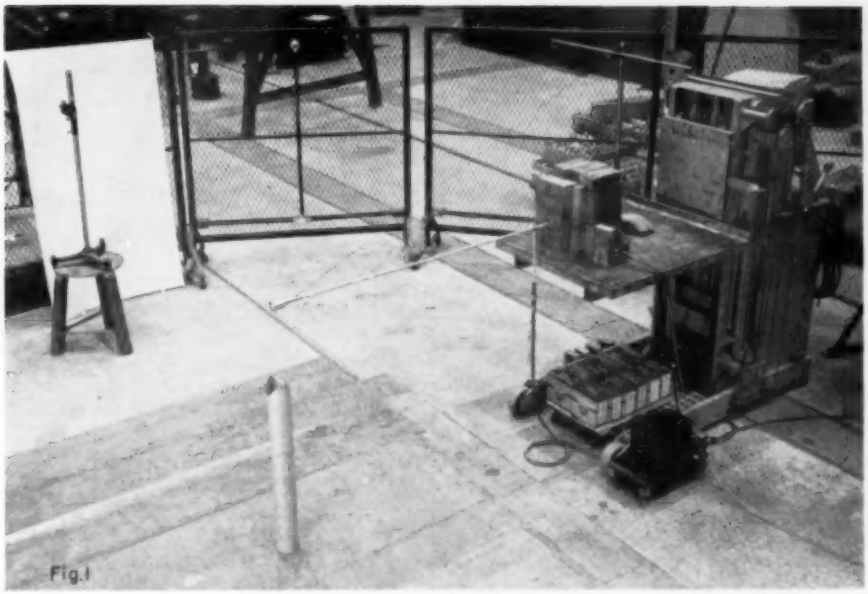

FIGURE 1. *Setup used for the preliminary radium measurements.*

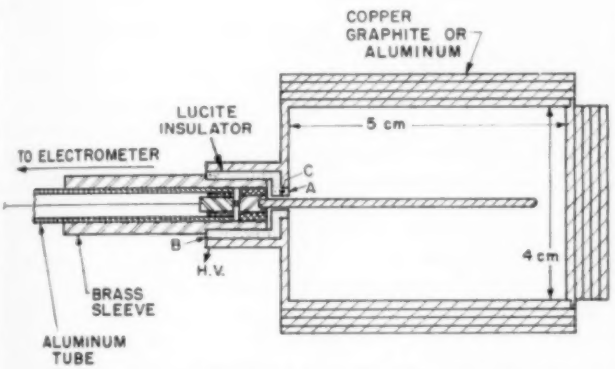

FIGURE 2. *Diagram of cavity-ionization chambers.*

The walls, of copper, aluminum, or graphite, were of variable thickness, and the central rod leading to the electrometer was, in each case, 3 mm in diameter and of the same material as the wall. The Lucite insulator was coated with graphite except for surfaces A and B. The graphite coating at C, the inside surface of the hole entering the chamber, was found to eliminate "soakage" effects when the voltage was first applied, and provided a guard ring for leakage of charge across surface A. Removing this graphite coating (from C) was found to have no effect on the steady state ionization in the chamber.

by the lead-covered floor. These were both very small and will be described in detail in section 3. Even with these corrections, the curves show considerable variation as a function of distance, the variation being twice as great for the aluminum chamber as for the graphite.

A calculation was carried out to take into account the inverse square effect of the size of the chamber and source, using the general approach of Mayneord and Roberts [6] and Clark and Brar [50]. The

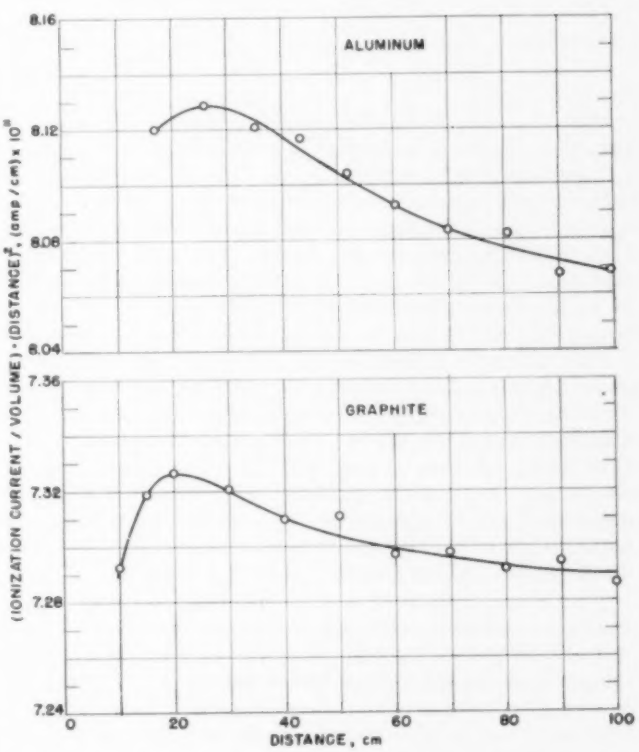

FIGURE 3. *Distance dependence of ionization in the graphite and aluminum cavity chambers.*

In each case, the radium source was located on a line perpendicular to the chamber axis and intersecting it at the geometrical center of the chamber.

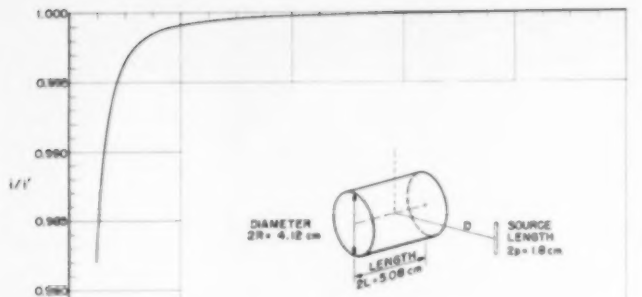

FIGURE 4. *Calculated divergence from inverse square law to be expected with the indicated geometry.*

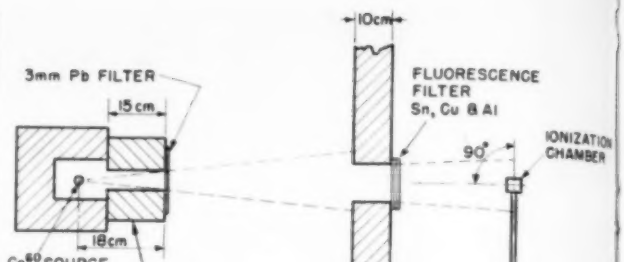

FIGURE 5. *Arrangement used for measuring the relative ionization produced by cobalt-60 γ-rays in copper, aluminum, and graphite chambers.*

The scatter shield removed scattered radiation produced in the air when the source was at large distances.

geometry was that indicated in figure 4, and the integration was carried over the three dimensions of the chamber and the length of the source, by a series expansion[4] in terms of (i/D^2). The resulting expression for the ionization in the chamber was:

$$i=i'\left[1+\frac{1}{D^2}\left(\frac{R^2}{2}-\frac{L^2}{3}-\frac{p^2}{3}\right)+\frac{1}{D^4}\left(\frac{L^4}{5}-\frac{2R^2L^2}{3}+\frac{2L^2p^2}{9}+\frac{R^4}{3}-\frac{R^2p^2}{3}+\frac{p^4}{5}\right)\right],$$

where i' is the ionization to be expected for a point source and point chamber separated by distance D, $2L$ is the internal length of the chamber, R its internal radius, and $2p$ the active length of the source. In the present case, where $2L$ is 5.08 cm, R is 2.06 cm, and $2p$ is 1.8 cm, the ratio (i/i') is as indicated in figure 4. The drop at small values of D is at least qualitatively shown by the curves in figure 3. However, (i/i') is flat within 0.1 percent for $D>20$ cm, unlike the results observed with these chambers. Such a calculation as this, of course, has nothing to say about the difference in slope of the aluminum and graphite curves, and ignores the fact that most of the cavity ionization is produced by electrons originating within the chamber walls. A more elaborate calculation taking these factors into account has not been attempted, and is probably not feasible with information now available.

The attenuation of γ-rays in the chamber walls was measured at different distances by the conventional method of varying the wall thickness, but the result was found to be independent of D. Extracameral collection of ionization and ion-recombination losses were also found experimentally to make a negligible contribution to the distance dependence of the ionization.

It appears then that the observed distance effect is not explained by the usual influencing factors. It was decided to explore the problem further by increasing the source-to-chamber distance to values greater than 1 m. In order to do this, it was necessary to employ larger Co^{60} sources (1 and 10 curies) to provide sufficient ionization for accurate measurement, and to collimate the beam to avoid complicating the issue with γ-ray scattering from surrounding objects. The geometry was as shown in figure 5.

Because the exact position of the source within the lead housing was not known, and because of scattering from the filter, only the ratios of ionizations in chambers of differing wall materials were considered as being significant. These ratios, relative to the graphite chamber, are shown in figure 6 (for 90° geometry), including the data for a copper chamber similar in dimensions to the graphite and the aluminum chambers, but with walls 1 mm in thickness. These data were taken with a filter of 3 mm Pb+2.4 mm Sn+0.5 mm Cu+0.8 mm Al to eliminate any scattered and fluorescent radiation originating in the source, housing, and diaphragm. Additional lead in the filter was found to have no effect upon the ratios; similarly, the presence of the fluorescence filter did not influence the results. Without any filter, the curves were of the same shape but somewhat higher due to the presence of low-energy radiation. The Al/C curve for 90° geometry in figure 6 decreases by 1.5 percent over the indicated range of distances, whereas the corresponding decrease of the Cu/C ratio is 5 percent. Neither curve shows any tendency to flatten out rapidly with distance, indicating that their slopes cannot be explained on the basis of a fixed difference in the effective centers of ionization in chambers of different wall materials. However, this behavior at large distances does suggest the possibility that the end walls of the chambers might in some way be responsible, perhaps through attenuation, because of the grazing incidence of the γ-rays upon those walls.

As a test of this hypothesis, the setup in figure 5 was changed to give a 50° instead of 90° angle between the chamber axis and the direction from which the rays were incident. With this geometry the Al/C and Cu/C curves were both flat within ±0.2 percent, as shown in figure 6. The work was repeated at 70°, to find out if there was any depend-

[4] The method of integrating was suggested by L. V. Spencer.

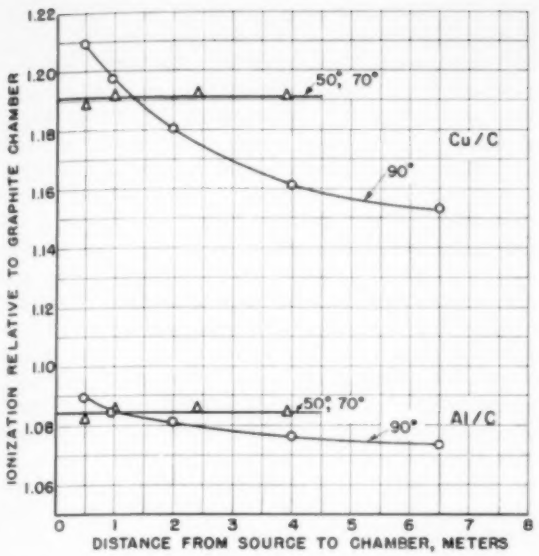

FIGURE 6. *Ionization in the copper and aluminum chamber relative to that in graphite for cobalt-60 γ-rays.*

The indicated angles are those between the chamber axis and the line joining the centers of the source and chamber.

ence on (nonglancing) angle, giving identical results. Thus, it appears clear that the distance effect is related to geometrical situations where the γ-rays strike the chamber at grazing incidence with respect to an appreciable area of chamber wall.[5] It is not definitely established, however, that attenuation is wholly responsible. It can account for the behavior at large distances, where the attenuation of γ-rays in the end walls of the copper chamber, for example, would certainly be much larger than in the graphite chamber because of the greater density of copper.[6] Thus, the copper end walls would contribute less than their share of ion-producing electrons, and the ionization would be reduced. However, as the distance from the source is diminished, one would expect this effect to become smaller, so that Cu/C and Al/C ratios would approach the values obtained at 50° and 70°. This is clearly not the case, as figure 6 indicates higher Cu/C and Al/C ratios at 90° than at 50° or 70° for distances less than about 1 m. At present there is no satisfactory explanation to account for this, and it therefore deserves further study.

For present purposes, however, the distance effect can be avoided by orienting the chamber so as to eliminate glancing-angle incidence of the γ-rays, thus obtaining unambiguous results for k(Ra), and for the experimental check of the stopping-power correction.

[5] G. N. Whyte [51] has also observed this effect, using cylindrical chambers with the γ-rays arriving at 0° with respect to the chamber axis. Greening's measurements [52] also show the effect to a small extent.

[6] Note that the decrease in the Cu/C ratio (for 90° geometry) over the range of distances shown in figure 6 is larger than the change in Al/C by the factor 3.1, which is nearly the ratio of densities of Cu/Al (3.3). Moreover, the distance-variation of $1/D^2$ shown in figure 3 is about 1.8 times as great for Al as for graphite; the corresponding density ratio is 1.6.

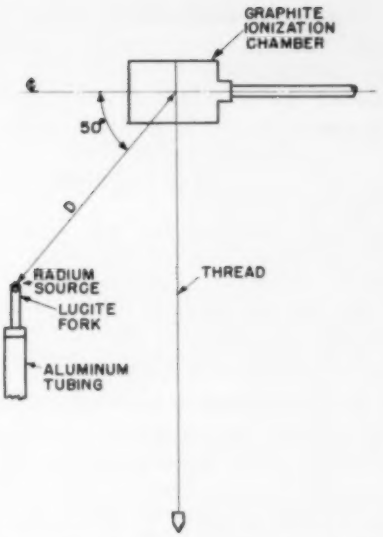

FIGURE 7. *Geometry employed in the final radium measurements.*

3. Final Radium Measurements

3.1. General Setup

The arrangement of the experiment was the same as that shown in figure 1 and described in section 2, except that the source was not directly below the chamber, and a 2-m stand of aluminum and Lucite was used in place of the paper tube. Figure 7 gives a schematic elevation of the final arrangement, in which there was a 50° angle between the chamber axis and the line joining centers of the source and chamber. The distance was determined by using two cathetometers, one vertical and the other horizontal. A fine thread supporting a plumb bob was suspended from the center of the chamber, positioned by a narrow groove cut into the chamber wall. This provided a reference point for the horizontal cathetometer measurement. Because of the time involved in making cathetometer readings before and after every ionization measurement, it was decided to substitute an exact replica of the radium source for this purpose to avoid unnecessary γ-ray exposure to the experimenters. This necessitated a more stable support for the source than the paper stand used previously.

The experimental setup was located in an air-conditioned room where the temperature fluctuations did not exceed a few tenths of a degree centigrade during the working day. Frequent readings were taken of the ambient temperature,[7] pressure and relative humidity, and all ionization data normalized to dry air at 0° C and a pressure of 760 mm of Hg. The room was 37 m long, 18 m wide, and 18 m high, the closest wall being 6 m distant.

[7] Blackening the bulb of the thermometer had no effect on its reading, indicating that radiant heat in the neighborhood of the graphite chamber was negligible.

3.2. Ionization Chamber

The graphite-walled ionization chamber was constructed as indicated in figure 2. Its dimensions were measured by a precision micrometer and its volume calculated to be 67.50 cm^3, allowing for the volume of the graphite collecting electrode, which was approximately 3 mm in diameter and extended into the chamber 3.7 cm.[8]

The purity of the graphite was checked spectroscopically and found to exceed 99.9 percent. A calculation of the effect of the remaining impurities (mainly iron) showed them to be entirely negligible. The density of the graphite was 1.7 g/cm^3, and it was found to be easily machinable to close tolerances.

3.3. Measurement of Ionization Current

A vibrating reed electrometer was used as a null detector in the current measurements, in the Townsend charge-compensation method [53]. The average rate of charge was measured during timed runs of about 60 sec duration by collecting the charge on a known capacitor (1014.8 $\mu\mu f$ ± 0.05 percent). The compensating potential was applied to the capacitor by a calibrated potentiometer accurate to ± 0.05 percent.

Time measurements were made by electronically counting the cycles in a 1 kc signal accurate to 1 part in 100,000. Runs were started and stopped by a relay in series with the electrometer milliammeter, using a device described by Costrell and Attix [54].

A potential of $\pm 1{,}000$ v was applied to the chamber wall to collect the ionization. This was sufficient to reduce the recombination losses to 0.1 percent, as determined from extrapolation on a plot of 1/ionization versus 1/collecting voltage. This 0.1 percent loss was corrected for in the calculation of k(Ra), and was independent of source-chamber distance. All ionization measurements were done with both polarities applied to the chamber, and the observed currents averaged to eliminate the effects of extracameral ionization generated in the connections. Usually the two polarities gave currents agreeing within a few tenths of a percent.

3.4. Radium Source

The principal radium source used in the absolute gamma-ray output measurement was NBS Secondary Standard No. 33420, containing nominally 100 mg of radium element. The platinum (10% iridium) capsule was cylindrical in shape, having 22 mm overall length, 18-mm active length, 3-mm outer diameter, and 0.5-mm wall thickness, with tolerances of ± 1 percent on these dimensions. It was completely filled with a homogeneous mixture of 142 mg of radium sulfate and 15 mg of barium sulfate, packed to a density of about 2.78 g/cm^3.

This source had been previously compared with the primary radium standards on the NBS Standard electroscope.[9] It had been found to have γ-radiation equivalent to that of 94.40 mg (± 0.3 percent) of radium element, in equilibrium with its products and contained in Thuringian glass 0.27 mm in thickness.[10] The γ-rays from the primary standard source are attenuated by 0.5 percent [56] in the glass wall and the radium salt itself. Hence, the γ-radiation from the secondary standard is equivalent to that from a bare, point source of (94.40 mg) $\times$ (0.995) = 93.93 mg (where only the harder γ-ray components are compared).

The actual radium content can be obtained by considering the physical dimensions of the source. Its nonpoint nature has two consequences: (1) Attenuation in the radium and barium salts; and (2) an increase in the effective thickness of the platinum wall because of its curvature. (From calculations by Owen and Naylor [57] our 0.5-mm platinum wall has an effective thickness of 0.56 mm.) The corrections are made in two steps, namely for:

(a) Attenuation in 0.56 mm platinum, using the coefficient 0.93 cm^{-1} for heavily filtered γ-rays.[11] This correction factor is 1/0.949.

(b) Attenuation in the salt for heavily filtered γ-rays. Interpolating Whyte's data for the components of the salts (Ra,Ba,S,O) one obtains an effective attenuation coefficient μ of 0.124 cm^{-1}. From calculations of Paterson, Walsh, and Higgins [59], the correction factor becomes $1/0.989_5$.

Applying corrections (a) and (b) to the 93.9_3-mg figure, the resulting radium content is $100.0_0 \pm 0.5$ mg. As a check on this figure, a calorimetric comparison with primary radium standard No. XIV was made by W. B. Mann, using the Peltier-effect twin microcalorimeter that was built for the comparison of a number of Hönigschmid standards [60]. This yielded a radium content of $99.6_2 \pm 0.3$ mg, which, being more directly obtained, is probably the more accurate of the two values. Thus, the two values have been averaged by weighting the calorimetric result twice, giving $99.7_5 \pm 0.3$ mg as the radium content as of October 1, 1956.

If this radium were located at a point centered within 0.5-mm platinum walls, no further correction would be necessary; the actual radium content would be used in calculating k(Ra). Instead, further corrections must be applied to obtain the effective radium content, taking into account the attenuation in the excess platinum wall thickness (due to its curvature), and the attenuation in the salt. For this purpose, the attenuation coefficients of Whyte [58] for lightly filtered radium γ-radiation were used, as follows:

a. Attenuation by the salt mixture itself, for radium γ-rays filtered by 0.56 mm platinum ($\mu = 0.170$ cm^{-1}), was calculated to give a correction factor of 0.986.

[8] A check on the volume of the aluminum chamber by water weighing was found to give agreement with the micrometer measurement to 4 parts in 10,000. This was not done with the graphite because of its porosity.

[9] This is essentially an aluminum-walled ionization chamber with thick (1 cm) lead outer walls to filter out the soft γ-rays.

[10] As of October 1, 1956. The radium contents of the primary standard sources were taken to be those given by the weighings of Hönigschmid, as described by Davenport et al. [55].

[11] G. N. Whyte has generously supplied, in private correspondence, the attenuation coefficients used for source corrections. His recent measurements were made with detectors of two types: (1) An ionization chamber with thick lead walls and an aluminum inside liner, and (2) a Victoreen chamber with thick Bakelite walls [58]. The measurements with (1) give the attenuation coefficients for heavily filtered radium γ-rays, whereas (2) gives those coefficients applying to lightly filtered γ-rays. Whyte's source was 30 mg of radium element in a glass capsule 2 mm in outside diameter and 0.25 mm in wall thickness. We will assume here that the radium salt plus glass wall had negligible filtering action on the radium spectrum compared to that of 0.5 mm of platinum.

b. Attenuation in the excess platinum wall thickness due to curvature (i. e., 0.56−0.50=0.06 mm Pt), for γ-rays filtered by the salt, plus 0.5 mm platinum, gave a correction factor of 0.991.

Applying these corrections to the true radium content of 99.7$_5$ mg gives an effective content of 97.4$_6$ mg of radium element. This is the figure used in calculating k(Ra).

A check of the γ-ray output as the source was rotated about its axis indicated that it was isotropic within ±0.1 percent.

As an over-all check on the source corrections, a second source of different dimensions was also used for the k(Ra) measurement. This was NBS Secondary Standard No. 33418, containing nominally 25 mg of radium in a platinum (10% iridium) capsule, 13 mm in over-all length, 9 mm in active length, 2.5 mm in external diameter, and having a wall thickness of 0.5 mm. By the same procedure described above for the other source (except for the omission of the calorimetric measurement of the radium content) the effective content of this source was found to be 24.3$_6$ mg of radium element, as of October 1, 1956.

4. Corrections for Scattering and Attenuation of the γ-Rays

4.1. Chamber Walls and Connector

The thickness of the chamber walls was more than enough to insure electronic equilibrium.[12] The cylindrical-wall thickness was 6.1 mm, the blank end wall 4.8 mm, and the connector end wall 3.2 mm. Attenuation and scattering in each of the walls was examined by increasing the thickness, using a series of graphite sleeves and disks, and extrapolating the observed ionization to zero wall thickness. These pieces were added as shown in figure 2, except that, for the 50°-angle geometry, they were placed in echelon fashion in line with the incoming γ-rays to avoid leaving a gap at the corner of the chamber. Scattered γ-radiation from the connector end wall and the connector was measured with the 50° angle altered to 130°, giving a "mirror image" of the usual geometry. Graphite disks and a replica of the chamber connecting assembly were then placed against the blank end of the chamber and their effect on the ionization observed. By this method, the scattered γ-radiation from the actual connector and connector end wall was estimated to be 0.2 percent. Attenuation in the other walls of the chamber amounted to some 3.1 percent,[13] giving an over-all correction of 2.9 percent for attenuation and scattering of γ-rays in the walls and connector.

Mayneord [62] has pointed out that the effective thickness of the wall, with respect to the γ-ray attenuation, is somewhat less than the actual thickness because the ionizing electrons are produced within the wall material. From data given by Gray [8], this reduction in effective thickness is about 0.26 mm of graphite for radium γ-rays. This results in a 0.1 percent decrease in the above attenuation correction of 2.9 percent, changing it to 2.8 percent.[14]

4.2. Air Scattering and Attenuation

The "true" absorption coefficient σ_a for radium γ-rays is 0.32 percent per meter of air at 1 atm and 20° C. However, the effective coefficient for attenuation near an isotropic point source will be less because of the contribution of backscattered rays. This coefficient was estimated to be about 0.2 percent per meter, obtained from a calculation assuming only single scattering. A somewhat lower value would result if multiple scattering were taken into account, but the correction is not important for the small distances (<1 m) used in this experiment.

4.3. Scattering From the Floor

Radiation scattered from the floor was measured by suspending the radium source in a small paper cradle attached by threads to the chamber. The height d of the source above the floor was then varied, keeping constant the distance D from source to chamber, and observing the ionization in the chamber. It was found that a 6-mm layer of lead on the thick concrete floor reduced the scattering by a factor of 1/3. Additional lead thickness made no difference.

Such a curve of ionization versus d is shown in figure 8, for D=100 cm and the lead covering on the floor.[15] The floor-scattered radiation arriving at the chamber with D=100 cm and d=200 cm is evidently about 0.2 percent. This applies strictly only when the source is directly below the chamber, as in the preliminary radium measurements (fig. 1). However, it is easy to show that changing to 50° geometry, as in figure 7, does not appreciably change the floor-scatter correction for a given d and D, if the scattering is small.

[12] The need for electronic equilibrium is discussed elsewhere, for example by Wilson 61]. Electronic equilibrium is a prerequisite for the measurement of exposure dose.

[13] Including a very small (<0.1%) calculated correction for attenuation in the central rod in the chamber.

[14] Corrections such as these (but measured with Co^{60} γ-rays) were also included in the data presented in figure 6. They were nearly the same as for radium.

[15] Actually the curve represents data obtained with several different D values. It was found that these could be normalized to fall on the same curve if the points were plotted with d(100 cm/D) cm as the abscissa. In other words, the amount of scatter "scales" with the ratio of distances d/D, as one might expect.

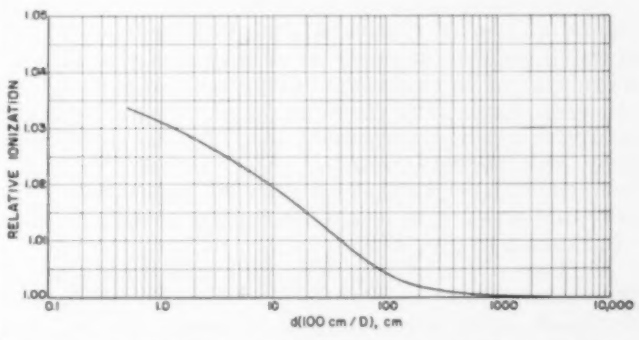

FIGURE 8. *Scattered γ-radiation from a lead-covered floor.*

The radium source is located at a distance d above the floor, and the graphite cavity chamber at a distance D above the source. (See footnote 15.)

4.4. Scattered Radiation From Other Objects

In addition to the sources of scattered radiation which have already been treated, the following were also considered.

The scattered radiation from the Lucite holder for the radium source was measured by doubling the thickness of the two blades of the "fork", and was found to be less than 0.1 percent.

The scattered radiation from all other objects together (including the lift truck and a concrete wall behind which the electrometer operator sat), was measured by interposing a lead block 10 cm square and 15 cm in thickness halfway between the source and chamber. This was supported on a light aluminum stand, which itself was observed to introduce no additional scattering.

With a distance of 94 cm between the source and chamber, the ionization with the lead block in place was found to be 0.7 percent of that obtained with the lead block removed. The scattering from the air (assumed to extend a great distance in all directions) amounts to some 0.6 percent of the unobstructed reading, while the lead-covered floor contributes another 0.2 percent. These total 0.8 percent, exceeding the observed ionization by 0.1 percent, which may be considered as agreement within experimental error. Thus the scattering by other objects is negligibly small.

5. Experimental Results

Table 1 presents the ionization in esu/cm^3-mgh (at 1 cm)[16] measured in the graphite chamber with geometry as in figure 7.

TABLE 1. *Ionization results with the graphite chamber*

Source	D	esu/cm^3-mgh at 1 cm
mg	*cm*	
100	31	8.25
100	50	8.26
100	72	8.28
100	94	8.24
25	32	8.26
Average		8.25_7

All the corrections for attenuation and scatter discussed above have been taken into account. There is apparently no systematic variation of the data as a function of D, this effect having been eliminated by the geometry. The check at 32 cm with the 25 mg source is in good agreement with the data obtained with the 100-mg source. The average of 8.25_7 esu/cm^3-mgh at 1 cm need only be multiplied by a stopping-power correction for the non-air-equivalence of graphite to give k(Ra).

Because of the existing uncertainty in the stopping-power correction, an auxiliary investigation was undertaken in an attempt to shed some light on that problem.

[16] Note that 1 coulomb = 2.998×10^9 esu.

6. Auxiliary Investigation of the Stopping-Power Correction

From the Bragg-Gray relation [2], the ionization J_{air} produced by γ-rays in free air is related to the ionization J_Z produced in a small cavity chamber with walls of atomic number Z by the equation

$$J_{air}=J_Z s^Z_{air},$$

where s^Z_{air} is the ratio of the effective electronic stopping power (per electron/cm^2) in the wall and air respectively, and it is assumed that only the Compton effect is active in delivering energy. This assumption holds for graphite, aluminum, and copper with cobalt-60 γ-rays. (Davisson and Evans [64] found no photoelectric effect in copper for cobalt-60 γ-rays.) If one measures J_Z for cavities having different wall materials, under identical conditions of irradiation, the respective values calculated for J_{air} should coincide if the stopping-power data (and the cavity theory) employed in calculating s^Z_{air} are correct.

Such measurements were made with cobalt-60 γ-rays in the course of the distance-effect study, and are shown in the form of J_{Cu}/J_C and J_A/J_C in figure 6. In order to apply properly the theoretical stopping-power factors s^Z_{air} to these data, further measurements at reduced air pressures were necessary, to ascertain whether the cavities were small enough to satisfy the requirements of cavity theory. Both the conventional Bragg-Gray theory and the Spencer cavity theory [49] require the cavity to be small in comparison with the average range of the primary electrons. Thus the following experiment was performed.

7. General Setup

The geometry was that shown in figure 5, except that the chamber in each case was enclosed within a cylindrical aluminum tank 7.3 cm in inner diameter, 25 cm in length, and having a side-wall thickness of 1.6 mm. The beam was oriented at 50° from the chamber axis.

The air in the tank was dried by passing it slowly through drying columns containing magnesium perchlorate. Pressures were measured by means of a mercury U-tube 12 mm in internal diameter, the other leg of which was continuously pumped to maintain it at about 0.1 mm of Hg. This low pressure was measured by a McLeod gage, taking care to eliminate vapors by means of a cold trap (CO_2 and trichlorethylene). Another cold trap separated the U-tube from the tank itself. The heights of the menisci were measured to ±0.1 mm of Hg with a cathetometer. A reservoir tank of 65 liters was connected to the system to provide "ballast", making it possible to maintain pressures constant to 0.1 mm of Hg for hours. Due care was exercised to avoid transient temperature effects after changing the tank pressure.

Most of the measurements were made with the cobalt-60 source (with filter) at 50 cm from the chamber. However, a check was made of the pressure dependence of the graphite chamber with a smaller

cobalt-60 source at a distance of 8 cm, yielding the same result within 0.1 percent. One may conclude that a geometrical effect such as that observed by White et al. [10] with spherical-shell chambers, is of no consequence here.

The effect of scattered radiation produced by the thin aluminum tank may be assumed to be of second order with respect to the pressure dependence of the cavity ionization.

8. Experimental Results

Ionization was measured in each chamber at pressures ranging from 0.1 to 1 atm. At each pressure and with each chamber, a saturation curve was taken with voltages up to 1,000 v. These are shown plotted as p/i versus $1/v$ in figures 9a, 9b, and 9c. By plotting against the reciprocal of the applied voltage, it is possible to extrapolate to $1/v=0$ to obtain the current at complete saturation, if the data are carried to sufficiently large voltages to give linear behavior [65]. Thus, the effect of variation of the degree of saturation with pressure can be eliminated.

Ordinarily the current measurements were made with both polarities and averaged. However, some gas multiplication was observed at high negative voltage and low pressure, causing the negative current to increase and diverge from the positive current. At 0.2 atm with −1,000 v applied to the chamber wall, and at 0.1 atm with −300 v, the increase was a few tenths of a percent. At 0.1 atmos, −1,000 v, it was about 9 percent. Onset of gas multiplication in air occurs at 20 v $cm^{-1}(mm\ Hg)^{-1}$ [66], or for the present chambers (assuming them to be simple cylinders) at −600 v for 0.1 atm, in reasonable agreement with observations. Because the multiplication occurs only in a small volume around the central electrode, it will be negligible for positive voltage on the chamber wall until it becomes very large for negative voltage. Thus, it was possible to avoid the effect by relying upon the positive current readings in cases where the negative current was influenced by multiplication.

The currents per unit pressure at $1/v=0$ are plotted (as solid curves) in figure 10 as a function of the air pressure (at 0° C) for copper, aluminum, and graphite. These curves are normalized to each other at room pressure ($\approx$0.92 atm) by means of the ratios Cu/C=1.191 and Al/C$\doteq$1.084 obtained from figure 6. The graphite curve shows a slight decrease with decreasing pressure, whereas aluminum and copper both have a pronounced rise. It would be difficult to extrapolate these curves to zero pressure with any confidence in the result, because of the increasing slope at low pressures.

9. Comparison with Cavity Theory

In calculating the values of s^z_{air}, the electron stopping-power formula of Bethe [43] was employed. Two sets of values for I, the mean excitation potential of the stopping material, were used with the Bethe formula; those of Bakker and Segre [44] and

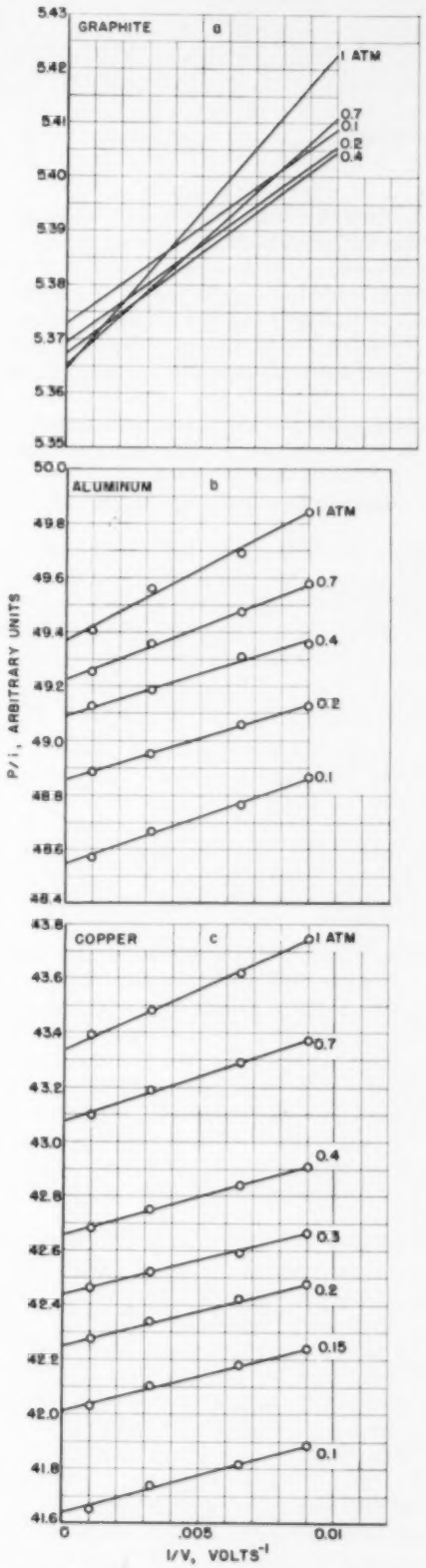

FIGURE 9*a,b,c. Saturation curves at various air pressures in the graphite, aluminum, and copper chambers, respectively, for cobalt-60 γ-rays, at an exposure dose rate of about 0.05 r/min.*

TABLE 2

	I_C	I_{Al}	I_{Cu}	I_{air}
	ev	*ev*	*ev*	*ev*
Bakker and Segre	76.4	150	279	80.5
Caldwell	78	163.1	377.5	94.9

those of Caldwell [46]. These are given in table 2.

For the Bakker and Segre set of I values, I_{air} was taken as 80.5 ev, which was found by Wilson [67] to be consistent with $I_{Al}=150$ ev. $I_{air}=94.9$ ev was obtained by multiplying the effective atomic number of air[17] (7.3) by 13, which is approximately the proportionality factor found by Caldwell to relate I and Z.

The density (or polarization) effect in the graphite, aluminum, and copper was treated according to the method of Steinheimer, using his data appropriate to the Bakker-Segre and Caldwell sets of I values [68,69].

The mean values of s^Z_{air} for cobalt-60 γ-rays were calculated from the usual Bragg-Gray theory approach by integrating s^Z_{air} over the electron energy from 0 to T_0, (the starting energy of a Compton recoil electron), and then integrating over the spectrum of starting energies [70]. Values of $\bar{s}^Z_{air}$ so obtained are given in table 3 for the two sets of I.

TABLE 3. $\bar{s}^Z_{air}$ *for* Co^{60} γ-*rays*[a]

	C	Al	Cu
Bakker and Segre	1.000	0.921	0.836
Caldwell	1.016	.928	.823

[a] Bragg-Gray treatment.

These data are compared with the experimental results in figure 10 by plotting $1/\bar{s}^{Cu}_{air}$, $1/\bar{s}^{Al}_{air}$, and $1/\bar{s}^{C}_{air}$ as short arrows along the vertical axis, having arbitrarily normalized to the experimental graphite curve at 0.085 atm. These theoretical values are seen to be too low to agree with any reasonable extrapolation of the experimental curves to zero pressure, where they are meant to be applied. Furthermore, the Bragg-Gray theory has nothing to say about the variation of ionization with cavity size (or gas pressure).

The modified cavity theory of Spencer [49], on the other hand, relates $\bar{s}^Z_{air}$ to a parameter Δ, taken to be the energy needed by an electron to cross the cavity. Secondary electrons (δ-rays) produced by collisions between electrons are included in the electron flux assumed to be crossing the cavity. The flux includes only electrons with energies greater than Δ, because it is assumed that all electrons with energies less than Δ lose their energy immediately, on the spot where they originate. The same general sort of calculation was carried out as was done for the Bragg-Gray theory, except that the integration over the degraded electron spectrum was taken from Δ to T_0. The resulting values of $\bar{s}^Z_{air}$ are given in table 4 for various values of Δ.

[17] Air was assumed to be 75.5 percent N_2, 23.2 percent O_2, and 1.3 percent A, by weight.

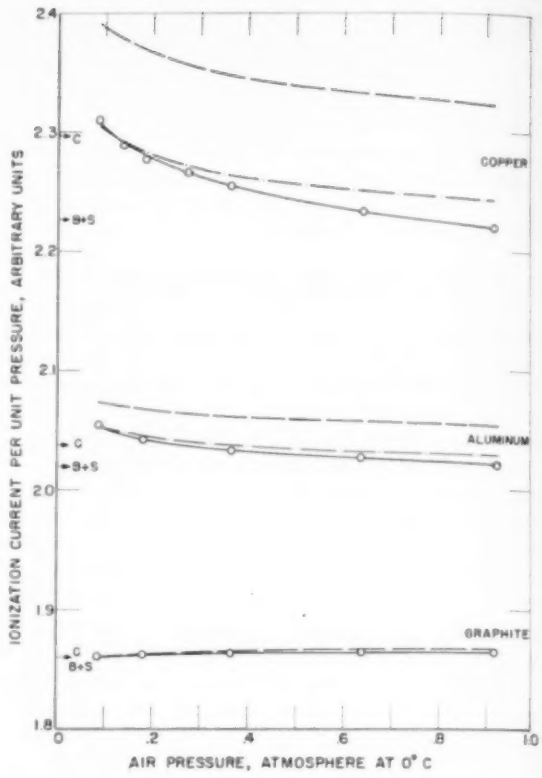

FIGURE 10. *Comparison of the relative ionizations in graphite, aluminum, and copper cavity chambers with theory, for cobalt-60* γ-*rays.*

The solid curves represent the observed ionizations per unit pressure as a function of pressure, for $1/v=0$ (see figs. 9a to c). The dashed curves were obtained, theoretically, by applying Caldwell stopping-power data to the Spencer cavity theory. The "dash-dot" curves were similarly obtained by applying Bakker and Segre stopping-power data to the Spencer theory. The short arrows at the ordinate axis represent the ionizations predicted by applying Bakker and Segre (B and S) and Caldwell (C) data to the conventional Bragg-Gray cavity theory. The results of each theory are normalized to the graphite experimental data at a pressure of 0.085 atmos.

TABLE 4. $\bar{s}^Z_{air}$ *calculated for cobalt-60* γ-*rays from Spencer, cavity theory* [49][a]

Z / Δ(kev)	10.2	20.4	40.9	81.8
C	1.001	1.001	1.000	1.000
	(1.021)	(1.019)	(1.017)	(1.016)
Al	0.905	0.911	0.917	0.921
	(0.914)	(0.919)	(0.924)	(0.928)
Cu	0.804	0.817	0.828	0.837
	(0.789)	(0.803)	(0.815)	(0.825)

[a] Δ=energy needed by an electron to cross the cavity. The values given in parentheses are calculated according to Caldwell's I values, the others are according to Bakker and Segre.

The choice of Δ for a particular chamber shape and gas pressure is fortunately not critical, because it would be difficult to calculate with accuracy. For the present experimental chambers, the diameter of 4 cm was taken as the effective track length of the electrons in crossing the cavity.[18] Range-energy

[18] 3 cm was taken as the mean diameter of the chamber, and the electrons were assumed to have linear ranges of ≈ 0.8 times their track lengths [71], thus giving ≈ 4 cm for the mean track length in the chamber. If 5 cm or 3 cm had been assumed instead of this 4 cm mean track length, $\bar{s}^{Cu}_{air}$ would be changed by about ± 0.4 percent, $\bar{s}^{Al}_{air}$ by ± 0.1 percent, $\bar{s}^{C}_{air}$ negligibly.

data for electrons in air were taken from Spencer [71], in relating Δ to the air pressure in the cavity.

Again normalizing the reciprocals of $\bar{s}^{C}_{air}$, $\bar{s}^{Al}_{air}$, and $\bar{s}^{Cu}_{air}$ to the graphite experimental curve at 0.085 atm, the resulting theoretical curves are shown in figure 10. The calculations based on Bakker-Segre I values are clearly the closer to the experimental results. Agreement is closest at low pressures where the limitation on the theory that $\Delta \ll T_0$ is best satisfied, as one might expect. At higher pressures, the air in the cavity begins to modify the spectrum of electrons crossing the cavity, which is assumed to be a negligible effect in the theory. It is thus apparent that a further refinement of the theory is necessary to account more exactly for the behavior of cavities where Δ is large. The present agreement at low pressure is, however, sufficiently good to warrant the conclusion that the Bakker-Segre I values, in conjunction with the modified cavity theory of Spencer, are to be preferred to the Caldwell I values in predicting the relative ionization in Cu-, Al-, and C-walled cavity chambers irradiated by cobalt–60 γ-rays.

It will be seen from the above discussion that this experiment does not directly affirm the accuracy of $I_{air}=80.5$ ev, relative to I_C, I_{Al}, and I_{Cu}, because only the ratios of ionizations among the latter materials are compared. However, there are other confirmations besides Wilson's work [67] indicating that $I_{air}=80.5$ ev is consistent with the Bakker-Segre I values.

Whyte [51] has recently suggested an empirical method for determining $\bar{s}^{Z}_{air}$ from an interpolation between the mean slopes of the ionization/pressure versus pressure curves for different wall materials. By this method, applied to air-filled cavity chambers of copper, aluminum, graphite, and beryllium, he arrives at a value of $\bar{s}^{C}_{air}=1.003 \pm 0.005$ for cobalt–60 γ-rays and $\Delta \approx 25$ kev. The corresponding value from table 4, based on the Bakker-Segre I data, would be $\bar{s}^{C}_{air}=1.001$, in close agreement. Applying Whyte's method to our experimental curves in figure 10, yields $\bar{s}^{C}_{air}=1.007 \pm 0.005$ or 0.6 percent more than the theoretical value. This must still be considered as fair agreement, however, because this empirical method is extremely sensitive to the slope of the experimental graphite curve. For example, if the ionization per unit pressure in the graphite chamber had gradually decreased by only 0.05 percent in place of the observed 0.15 percent in going from 0.92 to 0.085 atm, the value obtained for $\bar{s}^{C}_{air}$ would have been 1.002. This is about the range of accuracy one might expect of the graphite slope in this experiment.

Thompson [72] has recently measured the relative stopping powers of graphite, liquid nitrogen, and liquid oxygen for protons in the neighborhood of 270 Mev. His I values, relative to $I_{Cu}=279$ ev, are $I_C=70.2$ ev, $I_N=76.3$ ev, and $I_O=88.3$ ev. Taking this I_N and I_O in conjunction with $I_A=198$ ev for argon [73], one calculates $I_{air}=79.8$ ev. The $\bar{s}^{C}_{air}$ (at $\Delta=25$ kev) resulting from these data and Spencer cavity theory becomes 1.011, including the density correction according to Sternheimer [68]. This is apparently in disagreement with $\bar{s}^{C}_{air}=1.001$ obtained from Bakker-Segre I data. However, Whyte [51] has pointed out that part of the density effect, namely the "zero-energy" part, has not been taken into account here. If the Thompson measurements had compared the stopping powers of graphite with that of gaseous nitrogen and oxygen, a different value of I_{air}, closer to I_C, would have resulted. Sternheimer [74] has calculated the magnitude of the zero-energy density effect in solid (or liquid) air as 1.0 percent. Taking this into account corrects $\bar{s}^{C}_{air}$ from 1.011 to 1.001, in identical agreement with Bakker and Segre. Thus, there seems to be a fair amount of evidence in support of these results, and they may now be applied to the radium γ-ray measurements.

10. Calculation of k(Ra)

If one uses the Compton recoil-electron spectrum arising from the radium γ-ray spectrum in place of that from cobalt-60, the data for $\bar{s}^{C}_{air}$ given in table 4 are increased by only about 0.06 percent at each Δ, giving for the Bakker-Segre data:

Δ(kev)	10. 2	20. 4	40. 9	81. 8
$\bar{s}^{C}_{air}$	1. 002	1. 001	1. 001	1. 000

The dependence of the graphite-chamber ionization (per unit pressure) upon air pressure was found for radium γ-rays to be indiscernible from that obtained with cobalt-60, indicated in figure 10. Thus, it will be seen that k(Ra) based on the graphite chamber measurements is independent of pressure:

Pressure	esu/cm³/mgh	Δ	$\bar{s}^{C}_{air}$	k(Ra)
atmos		*kev*		
1	8.25_7	48	1.000_6	8. 26
0. 1	8.24_4	13	1.001_5	8. 26

11. Estimation of Limits of Error in k(Ra)

	Percent
(1) Effective content of radium source	± 0.4
(2) Chamber volume	± 0.1
(3) Compensating capacitor	± 0.05
(4) Compensating potentiometer	± 0.05
(5) Interval timer	≈ 0
(6) Distance measurements, source-to-chamber	± 0.2
(7) Measurements of ambient temperature, pressure and humidity (combined)	± 0.1
(8) Measurements of scattered radiation and chamber-wall attenuation	± 0.3
(9) Stopping-power correction ($\bar{s}^{C}_{air}$)	± 0.3

Combining these as random errors gives an estimated limit of error of ± 0.6 percent for k(Ra). Thus, we can write

$$k(\mathrm{Ra}) = 8.26 \pm 0.05 \text{ r/mgh at 1 cm.}$$

It must be stressed that this value of k(Ra) is based upon the validity of the conclusions reached in the discussion of the stopping-power correction $\overline{s}^{C}_{air}$. Future measurements of stopping power are not expected to disagree appreciably, but that possibility cannot be ruled out, in which case the value given here for k(Ra) can be adjusted to conform to the resulting improvements in $\overline{s}^{C}_{air}$.

12. Comparison With Results of Other Workers

A survey of the literature on the γ-ray emission of radium reveals that this constant has been measured in no fewer than 25 separate experiments. The results of some of these measurements have been included in table 5, for comparison with the present

TABLE 5. *Values of* k(Ra) *obtained previously by other workers.*

Author	Type of cavity chamber	k(Ra); r/mgh at 1 cm, 0.5 mm Pt filter		
		Value given by authors	Corrected for γ-ray attenuation in cavity wall	Corrected for non-air equivalence of wall
Friedrich and Schulze, 1935 [4].	Spherical, graphite, 4 mm thick.	7.8	8.0	8.0
Minder, 1937 [5].....	Spherical, graphite, 4 mm thick.	8.0	8.2	8.2
Mayneord and Roberts, 1947 [6].	Cylindrical, graphite, 4 mm thick. Central rod of elektron metal.	8.3	8.3	8.2
Gray, 1937 [7,8].....	Cylindrical, graphite, 3 mm thick.	8.4	8.4	8.3
Kaye and Binks, 1938 [9].	Cylindrical, graphite, 3 mm thick.	7.9_6	8.1	8.1
White, Marinelli, and Failla, 1940 [10].	Spherical Lucite shells, source in center.	8.4_7	8.4_7	8.3
Darden and Sheppard, 1951 [11].	Cylindrical, polystyrene.	8.3_9	8.3_9	8.2
Ghosh, Kastner, and Whyte, 1953 [12].	Cylindrical, polystyrene.	8.4_4	8.4_4	8.2[a]
			Average value.....	8.2[b]

[a] This figure also includes a correction factor of 0.995 to take into account the revised value of the Canadian radium standard according to the findings of Davenport et al. [55].

[b] This figure is consistent with the Bakker and Segre stopping-power data. If, instead, the calculations of Laurence [34] (based upon the assumption that the mean excitation potential I=13.5Z) are applied, the figure is changed to 8.4, which is the currently accepted value of k(Ra).

determination. These criteria were followed in selecting the data for this table:

(a) Free-air-chamber measurements were excluded on the grounds that, to date, none of them have been free of plate separation inadequacy, recombination losses, and/or electric field distortion.

(b) Measurements with cavity chambers having wall thicknesses inadequate for electronic equilibrium ($\approx$3 mm of graphite) were omitted, as were those in which the walls were not closely air equivalent (e. g., aluminum), or were not of well-defined composition (e. g., paper).

(c) Only the most recent determination by a given author was included.

The values of k(Ra) as given by these authors vary from 7.8 to 8.4_7, a spread of nearly 9 percent. However, if one applies corrections for attenuation of γ-rays in the cavity wall in cases where this was not included, and for the non-air-equivalence of the wall material (in accordance with the Bakker and Segre stopping-power results), the spread of results is reduced to 4 percent, and the average value is 8.2 r/mgh at 1 cm.

Another correction which has apparently been omitted from all these measurements (except that of Gray [7]), judging from the fact that it was not mentioned, is the correction for the decrease in electron density of the air, owing to humidity. This will be an upward correction to k(Ra), usually in the neighborhood of 0.3 percent. Thus, the 8.2 figure should be increased by roughly this amount. The resulting number for k(Ra) lies within the experimental error of the present result of 8.26 $\pm$0.05 r/mgh at 1 cm. Considering the many factors entering into such measurements, such close agreement may be to some extent fortuitous. However, it does indicate that k(Ra) is probably known with better accuracy than has been heretofore supposed.

Another interesting experiment was carried out by Gray [7], who applied cavity-ionization methods to determine the total energy absorbed in a large aluminum block enclosing a radon capsule. Gray averaged his result with a value obtained calorimetrically by Zlotowski [75] and arrived at 8.7_3 cal/hr per gram of radium (in equilibrium with its daughter products) as the best figure for the total γ-ray energy output. This can be reduced to a value for k(Ra) by application of eq 4 in Gray's paper, using $(\sigma_a)_{air}=0.0892\times10^{-24}$ cm^2/electron and $W_{air}=33.7$ ev per ion pair as given by Bay et al. [76]. The resulting value for k(Ra) is 9.0_0 r/mgh at 1 cm (for zero filtration of the radium source). The data of Whyte [58] indicate a transmission of 0.90_8 through 0.5 mm of platinum; thus, k(Ra) is given as 8.1_7 r/mgh at 1 cm; in reasonably good agreement with the results obtained by conventional cavity-chamber methods. Conversely, if one assumes 8.26 r/mgh at 1 cm for the value of k(Ra), the total γ-ray energy output becomes 8.84 cal/hr/g Ra. This is in good agreement with Zlotowski's result of 9.1 $\pm$0.15 cal/hr/g Ra, if one applies to it a correction factor of 0.98 for geometrical error and multiple scattering of γ-rays, as suggested by Gray, yielding a value of 8.9 $\pm$0.15 cal/hr/g Ra.

The authors thank H. O. Wyckoff for frequent discussions on the various phases of the work; L. V. Spencer for his contributions in the interpretation of the cavity-chamber measurements; and W. B. Mann for his calibration of the radium source by the calorimetric method.

13. References

[1] 1956 Report of the International Commission on Radiological Units and Measurements.
[2] L. H. Gray, Proc. Roy. Soc. (London) [A] **156,** 578 (1936).
[3] W. H. Bragg, Studies in radioactivity, p. 94 (MacMillan and Co., New York, N. Y., 1912).
[4] W. Friedrich and R. Schulze, Strahlentherapie, **54,** 553 (1935).
[5] W. Minder, Acta Radiol. **17,** 761 (1937).
[6] W. V. Mayneord and J. E. Roberts, Brit. J. Radiol. **10,** 365 (1937).
[7] L. H. Gray, Proc. Roy. Soc. (London) [A] **159,** 263 (1937).
[8] L. H. Gray, Brit. J. Radiol. **10,** 721 (1937).
[9] G. W. Kaye and W. Binks, Am. J. Roentgenol. and Radium Therapy **40,** 80 (1938).
[10] T. N. White, L. D. Marinelli, and G. Failla, Am. J. Roentgenol. and Radium Therapy **44,** 889 (1940).
[11] E. B. Darden and C. W. Sheppard, Oak Ridge National Laboratory Report No. 1002 (Instrumentation, July 9, 1951).
[12] A. Ghosh, J. Kastner, and G. N. Whyte, Nucleonics **11,** No. 6, 70 (1953).
[13] A. S. Eve, Phil. Mag. **22,** 551 (1911).
[14] A. S. Eve, Phil. Mag. **27,** 394 (1914).
[15] H. Behnken and R. Jaeger, Strahlentherapie **29,** 483 (1928).
[16] M. Jona, Strahlentherapie **32,** 775 (1929).
[17] M. Bruzau, Ann. phys. **11,** 1 (1929).
[18] O. Glasser and F. R. Mautz, Radiology **15,** 93 (1930).
[19] G. Failla and P. S. Henshaw, Radiology **17,** 1 (1931).
[20] W. V. Mayneord, Brit. J. Radiol. **4,** 693 (1931).
[21] A. W. Reitz, Z. Physik **69,** 259 (1931).
[22] W. V. Mayneord, Brit. J. Radiol. **6,** 598 (1933).
[23] R. Paterson and H. M. Parker, Brit. J. Radiol. **7,** 592 (1934).
[24] R. M. Sievert, Acta Radiol. **15,** 193 (1934).
[25] W. Friedrich, K. G. Zimmer, and R. Schulze, Strahlentherapie **51,** 7 (1934).
[26] W. V. Mayneord and J. E. Roberts, Brit. J. Radiol. **7,** 158 (1934).
[27] L. G. Grimmett and J. Read, Brit. J. Radiol. **8,** 702 (1935).
[28] W. Friedrich, Strahlentherapie **54,** 397 (1935).
[29] J. Murdoch and E. Stahel, Strahlentherapie **53,** 102 (1935).
[30] G. W. C. Kaye and W. Binks, Strahlentherapie **56,** 608 (1936).
[31] J. Murdoch, E. Stahel, and S. Simons, Strahlentherapie **57,** 87 (1936).
[32] O. Glasser and L. Rovner, Am. J. Roentgenol. and Radium Therapy **36,** 94 (1936).
[33] K. G. Zimmer, Radiumdosimetrie, Georg Thieme, Leipzig (1936).
[34] G. C. Laurence, Can. J. Research **15,** 67 (1937).
[35] G. Failla and L. D. Marinelli, Am. J. Roentgenol. and Radium Therapy **38,** 312 (1937).
[36] H. Smereker, Strahlentherapie **58,** 267 (1937).
[37] R. Schulze, Ann. Physik **31,** 633 (1938).
[38] W. Friedrich, Am. J. Roentgenol. and Radium Therapy **40,** 69 (1938).
[39] G. C. Laurence, Am. J. Roentgenol. and Radium Therapy **40,** 92 (1938).
[40] L. Rovner, Am. J. Roentgenol. and Radium Therapy **40,** 104 (1938).
[41] W. Minder, Radiumdosimetrie (Julius Springer, Vienna, 1941).
[42] L. S. Taylor and G. Singer, J. Research NBS **24,** 247 (1940) RP1283.
[43] H. A. Bethe and J. Ashkin, Experimental nuclear physics, E. Segre, Ed., Vol. I, p. 254 (eq 52) (John Wiley & Sons, Inc., New York, N. Y., 1953).
[44] C. J. Bakker and E. Segre, Phys. Rev. **81,** 489 (1951).
[45] R. L. Mather and E. Segre, Phys. Rev. **84,** 191 (1951).
[46] D. O. Caldwell, Phys. Rev. **100,** 291 (1955).
[47] H. Bichsel and R. F. Mozley, Phys. Rev. **94,** 764 (1954).
[48] W. Brandt, Phys. Rev. **104,** 691 (1956).
[49] L. V. Spencer and F. H. Attix, Rad. Research **3,** 239 (1955).
[50] R. K. Clark and S. S. Brar, Nucleonics **12,** No. 8, 28 (1954).
[51] G. N. Whyte, Rad. Research **6,** 371 (1957).
[52] J. R. Greening, Brit. J. Radiol. **30,** 254 (1957).
[53] J. W. Boag, Radiation dosimetry, ed. Hine and Brownell, p. 194 (Academic Press Inc., New York, N. Y., 1956).
[54] L. Costrell and F. H. Attix, Nucleonics **15,** No. 2, 203 (1957).
[55] T. I. Davenport, W. B. Mann, C. C. McCraven, and C. C. Smith, J. Research NBS, **53,** 267 (1954) RP2544.
[56] W. E. Perry, Proc. Phys. Soc. London [A], **68,** 942 (1955).
[57] E. A. Owen and B. Naylor, Proc. Phys. Soc. London **34,** 92 (1922).
[58] G. N. Whyte, Brit. J. Radiol. **28,** 635 (1955).
[59] C. C. Paterson, J. W. T. Walsh, and W. F. Higgins, Proc. Phys. Soc. London **29,** 215 (1917).
[60] W. B. Mann, J. Research NBS **53,** 277 (1954) RP2545.
[61] C. W. Wilson, Radium therapy, its physical aspects, p. 72 (Chapman Hall, London, 1948).
[62] W. V. Mayneord, Brit. J. Radiol., Suppl. No. 2, 226 (1950).
[63] Gladys White Grodstein, X-ray attenuation coefficients, NBS Circ. 583 (1957).
[64] C. M. Davisson and R. D. Evans, Phys. Rev. **81,** 404 (1951).
[65] E. Kara-Michailova and D. E. Lea, Proc. Cambridge Phil. Soc. **36,** 101 (1940).
[66] L. B. Loeb, Fundamental processes of electrical discharge in gases, p. 338 (John Wiley & Sons, Inc., New York, N. Y., 1939).
[67] R. R. Wilson, Phys. Rev. **60,** 749 (1941).
[68] R. M. Sternheimer, Phys. Rev. **88,** 851 (1952).
[69] R. M. Sternheimer, Phys. Rev. **103,** 511 (1956).
[70] A. T. Nelms, Graphs of the Compton energy-angle relationship and the Klein-Nishina formula from 10 kev to 500 mev, NBS Circ. 542 (1953).
[71] L. V. Spencer, Phys. Rev. **98,** 1, 597 (1955).
[72] T. J. Thompson, Effect of chemical structure on stopping powers for high-energy protons, UCRL–1910, University of California Thesis (August 11, 1952).
[73] W. A. Aron, The passage of charged particles through matter, UCRL–1325, University of California Thesis (May 1951).
[74] R. M. Sternheimer, Phys. Rev. **93,** 351 (1953).
[75] I. Zlotowski, J. phys. radium **6,** 241 (1935).
[76] Z. Bay, W. B. Mann, H. H. Seliger, and H. O. Wyckoff, W_{ai} for sulphur-35 beta rays, Rad. Research (to be published).

Washington, March 15, 1957.

Journal of Research of the National Bureau of Standards Vol. 59, No. 5, November 1957 Research Paper 2802

Radiation From Slots on Dielectric-Clad and Corrugated Cylinders

James R. Wait and Alyce M. Conda

An approximate formula is derived for the radiation pattern of an axially slotted cylinder with a thin dielectric coating. The accuracy of the formula is shown to be sufficient for practical purposes. Using a similar method, the pattern function for a slot on a corrugated cylinder is derived. Extensive numerical results are presented for both dielectric-clad and corrugated cylinders.

1. Introduction

The radiation from slots on smooth circular cylinders is now well understood. However, if the cylindrical surface is coated with a dielectric film, the patterns can be appreciably modified. Although a rigorous expression can be derived for the fields of an arbitrary slot on a circular cylinder with a dielectric coating, the resulting formulas are very cumbersome.[1] For this reason, it seems worthwhile to modify the final expressions for the field by making several approximations on the basis that the thickness of the dielectric film is small. Furthermore, it is of interest to consider the problem by using approximate boundary conditions. This latter method can also be used to treat the corrugated cylinder under the restriction that the teeth are closely spaced with respect to the wavelength.

An attempt will be made in the present paper to investigate the accuracy of the simplifying approximations for dielectric-clad cylinders. A comparison is also made between thin dielectric coatings and corrugations on an axially slotted circular cylinder, from the standpoint of the directionality of the radiation.

2. Dielectric-Clad Cylinder

The cylinder is taken to be of radius a and the concentric dielectric coating has a radius b, as indicated in figure 1a and 1b. Cylindrical coordinates (ρ,ϕ,z) are chosen to be coaxial with the cylinder. The electrical constants of the coating are ϵ and μ, and those of the homogeneous (air) space outside are ϵ_0 and μ_0. The tangential electric fields on the slot are to be specified. In the case of a thin axial slot (where the slot is parallel to the cylinder axis), the electric field, E, in the equatorial plane is vertically polarized, possessing only a z component. It was shown before that (see footnote 1)

$$E_\phi=\left[\frac{k_0}{2\pi^2}\int_{z_1}^{z_2}V(z')dz'\right]\frac{e^{-ik_0\rho}}{\rho}P(\phi) \qquad (1a)$$

where $k_0=(\epsilon_0\mu_0)^{1/2}\omega=2\pi/$free space wavelength, and where $V(z')$ is the transverse voltage along the slot

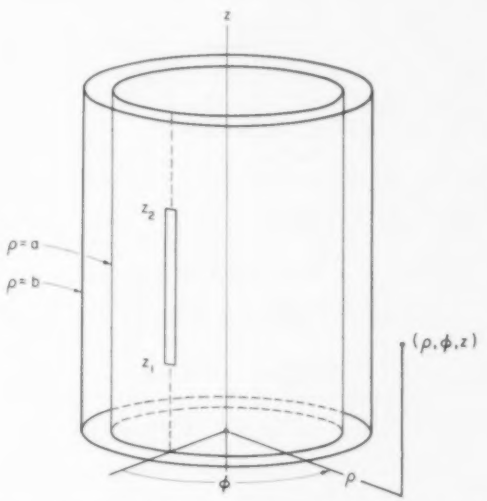

FIGURE 1a. *Axial slot on a metallic circular cylinder of infinite length with a dielectric coating.*

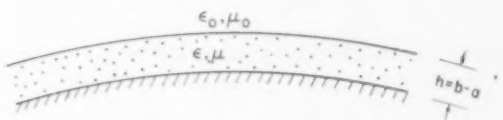

FIGURE 1b. *Sectional view of the dielectric coating.*

that extends from $z=z_1$ to z_2 at $\rho=a$ and $\phi=0$. The pattern factor that characterizes the azimuthal variation of the radiated field is given by

$$P(\phi)=\frac{2i}{\pi(kb)(k_0a)}\sum_{m=0}^{\infty}\frac{\epsilon_m\cos m\phi e^{im\pi/2}}{\left(\frac{k_0\mu}{k\mu_0}\right)H_m(k_0b)T_m-H'_m(k_0b)L_m} \qquad (2)$$

where

$$T_m=J'_m(kb)H'_m(ka)-J'_m(ka)H'_m(kb), \qquad (3a)$$

$$L_m=J_m(kb)H'_m(ka)-J'_m(ka)H_m(kb), \qquad (3b)$$

$k=(\epsilon\mu)^{1/2}\omega$, and J_m and H_m are the Bessel function and the Hankel function of the second kind, of order m, respectively. The prime indicates the derivative with respect to the argument of the

[1] J. R. Wait and W. E. Mientka, Slotted-cylinder antenna with a dielectric coating, J. Research NBS **58**, 287 (1957) RP2762.

function. When the slot is of infinite length, the radiated field is a cylindrical wave[2] and the field is given by

$$E_\phi = -i60\epsilon_0\omega V\left(\frac{2}{\pi k_0\rho}\right)^{\frac{1}{2}} e^{-i(k_0\rho-\pi/4)}P(\phi) \qquad (1b)$$

which has the same azimuthal dependence as the spherical wave radiated from a finite slot.

Some numerical values for the function $P(\phi)$ were given in a previous paper (see footnote 1). The cases considered were for $ka=2$ and 3, and various values of b/a, ϵ/ϵ_0 and μ/μ_0. The numerical work involved is extensive. In view of the complexity of the above formula for $P(\phi)$, an effort was made to simplify it by making several judicious approximations. The validity of this procedure is best checked by comparing the numerical values computed from the approximate and the exact formulas. This work will be described in what follows.

Noting the Taylor expansions

$$J'_m(ka)=J'_m(kb)+(ka-kb)J''_m(kb)+\ \ldots\ ,$$

$$H'_m(ka)=H'_m(kb)+(ka-kb)H''_m(kb)+\ \ldots\ ,$$

it follows that to a first order in $k(b-a)$,

$$T_m\simeq-[J'_mH''_m-J''_mH'_m]\,k(b-a). \qquad (4)$$

The argument of the Bessel functions, J_m and H_m, is kb, and the double prime indicates a second derivative with respect to kb. Making repeated use of the recursion formulas

$$J'_{m+1}=-\frac{m+1}{kb}J_{m+1}+J_m \qquad (5a)$$

$$J'_m=\frac{m}{kb}J_m-J_{m+1} \qquad (5b)$$

and utilizing the Wronskian relation

$$J_mH'_m-H_mJ'_m=\frac{2}{\pi ikb} \qquad (6)$$

it is easy to show that

$$T_m\simeq\frac{2i}{\pi}\left(1-\frac{m^2}{k^2b^2}\right)\left(\frac{b-a}{b}\right). \qquad (7)$$

In a similar manner, an expansion in ascending powers of $k(b-a)$ can be developed for L_m. Retaining terms to first order in $k(b-a)$ leads to

$$L_m\simeq\frac{2}{\pi ikb}-\frac{b-a}{b}\,[J_mH_{m+1}-J_{m+1}H_m]$$

$$\simeq\frac{2}{\pi ikb}+\frac{b-a}{b}\left[\frac{2}{\pi ikb}\right]$$

$$\simeq\frac{2}{\pi ika}. \qquad (8)$$

[2] J. R. Wait, Slotted-cylinder antenna with a dielectric coating, Addendum to Radio Physics Lab. Project Report 19-0-11 (Ottawa, November 1954).

On the basis of the above derivation it would be expected that these formulas for T_m and L_m are valid if $(b-a)\ll b$ and $k(b-a)<1$.

The expression for the pattern factor now takes the relatively simple form

$$P(\phi)\simeq\frac{1}{B}\sum_{m=0}^{\infty}\frac{\epsilon_m\cos m\phi\, e^{im\pi/2}}{H'_m(B)+G_mH_m(B)} \qquad (9)$$

where

$$G_m=(\mu/\mu_0)(B-A)\left(1-\frac{m^2}{N^2B^2}\right)\frac{A}{B} \qquad (10)$$

with $A=k_0a$, $B=k_0b$, $N=k/k_0$. It can be seen that if $k=k_0$, or if $b=a$, the equation for the pattern becomes

$$P(\phi)=\frac{1}{A}\sum_{m=0}^{\infty}\frac{\epsilon_m\cos m\phi\, e^{im\pi/2}}{H'_m(A)} \qquad (11)$$

which is the well-known result for the uncoated cylinder (see footnote 1).

3. Corrugated Cylinder

Before discussing numerical results, it is of some interest to consider a closely related problem. A line magnetic source (of strength K volts) is located at $\rho=\rho_0$, $\phi=0$, parallel to a circular cylinder of radius b and infinite length (see fig. 2). The ratio between the tangential electric field (E_ϕ) and the tangential magnetic field (H_z) on the surface of the cylinder is to be specified. That is,

$$\left[E_\phi=\frac{i}{\epsilon_0\omega}\frac{\partial\psi}{\partial\rho}=-Z\psi\right]_{\rho=b}$$

where $\psi=H_z$ and where Z is the boundary impedance. Following the method suggested previously (see footnote 1) the solution for $\rho>b$ can be written

$$\psi=\frac{\epsilon_0\omega K}{4}\sum_{m=0}^{\infty}\epsilon_mH_m(k_0\rho_0)[J_m(k_0\rho)+A_mH_m(k_0\rho)]$$

$$\cos m\phi \text{ for } \rho<\rho_0 \qquad (12a)$$

and

$$\psi=\frac{\epsilon_0\omega K}{4}\sum_{m=0}^{\infty}\epsilon_mH_m(k_0\rho)[J_m(k_0\rho_0)+A_mH_m(k_0\rho_0)]$$

$$\cos m\phi \text{ for } \rho>\rho_0 \qquad (12b)$$

where A_m is to be determined from the boundary condition at $\rho=b$. In the present case it is easily found that

$$A_m=-\left[\frac{J'_m(k_0b)+GJ_m(k_0b)}{H'_m(k_0b)+GH_m(k_0b)}\right], \qquad (12c)$$

where $G=-iZ/\eta_0$, $\eta_0=\sqrt{\mu_0/\epsilon_0}$.

The above result is now specialized in two ways. Firstly, the far field approximation is made ($k_0\rho\gg1$) and, consequently, the leading term of the asymp-

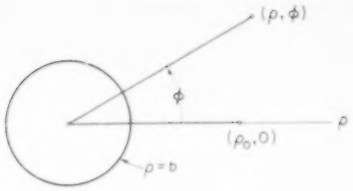

FIGURE 2. *Illustrating a line magnetic source at $(\rho_0,0)$ outside a circular cylinder whose average surface impedance, at $\rho=b$, is to be specified.*

totic expansion of $H_m(k_0\rho)$ can be used. Secondly, the source is allowed to approach the cylinder $(\rho_0 \to b)$. Then, utilizing the Wronskian for J_m and H_m, the far field can be written

$$E_\phi = -i60\epsilon_0\omega V\left(\frac{2}{\pi k_0\rho}\right)^{1/2} e^{-i(k_0\rho-\pi/4)}Q(\phi) \tag{13}$$

where the pattern factor $Q(\phi)$ is given by

$$Q(\phi)=\frac{1}{B}\sum_{m=0}^{\infty}\frac{\epsilon_m \cos m\phi e^{im\pi/2}}{H_m'(B)+GH_m(B)} \tag{14}$$

where $B=k_0b$.

This formula is almost identical in form to that for $P(\phi)$, the pattern of a slotted cylinder with a dielectric coating. The surface impedance function, Z, although not strictly applicable to curved surfaces, would be given by

$$Z\simeq i\sqrt{\mu/\epsilon}\tan k(b-a)\simeq i\sqrt{\mu/\epsilon}\,k(b-a), \tag{15}$$

which is the appropriate value for a thin dielectric film of thickness $b-a$ on a flat perfect conductor for a plane wave at normal incidence. Therefore,

$$G\simeq\frac{\mu}{\mu_0}\cdot\frac{1}{N}\tan N(B-A)$$

$$\simeq\frac{\mu}{\mu_0}(B-A). \tag{16}$$

It is interesting to note that

$$\frac{G_m}{G}\simeq\left(1-\frac{m^2}{N^2B^2}\right)\frac{A}{B}\simeq\left(1-\frac{m^2}{N^2B^2}\right). \tag{17}$$

If the refractive index, N, of the coating is large, the quantity m^2/N^2B^2 is small compared to unity for significant values of m (i. e., $m<2A$) in the summation. Consequently, $G_m\simeq G$, for thin dielectric coatings of high refractive index. In the case of polystyrene and other such dielectric materials, N is of the order of 2 and the term m^2/N^2B^2 is comparable to unity for values of m of the order of A. In this case, it is not justified to use an approximate boundary condition.[3]

Although there are severe limitations to the use of approximate boundary conditions for dielectric-clad surfaces, they become very suitable for characterizing corrugated surfaces. For example, if axial grooves of width, w, and depth, h, are cut circumferentially around the metal cylinder, it follows that the average surface impedance at $\rho=b$ is

$$Z\simeq i\eta_0\left(\frac{\mu}{\mu_0}\right)\left(\frac{w}{dN}\right)\tan Nk_0h \tag{18a}$$

where d is the periodicity of the grooves in the circumferential direction, and N is the refractive index of the material filling the grooves. Equation (18a) is obtained by regarding the grooves as shorted transmission lines of electrical length, Nkh, and considering only the fundamental (TEM) mode. This can be expected to be valid [4] if d is small compared to the wavelength. In the limiting case where h tends to zero, the cylinder again behaves as a perfectly conducting object. When the width of the teeth is small compared to the width of the grooves, such that $w\simeq d$, it is seen that

$$Z\simeq i\eta_0\left(\frac{\mu}{\mu_0}\right)\frac{1}{N}\tan Nk_0h \tag{18b}$$

or

$$G\simeq\frac{\mu}{\mu_0}\frac{1}{N}\tan N(B-A),$$

where Z corresponds to the surface impedance for a plane wave at normal incidence on a dielectric film of thickness $b-a$. In the present instance, this always can be expected to be a good approximation since energy flow in the circumferential direction in the dielectric film is not permitted because of the presence of the teeth.

The relative location of the slot and the teeth on the corrugated surface has not been specified. Presumably the slot could be cut in the bottom of one of the grooves.

4. Numerical Results

The approximate formula for the pattern function of an axial slot (of finite or infinite length) on a pure dielectric $(\mu=\mu_0)$ clad cylinder is

$$P(\phi)\simeq\frac{1}{B}\sum_{m=0}^{\infty}\frac{\epsilon_m\cos m\phi e^{im\pi/2}}{H_m'(B)+G_mH_m(B)} \tag{19}$$

[3] Some improvement might be obtained if the value of the surface impedance for a plane wave at grazing incidence on a thin dielectric coating on a plane conductor was used. This would lead to

$$G\simeq\frac{\mu}{\mu_0}(B-A)\left(1-\frac{1}{N^2}\right).$$

[4] R. S. Elliott, Azimuthal surface waves on corrugated cylinders, J. Appl. Phys. **38**,368 (April, 1955).

where $G_m=(B-A)\,[1-(m^2/N^2B^2)]\,A/B$. The amplitude and phase of $P(\phi)$ for ϕ from 0° to 180° are shown listed in tables 1 and 2. The columns labeled "exact" are based on the exact formula for $P(\phi)$ given by eq (2), and the columns labeled "approx." are based on eq (19). The amplitude values shown are normalized to unity at $\phi=0$ and the phase, which is -arg. $P(\phi)$, is normalized to 0° at $\phi=0$.

The cases for the smaller cylinders ($A=2$ and 3) are treated by both the approximate and exact techniques. The excellence of the approximate formula is evidenced by a comparison of the appropriate columns. For the case of the large cylinder ($A=8$), only the numerical results from the approximate formula have been obtained. The corresponding exact numerical data for $A=8$ could be obtained only from extensive and tedious computations. It is believed, however, that the approximate results for this larger cylinder would not differ more than 5 percent in amplitude and 10° in phase from reality.

The corresponding formula for $Q(\phi)$, the pattern of a slot on a corrugated cylinder, is identical in form to that for $P(\phi)$, except G_m is replaced by G where

$$G=\frac{1}{N}\tan\,[N(B-A)].$$

In this case, the teeth are of small width compared to their separation. The refractive index of the dielectric material filling the grooves is N and the depth of the grooves is $b-a$. One might describe this situation as a dielectric-clad cylinder with radial fins contained within the dielectric coating (see fig. 3). For purposes of comparison with the noncorrugated cylinder, $Q(\phi)$ has been calculated for the same range of values of A, B, and N. Results for

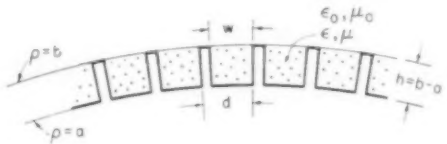

FIGURE 3. *Sectional view of the corrugated surface.*

TABLE 1. *Amplitude of P (φ)*

φ	A=2.0 B=2.0	A=2.0 B=2.1 Exact N=2	A=2.0 B=2.1 Approx. N=2	A=2.0 B=2.2 Exact N=2	A=2.0 B=2.2 Approx. N=2	A=2.0 B=2.3 Exact N=2	A=2.0 B=2.3 Approx. N=2	A=2.0 B=2.2 Exact N=1.5	A=2.0 B=2.2 Approx. N=1.5	A=3.0 B=3.0	A=3.0 B=3.2 Exact N=2	A=3.0 B=3.2 Approx. N=2	A=8.0 B=8.0	A=8.0 B=8.1 Approx. N=2	A=8.0 B=8.2 Approx. N=2
0°	1.000	1.000	1.000	1.000	1.000	1.000	1.000	1.000	1.000	1.000	1.000	1.000	1.000	1.000	1.000
10°	1.000	0.999	1.000	1.002	0.995	1.003	1.002	1.001	0.996	0.997	1.003	1.004	0.997	0.995	0.998
20°	0.990	.985	0.997	1.005	.987	1.012	1.012	1.001	.986	.987	1.007	1.014	.992	.988	.985
30°	.976	.985	.988	1.005	.979	1.021	1.024	0.995	.974	.966	1.002	1.020	.986	.988	.990
40°	.942	.961	.967	0.993	.971	1.021	1.031	.975	.961	.934	0.974	1.004	.966	.972	.988
50°	.900	.920	.927	.957	.950	0.995	1.081	.936	.934	.895	.924	0.955	.945	.953	.957
60°	.838	.861	.868	.894	.899	.932	0.971	.876	.881	.869	.874	.901	.905	.928	.957
70°	.780	.796	.800	.810	.813	.836	.847	.803	.801	.828	.853	.874	.845	.866	.887
80°	.732	.742	.743	.733	.722	.739	.797	.738	.719	.779	.842	.866	.788	.822	.869
90°	.698	.711	.711	.693	.674	.691	.739	.703	.676	.693	.784	.814	.680	.716	.753
100°	.670	.695	.695	.689	.678	.706	.742	.694	.677	.585	.657	.688	.601	.659	.724
110°	.622	.661	.664	.680	.692	.729	.760	.673	.674	.539	.539	.569	.479	.522	.568
120°	.536	.582	.587	.620	.641	.692	.719	.603	.616	.490	.535	.548	.401	.486	.561
130°	.412	.454	.459	.493	.518	.563	.589	.473	.484	.463	.562	.579	.295	.333	.375
140°	.282	.305	.308	.327	.323	.366	.391	.316	.310	.367	.483	.502	.282	.348	.428
150°	.227	.232	.231	.238	.215	.223	.245	.233	.215	.215	.282	.300	.155	.179	.208
160°	.285	.305	.303	.331	.321	.331	.343	.308	.312	.162	.177	.181	.205	.286	.348
170°	.361	.402	.401	.451	.453	.485	.496	.413	.432	.271	.350	.335	.047	.056	.066
180°	.392	.441	.440	.499	.499	.546	.557	.454	.478	.325	.436	.449	.182	.265	.323

TABLE 2. *Normalized phase of P (φ)*

φ	A=2.0 B=2.0	A=2.0 B=2.1 Exact N=2	A=2.0 B=2.1 Approx. N=2	A=2.0 B=2.2 Exact N=2	A=2.0 B=2.2 Approx. N=20	A=2.0 B=2.3 Exact N=2	A=2.0 B=2.3 Approx. N=2	A=2.0 B=2.2 Exact N=1.5	A=2.0 B=2.2 Approx. N=1.5	A=3.0 B=3.0	A=3.0 B=3.2 Exact N=2	A=3.0 B=3.2 Approx. N=2	A=8.0 B=8.0	A=8.0 B=8.1 Approx. N=2	A=8.0 B=8.2 Approx. N=2
0°	0°	0°	0°	0°	0°	0°	0°	0°	0°	0°	0°	0°	0°	0°	0°
10°	1.6	1.6	1.7	1.8	2.1	2.0	2.1	1.6	2.1	2.4	2.6	2.8	7.9	6.9	6.2
20°	6.2	6.6	5.0	6.9	8.4	7.6	8.3	6.5	8.0	9.6	10.1	10.3	27.5	27.8	27.0
30°	13.9	14.5	15.0	15.1	18.3	16.3	17.8	14.5	17.3	21.5	22.3	23.3	60.7	61.6	62.3
40°	24.4	25.4	26.4	26.0	3[illegible]6	27.6	30.0	25.4	29.3	38.2	39.1	40.1	105.8	107.1	108.0
50°	37.9	39.2	39.8	39.5	45.0	41.0	44.4	39.2	43.2	59.6	61.1	61.7	161.8	164.5	166.8
60°	54.6	56.1	61.8	55.9	60.5	57.2	61.3	56.0	59.3	85.0	88.7	89.6	226.1	229.6	233.1
70°	74.4	76.5	82.9	76.2	79.6	77.2	84.3	76.3	78.5	112.5	119.9	121.3	298.9	303.7	307.9
80°	96.8	100.1	107.3	100.9	103.7	102.7	106.2	100.3	102.3	141.1	150.9	138.0	374.9	382.5	388.8
90°	120.1	125.1	132.1	128.6	132.3	132.9	136.4	126.4	129.7	171.2	180.9	184.4	459.6	466.6	473.2
100°	142.4	148.9	156.1	155.1	160.1	162.1	166.1	151.3	151.2	205.4	214.0	216.3	543.8	552.9	562.5
110°	162.6	169.9	176.1	177.8	181.9	185.7	188.7	172.8	177.5	244.9	256.4	254.7	632.3	641.8	650.7
120°	181.6	189.0	194.6	197.1	199.3	204.5	210.8	191.7	195.0	282.8	301.6	304.1	718.1	730.9	744.5
130°	202.0	208.8	213.3	216.4	216.1	221.8	229.2	211.0	212.2	312.7	334.2	337.1	814.0	821.4	832.5
140°	231.2	237.1	238.3	243.7	243.7	245.3	253.3	238.7	237.7	337.6	357.9	361.5	894.2	910.7	928.7
150°	278.4	287.4	281.5	296.9	297.2	300.3	306.0	289.8	292.8	371.1	386.4	389.1	988.4	1001.8	1014.4
160°	317.8	330.1	322.9	342.9	346.3	356.5	361.5	335.0	339.9	445.3	469.7	472.6	1089.1	1090.4	1112.5
170°	334.6	347.2	342.2	359.7	362.0	374.0	379.9	352.7	355.6	485.1	514.6	518.5	1168.1	1179.3	1195.5
180°	339.1	351.6	347.6	364.0	366.6	378.1	384.5	357.3	359.5	492.8	521.8	525.8	1249.3	1270.3	1293.9

the normalized amplitude and phase of $Q(\phi)$ are listed in tables 3 and 4.

TABLE 3. *Amplitude of $Q(\phi)$*

ϕ	$A=2.0$ $B=2.0$	$A=2.0$ $B=2.1$ $N=2$	$A=2.0$ $B=2.2$ $N=2$	$A=2.0$ $B=2.3$ $N=2$	$A=8.0$ $B=8.0$	$A=8.0$ $B=8.1$ $N=2$	$A=8.0$ $B=8.2$ $N=2$
0°	1.000	1.000	1.000	1.000	1.000	1.000	1.000
10°	1.000	1.001	0.995	1.000	0.997	0.991	1.007
20°	0.990	1.001	.996	1.006	.992	.986	0.999
30°	.976	0.996	1.006	1.027	.986	1.005	.996
40°	.942	.978	1.023	1.062	.966	1.000	1.005
50°	.900	.941	1.026	1.089	.945	0.976	0.987
60°	.838	.882	0.983	1.072	.905	.949	.985
70°	.780	.811	.886	0.988	.845	.905	.921
80°	.732	.748	.768	.856	.788	.883	.908
90°	.698	.718	.708	.757	.680	.749	.795
100°	.670	.707	.737	.776	.601	.669	.781
110°	.622	.683	.783	.859	.479	.553	.652
120°	.536	.610	.754	.879	.401	.538	.635
130°	.412	.480	.618	.759	.295	.356	.424
140°	.282	.320	.412	.507	.282	.391	.513
150°	.227	.234	.282	.265	.155	.193	.241
157.5°					.205	.268	.400
160°	.285	.312	.390	.394	.205	.285	.439
170°	.361	.419	.541	.624	.047	.083	.088
180°	.392	.462	.600	.713	.182	.309	.415

TABLE 4. *Normalized phase of $Q(\phi)$*

ϕ	$A=2.0$ $B=2.0$	$A=2.0$ $B=2.1$ $N=2$	$A=2.0$ $B=2.2$ $N=2$	$A=2.0$ $B=2.3$ $N=2$	$A=8.0$ $B=8.0$	$A=8.0$ $B=8.1$ $N=2$	$A=8.0$ $B=8.2$ $N=2$
0°	0°	0°	0°	0°	0°	0°	0°
10°	1.6	8.6	12.5	7.8	7.9	7.0	6.2
20°	6.2	13.5	19.9	15.7	27.5	28.5	26.6
30°	13.9	20.3	30.8	27.7	60.7	62.8	63.0
40°	24.4	32.4	43.7	42.1	105.8	108.1	109.6
50°	37.9	46.1	57.6	57.6	161.8	165.7	168.1
60°	54.6	62.9	72.8	74.2	226.1	231.8	237.1
70°	74.4	83.4	91.2	93.3	298.9	307.0	310.9
80°	96.8	107.5	115.7	117.9	374.9	384.7	395.7
90°	120.1	133.6	146.8	150.6	459.6	467.1	478.1
100°	142.4	158.4	176.9	178.3	543.8	556.8	572.5
110°	162.6	170.2	200.0	213.7	632.3	647.5	657.6
120°	181.6	199.1	217.5	233.8	718.1	735.8	757.8
130°	202.0	209.5	234.3	250.0	804.0	824.5	841.1
140°	231.2	245.9	258.0	270.0	894.2	917.1	945.0
150°	278.4	297.0	309.1	302.3	988.4	1001.7	1024.3
160°	317.8	341.1	357.3	350.0	1089.1	1100.3	1130.8
170°	334.6	358.5	374.3	408.8	1168.1	1204.6	1206.1
180°	339.1	364.0	378.4	412.8	1249.3	1277.5	1312.9

5. Graphical Presentation of Results

The salient features of the radiation patterns are best illustrated by graphical presentation. In figure 4a, $|P(\phi)|$, using the exact formula, is plotted for $A=2.0$, and $B=2.0$, 2.1, 2.2, 2.3 with $N=2.0$. This shows clearly the effect of varying the thickness of the dielectric film. The corresponding results for $|P(\phi)|$, using the approximate formula, are shown in figure 4b. The two sets of patterns are identical in appearance. The most significant feature is that the dielectric film enhances the field to the rear. The pattern $|Q(\phi)|$ for the corrugated cylinder for the same values of A, B, and N is shown in figure 4c. There is a general similarity between these and the corresponding patterns for the uncorrugated dielectric film (i. e., fig. 4a or 4b). It appears that the corrugations further enhance the field in the backward direction.

The effect of varying N, the refractive index of the dielectric coating, is shown in figures 5a and 5b where $|P(\phi)|$ is plotted for $A=2.0$, $B=2.2$, and $N=1.5$ and 2.0. As would be expected, the distortion of the pattern for $N=1.5$ from the uncoated case (i. e., $A=B=2.0$) is less than for the higher value of N. The corresponding patterns for $Q(\phi)$ and $N=1.5$ also have less distortion than that for $N=2.0$, which was plotted in figure 4c. This is readily evident from the formula

$$G=\frac{1}{N}\tan N(B-A)\cong(B-A)+\frac{N^2(B-A)^3}{3}+\cdots$$

which to a first order in $(B-A)$ is independent of N, but tends to increase with N when $B-A$ is not small.

The patterns, $P(\phi)$, for a slightly larger cylinder, $(A=3.0)$, are shown in figures 6a and 6b using the exact and approximation formulas, respectively. The rear lobes are now becoming smaller. The enhancement, resulting from the presence of the coating of the field in the backward direction, is again quite significant.

Finally, the pattern $|P(\phi)|$ for the large dielectric-coated cylinder is shown in figure 7a for several thicknesses of the coating. The corresponding pattern $|Q(\phi)|$ for the corrugated cylinder is shown in figure 7b. It is strikingly noted here that the pattern for the corrugated cylinder has a pronounced lobe structure. This is evidence that surface waves are being guided more efficiently, due to the presence of the corrugations. This viewpoint is further substantiated when eq (19) is transformed to a Watson-Bremmer type[5] residue series. The individual terms of this mode series are then in the form of peripheral surface waves. The dominant mode is of the type studied by Elliott (see footnote 3).

6. Conclusion

It is seen that considerable simplification can be made to the general formula for radiation from a dielectric-coated, axially slotted cylinder. This new approximate formula, which is valid for thin coatings, is only slightly more complicated than its counterpart for an uncoated cylinder. It is shown that a direct approach, using approximate boundary conditions, is not generally valid for curved dielectric-clad surfaces due to the azimuthal flow of energy within the dielectric. On the other hand, the formulas derived using the surface impedance concept are applicable to a corrugated surface, and the patterns calculated therefrom have similar characteristics to their dielectric-clad counterpart. Generally speaking, for a specified normal surface impedance, the corrugated cylinder modifies the pattern to a greater extent than the dielectric-clad cylinder.

[5] H. Bremmer, Terrestrial radio waves (Elsevier Publishing Company, New York, N. Y., 1949).

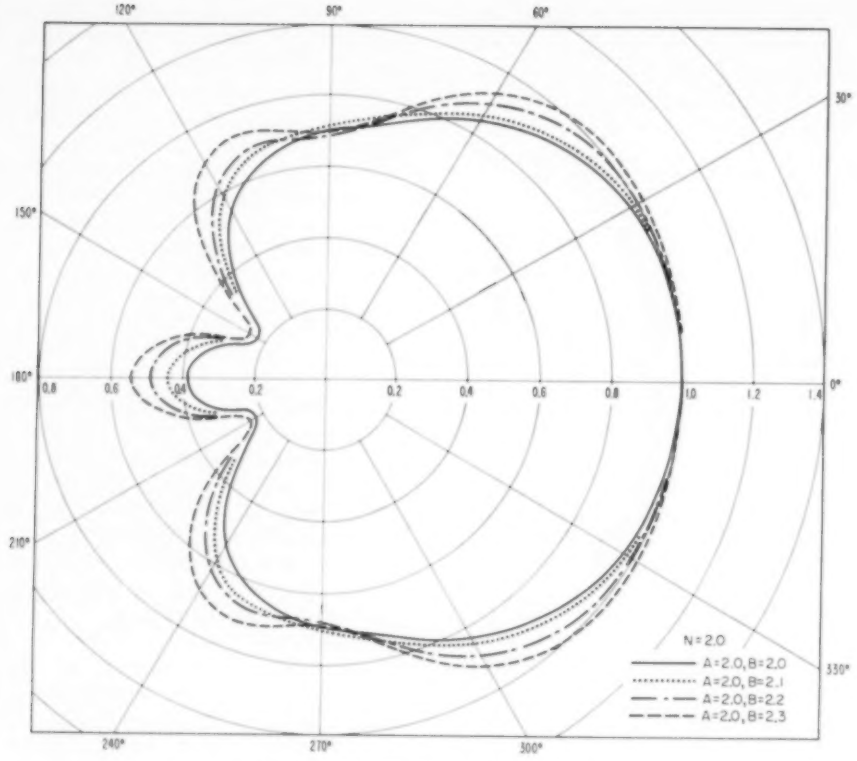

FIGURE 4a. *Pattern* $|P(\phi)|$ *(exact).*

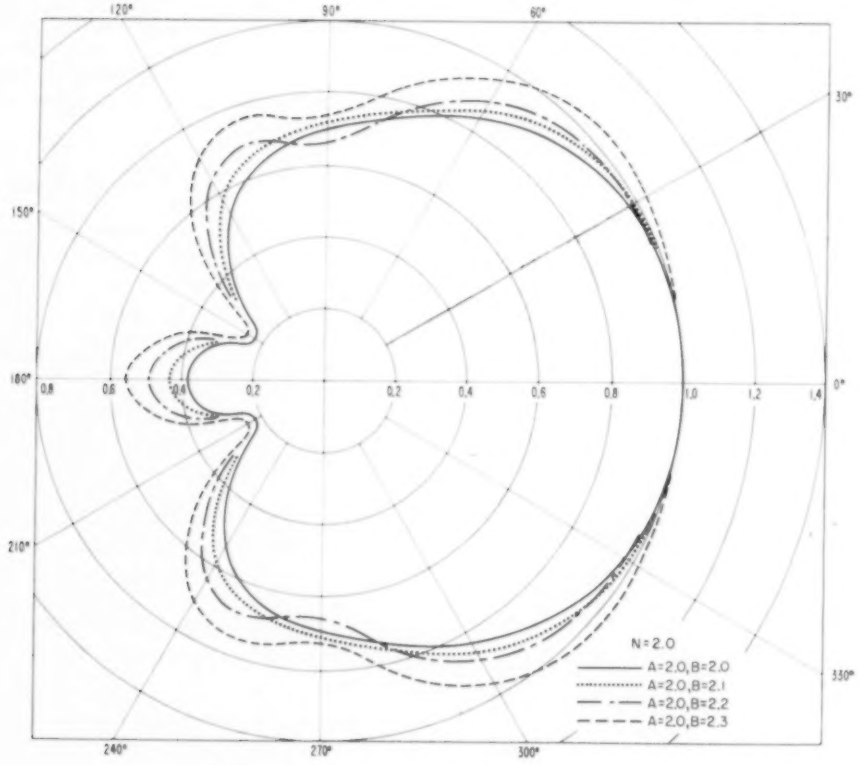

FIGURE 4b. *Pattern* $|P(\phi)|$ *(approximate).*

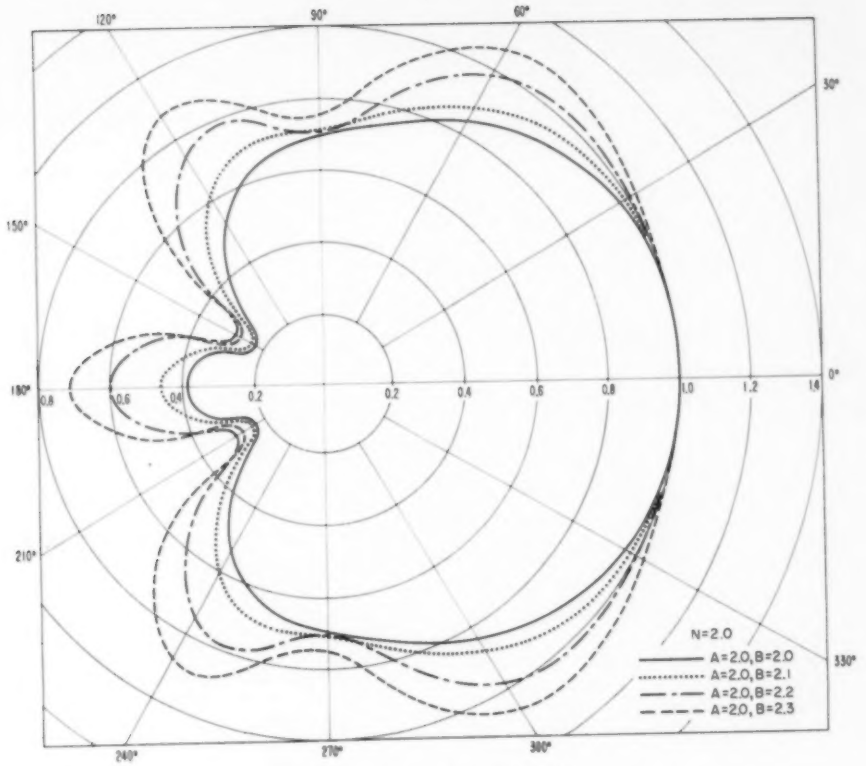

FIGURE 4c. *Pattern* $|Q(\phi)|$.

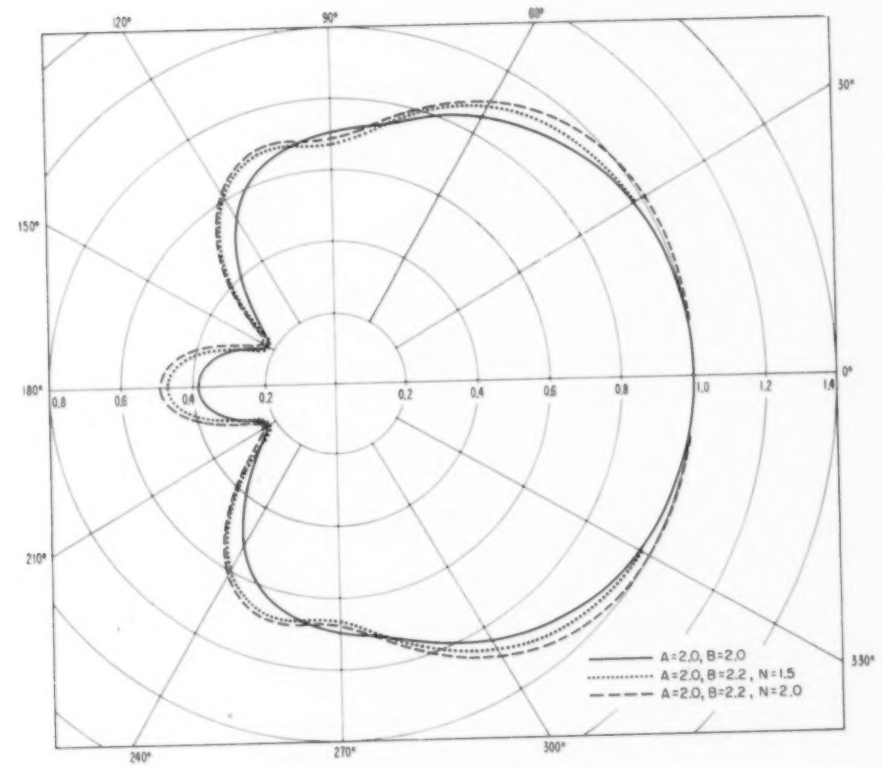

FIGURE 5a. *Pattern* $|P(\phi)|$ *(exact)*.

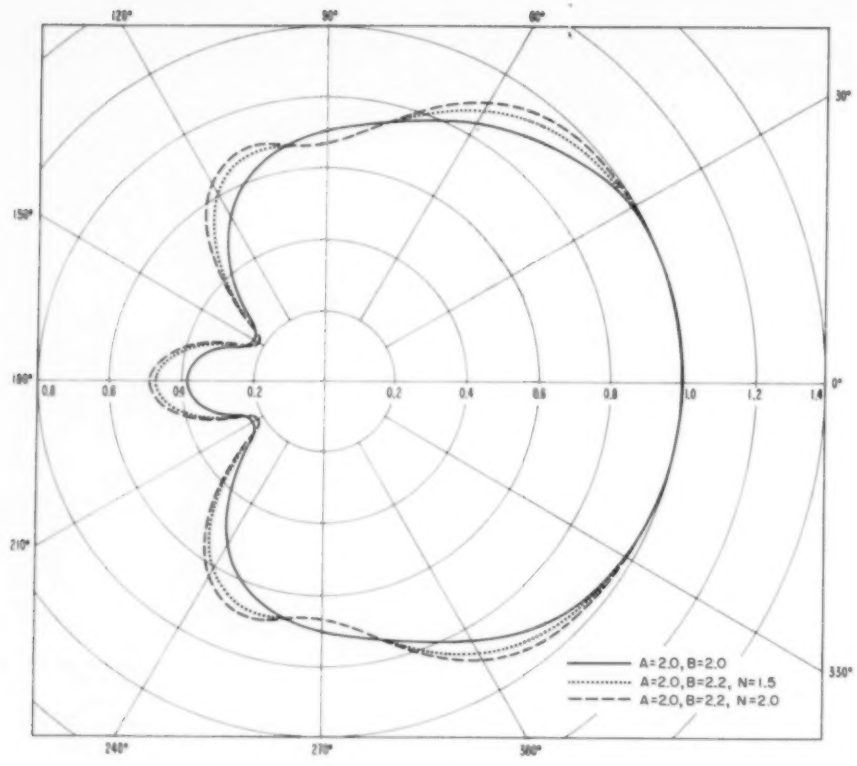

FIGURE 5b. *Pattern* $|P(\phi)|$ *(approximate).*

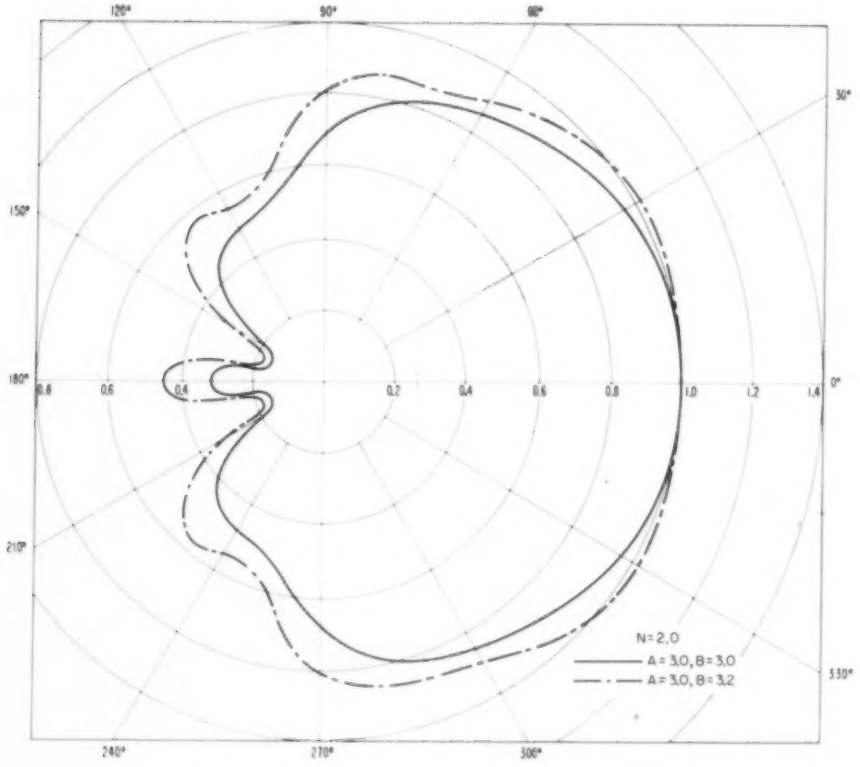

FIGURE 6a. *Pattern* $|P(\phi)|$ *(exact).*

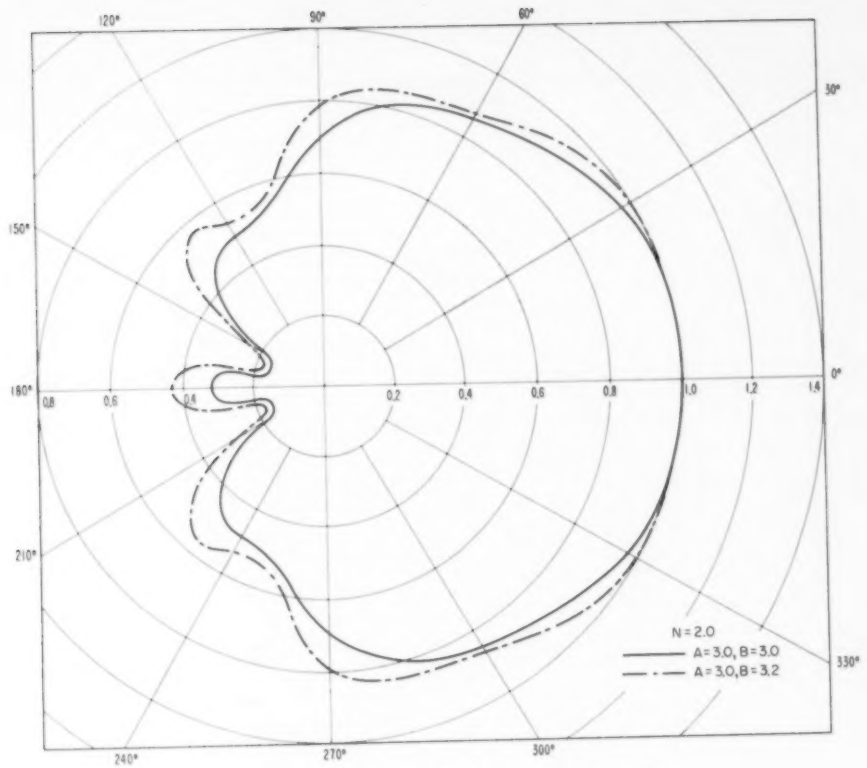

FIGURE 6b. *Pattern* $|P(\phi)|$ *(approximate).*

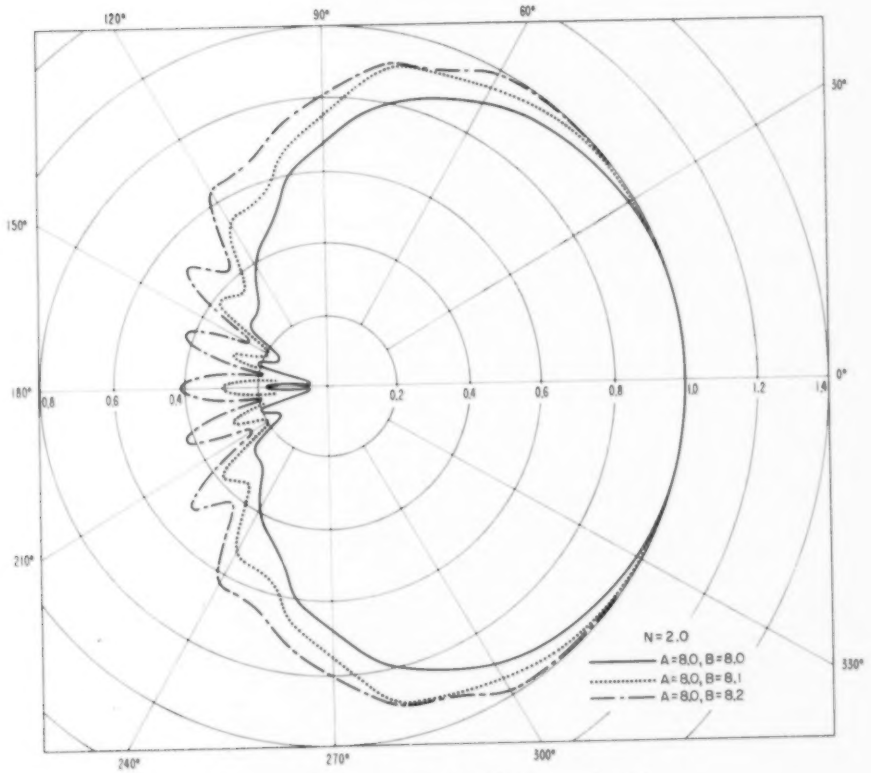

FIGURE 7a. *Pattern* $|P(\phi)|$ *(approximate).*

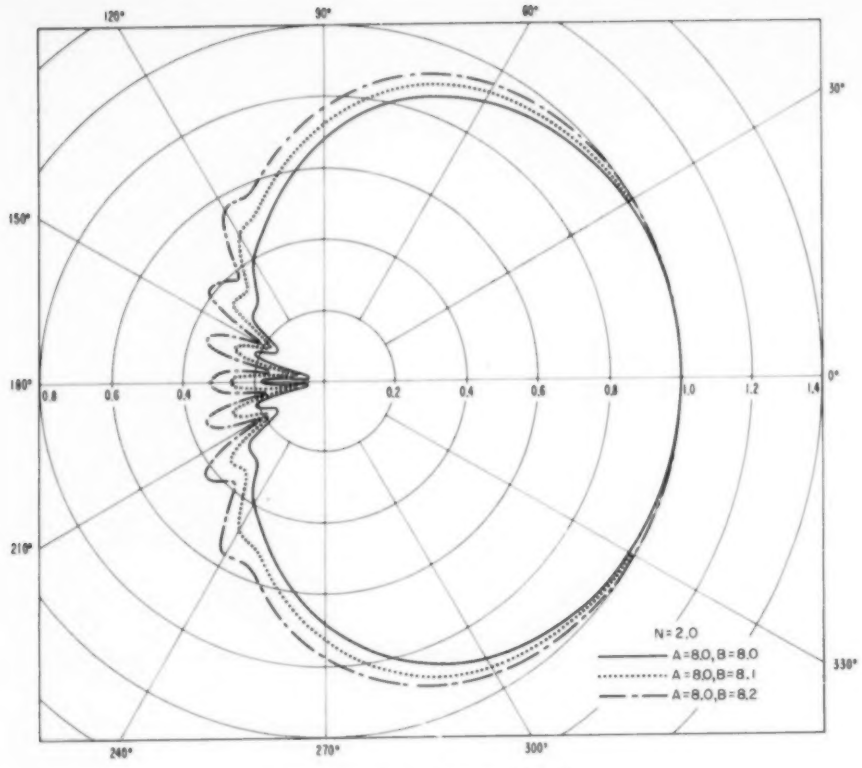

FIGURE 7b. *Pattern* $|Q(\phi)|$.

BOULDER, COLO., May 9, 1957.

Journal of Research of the National Bureau of Standards Vol. 59, No. 5, November 1957 Research Paper 2803

Infrared Emission Spectrum of Methane at 3.3 Microns[1]

Earle K. Plyler and Lamdin R. Blaine

The emission spectrum of methane from the flame of a Bunsen burner has been observed in the region from 2,820 to 3,180 cm^{-1}. Many lines have been measured in the *P*-, *Q*-, and *R*-branches. The *P*-branch was observed to *P*-28 and the *R*-branch to *R*-17.

The spectrum was observed from the inner cone of the flame and with a rich fuel mixture the *P*-12 line was most intense. This intensity distribution indicated a temperature of about 1,200° K for the heated gas.

1. Introduction

In the measurement of the emission spectrum from a flame [1] [2] with methane gas as a fuel, it was shown that the bands of greatest intensity were produced by the molecules of H_2O and CO_2 at elevated temperatures. In further studies it was shown [2] that weak bands are produced in the infrared spectra of flames from the molecules of OH, CO, and C_2. A weak emission band was observed also in the region of 3.3 μ from the inner cone of a methane-oxygen flame. This band was identified as arising from the heated methane molecules before combustion took place. No rotational structure was observed in the band, but the position and type of band observed made it highly probable that it was an emission band of methane. The present work was undertaken to ascertain if the spectrum when measured under high resolution contained a rotational structure which was similar to that of methane. Also from the spectrum under high resolution it would be possible to determine the temperature of the heated gas.

2. Experimental Method

The spectra were measured by the use of a grating spectrometer having a grating of 10,000 lines per inch. Other details concerning the spectrometer have been given in a previous publication [3].

Under the most suitable conditions a resolution of 0.05 cm^{-1} is obtained in the region of 3.3 μ, but on account of the low intensity of the emission of the flame, it was necessary to widen the slits so that the resolution obtained in this work is about 0.10 cm^{-1}. Two types of burners were used for obtaining the methane spectrum. The first type was a glass-blower's torch where mixtures of methane and oxygen were burned. The intensity was then compared with that obtained from a flame of a Bunsen burner in which a mixture of methane and air was used. It was found that the radiation from the inner cone of the flame of a Bunsen burner was more intense in the region of the methane band, and it was used for measuring the spectrum. The flame was low in intensity and a group of mirrors was used to increase the available energy on the entrance slit of the spectrometer [4]. In the use of the optical system, part of the radiation is focused back on the flame. The flame absorbs some of the reflected energy, but the amount is small. It was found that the strongest lines showed an increase in the energy on the entrance slit by a factor of 3.5. This factor of increased energy approaches the value of 4, which would be the gain in energy if there were no absorption in the flame and no reflection losses from the mirrors.

In observing the spectrum in the 3.3-μ region a rich fuel mixture was used for the flame. The Bunsen burner was adjusted so that an inner cone 4 in. in height was obtained, and a section of the inner cone about 3 in. above the top of the burner was focused on the entrance slit of the spectrometer.

3. Results

The observed spectrum from 2,820 to 3,180 cm^{-1} is shown in figure 1. The *P*-, *Q*-, and *R*-branches of the $1 \rightarrow 0$ transition of methane stand out clearly, but there are present a number of lines that are not a part of the transition producing this band. Some of the extra lines are part of the emission spectrum of H_2O. The emission spectrum of water became so intense at 3,180 cm^{-1} and at higher frequencies that the methane lines beyond *R*-18 could not be identified. In addition to the water vapor spectrum, many small lines between the main series in the *P*-branch arise from hot bands, but they were not classified and no other bands except the $1 \rightarrow 0$ transition were identified. On increasing the slit width a large number of lines became sufficiently intense for detection and the band extended to longer wavelengths. However, measurements were made on the positions of the lines with a narrow slit and under these conditions the main lines of the *P*- and *R*-branches were overlapped only slightly.

In several scannings of the spectrum the *P*-12 line was the most intense. Calculation shows that this intensity distribution of the rotational lines leads to a temperature of about 1,200° K for the heated gas. This is an average across the inner cone. The molecules on the outer periphery of the inner cone, close to the burning gas, are probably at a somewhat higher temperature and those at the center of the cone may be cooler than 1,200° K.

The present study shows that a molecule used as a fuel for combustion may radiate its own characteristic spectra if it is sufficiently heated before combus-

[1] This work was supported in part by the Geophysics Research Directorate, Air Force Cambridge Research Center.

[2] Figures in brackets indicate the literature references at the end of this paper.

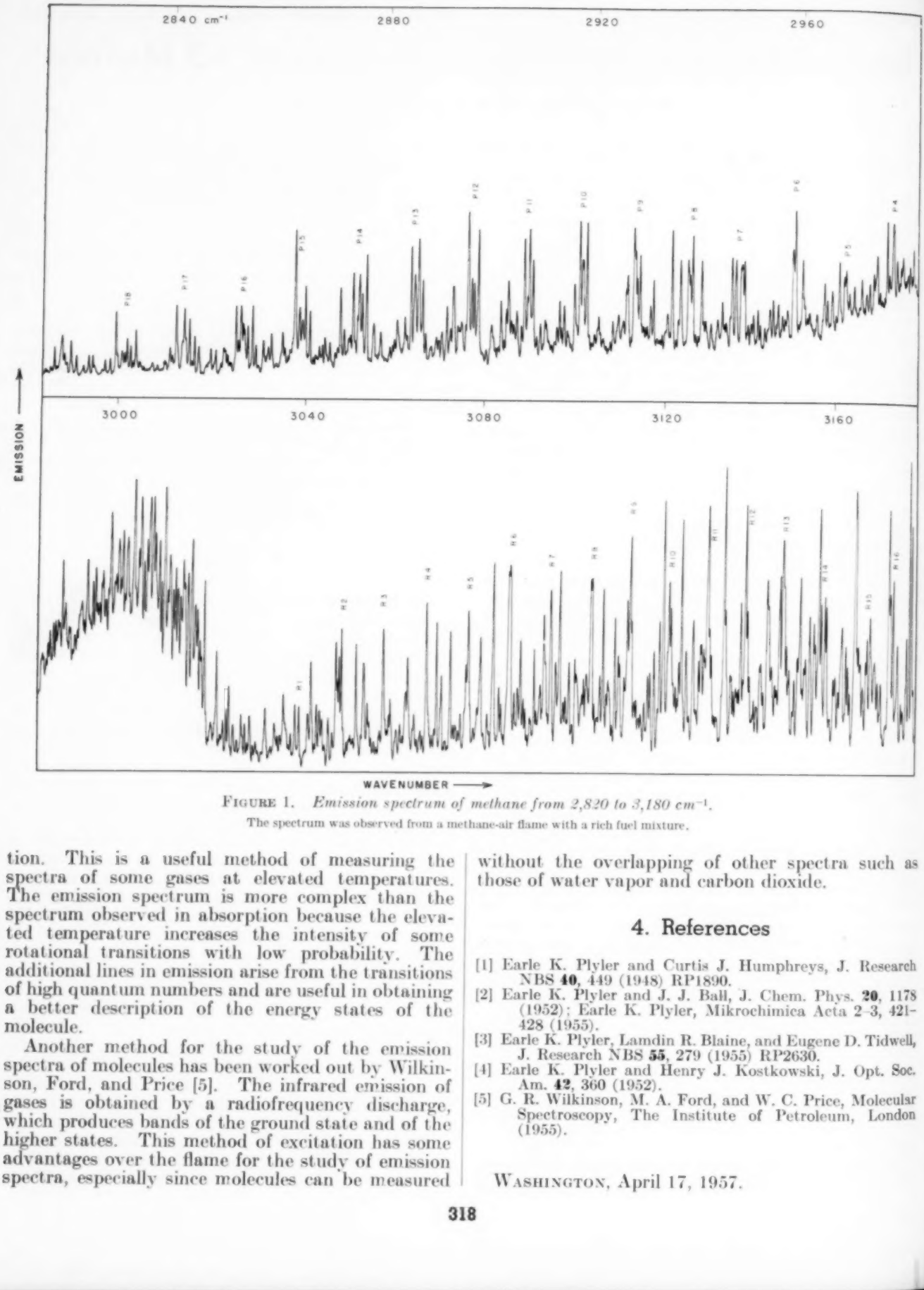

FIGURE 1. *Emission spectrum of methane from 2,820 to 3,180 cm⁻¹.*

The spectrum was observed from a methane-air flame with a rich fuel mixture.

tion. This is a useful method of measuring the spectra of some gases at elevated temperatures. The emission spectrum is more complex than the spectrum observed in absorption because the elevated temperature increases the intensity of some rotational transitions with low probability. The additional lines in emission arise from the transitions of high quantum numbers and are useful in obtaining a better description of the energy states of the molecule.

Another method for the study of the emission spectra of molecules has been worked out by Wilkinson, Ford, and Price [5]. The infrared emission of gases is obtained by a radiofrequency discharge, which produces bands of the ground state and of the higher states. This method of excitation has some advantages over the flame for the study of emission spectra, especially since molecules can be measured without the overlapping of other spectra such as those of water vapor and carbon dioxide.

4. References

[1] Earle K. Plyler and Curtis J. Humphreys, J. Research NBS **40**, 449 (1948) RP1890.

[2] Earle K. Plyler and J. J. Ball, J. Chem. Phys. **20**, 1178 (1952); Earle K. Plyler, Mikrochimica Acta 2–3, 421–428 (1955).

[3] Earle K. Plyler, Lamdin R. Blaine, and Eugene D. Tidwell, J. Research NBS **55**, 279 (1955) RP2630.

[4] Earle K. Plyler and Henry J. Kostkowski, J. Opt. Soc. Am. **42**, 360 (1952).

[5] G. R. Wilkinson, M. A. Ford, and W. C. Price, Molecular Spectroscopy, The Institute of Petroleum, London (1955).

WASHINGTON, April 17, 1957.

Journal of Research of the National Bureau of Standards Vol. 59, No. 5, November 1957 Research Paper 2804

Term Analysis of the First Spectrum of Rhenium (Re I)

P. F. A. Klinkenberg,[1] W. F. Meggers, R. Velasco,[2] and M. A. Catalán[2]

With the aid of new data on wavelengths, intensities, and the Zeeman effect, the structural analysis of the first spectrum of rhenium (Re I) has been extended to include 2,764 lines that are explained as transitions among 282 atomic energy levels. This analysis accounts for 90 percent of the total observed intensity, although only 64 percent of the total number of lines has been classified. From the Zeeman effect, magnetic splitting factors have been derived for 75 percent of the levels, and nearly 40 percent of these have been grouped into designated spectral terms ascribed to specific configurations of electrons. The normal state of neutral Re atoms is $5d^5\,6s^2\,{}^6S_{2\frac{1}{2}}$, and the ionization limit is approximately 63530 kaysers or 7.87 electron volts.

1. Introduction

For a quarter century the atomic emission spectra of rhenium have been investigated intermittently by several researchers, and now a full report on the present status of the analysis and interpretation of the first spectrum of rhenium (Re I) is presented in this paper.

In 1931 the first useful description (2500.59 to 8797.6 A) and partial analysis of Re I was published by Meggers [1],[3] who classified about 500 lines as combinations of 115 atomic energy levels, 24 of which were assigned spectral term symbols. In a second paper [2] the spectrum was extended to longer waves (10639.44 A), and 5 additional metastable energy levels were reported. In 1947 the analysis of Re I was considerably extended by Klinkenberg [3] who used new data in the MIT Wavelength Tables [4], principally between 2500 and 2000 A, and increased the number of levels to 172 and the number of classified lines to 1,171. In a second paper [5], he increased the number of levels to 221, the number of classified lines to 1,624, and identified many terms (of even parity) with electron configurations. Since 1946 Velasco has also worked independently on Re I; in 1949 he [6] pointed out some discrepancies between his levels and Klinkenberg's, and in 1952 he [7] reported measurements between 2000 and 1500 A, revised some levels reported by Meggers [1], classified about 150 lines with 29 new levels, and correlated many spectral terms (even and odd) with electron configurations.

The above mentioned contributions to the interpretation of Re I were all made without the benefit of Zeeman effect; they were based entirely on wave numbers and intensities, and were guided by comparisons with other analyzed spectra, and by quantum theoretical predictions. In order to make further progress with the analysis of Re I it was felt necessary to make new descriptions of the arc and spark spectra of rhenium and to investigate the Zeeman effect.

A new description of the arc and spark spectra of rhenium was supplied by Meggers [8], who used solid electrodes of pure rhenium and obtained wavelengths and intensities for approximately 6,000 lines of which about 4,200 were assigned to Re I. These data, supplemented by those of Velasco [7] from arc spectrograms made by Catalán with a vacuum spectrograph at Princeton University, comprise an improved list of Re I lines ranging in wavelength from about 1700 A in the extreme ultraviolet to 12000 A, the photographic limit in the infrared. This list was used by Klinkenberg in making this final attack on the Re I spectrum; new levels were found and the relative values of all atomic energy levels were recalculated.

The splitting of spectral lines by magnetic fields (Zeeman effect) is extremely useful in analyses of complex spectra because it reveals (by the number of components) the inner-quantum numbers (J) of both levels, and often identifies (by the splitting factors, g) the term types (L) and multiplicities (r). At the Massachusetts Institute of Technology the Bitter magnet [9] was constructed and operated for this purpose, and the MIT wavelength project [10] included Zeeman spectrograms of rhenium. These spectrograms were made just before World War II and during the war years they were in the possession of graduate students who had no opportunity to measure and interpret them. They were finally loaned to the National Bureau of Standards where they were examined and stored. In 1949, through the courtesy of G. R. Harrison, Meggers made greatly superior Zeeman spectrograms of rhenium in the Spectroscopy Laboratory at MIT. These were hand-measured at the Bureau, the wavelengths of Zeeman components were computed, and some resolved patterns gave a start on the analysis of Re II in 1950. At that time the record books were turned over to Catalán and Velasco, who fully exploited the Zeeman data for the determination of J-values and calculation of g-factors for energy levels in the first two spectra of rhenium, Re I and Re II. A preliminary report [11] on these results indicated that g-values had been derived for 164 Re I levels, and for 39 Re II levels. The combined efforts of three research groups in accumulating and analyzing spectral data for Re I have improved and extended the analysis to include 2764 classified lines arising from permitted transitions among 51 low even, 20 high even, and 211 middle odd levels, with g-values evaluated for 75 percent of all levels.

[1] Zeeman Laboratorium, Amsterdam, The Netherlands.
[2] Instituto de Optica, Madrid, Spain.
[3] Figures in brackets indicate the literature references on page 326.

The details concerning established levels and classified lines are presented in tables below, and are followed by a discussion of the experimental and theoretical structure of the Re I spectrum.

2. Atomic Energy Levels of Re I

Before this analysis could proceed it was necessary to convert the newly measured wavelengths to vacuum wave numbers, and for this purpose the Edlén formula for the dispersion of standard air [12] was used as recommended in 1952 by the Joint Commission for Spectroscopy [13]. Then all previously discovered atomic energy levels of Re I were recalculated with the new data so that old and new levels would be consistent. Many new lines in the list could be immediately classified as transitions between known levels, and nearly all levels adopted previously [3,5] were confirmed. The exceptions are $3341_{1/2}$, $3389_{1/2}$, $3481_{5/2}$, $3575_{1/2}$, $3641_{5/2}$, $3801_{1/2}$, $3955_{9/2}$, $5366_{7/2}$, $5626_{1/2}$, and $5829_{11/2}$, four of which had been characterized as questionable before [5]. All the rejected levels belong to the odd group. The analysis was continued with the remaining unclassified Re I lines with the result that 12 low even levels, 3 high even levels, and 46 odd levels could be added to those previously found; they are reported for the first time in this paper. In addition, 11 of the odd levels proposed by Velasco [7], and 8 qualified as provisional by Klinkenberg [5], have been confirmed. The total number of established atomic energy levels resulting from this analysis of the Re I spectrum is now 282 which is the sum of 51 low even, 20 high even, and 211 odd levels. These energy levels are listed in table 1 in which successive columns display an abbreviated designation, the level value (in $K=cm^{-1}$), the inner quantum number J, the magnetic splitting factor g, and the origin of the level. The abridged designation of levels is according to the system adopted by Klinkenberg [3] in 1947: "The odd and high even levels are given by the first 4 digits, the ground levels (which are more widely spaced) by the first 3 digits; however where ambiguities occur an alteration by one or more units of the last figure is allowed. The odd terms are printed in italics".

The J-values have been fixed either by the Zeeman effect or by the combinations, and a number of the J-values in earlier papers have been corrected in this analysis: for level 261 the value 5/2 has been changed to 3/2; for level 278, 5/2 to 3/2; for level *3991*, 9/2 to 11/2; for level *4081*, 3/2 to 1/2; for level *4614*, 3/2 to 1/2; for level *4637*, 11/2 to 9/2; for level *5097*, 3/2 to 5/2; for level *5221*, 3/2? to 5/2; and for level *5482*, 3/2 to 5/2. An important contribution of the Zeeman effect has been the *absolute* determination of the J-values of the levels for lines whose magnetic splitting has been completely observed and resolved. In all previous analyses of the Re I spectrum the J-values were assumed to be those required by theory for the identified terms and the remainder were then derived from the level combinations according to the selection rule that $\Delta J=0$ or ± 1 for permitted transitions.

The Zeeman-effect spectrograms were made with magnetic field intensity of 81,000 oersteds, the field intensity being determined from the splitting of impurity lines of Ag, Cu, Mg, and Ca. Their measurement was complicated by hyperfine structures, and by dissymmetries usually due to partial Paschen-Back effect. These difficulties are illustrated respectively in the two small samples of Re I spectra reproduced in figure 1. The upper strip of spectrum shows the resonance lines ^6S–$^6P^\circ$; the Zeeman components are complex and wide with hyperfine structure except when the magnetic quantum number is 1/2. The lower strip displays a portion of the Re I spectrum in which most Zeeman patterns are so badly perturbed that they cannot be interpreted without great difficulty. When the classification of these lines is examined in table 2 it is obvious that the asymmetrical Zeeman patterns arise from strong Paschen-Back interaction of the closely spaced even levels designated as $5097_{5/2}$, $5098_{7/2}$, $5099_{9/2}$ and $5103_{3/2}$, $5104_{5/2}$, $5105_{1/2}$. Often even fully resolved, symmetrical Zeeman patterns of Re lines are not easy to interpret (apart from J-values) because the splitting factors (g) usually depart more or less from Landé values. In fact these g-factors prove that besides configuration interaction the electron coupling in Re is neither LS nor JJ, but usually intermediate; this will be discussed in connection with spectral term designations. A few of the levels in table 1 have two g-values owing to incomplete observations of the Zeeman patterns; in these cases the second possible value of g is given in parentheses. Magnetic splitting factors, g, are now known for more than 75 percent of all known levels of Re I.

In table 1 the column headed "Origin" shows where levels previously known have been reported for the first time, according to the code explained at the end of that table. This gives a view of the progress from 1931 to 1956 in searching for atomic energy levels in the first spectrum of rhenium. Finally figure 2 gives a survey of the positions of presently known Re I energy levels grouped according to J-values.

3. Spectral Lines of Re I

Attempts to describe the spectra of rhenium, including the magnetic splitting (Zeeman effect), are plagued by relatively coarse hyperfine structure exhibited by most of the lines, many of which have 6 components (see fig. 1). This makes it difficult to estimate relative intensities and in some cases hyperfine structure is easily mistaken for fine structure. For lines that show flag patterns a mean wavelength was recorded, but when hyperfine components appear as two lines or groups of lines it is impossible to distinguish them from close fine structures. A good example of the latter are the two close levels 27384.40 and 27385.20 K, both having $J=½$, which are retained in tables 1 and 2 as individual atomic energy levels although there is evidence that they are hyperfine levels. Another example is $44703.37_{5/2}$ whose combinations are

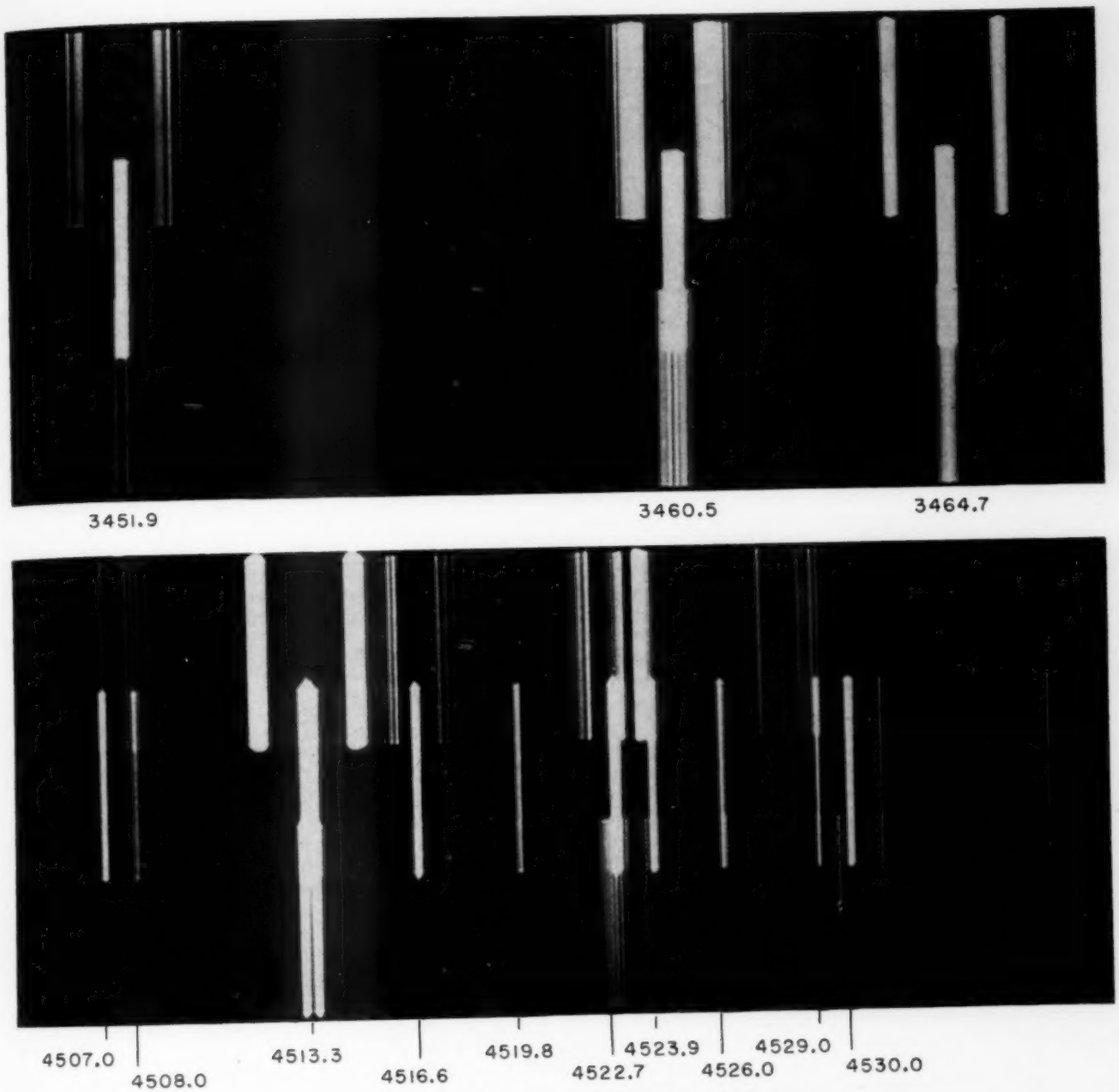

FIGURE 1. *Zeeman patterns of* Re I *lines at 81,000 oersteds.*

Upper: σ components—perpendicular polarization.
Center: Arc spectrum without magnetic field.
Lower: π components—parallel polarization.
Numbers: Wavelengths of Re I lines in angstroms.

usually observed as widened doublets which possibly represent perturbed or mutilated hyperfine multiplets (see note 28 at end of table 2). Several combinations of level $15165.89_{1/2}$ are double (4394, 4417, 4565 A) but this seems to be caused by the involved odd levels, because most combinations of $151_{1/2}$ are single (see note 24 at end of table 2). As compensation for the complication introduced by hyperfine structure it may be said that the width and shading of flag patterns confirm this analysis qualitatively and have aided in the assignment of levels to electron configurations and term groups. Detailed proof of this statement is omitted in this paper which deals primarily with fine structure and therefore ignores hyperfine structure (excepting the complications mentioned above). Information about the resolution, width, and shading of flag patterns in rhenium spectra is given in Meggers' recent description of these spectra [8] which provided most of the material for this analysis.

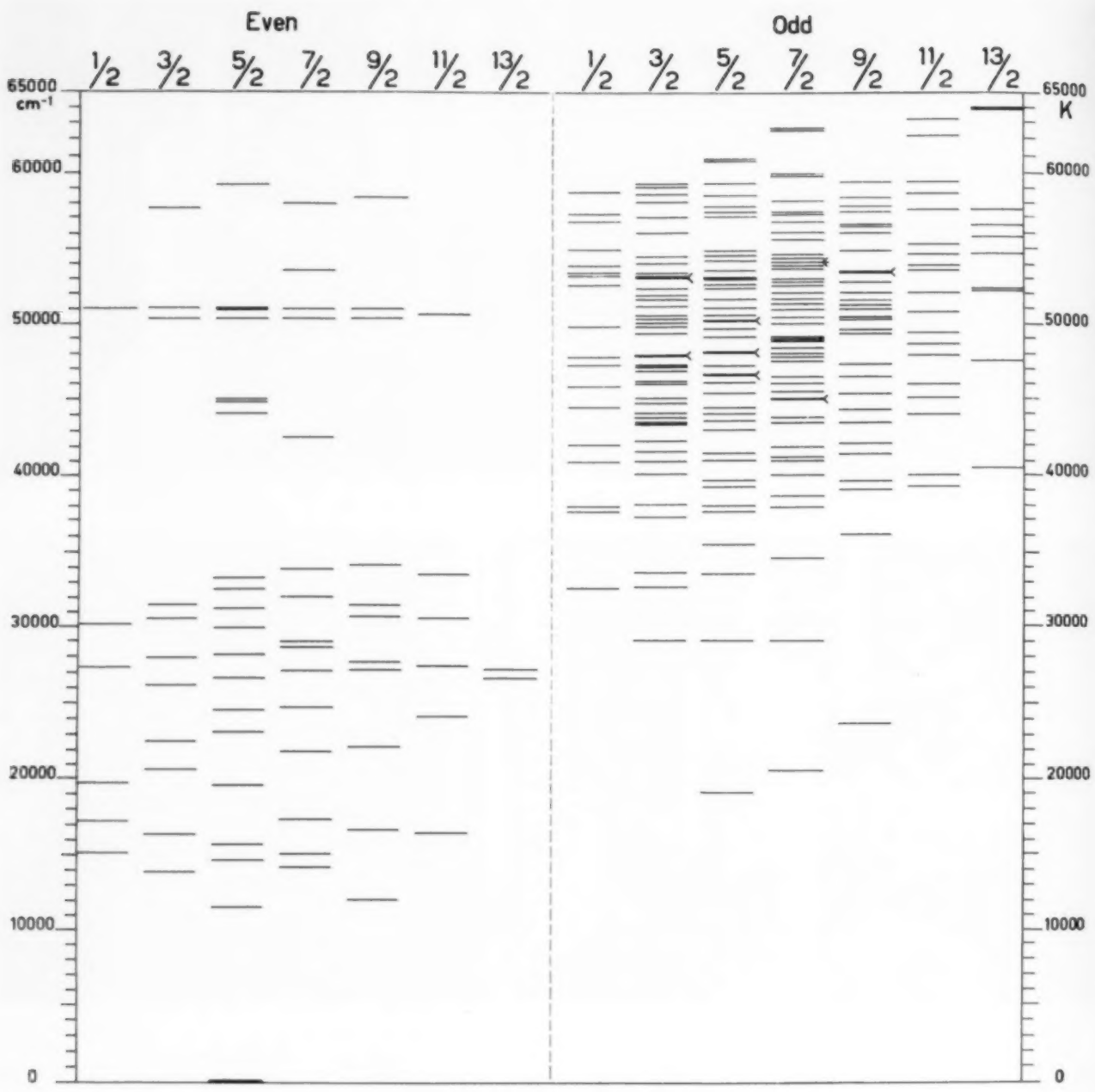

FIGURE 2. *Energy-level diagram of* Re I.

Abscissae: *J*-values
Ordinates: kaysers, 1 K = 1 cm⁻¹

Table 2 contains all relevant data on the classified lines of Re I, including estimated relative intensities, measured wavelengths, derived vacuum wave numbers, observed Zeeman patterns, transitions between designated atomic energy levels, differences between wave numbers derived from measured wavelengths and those calculated from atomic energy levels, and notes that are appended to the table.

In table 2, column 4, the observed displacements of magnetic components are given in Lorentz units, the π components being inclosed by parentheses and followed by the σ components. When there are more than one component of either type the strongest is shown in bold face. Many unresolved Zeeman patterns are accompanied by letters A, B, C, or D which were adopted for conveniently indicating standard types according to Back and Landé [14]. The letter A means that the strongest π components have the greatest displacement whereas the displacement of the strongest σ components is the

average of all. B means that the strongest π components are least and the strongest σ components most displaced. C indicates that the strongest π and σ are both least displaced. The letter D applies to relatively weak lines for which no σ components were observed, so that it is impossible to distinguish between types B and C. A dagger (†) means that the pattern is unsymmetrical, and an asterisk (*) that the observed Zeeman pattern belongs to a Re II line. P-B indicates that a perturbation of Paschen-Back type has been observed.

The total number of classified lines of Re I in the region 1700 to 12000 A is now 2,764. Of these 116 are doubly and 5 are trebly classified, because the resolving power was inadequate to separate them. There are 6 cases where two observed lines have been classified as one transition, because the doubling is believed to be caused by perturbed hyperfine structures. Thus for some purposes the employed resolving power was too small and for others it was too large. Some of the complications that arose on account of hyperfine structure were mentioned in the preceding section.

A few lines classified as Re I were observed only on spark spectrograms measured in the Zeeman laboratory. Some of these have also been classified as Re II lines, and in these complex spectra it is certainly probable that occasionally Re I and Re II lines coincide within the limits of spectrographic resolving power employed. In any case such lines appearing in table 2 represent permitted transitions between established energy levels of Re I within reasonable limits of tolerance for these transitions.

Excepting lines of very short wavelengths, near 2000 A for which an error of 0.01 A corresponds to 0.25 K, the difference between observed and calculated wave number (O–C in table 2) of classified Re I lines rarely exceeds 0.3 K. For 563 lines in table 2 this difference is naught; for the remainder it is $\pm 0.06_5$ K and for the total number the average difference is ± 0.05 K. Recalling that on account of hyperfine structure many Re lines have widths of the order of 2 K, this small average departure of calculated from observed wave number of classified Re I must be regarded as satisfactory; it gives assurance that the mean wavelength of the wide lines is very near the actual center of gravity.

In the recent description of the arc spectrum of rhenium by Meggers [8] there are 4,143 lines that may be ascribed to Re I. Of these 2,660 are classified in this analysis (table 2). Although this number of classified Re I lines is only 64 percent of the total number it accounts for 90 percent of the total observed intensity. The remaining unclassified lines, with few exceptions, are of low intensity, between 40 and 1. This is obvious from table 3 which lists all the unclassified Re I lines having intensity 50 or more. Only two of these are visible; the remainder are all in the ultraviolet short of 3000 A. This suggests that some high energy levels of Re I are still unknown, and that further progress in the analysis of this spectrum might be made if an improved description in the extreme ultraviolet could be obtained.

4. Interpretation of the Re I Levels

Previous interpretations [1, 2, 3, 5, 6, 7] of certain Re I levels were made without the aid of Zeeman effect; they were guided by the simple interval and intensity rules of multiplet structure and by comparison with the known terms of Mn I. Now despite the large number of observed Zeeman patterns and computed g-factors, there are still only relatively few Re I levels that can be interpreted with certainty; 61 percent (171 out of 282) of the established levels must be characterized as "miscellaneous". However, compared with the earlier identifications, definite progress has resulted from the Zeeman-effect data despite many departures of g-factors from the Landé values associated with conventional spectral-term notation. We are pleased to report that most of the previous interpretations have been confirmed by the g-factors found, even those of $d^5\,s^2\,{}^4P$ which had been questioned [6]. The Re I levels, terms, and interpretations are displayed in table 4.

Because manganese, technetium, and rhenium are homologous chemical elements their spectra are bound to show similarities. Indeed, such similarities, when first discovered in Re and Tc, were regarded as proof that these elements are really homologs of Mn. In each case the spectra are highly complex because there are 7 optical electrons, and spectral terms of 4 different multiplicities (doublets, quartets, sextets, and octets) occur. Because the d-shell of electrons is usually half (or more) filled the terms are partly regular, partly inverted, and sometimes partially inverted. The principal differences between the three spectra, in general, are exhibited by larger term intervals for heavier atoms, and by the relative stability of various configurations of electrons.

In general, the structure of the low even system of Re I is comparable to that of Mn I [15]. The relative positions of the Re I lowest terms from $d^5\,s^2$ and $d^6\,s$ are very similar to those of Mn I, and quite different from those of Tc I [16]. However, in Re I the terms from $d^5\,s^2$ are somewhat better known than in Mn I. This is due partly to the fact that intersystem combinations are much stronger in Re I because of departures from LS coupling, so that many doublet levels could be found in Re I that were unknown in Mn I. The second reason is that the mutual electrostatic interactions in Re I are rather different from those in Mn I. This is immediately obvious from the fact that in the $d^5\,s^2$ configuration ${}^4P$ is below ${}^4G$ in Re I, whereas the opposite obtains in Mn I. When taking this into account one finds from theoretical consideration [17] that the doublet terms should be depressed with respect to the quartets in Re I as compared with Mn I. An analogous situation exists in the spectra of W I versus Cr I.

The same $d^6\,s$ terms are found in Re I and Mn I excepting two doublets above 38000 K in the latter. The new 13/2 level 270 in Re I has much stronger combinations than the previously found 13/2 level 263 that was interpreted [5] as ${}^4H$. This, and the fact that the new level had a g-value much nearer to the Landé value for ${}^4H_{13/2}$ led us to identify level

270 as $(5d^6\,6s)^4H_{13/2}$. This is certainly the most plausible interpretation because there are only three 13/2 levels anticipated in the low even system, namely $d^5\,s^2\,^2I_{13/2}$, $d^6\,s\,^4H_{13/2}$, and $d^6\,s\,^2I_{13/2}$. The lower level 263 is readily explained as the first ^2I whereas the other ^2I presumably lies too high to be detected. In view of recent progress with the analysis of Mn I [15] the earlier interpretation [5] of four Re I levels above 22000 K as $5d^7\,^4F$ cannot be maintained; it is concluded that no d^7 levels have been found in Re I. In fact all the known low even levels of Re I have been assigned to $d^5\,s^2$ or $d^6\,s$. Besides the identifications mentioned above, additional assignments of conventional term symbols have been suggested by R. E. Trees, who calculated approximately the relative positions of known and anticipated spectral terms; these calculations will be reported in a separate paper by Trees.

A brief discussion of the Re I level $273_{1/2}$ seems justified because of the trouble caused by hyperfine structure. At first two levels were detected at nearly the same value, viz., 27384.40 and 27385.20 K. Generally these combined with the same odd levels, thus yielding 10 pairs of very close lines of comparable intensities. In three more cases only a somewhat broadened line was observed with a wave number intermediate between the calculated values. In some other cases only the transition to 273′ or 273″ was present and because 273″ had two combinations with odd 5/2 levels while 273′ had none, the latter was regarded as a 1/2 level and the former as a 3/2, with the possible interpretations $d^6\,s\,^4P_{1/2}$ and $d^5\,s^2\,^4D_{3/2}$. All the lines involved were relatively weak. For 273″ no Zeeman-effect measurements were available, but for 273′ there was a measurement of two π components of 4369.64 A ($273'_{1/2}$–$5026_{3/2}$). This splitting pointed to a g-value of either 2.396 or 0.072, the first being compatible with the interpretation of 273′ as $^4P_{1/2}$ and the second with $^4D_{1/2}$. Upon remeasurement of the Zeeman spectrogram the two π components were found to be symmetrical around the wavelength 4369.70 A, just the average of the wavelengths 4369.64 and 4369.77 A reported [8] for Re I. Hence we must conclude that these lines are hyperfine structure components of one and the same transition and that 273′ and 273″ are hyperfine structure sublevels of one electronic level having $J=1/2$. In tables 1 and 2, it was found practical to retain the notation 273′ and 273″, but in table 4 a single level 27384.80 K is interpreted as $d^6\,s\,^4D_{1/2}$.

The departures of the observed g-factors from their Landé values are often very large but in opposite directions, so that the g-sums are not very irregular even when some levels of the same J-value are not known. There are a few instances of g-sharing which suggest a strong mutual perturbation of two levels with exclusion of the rest. The most conspicuous example is $d^5\,s^2\,^4G_{7/2}$ (with $\Delta g=+0.17$) and $d^6\,s\,^4D_{7/2}$ (with $\Delta g=-0.17$). Furthermore, we have the two levels $d^6\,s\,^6D_{1/2}$ ($\Delta g=-0.81$) and $(d^6\,s)^4D_{1/2}$ ($\Delta g=+0.98$). Also two levels with $J=13/2$ have opposite but equal g-departures ($d^5\,s^2\,^2I_{13/2}$ has $\Delta g=+0.02$ and $d^6\,s\,^4H_{13/2}$ has $\Delta g=-0.02$), so that the remaining unknown 13/2 level ($d^6\,s\,^2I_{13/2}$) should have a normal g-factor. Attention was called [11] to large negative deviations of g-values for Re I terms that converge to $d^5\,s\,^5S_2$ in Re II, which lacks 0.29 Lorentz unit from Landé value for that term. The present data are insufficient to test the sum rule for g-values of any configuration in Re I.

The first identifications in the low even system served as a basis for the interpretation of a number of odd levels by means of the observed intensities of the combinations. When g-values became available these identifications could be extended, and verified by comparison with the parent structure of Re II. For example the low $^6G^\circ$ from $d^5\,s(^5G)6p$ of Re I was not expected where found, but it is confirmed by the low ^5G from $d^5\,s$ found in Re II by Meggers, Catalán, and Sales [18].

From comparison of the transitions $d^4\,s\,^6D_{9/2}$–$d^4\,p\,^6F^\circ_{11/2}$ in V I, Nb I, and Ta I, and $(d^6\,s)^6D_{9/2}$–$d^6\,p\,^6F^\circ_{11/2}$ in Mn I and Tc I, it could be inferred that the corresponding transition in Re I should have a wave number of about 35000 K. In agreement herewith $d^6\,p\,^6F^\circ_{11/2}$ has been located in Re I at 45082.63 K, and the line in question at 33328.06 K. Beyond completing this $^6F^\circ$ term no further identifications in the $d^6\,p$ configuration of Re I have been attempted. Excepting $d^5\,sp\,^8P^\circ$ and $^6P^\circ$ the low odd terms of Re I belong to $d^4\,s^2p$. The terms ^6D and ^6F derived from the parent term $d^4\,s^2\,^5D$ of Re II (which is about 14000 K above the ground state $d^5(^6S)s\,^7S$) have been identified. In accordance with this assignment the levels with small J-values are the lower ones, whereas the terms derived from $d^6\,^5D$ should be inverted, as they are.

Seventeen high even levels of Re I could readily be interpreted in connection with the known low Re II levels [18]. The previous interpretation [3] of level $5097_{3/2}$ as $d^5\,s(^7S)d\,^6D$ has been abandoned. The levels $5103_{3/2}$ and $5104_{5/2}$ turned out to belong to one multiple term because they show partial Paschen-Back effects of transitions to the same odd level. The grouping of nearby levels with proper J-values led to recognition of the partially inverted term designated $e\,^6D$. Both $e\,^6D$ and $e\,^8D$ have small intervals because their series limit is a ^7S in Re II, and the available g-factors confirm the designations. The former interpretation [5] of level $5766_{3/2}$ was changed because the lower ^5D in Re II was assigned [18] to $d^4\,s^2$ instead of d^6. In the course of this analysis of Re I we succeeded in supplementing this 3/2 level with 5/2, 7/2, and 9/2 to form the term designated as $f\,^6D$, with only the 1/2 level still lacking. These interpretations are supported by the observed intensities of the transitions to the odd levels which are displayed in figure 3, where the observed intensity is roughly represented by the size of the black circle, and shaded circles indicate outstanding intensities. The most striking feature of figure 3 is that the levels of $d^5\,s(^5D)s\,^6D$ combine much more strongly with the higher odd ^6D than with the lower one. The explanation is that the former transitions (to $d^5\,s(^5P)p\,^6D$) require only one electron jump (p to s), whereas the latter transitions (to $d^4\,s^2(^5D)p\,^6D$)

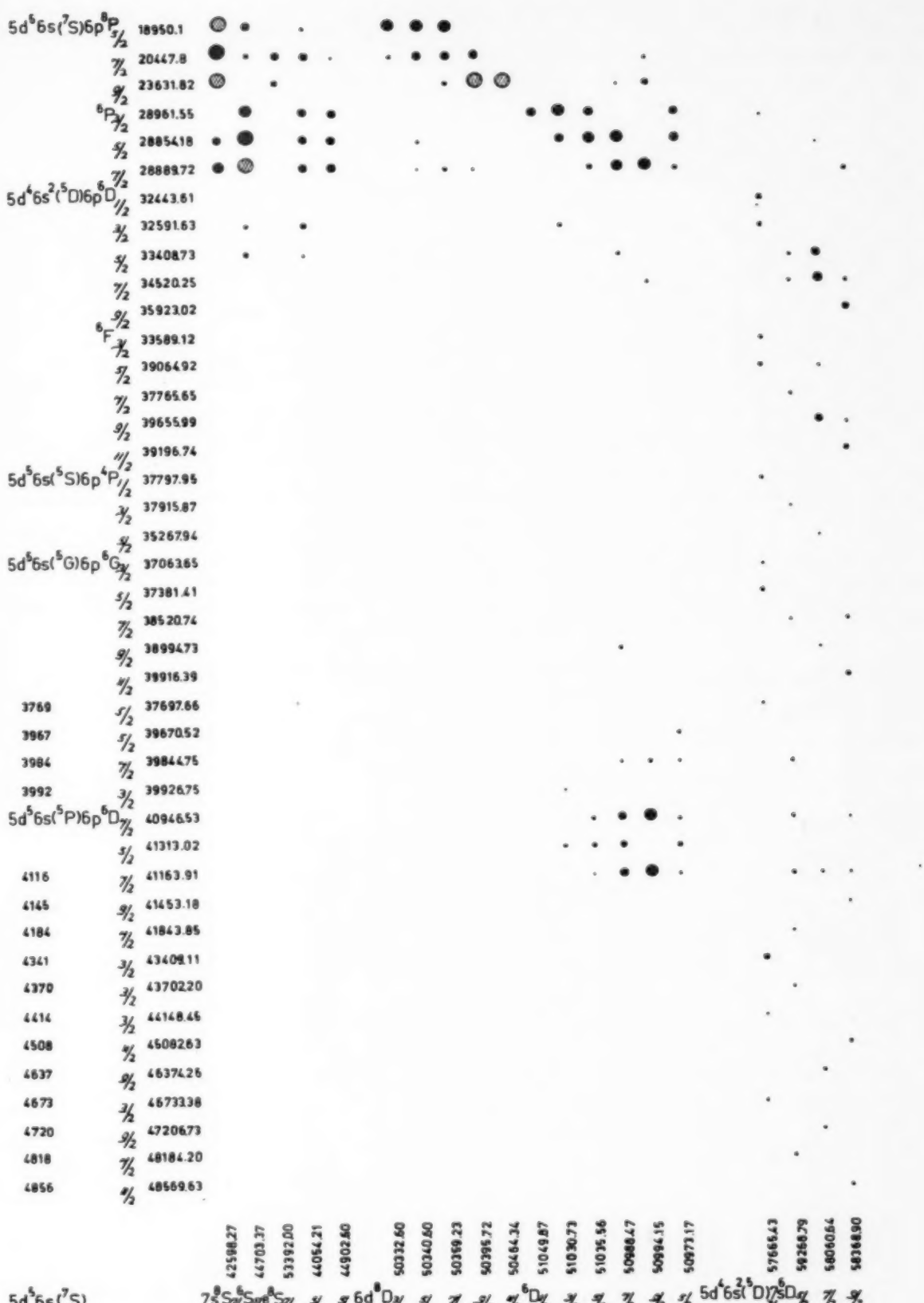

FIGURE 3. *Line intensities of transitions between* Re I *levels.*

involve a simultaneous jump of two electrons (p to s and s to d).

In the high even group of Re I there are two 5/2 levels the parent terms of which should be very low in Re II, but are still unknown. The Re I levels in question have values 44054.21 and 44902.60 K; they are well established (see fig. 3) but without g-factors. These levels suggest the existence of Re II levels between 0 and 13777 K, for which supposition there is no further evidence except that $d^6\ ^5D$ is still unknown. Another unidentified high even level in Re I is at 50973.17 K, but in this energy range there are more possibilities, and this lone level is left as an invitation to further analysis and interpretation.

In his first paper Meggers [1] derived from two ^8S terms in series a spectroscopic convergence limit of 63530 K for Re I. In his second paper Klinkenberg [5] derived from two ^6S terms a Rydberg-series limit of 65560 K, which he regarded as an upper limit because the proper correction is unknown. If the Rydberg denominator deviates only 0.04 from unity this limit would be reduced to 63000 K. Because there is at present no further information on spectral series in Re I the original limit is accepted, and the ionization potential remains near 7.87 electron volts.

The present description and interpretation of Re I has been a long and difficult task; it is still far from satisfactory or complete but may require additional experimental and theoretical study before it can be continued. This analysis has been pushed to its present state primarily so that table 4 could be reproduced in Volume III of Atomic Energy Levels [19], where detailed comparisons with other tables may give inspiration for further progress in the quantum interpretation of complex atomic spectra.

5. References

[1] W. F. Meggers, BS J. Research **6,** 1027 (1931) RP322.
[2] W. F. Meggers, BS J. Research **10,** 757 (1933) RP564.
[3] P. F. A. Klinkenberg, Physica **13,** 581 (1947).
[4] G. R. Harrison, MIT Wavelength Tables (John Wiley & Sons, Inc., New York, N. Y., 1939).
[5] P. F. A. Klinkenberg, Physica **14,** 269 (1948).
[6] R. Velasco, Anales real soc. espan. fis. y quim. [A] **45,** 215 (1949).
[7] R. Velasco, Anales real soc. espan. fis. y quim. [A] **48,** 55 (1952).
[8] W. F. Meggers, J. Research NBS, **49,** 187 (1952) RP2355.
[9] G. R. Harrison and F. Bitter, Phys. Rev. **57,** 15 (1940).
[10] G. R. Harrison, Repts. Progr. in Phys. **8,** 212 (1941).
[11] W. F. Meggers, M. A. Catalán, and R. Velasco, J. Opt. Soc. Am. **42,** 288 (1952).
[12] B. Edlén, J. Opt. Soc. Am. **43,** 339 (1953).
[13] Transactions of the Joint Commission for Spectroscopy, J. Opt. Soc. Am. **43,** 412 (1953).
[14] E. Back and A. Landé, Zeeman effect und Multiplet-struktur der Spektrallinien, 168 (Springer, Berlin, 1925).
[15] C. E. Moore, Atomic Energy Levels II, 27–32, NBS Circ. 467 (1952).
[16] W. F. Meggers, J. Research NBS **47,** 7 (1951) RP2221.
[17] O. Laporte and J. R. Platt, Phys. Rev. **61,** 305 (1942).
[18] W. F. Meggers, M. A. Catalán, and M. Sales (in press).
[19] C. E. Moore, Atomic Energy Levels, III, NBS Circ. 467 (in press).

TABLE 1. *Energy levels of the* Re *atom*

Designation	Value	J	g	Origin	Designation	Value	J	g	Origin
				LOW EVEN GROUP					
0	0.00	5/2	1.950	M 31	266	26661.43	5/2	1.32	K 47
115	11583.96	5/2	1.278	M 31	270	27130.14	13/2	1.20$_8$	------
117	11754.52	9/2	1.545	M 31	271	27141.13	7/2	1.34	M 33
138	13826.12	3/2	1.485	M 31	272	27161.35	9/2	----------	K 47
142	14216.86	7/2	1.567	M 31	273	27243.88	11/2	1.18	K 48
146	14621.46	5/2	1.151	M 31	273′	27384.40	1/2	2.396 (0.072)	------
150	15058.19	7/2	1.153	M 31	273″	27385.20	1/2	----------	------
151	15165.89	1/2	2.368	K 47	275	27514.31	9/2	1.13	K 47
157	15770.42	5/2	1.309	M 31	278	27827.65	3/2	0.888	K 48
163	16307.15	11/2	1.242	M 31	280	28030.32	5/2	1.12	K 48
164	16327.51	3/2	1.706	M 31	285	28542.13	7/2	----------	K 48
166	16619.28	9/2	1.175	M 31	288	28809.87	7/2	0.93 (1.44)	------
172	17238.30	1/2	2.521	M 31	298	29800.38	5/2	~1.17	K 48
173	17330.82	7/2	1.255	M 31	301	30131.57	1/2	----------	K 48
194	19457.89	5/2	1.361	M 33	304	30526.60	3/2	----------	------
197	19757.91	1/2	0.983	K 47	305	30559.91	11/2	1.07	------
204	20481.73	3/2	1.451	K 47	306	30645.33	9/2	----------	K 48
217	21775.40	7/2	1.135	M 31	311	31186.08	5/2	1.17?	------
221	22160.04	9/2	1.198	K 47	313	31399.30	9/2	----------	K 48
224	22422.83	3/2	0.781	K 47	314	31460.62	3/2	----------	K 48
231	23154.81	5/2	1.189	M 33	319	31982.99	7/2	----------	K 48
239	23956.00	11/2	0.995	K 47	324	32435.14	5/2	----------	------
244	24425.40	5/2	1.067	K 47	332	33281.65	5/2	----------	------
247	24724.22	7/2	1.03	M 33	333	33317.57	11/2	----------	------
261	26131.57	3/2	0.650	M 33	338	33823.66	7/2	----------	------
263	26348.96	13/2	1.100	K 48	341	34194.27	9/2	----------	------

TABLE 1. *Energy levels of the* Re *atom*—Continued

Designation	Value	J	g	Origin	Designation	Value	J	g	Origin
				HIGH EVEN GROUP					
4259	42598. 27	7/2	1. 957	M 31	5098	50988. 47	7/2	1. 558	M 31
4405	44054. 21	5/2	----------	M 31	5099	50994. 15	9/2	1. 548	M 31
4470	44703. 37	5/2	1. 866	M 31	5103	51030. 73	3/2	----------	M 31
4491	44902. 60	5/2	----------	M 31	5104	51035. 56	5/2	1. 546	M 31
5033	50332. 60	3/2	----------	M 31	5105	51049. 87	1/2	----------	C 53
5034	50340. 62	5/2	2. 027	M 31	5339	53392. 00	7/2	----------	M 31
5035	50359. 23	7/2	1. 820	M 31	5766	57665. 43	3/2	----------	K 48
5039	50395. 72	9/2	1. 690	M 31	5806	58060. 64	7/2	----------	------
5047	50464. 34	11/2	1. 629	M 31	5836	58368. 90	9/2	----------	------
5097	50973. 17	5/2	1. 489	M 31	5926	59268. 79	5/2	----------	------
				ODD GROUP					
1895	*18950. 1*	5/2	2. 274	M 31	*4394*	*43949. 98*	5/2	1. 385	K 47
2044	*20447. 8*	7/2	1. 926	M 31	*4399*	*43996. 30*	11/2	1. 26	K 47
2363	*23631. 82*	9/2	1. 768	M 31	*4414*	*44148. 45*	3/2	1. 573	K 47
2885	*28854. 18*	5/2	1. 871	M 31	*4422*	*44224. 58*	9/2	1. 244	M 31
2889	*28889. 72*	7/2	1. 709	M 31	*4430*	*44308. 73*	5/2	1. 223	M 31
2896	*28961. 55*	3/2	2. 333	M 31	*4441*	*44416. 33*	1/2	0. 15	K 47
3244	*32443. 61*	1/2	----------	M 31	*4472*	*44720. 09*	3/2	1. 330	K 47
3259	*32591. 63*	3/2	1. 762	M 31	*4490*	*44901. 15*	7/2	1. 253	M 31
3340	*33408. 73*	5/2	1. 500	M 31	*4494*	*44946. 12*	7/2	0. 905	K 47
3358	*33589. 12*	3/2	2. 335	M 31	*4508*	*45082. 63*	11/2	1. 40	M 31
3452	*34520. 25*	7/2	1. 454	M 31	*4512*	*45121. 81*	3/2	0. 674	K 47
3526	*35267. 94*	5/2	1. 385	M 31	*4533*	*45332. 03*	5/2	1. 088	K 48
3592	*35923. 02*	9/2	1. 440	M 31	*4534*	*45343. 57*	9/2	1. 131	M 31
3706	*37063. 65*	3/2	0. 626	M 31	*4546*	*45462. 83*	7/2	1. 300	M 31
3738	*37381. 41*	5/2	0. 990	M 31	*4581*	*45817. 26*	1/2	2. 197	
3769	*37697. 66*	5/2	1. 219	M 31	*4587*	*45876. 34*	3/2	1. 384	K 47
3776	*37765. 65*	7/2	1. 335	M 31	*4590*	*45904. 25*	11/2	1. 175	K 47
3779	*37797. 95*	1/2	2. 620	------	*4593*	*45937. 18*	7/2	1. 298	M 31
3791	*37915. 87*	3/2	1. 495	M 31	*4611*	*46112. 24*	5/2	1. 405	M 31
3852	*38520. 74*	7/2	1. 216	M 31	*4614*	*46141. 11*	1/2	0. 716	M 31
3899	*38994. 73*	9/2	1. 25	M 31	*4635*	*46352. 99*	7/2	1. 271	M 31
3906	*39064. 92*	5/2	1. 335	M 31	*4637*	*46374. 25*	9/2	1. 341	M 31
3919	*39196. 74*	11/2	1. 405	M 31	*4650*	*46509. 40*	5/2	1. 371	M 31
3965	*39655. 99*	9/2	1. 444	M 31	*4664*	*46649. 42*	5/2	1. 334	M 31
3967	*39670. 52*	5/2	1. 107	M 31	*4673*	*46733. 38*	3/2	1. 858	K 47
3984	*39844. 75*	7/2	1. 223	M 31	*4700*	*47004. 34*	3/2	1. 285	M 31
3991	*39916. 39*	11/2	1. 314	M 31	*4710*	*47101. 61*	5/2	0. 893	K 47
3992	*39926. 75*	3/2	0. 745	K 47	*4717*	*47172. 1*	3/2		
4049	*40493. 34*	13/2	1. 364	------	*4718*	*47172. 9*	1/2	2. 215	
					4720	*47205. 73*	9/2	1. 106	M 31
4080	*40808. 85*	3/2	1. 351	M 31					
4081	*40810. 17*	1/2	----------	M 31	*4735*	*47358. 36*	7/2	1. 151	K 47
4082	*40821. 83*	5/2	1. 126	M 31	*4750*	*47506. 79*	13/2	1. 26	K 48
4094	*40946. 53*	7/2	1. 534	M 31	*4765*	*47664. 74*	1/2	1. 50	
4116	*41163. 91*	7/2	1. 325	M 31	*4766*	*47669. 01*	7/2	1. 196	M 31
					4770	*47703. 78*	3/2	1. 443	K 48
4131	*41313. 02*	5/2	1. 278	M 31	*4777*	*47779. 91*	3/2	1. 362	K 47
4145	*41453. 18*	9/2	1. 372	M 31	*4785*	*47859. 93*	11/2	1. 20	M 31
4155	*41557. 08*	3/2	1. 655	M 31	*4789*	*47899. 22*	5/2	1. 217	M 31
4184	*41843. 85*	7/2	1. 190	M 31	*4793*	*47932. 55*	7/2	1. 31	M 31
4199	*41991. 56*	1/2	0. 61	K 48	*4797*	*47970. 82*	5/2	1. 169	M 31
4214	*42140. 06*	9/2	1. 249	M 31	*4818*	*48184. 20*	7/2	1. 252	M 31
4225	*42254. 19*	3/2	1. 578	K 47	*4856*	*48569. 63*	11/2	1. 27	M 31
4304	*43044. 02*	5/2	1. 449	K 47	*4878*	*48786. 35*	7/2	1. 53	K 47
4334	*43341. 85*	3/2	0. 975	M 31	*4885*	*48857. 60*	7/2		K 47
4340	*43407. 87*	7/2	1. 368	M 31	*4902*	*49022. 77*	5/2	1. 495	M 31
4341	*43409. 11*	3/2	----------	M 31	*4903*	*49027. 85*	7/2	1. 499	M 31
4345	*43453. 30*	9/2	1. 336	M 31	*4917*	*49170. 76*	9/2	1. 135	K 47
4356	*43569. 36*	5/2	1. 504	M 31	*4925*	*49250. 02*	3/2	1. 263	K 47
4370	*43702. 20*	3/2	1. 962	M 31	*4928*	*49286. 07*	11/2	1. 075	
4381	*43815. 01*	7/2	1. 348	K 47	*4954*	*49540. 96*	5/2		K 48

TABLE 1. *Energy levels of the* Re *atom*—Continued

Designation	Value	J	g	Origin	Designation	Value	J	g	Origin
ODD GROUP—continued									
4957	*49573. 11*	5/2	1. 344	K 47	*5401*	*54018. 19*	7/2	0. 723 (1. 895)	K 48
4958	*49582. 61*	9/2	1. 058	K 47	*5408*	*54086. 67*	7/2	1. 22	K 48
4966	*49667. 25*	3/2	1. 272	K 47	*5417*	*54177. 25*	7/2	1. 273	K 47
4985	*49859. 53*	1/2	0. 410		*5426*	*54268. 18*	5/2	1. 290	
4986	*49863. 22*	7/2	1. 175	K 47	*5440*	*54409. 61*	5/2	1. 069	K 48
4989	*49895. 57*	3/2	1. 989	K 47	*5446*	*54467. 40*	3/2	1. 361	
5011	*50110. 28*	5/2	1. 765	M 31	*5451*	*54513. 84*	7/2		K 47
5015	*50158. 87*	5/2	1. 422	K 47	*5455*	*54554. 61*	11/2		K 48
5019	*50196. 94*	9/2	1. 345	K 48	*5472*	*54729. 52*	13/2		
5026	*50263. 22*	3/2	1. 234		*5481*	*54813. 12*	9/2	1. 185 (1. 949)	K 47
5031	*50310. 70*	7/2	1. 170		*5482*	*54823. 02*	5/2	1. 183	K 48
5040	*50401. 01*	9/2	1. 055	K 47	*5496*	*54968. 85*	1/2	1. 314	
5046	*50463. 80*	5/2	1. 144	K 47	*5522*	*55223. 85*	11/2	1. 149	
5057	*50571. 02*	3/2	0. 935	K 48	*5545*	*55454. 48*	7/2	1. 17	
5066	*50663. 51*	11/2	1. 220	K 48	*5577*	*55776. 51*	13/2	1. 056	
5086	*50869. 00*	7/2	1. 240	K 48	*5589*	*55901. 20*	7/2	1. 22	
5093	*50934. 18*	5/2	1. 385	M 31	*5590*	*55902. 01*	3/2	0. 447 (1. 115)	
5102	*51027. 96*	9/2		K 47	*5591*	*55912. 42*	9/2	1. 06	K 48
5118	*51183. 00*	3/2	1. 456	V 52	*5630*	*56307. 97*	9/2		
5119	*51193. 49*	9/2		K 48	*5641*	*56411. 22*	9/2		
5122	*51229. 64*	7/2	1. 231	K 47	*5645*	*56451. 87*	1/2	1. 287	
5147	*51477. 15*	5/2	0. 97	K 47	*5652*	*56523. 41*	13/2		
5148	*51486. 29*	9/2	1. 20	K 48	*5669*	*56699. 41*	7/2	1. 25	V 52
5157	*51578. 05*	3/2		K 48	*5682*	*56822. 75*	5/2		V 52
5159	*51590. 08*	5/2	1. 02	K 48	*5686*	*56866. 06*	3/2	1. 099	
5164	*51647. 82*	7/2	1. 139	K 47	*5707*	*57073. 31*	1/2	0. 94	
5187	*51874. 43*	3/2	1. 29	V 52	*5709*	*57090. 29*	7/2		
5194	*51945. 94*	11/2		K 48	*5717*	*57172. 70*	7/2	1. 19	
5195	*51955. 02*	7/2	1. 200	K 47	*5728*	*57280. 86*	9/2	1. 19	K 48
5200	*52001. 37*	9/2	1. 357	K 47	*5737*	*57371. 75*	7/2		K 47
5212	*52122. 35*	13/2	1. 17	K 48	*5739*	*57391. 44*	11/2	1. 30	K 48
5221	*52218. 11*	5/2	1. 208	K 47	*5745*	*57452. 83*	13/2		K 48
5222	*52227. 20*	13/2		K 48	*5752*	*57524. 31*	5/2	~1. 40	
5227	*52278. 28*	3/2	1. 422	K 47	*5765*	*57656. 85*	9/2	1. 19	K 47
5237	*52373. 12*	7/2		K 47	*5805*	*58050. 58*	3/2	1. 111	
5246	*52469. 45*	1/2	1. 315		*5826*	*58260. 03*	7/2	1. 43	V 52
5247	*52472. 31*	5/2		V 52	*5827*	*58279. 31*	9/2		K 48
5261	*52610. 01*	7/2		V 52	*5833*	*58332. 42*	5/2		K 48
5274	*52741. 30*	9/2		K 47	*5844*	*58442. 51*	3/2	1. 32	K 48
5285	*52857. 44*	7/2	1. 30	K 47	*5854*	*58541. 88*	1/2		
5288	*52881. 34*	5/2	1. 05	K 47	*5861*	*58619. 32*	11/2	1. 165	K 48
5295	*52951. 59*	3/2	1. 14	K 48	*5912*	*59127. 30*	3/2	1. 20	V 52
5296	*52954. 46*	3/2		V 52	*5917*	*59171. 73*	5/2		V 52
5305	*53058. 74*	5/2	1. 184	K 47	*5929*	*59293. 45*	3/2		
5312	*53125. 19*	3/2	1. 145	K 47	*5939*	*59394. 29*	9/2		K 47
5328	*53288. 28*	1/2	1. 372		*5941*	*59412. 46*	11/2	1. 15	K 47
5329	*53293. 72*	3/2	1. 323	K 47	*5978*	*59784. 67*	7/2		
5332	*53320. 95*	9/2	1. 38	K 47	*5992*	*59926. 91*	7/2	1. 100 (1. 170)	
5333	*53335. 94*	7/2	1. 290	V 52	*6073*	*60737. 28*	5/2		K 48
5337	*53379. 35*	9/2	1. 09	K 47	*6083*	*60837. 10*	5/2	1. 22	
5338	*53389. 73*	5/2	1. 19	K 48	*6214*	*62142. 97*	11/2		
5346	*53467. 57*	11/2	1. 20	K 48	*6235*	*62350. 13*	7/2		
5373	*53738. 46*	7/2	1. 203	K 47	*6249*	*62493. 51*	7/2	~1. 17	
5384	*53842. 53*	3/2	1. 169	K 47	*6326*	*63267. 63*	11/2	1. 135	
5392	*53928. 90*	1/2	1. 113		*6377*	*63772. 40*	13/2		
5394	*53948. 73*	11/2	1. 13		*6393*	*63934. 76*	13/2	1. 07	

When no symbol is inserted in the column headed "origin" the corresponding level is a new one. The symbols ave the following meaning:
M 31, W. F. Meggers, BS J. Research **6,** 1027 (1931) RP322.
M 33, W. F. Meggers, BS J. Research **10,** 757 (1933) RP564.
K 47, P. F. A. Klinkenberg, Physica **13,** 581 (1947).
K 48, P. F. A. Klinkenberg, Physica **14,** 269 (1948).
V 52, R. Velasco, Anales real soc. espan. fis. y quim. **48,** 55 (1952).
C 53, M. A. Catalan, communicated in letter from Velasco to Klinkenberg, dated July 22, 1953.

Int.	λ_{vac}	σ_{vac}	Zeeman effect	Transition	O–C	Notes	Int.	λ_{vac}	σ_{vac}	Zeeman effect	Transition	O–C	Notes
	A	*K*					*A*	*K*					
(12)	1716.45	58259.8		$0_{5/2} - 5826_{7/2}$	−0.2	1	2	2215.535	45121.77		$0_{5/2} - 4512_{3/2}$	−.04	
0	1758.55	56865.0		$0_{5/2} - 5686_{3/2}$	−1.1	..	10	2220.577	45619.33		$173_{7/2} - 6235_{7/2}$	+.02	..
3	1759.83	56823.7		$0_{5/2} - 5682_{3/2}$	+0.9	..	5	2223.16	44967.1		$157_{5/2} - 6073_{5/2}$	+.3	..
0	1763.70	56699.0		$0_{5/2} - 5669_{7/2}$	−.4	..	3	2223.77	44954.7		$142_{7/2} - 5917_{5/2}$	−.2	..
1w	1788.96	55898.4		$0_{5/2} - 5589_{7/2}$	−2.8	..	(10)	2224.21	44945.8		$0_{5/2} - 4494_{7/2}$	−.3	3
1	1845.77	54177.9		$0_{5/2} - 5417_{7/2}$	+0.6	..	300R	2226.418	44901.24	(**.342**, 1.015. . .)	$0_{5/2} - 4490_{7/2}$	+.09	..
(12)	1848.88	54086.8		$0_{5/2} - 5408_{7/2}$	+.1	1	30	2228.05	44868.4		$150_{7/2} - 5992_{7/2}$	−.3	..
0h	1851.23	54018.1		$0_{5/2} - 5401_{7/2}$	−.1	..	7	2235.110	44726.64		$150_{7/2} - 5978_{7/2}$	+.16	..
(3)	1857.34	53840.4		$0_{5/2} - 5384_{5/2}$	−2.1	1	50r	2235.440	44720.04		$0_{5/2} - 4472_{5/2}$	−.05	..
(5)	1873.03	53389.4		$0_{5/2} - 5338_{5/2}$	−0.3	1	2	2237.85	44672.0		$146_{5/2} - 5929_{3/2}$	.0	..
(15r)	1874.93	53335.3		$0_{5/2} - 5333_{7/2}$	−.6	1	40r	2238.603	44656.85		$117_{9/2} - 5641_{9/2}$	+.15	..
4	1876.36	53294.7		$0_{5/2} - 5329_{1/2}$	+1.0	..	30	2240.63	44616.4		$138_{3/2} - 5844_{3/2}$	.0	..
(3)	1884.70	53058.8		$0_{5/2} - 5305_{5/2}$	+0.1	1	8	2243.79	44553.6		$117_{9/2} - 5630_{9/2}$	+.1	..
(10)	1888.43	52954.0		$0_{5/2} - 5296_{3/2}$	−.5	1	2	2246.18	44506.2		$138_{3/2} - 5833_{3/2}$	−.1	..
(10)	1891.04	52881.0		$0_{5/2} - 5288_{5/2}$	−.3	1	30	2254.790	44336.30		$150_{7/2} - 5939_{9/2}$	+.20	..
(50R)	1900.83	52608.6		$0_{5/2} - 5261_{7/2}$	−1.4	1	100r	2255.729	44317.83		$115_{5/2} - 5550_{3/2}$	−.21	6
(50R)	1905.74	52473.1		$0_{5/2} - 5247_{5/2}$	+0.8	1					$115_{5/2} - 5589_{7/2}$	+.59	
(50R)	1909.36	52373.6		$0_{5/2} - 5237_{7/2}$	+.5	1	150R	2256.193	44308.72		$0_{5/2} - 4430_{5/2}$	−.01	..
2h	1912.81	52279.1		$0_{5/2} - 5227_{3/2}$	+.8	..	5	2260.50	44224.31		$138_{3/2} - 5805_{3/2}$	−.15	5
3	1915.01	52219.0		$0_{5/2} - 5221_{5/2}$	+.9	..	10	2263.96	44156.7		$157_{5/2} - 5992_{7/2}$	+.2	..
(15)	1924.74	51955.1		$0_{5/2} - 5195_{7/2}$	+.1	1	200R	2264.393	44148.28	(**.186**, .547) 1.789, 2.150, **2.512**	$0_{5/2} - 4414_{3/2}$	−.17	..
(15r)	1927.72	51874.8		$0_{5/2} - 5187_{7/2}$	+.4	1							
8	1941.33	51511.1		$117_{9/2} - 6326_{11/2}$	−2.0	..							
(5)	1942.61	51477.1		$0_{5/2} - 5147_{5/2}$	−0.1	1	30	2266.072	44115.58		$142_{7/2} - 5833_{5/2}$	+.02	..
12	1952.00	51229.5		$0_{5/2} - 5122_{7/2}$	−.1	..	2	2266.18	44113.5		$150_{7/2} - 5917_{5/2}$	.0	5
(5R)	1953.77	51185.1		$0_{5/2} - 5118_{3/2}$	+2.1	1	10	2268.803	44062.49		$142_{7/2} - 5827_{9/2}$	+.04	..
(15R)	1963.38	50932.4		$0_{5/2} - 5093_{5/2}$	−1.8	1	2	2269.793	44043.26		$142_{7/2} - 5826_{7/2}$	+.09	5
(5)	1965.83	50869.1		$0_{5/2} - 5086_{7/2}$	+0.1	1	40r	2271.300	44014.05		$157_{5/2} - 5878_{7/2}$	−.20	..
0	1969.87	50764.8		$115_{5/2} - 6235_{7/2}$	−1.4	..	4	2274.016	43961.47		$151_{1/2} - 5912_{3/2}$	+.06	..
2s	1976.80	50740.8		$117_{9/2} - 6249_{7/2}$	+1.2	..	300R	2274.618	43949.84	(2.259, 2.804, **3.352**) .530, 1.100, **1.671**, 2.242, 2.812	$0_{5/2} - 4394_{5/2}$	−.14	..
2	1977.48	50569.4		$0_{5/2} - 5057_{3/2}$	−1.6	..							
(5)	1981.62	50463.8		$0_{5/2} - 5046_{3/2}$	0.0	1							
(20R)	1995.61	50110.0		$0_{5/2} - 5011_{5/2}$	−.3	1							
	λ_{air}						10	2278.73	43870.6		$115_{5/2} - 5545_{7/2}$	+.1	..
50R	2003.532	49895.70		$0_{5/2} - 4989_{1/2}$	+.13	2	10	2281.29	43821.4		$146_{3/2} - 5844_{3/2}$	+.3	..
(10)	2004.84	49863.2		$0_{5/2} - 4986_{7/2}$	.0	3	200R	2281.620	43814.99	(**.297**, .898, 1.500)	$0_{5/2} - 4381_{7/2}$	−.02	..
(2)	2012.74	49667.5		$0_{5/2} - 4966_{5/2}$	+.3	4							
20r	2016.56	49573.4		$0_{5/2} - 4957_{5/2}$	+.3	..	400R	2287.506	43702.24	(.000) 1.940. . .	$0_{5/2} - 4370_{3/2}$	+.04	..
200R	2017.866	49541.32		$0_{5/2} - 4954_{5/2}$	+.36	..	400R	2294.486	43569.32	(.206, .664, **1.121**) .832, 1.275, **1.717**, 2.160, 2.600	$0_{5/2} - 4356_{5/2}$	−.04	..
5	2029.70	49252.6		$115_{5/2} - 6083_{5/2}$	−.5	..							
20r	2033.78	49153.8		$115_{5/2} - 6073_{5/2}$	+.5	..							
30r	2038.99	49028.0		$0_{5/2} - 4903_{7/2}$	+.1	..							
50r	2039.204	49022.99		$0_{5/2} - 4902_{5/2}$	+.22	..	40r	2296.926	43523.03		$157_{5/2} - 5929_{3/2}$	.00	..
(7)	2046.09	48848.0		$0_{5/2} - 4885_{7/2}$	+.4	5	7	2297.81	43506.3		$173_{7/2} - 6083_{5/2}$	.0	..
400R	2049.079	48786.77		$0_{5/2} - 4878_{7/2}$	+.42	..	20	2299.769	43469.25		$117_{9/2} - 5522_{11/2}$	−.08	..
20r	2067.89	48343.0		$115_{5/2} - 5992_{7/2}$	.0	..	8	2301.318	43439.98		$142_{7/2} - 5765_{9/2}$	−.01	..
20r	2074.70	48184.4		$0_{5/2} - 4818_{7/2}$	+.2	..	4	2301.884	43429.30		$146_{5/2} - 5805_{3/2}$	+.18	..
5	2075.20	48172.8		$117_{9/2} - 5992_{7/2}$	+.4	..	150R	2302.992	43408.41		$0_{5/2} - 4341_{5/2}$	−.70	6
7	2081.35	48030.5		$117_{9/2} - 5978_{7/2}$	+.3	..					$0_{5/2} - 4340_{7/2}$	+.54	
40r	2083.925	47971.11		$0_{5/2} - 4797_{5/2}$	+.29	..	3	2303.370	43401.29		$157_{5/2} - 5917_{5/2}$	−.02	..
200R	2085.594	47932.71		$0_{5/2} - 4793_{7/2}$	+.16	..	10	2304.714	43375.99		$151_{1/2} - 5854_{1/2}$	.00	..
3h	2088.23	47872.3		$146_{5/2} - 6249_{7/2}$	+.2	..	10	2305.726	43356.96		$157_{5/2} - 5912_{3/2}$	+.08	..
50r	2092.24	47780.4		$0_{5/2} - 4777_{3/2}$	+.5	..	60r	2306.540	43341.64	(**.495**, **1.456**) . . . . , 2.615, **3.568**.	$0_{5/2} - 4334_{3/2}$	−.21	..
5	2094.50	47728.8		$146_{5/2} - 6235_{7/2}$	+.1	..							
2	2095.33	47709.9		$115_{5/2} - 5929_{1/2}$	+.4	..							
100R	2097.122	47669.26		$0_{5/2} - 4766_{7/2}$	+.25	..					$166_{9/2} - 5992_{7/2}$	−.04	..
4	2097.603	47658.33		$117_{9/2} - 5941_{11/2}$	+.39	5	20	2308.354	43307.59		$142_{7/2} - 5752_{5/2}$	+.14	..
4	2098.41	47639.9		$117_{9/2} - 5939_{9/2}$	+.1	..	3	2310.00	43276.7		$151_{1/2} - 5844_{3/2}$	+.1	..
3	2102.67	47543.4		$115_{5/2} - 5512_{3/2}$	+.1	..	10	2310.134	43274.21		$150_{7/2} - 5833_{5/2}$	−.02	..
4	2106.13	47465.4		$163_{11/2} - 6377_{13/2}$	+.1	..	8	2311.576	43247.23		$138_{3/2} - 5707_{1/2}$	+.04	..
60r	2107.452	47435.63		$150_{7/2} - 6249_{7/2}$	+.31	..	7	2312.011	43239.09		$115_{5/2} - 5482_{5/2}$	+.03	..
30r	2113.87	47291.6		$150_{7/2} - 6235_{7/2}$	−.3	..	1Cr	2312.971	43221.15		$150_{7/2} - 5827_{9/2}$	+.03	..
4	2128.773	46960.59		$163_{11/2} - 6326_{11/2}$	+.11	..	30r	2315.956	43165.44		$166_{9/2} - 5978_{7/2}$	+.05	..
2	2131.01	46911.4		$138_{3/2} - 6073_{5/2}$	+.2	..	30	2316.523	43154.88		$142_{7/2} - 5737_{7/2}$	−.01	..
2	2133.122	46864.86		$117_{9/2} - 5861_{11/2}$	+.06	5	30r	2319.19	43105.3		$163_{11/2} - 5941_{11/2}$	.0	..
5	2133.41	46858.6		$115_{5/2} - 5844_{3/2}$	.0	..	50r	2320.162	43087.20		$163_{11/2} - 5939_{9/2}$	+.06	..
5h	2138.44	46748.4		$115_{5/2} - 5833_{3/2}$	−.1	..	10	2321.41	43064.1		$142_{7/2} - 5728_{9/2}$	+.1	..
6	2141.745	46676.19		$115_{5/2} - 5826_{7/2}$	+.12	..	10	2321.70	43058.7		$117_{9/2} - 5481_{9/2}$	+.1	..
20r	2142.97	46649.4		$0_{5/2} - 4664_{5/2}$	.0	..	50R	2322.490	43044.02	(.255, .764 **1.273**) .687, 1.194, **1.703**, 2.210, 2.714.	$0_{5/2} - 4304_{5/2}$	.00	..
3	2148.92	46520.3		$142_{7/2} - 6073_{5/2}$	−.1	..							
5	2149.43	46509.3		$0_{5/2} - 4650_{5/2}$	−.1	..							
1	2149.59	46505.8		$117_{9/2} - 5826_{7/2}$	+.3	5							
4	2151.40	46466.7		$115_{5/2} - 5805_{3/2}$	+.1	..	4	2322.700	43040.13		$138_{3/2} - 5686_{3/2}$	+.19	..
100R	2156.673	46353.14		$0_{5/2} - 4635_{7/2}$	+.15	..	10	2322.945	43035.59		$194_{5/2} - 6249_{7/2}$	−.03	..
10	2163.10	46215.4		$146_{5/2} - 6083_{5/2}$	−.2	..	20	2325.045	42996.72		$138_{3/2} - 5682_{5/2}$	+.09	..
200R	2167.938	46112.32		$0_{5/2} - 4611_{5/2}$	+.08	..	30r	2328.664	42929.90	(.000) 1.216. . . .	$115_{5/2} - 5451_{7/2}$	+.03	..
200R	2176.206	45937.13		$0_{5/2} - 4593_{7/2}$	−.05	..	4	2330.706	42892.30		$194_{5/2} - 6235_{7/2}$	+.06	..
2	2177.851	45902.45		$117_{9/2} - 5765_{9/2}$	+.12	5	20	2331.135	42884.41		$172_{1/2} - 5835_{3/2}$	−.28	..
(5)	2179.09	45876.4		$0_{5/2} - 4587_{1/2}$	+.1	4	(3)	2331.19	42883.3		$115_{5/2} - 5446_{3/2}$	−.1	4
8	2179.18	45874.5		$166_{9/2} - 6249_{7/2}$	+.3	..	20	2331.73	42873.4		$142_{7/2} - 5709_{7/2}$	.0	..
20	2181.02	45835.8		$163_{11/2} - 6214_{11/2}$	.0	..	20	2333.32	42844.2		$164_{3/2} - 5917_{5/2}$	.C	..
100R	2183.72	45779.2		$150_{7/2} - 6083_{5/2}$	+.3	..	20r	2334.33	42825.6	(.547) 1.016h. . .	$115_{5/2} - 5440_{5/2}$	−.1	..
3	2187.02	45710.1		$142_{7/2} - 5992_{7/2}$	.0	..	20r	2335.730	42800.05		$117_{9/2} - 5455_{11/2}$	−.04	..
6	2188.50	45679.2		$150_{7/2} - 6073_{5/2}$	+.1	..	20r	2336.10	42793.2		$166_{9/2} - 5941_{11/2}$	.0	..
10	2190.518	45637.03		$117_{9/2} - 5739_{11/2}$	+.11	..	10	2337.092	42775.09		$166_{9/2} - 5939_{9/2}$	+.08	..
40	2191.471	45617.19		$117_{9/2} - 5737_{7/2}$	−.04	..	40R	2337.953	42759.35	(**.148**, .417).	$117_{9/2} - 5451_{7/2}$	+.03	..
3	2192.84	45588.6		$115_{5/2} - 5717_{7/2}$	−.1	..	20	2338.451	42750.24		$146_{5/2} - 5737_{7/2}$	−.05	..
5	2193.85	45567.6		$142_{7/2} - 5978_{7/2}$	−.2	..	2	2342.06	42684.3		$115_{5/2} - 5426_{5/2}$	+.1	..
8	2195.84	45526.4		$117_{9/2} - 5728_{9/2}$	+.1	..	30	2342.731	42672.15		$157_{5/2} - 5844_{3/2}$	+.06	..
10	2195.97	45523.7		$166_{9/2} - 6214_{11/2}$	.0	—	20r	2345.282	42625.75		$138_{3/2} - 5645_{1/2}$	.00	..
200R	2198.914	45462.79		$0_{5/2} - 4546_{7/2}$	−.04	..	4h	2346.37	42606.0		$142_{7/2} - 5682_{5/2}$	+.1	..
8	2201.075	45418.17		$117_{9/2} - 5717_{7/2}$	−.01	..	6	2346.774	42598.64		$150_{7/2} - 5765_{9/2}$	−.02	..
4	2206.76	45301.1		$138_{3/2} - 5912_{3/2}$	−.01	..	10	2347.064	42593.37	(.000) 1.261. . . .	$115_{5/2} - 5417_{7/2}$	+.08	..
20	2207.680	45282.31		$115_{5/2} - 5686_{3/2}$	+.21	..	8	2348.792	42562.05		$157_{5/2} - 5833_{5/2}$	+.05	..
30	2209.800	45238.86		$115_{5/2} - 5682_{5/2}$	+.07	..	30r	2349.391	42551.20	(.000) 1.271. . . .	$146_{5/2} - 5717_{7/2}$	−.04	..
10	2212.809	45177.36		$142_{7/2} - 5939_{9/2}$	−.07	..	100R	2352.069	42502.75	(0w) 1.110h D.	$115_{5/2} - 5408_{7/2}$	+.04	..
2	2213.50	45163.2		$146_{5/2} - 5978_{7/2}$	.0	..	5	2353.18	42482.7		$142_{7/2} - 5669_{7/2}$	+.1	..

TABLE 2. *Classified lines of* Re I—Continued

Int.	λ_{vac}	σ_{vac}	Zeeman effect	Transition	O-C	Notes
	A	*K*				
30r	2353.95	42468.8		$146_{5/2}$ —$5709_{7/2}$	.0	--
30r	2354.08	42466.5		$150_{7/2}$ —$5752_{5/2}$	+.4	--
15	2354.773	42453.96		$173_{7/2}$ —$5978_{7/2}$	+.11	--
10	2355.868	42434.21		$115_{5/2}$ —$5401_{7/2}$	−.02	--
30r	2356.496	42422.91		$117_{9/2}$ —$5417_{7/2}$	+.18	--
20	2362.64	42312.6		$163_{11/2}$—$5861_{11/2}$	+.4	--
3	2364.44	42280.4		$157_{5/2}$ —$5805_{3/2}$	+.2	--
20r	2365.666	42258.47		$115_{5/2}$ —$5384_{3/2}$	−.10	--
150R	2365.90	42254.4	(**.184**, .556) . . . 1.747, 2.121, **2.496.**	$0_{5/2}$ —$4225_{3/2}$	+.2	--
50r	2367.683	42222.49	(.000) 1.171. . . .	$150_{7/2}$ —$5728_{9/2}$	−.18	--
4	2368.12	42214.8		$164_{3/2}$ —$5854_{3/2}$	+.3	--
15	2368.88	42201.2		$146_{5/2}$ —$5682_{3/2}$	−.1	--
50r	2369.27	42194.3	(**.167**, .500, .832) **.163**, .493, .823	$142_{7/2}$ —$5641_{9/2}$ / $117_{9/2}$ —$5394_{11/2}$	−.1 / +.1	19
30r	2371.500	42154.53	(0w) 1.000B. . .	$115_{5/2}$ —$5373_{7/2}$	+.03	--
15	2373.747	42114.62		$150_{7/2}$ —$5717_{7/2}$	+.11	--
100r	2375.073	42091.12		$142_{7/2}$ —$5639_{9/2}$	+.01	--
15r	2375.815	42077.97	(0w) 1.412hD.	$146_{5/2}$ —$5669_{7/2}$	+.02	--
10	2375.93	42075.9		$138_{3/2}$ —$5590_{3/2}$	.0	--
10	2376.629	42063.57		$173_{7/2}$ —$5939_{9/2}$	+.10	--
10	2377.104	42055.15		$172_{1/2}$ —$5929_{3/2}$	.00	--
3	2378.40	42032.2		$150_{7/2}$ —$5708_{7/2}$	+.1	--
5	2379.950	42004.87		$164_{3/2}$ —$5835_{5/2}$	−.04	--
20	2380.225	42000.02	(.000) 1.124. . .	$166_{9/2}$ —$5861_{11/2}$	−.02	--
40	2381.136	41983.96	(**.159**, .488, .817)	$117_{9/2}$ —$5373_{7/2}$	+.02	--
6	2381.81	41972.0		$163_{11/2}$ —$5827_{9/2}$	−.2	--
15	2385.48	41907.5		$151_{1/2}$ —$5707_{1/2}$	+.1	--
10	2386.536	41888.95		$172_{1/2}$ —$5912_{3/2}$	−.05	--
20r	2389.110	41843.84	(**.376**, 1.118) . . .	$0_{3/2}$ —$4184_{7/2}$	+.01	--
5	2389.270	41841.03		$173_{7/2}$ —$5917_{7/2}$	+.08	--
30r	2391.278	41805.89		$115_{5/2}$ —$5338_{5/2}$	+.12	--
50r	2393.645	41764.56		$150_{7/2}$ —$5682_{5/2}$	.00	--
4	2394.252	41753.98		$157_{5/2}$ —$5752_{3/2}$	+.09	--
30r	2394.37	41751.9	(.000) 1.311. . . .	$115_{5/2}$ —$5333_{7/2}$	−.1	--
7	2396.03	41723.0		$164_{3/2}$ —$5805_{3/2}$	−.1	--
(10)	2396.60	41713.1		$117_{9/2}$ —$5346_{11/2}$	.0	7
40r	2396.791	41709.74	(.000) 1.245. . . .	$115_{5/2}$ —$5329_{3/2}$	−.02	--
50	2397.31	41700.7	(.626) .465. . . .	$151_{1/2}$ —$5686_{3/2}$	+.5	8
4	2397.605	41695.59		$142_{7/2}$ —$5591_{9/2}$	+.03	--
10	2398.25	41684.4		$142_{7/2}$ —$5589_{7/2}$	+.1	--
6	2399.648	41660.10		$166_{9/2}$ —$5827_{9/2}$	+.07	--
20	2400.72	41641.5		$150_{7/2}$ —$5669_{7/2}$	+.3	--
30	2401.680	41624.85	(.705, 1.178, 1.650, **2.125**), .388, .847, **1.306**, 1.765.	$117_{9/2}$ —$5337_{9/2}$	+.02	--
10	2403.036	41601.36		$157_{3/2}$ —$5737_{7/2}$	+.03	5
300R	2405.056	41566.42	(.730)1.547wA	$117_{9/2}$ —$5339_{9/2}$	−.01	--
200r	2405.602	41556.99	(**.152**, .444) 1.789, 2.086, **2.386.**	$0_{5/2}$ —$4155_{1/2}$	−.09	--
30r	2410.37	41474.8	(.210) 1.235h. . .	$115_{5/2}$ —$5305_{5/2}$	.0	--
30r	2414.587	41402.36	(0w) .965hC. . . .	$157_{5/2}$ —$5717_{7/2}$	+.08	--
4h	2415.93	41379.4		$194_{5/2}$ —$6083_{5/2}$	+.2	--
10	2416.441	41370.60		$115_{5/2}$ —$5296_{3/2}$	+.10	--
15	2417.661	41349.72	(0w) 1.438D. . . .	$163_{11/2}$—$5765_{9/2}$	+.02	--
60r	2419.404	41319.94		$157_{3/2}$ —$5709_{7/2}$	+.07	--
100r	2419.807	41313.06	(.335, 1.004, **1.673**) .287, .956, **1.616**, 2.279, 2.948.	$0_{3/2}$ —$4131_{3/2}$	+.04	--
5	2420.35	41303.7		$172_{1/2}$ —$5854_{1/2}$	+.1	--
5	2420.72	41297.4		$115_{5/2}$ —$5288_{3/2}$	.0	--
30	2421.38	41286.1		$151_{1/2}$ —$5645_{1/2}$	+.1	--
40r	2421.730	41280.26	(0w) 1.198. . . .	$146_{5/2}$ —$5590_{3/2}$ / $146_{5/2}$ —$5589_{7/2}$	−.29 / +.52	6
2	2422.11	41273.7		$115_{5/2}$ —$5285_{7/2}$	+.2	--
30	2423.50	41250.0		$156_{7/2}$ —$5630_{9/2}$	+.2	--
10	2426.195	41204.28		$172_{1/2}$ —$5844_{3/2}$	+.07	--
30	2426.635	41196.81	(000) .994. . . .	$164_{3/2}$ —$5752_{3/2}$	+.01	11
300R	2428.576	41163.90	(**.319**, .972, 1.625) **.319**, .965, 1.611, 2.255.	$0_{5/2}$ —$4116_{7/2}$	−.01	--
10	2429.648	41145.74		$163_{11/2}$—$5745_{13/2}$	+.06	--
80	2432.18	41102.9	(**.125**, .412, .696).	$117_{9/2}$ —$5285_{7/2}$	.0	--
5	2432.617	41095.52		$157_{5/2}$ —$5686_{3/2}$	−.08	--
20	2433.28	41084.3	(.172) 1.256h. . .	$163_{11/2}$—$5739_{11/2}$	.0	--
10	2436.046	41037.67	(.000) 1.182. . . .	$166_{9/2}$ —$5765_{9/2}$	+.10	--
(10)	2436.74	41026.0	(000) 1.095. . . .	$115_{5/2}$ —$5261_{7/2}$	−.1	7
30	2438.462	40997.03	(**.156**, .467) **.715**, 1.026, 1.338.	$138_{3/2}$ —$5482_{3/2}$	+.13	--
30	2439.06	40987.0		$117_{9/2}$ —$5274_{9/2}$	+.2	--
3	2439.86	40973.5		$163_{11/2}$—$5728_{9/2}$	−.2	--
3	2441.35	40948.5		$173_{7/2}$ —$5827_{9/2}$	.0	5
100R	2441.47	40946.5	(**.211**, .628, 1.046) **.490**, .906, 1.319, 1.730, 2.143, 2.556.	$0_{5/2}$ —$4094_{7/2}$	.0	--
40r	2442.510	40929.09	. . . .	$173_{7/2}$ —$5826_{7/2}$ / $157_{5/2}$ —$5669_{7/2}$	−.12 / +.10	9
70r	2444.943	40888.35	(.427, **.717**). . . .	$115_{5/2}$ —$5247_{5/2}$	.00	--
30	2446.978	40854.36		$150_{7/2}$ —$5591_{9/2}$	+.13	--
5	2447.656	40843.04		$150_{7/2}$ —$5589_{7/2}$	+.03	--
1	2448.26	40833.0		$146_{5/2}$ —$5545_{7/2}$	.0	5
60r	2449.710	40808.79	(000) 2.856	$0_{3/2}$ —$4080_{3/2}$	−.06	10, 26
30	2450.895	40789.07	(0w)?	$115_{5/2}$ —$5237_{7/2}$	−.09	--
8	2451.910	40772.19		$166_{9/2}$ —$5739_{11/2}$	+.03	--
10	2453.493	40745.87	(.387).	$164_{3/2}$ —$5707_{1/2}$	+.07	--
3	2454.082	40736.10		$151_{1/2}$ —$5590_{3/2}$	−.02	--
2	2458.577	40661.62		$166_{9/2}$ —$5728_{9/2}$	+.04	--
4	2459.81	40641.3		$138_{3/2}$ —$5446_{3/2}$	.0	--
20	2460.24	40634.2	(.160) 1.231h. . .	$115_{5/2}$ —$5221_{3/2}$	.0	--
200R	2461.196	40618.35	(0h) 1.503h D. .	$117_{9/2}$ —$5237_{7/2}$	−.25	--
10	2462.539	40596.21	(**.194**, .574, .952).	$142_{7/2}$ —$5481_{9/2}$	−.05	--
15	2463.307	40583.55	(**.213**, .628) **.445**, .860, 1.274.	$138_{3/2}$ —$5440_{5/2}$	+.06	--
5	2463.84	40574.7		$217_{7/2}$ —$6235_{7/2}$	.0	--
30	2465.13	40553.5	(000) 1.111. . . .	$166_{9/2}$ —$5717_{7/2}$	+.1	--
5	2466.042	40538.54		$164_{3/2}$ —$5686_{3/2}$	−.01	--
4	2470.164	40470.90		$166_{9/2}$ —$5708_{7/2}$	−.20	--
3	2470.275	40469.08		$194_{5/2}$ —$5992_{7/2}$	+.06	--
2	2471.93	40441.9		$138_{3/2}$ —$5426_{3/2}$	−.2	--
15	2474.725	40396.32	(000) 1.154. . . .	$150_{7/2}$ —$5545_{7/2}$	+.03	--
5	2476.275	40371.04		$115_{5/2}$ —$5195_{7/2}$	−.02	--
2h	2478.58	40333.5		$221_{9/2}$ —$6849_{7/2}$	.0	--
20	2479.02	40326.3		$194_{3/2}$ —$5978_{7/2}$ / $173_{7/2}$ —$5765_{9/2}$	−.5 / +.3	--
20	2480.820	40297.08	(.471, .792, **1.114**).	$142_{7/2}$ —$5451_{7/2}$	+.1	--
4	2481.226	40290.49		$115_{5/2}$ —$5187_{3/2}$	+.02	--
5	2483.38	40255.5		$204_{1/2}$ —$6073_{3/2}$	−.1	--
200R	2483.920	40246.79	(.875) 1.452A. .	$117_{9/2}$ —$5393_{9/2}$	−.06	--
20	2485.805	40216.28		$163_{11/2}$—$5652_{13/2}$	+.02	--
30	2486.779	40200.53	(**.171**, .490, .809).	$117_{9/2}$ —$5195_{7/2}$	+.03	--
5	2487.21	40193.6		$173_{7/2}$ —$5752_{5/2}$	+.1	--
200R	2487.331	40191.60		$117_{9/2}$ —$5194_{11/2}$	+.18	--
9	2491.07	40131.3		$157_{5/2}$ —$5590_{3/2}$ / $157_{5/2}$ —$5589_{7/2}$	−.3 / +.5	--
2	2491.497	40124.40		$164_{3/2}$ —$5645_{1/2}$	+.04	--
8	2492.751	40104.22		$163_{11/2}$—$5641_{9/2}$	+.15	--
3	2492.838	40102.82	(.192) 1.738. . .	$138_{3/2}$ —$5392_{1/2}$	+.04	--
3	2494.250	40080.12		$166_{9/2}$ —$5669_{7/2}$	−.01	--
8	2495.263	40063.84		$115_{5/2}$ —$5164_{7/2}$	−.02	--
30	2496.039	40051.39	(**.142**, .419, .697) .835f.	$142_{7/2}$ —$5426_{5/2}$	+.07	11
10	2496.692	40040.92		$173_{7/2}$ —$5737_{7/2}$	−.01	--
20	2498.215	40016.51	(.479) 1.010, 1.345, **1.678**f.	$138_{3/2}$ —$5384_{1/2}$	+.10	--
20	2498.861	40006.17	(.394, **.661**) 1.386.	$115_{5/2}$ —$5159_{5/2}$	+.05	12
1	2499.19	40001.0		$163_{11/2}$—$5630_{9/2}$	+.2	--
2	2499.608	39994.22		$115_{5/2}$ —$5157_{3/2}$	+.13	--
10	2500.312	39982.95		$221_{9/2}$ —$6814_{11/2}$	+.02	--
10	2500.568	39978.85	(0w) D.	$239_{11/2}$—$6393_{13/2}$	+.09	--
50r	2501.721	39960.43	(.453, .759, **1.062**) .529, .819, 1.113, **1.417**, 1.707, 1.992.	$142_{7/2}$ —$5417_{7/2}$	+.04	--
30	2505.945	39893.08	(.485, **.805**) 1.146.	$115_{5/2}$ —$5147_{5/2}$	−.11	--
30	2507.403	39869.89	(.566, .907, **1.251**).	$142_{7/2}$ —$5408_{7/2}$	+.08	12
200R	2508.991	39844.65	(.366, 1.094, **1.821**).	$0_{5/2}$ —$3984_{7/2}$	+.10	12
5	2509.562	39835.59		$194_{5/2}$ —$5929_{7/2}$	+.03	--
(5)	2510.771	39816.41		$239_{11/2}$—$6377_{13/2}$	+.01	7
5	2511.616	39803.02		$151_{1/2}$ —$5496_{1/2}$	+.06	--
2	2511.720	39801.37		$142_{7/2}$ —$5461_{7/2}$	+.04	--
4	2512.317	39791.92		$166_{9/2}$ —$5641_{9/2}$	−.02	--
15	2512.550	39788.23	(.210) 1.051A. .	$146_{5/2}$ —$5440_{5/2}$	+.08	--
2h	2514.35	39759.7		$173_{7/2}$ —$5709_{7/2}$	+.2	--
5	2514.651	39754.98		$150_{7/2}$ —$5481_{9/2}$	+.05	--
150r	2516.120	39731.77	(.506, .857, 1.209, **1.558**) 000, .341, .682, 1.023, **1.368**, 1.708, 2.043, 2.384, 2.729.	$117_{9/2}$ —$5148_{9/2}$	.0	--
5	2518.87	39688.4		$166_{9/2}$ —$5630_{9/2}$	−.3	--
6	2519.139	39684.16		$157_{5/2}$ —$5545_{7/2}$	+.10	--
50r	2520.009	39670.46	(.417, 1.266, **2.112**) −.146, .684, **1.526**, 2.369, 3.211.	$0_{5/2}$ —$3967_{7/2}$	−.06	--
10	2521.50	39647.0		$146_{5/2}$ —$5426_{7/2}$	+.3	--
5	2521.59	39645.6		$115_{5/2}$ —$5122_{7/2}$	−.1	--
5	2522.719	39627.84		$172_{1/2}$ —$5686_{1/2}$	+.08	--
5	2524.155	39605.30		$163_{11/2}$—$5591_{9/2}$	+.03	--
6	2524.546	39599.17		$115_{5/2}$ —$5118_{3/2}$	+.13	--
10	2526.809	39563.70		$138_{3/2}$ —$5338_{5/2}$	+.09	--
5	2527.311	39555.85		$146_{5/2}$ —$5417_{7/2}$	+.06	--
(1)	2528.62	39535.4		$197_{1/2}$ —$5929_{3/2}$	−.1	5
15	2529.50	39521.6		$142_{7/2}$ —$5373_{7/2}$	.0	--
5	2531.404	39491.89		$173_{7/2}$ —$5682_{5/2}$	−.04	--
5	2532.48	39475.1		$117_{9/2}$ —$5122_{7/2}$	.0	--
5	2532.848	39469.38		$163_{11/2}$—$5577_{13/2}$	+.02	--

TABLE 2. *Classified lines of* Re I—Continued

Int.	λ_{vac}	σ_{vac}	Zeeman effect	Transition	O–C	Notes
	A	*K*				
4	2532.963	39467.59		$138_{3/2}$ —$5329_{3/2}$	−.01	--
4	2533.119	39465.16		$146_{5/2}$ —$5408_{7/2}$	−.05	--
15r	2533.310	39462.19		$138_{3/2}$ —$5328_{1/2}$	+.03	--
1	2533.74	39455.5		$150_{7/2}$ —$5451_{7/2}$	−.2	--
30	2534.805	39438.91	(**260**, .**775**, **1.288**)	$117_{9/2}$ —$5119_{9/2}$	−.06	12
4	2537.517	39396.77		$146_{5/2}$ —$5401_{7/2}$	+.04	--
20	2539.326	39368.69		$173_{7/2}$ —$5669_{7/2}$	+.10	--
3	2540.45	39351.3		$150_{7/2}$ —$5440_{5/2}$	−.1	--
40r	2540.513	39350.31	(.**252**) **1.342** A..	$115_{5/2}$ —$5093_{5/2}$	+.09	--
20h	2541.27	39338.6		$231_{5/2}$ —$6249_{7/2}$	−.1	--
2	2543.022	39311.48		$239_{11/2}$—$6326_{11/2}$	−.15	--
10	2543.671	39301.45	(.**495**) .**866**.....	$151_{1/2}$ —$5446_{3/2}$	−.06	5
8	2543.835	39298.92		$138_{3/2}$ —$5312_{3/2}$	−.15	--
10	2544.215	39293.05	(.**736**) A..	$166_{9/2}$ —$5591_{9/2}$	−.09	--
100r	2544.739	39284.96	(**0w**) **1.169** D..	$115_{5/2}$ —$5086_{7/2}$	−.08	--
8	2544.952	39281.67	(**0w**) **1.047**.....	$166_{9/2}$ —$5589_{7/2}$	−.25	--
30r	2545.485	39273.45	(.**993**, **1.447**, **1.898**).	$117_{9/2}$ —$5102_{9/2}$	+.01	--
10	2548.136	39232.59	(**.151**, .457) **.762**, **1.068**.	$138_{9/2}$ —$5305_{5/2}$	−.03	--
20	2548.885	39221.06	(**000**) **1.143**.....	$146_{5/2}$ —$5384_{3/2}$	−.01	--
6	2549.372	39213.57		$172_{1/2}$ —$5645_{1/2}$	.00	--
40r	2552.021	39172.87	(**.189**, .575, .961) **1.018**, **1.396**, **1.774**, **2.152**, **2.526**.	$142_{7/2}$ —$5338_{5/2}$	.00	--
6	2554.929	39128.29		$138_{3/2}$ —$5296_{3/2}$	−.05	--
2	2555.116	39125.42		$138_{3/2}$ —$5295_{3/2}$	−.05	--
4	2555.531	39119.06		$142_{7/2}$ —$5333_{7/2}$ $150_{7/2}$ —$5417_{7/2}$	−.02 .00	-- --
5	2555.666	39117.00		$146_{5/2}$ —$5373_{7/2}$	.00	--
80R	2556.512	39104.06	(.**101**, .**302**, .**502**, **.803**) **.697**, .**893**, **1.090**, **1.286**, **1.483**, **1.679**.	$142_{7/2}$ —$5332_{9/2}$	−.03	--
10	2558.062	39080.37		$173_{7/2}$ —$5641_{9/2}$	−.03	--
20R	2559.076	39064.88	(.**291**, .**916**, **1.540**) .**406**, **1.031**, **1.656**, **2.280**, **2.903**.	$0_{3/2}$ —$3906_{5/2}$	−.04	--
6	2559.707	39055.25		$138_{3/2}$ —$5288_{3/2}$	+.03	--
6	2559.882	39052.58		$157_{5/2}$ —$5488_{3/2}$	−.02	--
8	2561.462	39028.50	(.**159**) **1.162**A..	$150_{7/2}$ —$5408_{7/2}$	+.02	--
50R	2564.186	38987.03	(**.167**, .**505**) .**781**, **1.113**, **1.446**, **1.778**.	$115_{5/2}$ —$5057_{3/2}$	−.03	--
10	2564.347	38984.59		$194_{5/2}$ —$5844_{3/2}$	−.03	--
6	2565.839	38961.92		$217_{7/2}$ —$6073_{5/2}$	+.04	--
3	2565.967	38959.98		$150_{7/2}$ —$5401_{7/2}$	−.02	--
2	2568.817	38916.75		$163_{11/2}$—$5522_{11/2}$	+.05	--
4	2569.327	38909.03		$117_{9/2}$ —$5066_{11/2}$	+.04	--
10	2571.255	38879.87	(.**332**) A..	$115_{5/2}$ —$5046_{5/2}$	+.03	--
1	2571.605	38874.58		$194_{5/2}$ —$5833_{5/2}$	+.05	--
20	2573.760	38842.02	(**.192**. .**570**, .**947**) .**633**, **1.012**, **1.389**, **1.767**, **2.144**, **2.521**.	$142_{7/2}$ —$5305_{5/2}$	+.14	--
6	2574.211	38835.22		$166_{9/2}$ —$5545_{7/2}$	+.06	--
4	2576.408	38802.10		$194_{5/2}$ —$5826_{7/2}$	−.04	--
6	2577.614	38783.95		$197_{1/2}$ —$5854_{1/2}$	−.02	--
10	2579.005	38763.04	(.**619**) **1.732**.....	$151_{1/2}$ —$5392_{1/2}$	+.03	--
7	2580.311	38743.42		$157_{5/2}$ —$5451_{7/2}$	.00	5
9hl	2581.438	38726.50		$115_{5/2}$ —$5031_{7/2}$	−.24	--
2	2582.240	38714.47		$146_{5/2}$ —$5333_{7/2}$	−.01	--
3	2583.406	38697.00		$157_{5/2}$ —$5446_{3/2}$	+.02	--
4	2583.873	38690.01		$204_{3/2}$ —$5917_{5/2}$	+.01	--
6	2584.523	38680.29		$150_{7/2}$ —$5373_{7/2}$	+.02	--
10	2584.768	38676.62	(.**594**) .**594**, **1.304**†?.	$151_{1/2}$ —$5384_{3/2}$	−.02	12
6	2585.061	38672.22		$146_{5/2}$ —$5329_{3/2}$	−.04	--
8	2585.580	38664.46		$142_{7/2}$ —$5288_{3/2}$	−.02	--
50R	2586.788	38646.41	(.**704**, **1.195**, **1.686**, **2.178**).	$117_{9/2}$ —$5040_{9/2}$	−.08	--
7	2586.998	38643.28		$138_{3/2}$ —$5246_{1/2}$	−.05	--
6	2589.594	38604.53	(**000**) **1.082**.....	$166_{9/2}$ —$5552_{11/2}$	−.04	--
6	2591.133	38581.61		$173_{7/2}$ —$5591_{9/2}$	+.01	--
30r	2591.582	38574.93	(.**373**) A..	$115_{5/2}$ —$5015_{3/2}$	+.02	--
10	2591.889	38570.36		$173_{7/2}$ —$5589_{7/2}$	−.02	--
10	2592.843	38556.17		$117_{9/2}$ —$5031_{7/2}$	−.01	--
30R	2594.854	38526.29		$115_{5/2}$ —$5011_{5/2}$	−.03	--
5	2594.982	38524.39		$142_{7/2}$ —$5274_{9/2}$	−.05	--
60R	2595.234	38520.65		$0_{3/2}$ —$3852_{7/2}$	−.09	--
10r	2596.780	38497.72	(**000**) **1.300**.....	$157_{5/2}$ —$5426_{3/2}$	−.04	--
50R	2599.856	38452.17	(**000**) **1.457**.....	$138_{3/2}$ —$5227_{3/2}$	+.01	--
5	2600.518	38442.39		$117_{9/2}$ —$5019_{9/2}$	−.03	--
10	2600.866	38437.24	(**0d?**) **1.166**..	$146_{5/2}$ —$5305_{3/2}$	−.04	--
15	2601.874	38422.36		$163_{11/2}$—$5472_{13/2}$	−.01	--
10	2602.926	38406.82	(**0d?**) **1.200**.....	$157_{5/2}$ —$5417_{7/2}$	−.01	--
10	2607.936	38333.04		$146_{5/2}$ —$5296_{3/2}$	+.04	--
3	2608.043	38331.47		$150_{7/2}$ —$5338_{5/2}$	−.07	--
3	2608.746	38321.15		$150_{7/2}$ —$5337_{9/2}$	−.11	--
5	2609.085	38316.17		$157_{5/2}$ —$5408_{7/2}$	−.08	--
5	2609.204	38314.42		$224_{3/2}$ —$6073_{5/2}$	−.03	--
9	2609.404	38311.49		$115_{5/2}$ —$4989_{1/2}$	−.12	--
4	2610.690	38292.60		$197_{1/2}$ —$5805_{1/2}$	−.07	--
40R	2611.603	38279.22	(**000**) .**910** C†..	$115_{5/2}$ —$4986_{7/2}$	−.04	--
5	2611.702	38277.77		$150_{7/2}$ —$5333_{7/2}$	+.02	--
10	2612.730	38262.71		$150_{7/2}$ —$5332_{9/2}$	−.05	--
5	2612.929	38259.80		$146_{5/2}$ —$5288_{5/2}$	−.08	--
10	2613.235	38255.32		$142_{7/2}$ —$5247_{5/2}$	−.13	--
15	2613.744	38247.87	(.**293**) A..	$157_{3/2}$ —$5401_{7/2}$	+.10	--
50R	2614.558	38235.96	(**0w**) **1.662** B..	$146_{5/2}$ —$5285_{7/2}$	−.02	--
10	2617.442	38193.84		$166_{9/2}$ —$5481_{9/2}$	.00	--
40R	2620.026	38156.17	(.**341**) **1.485** A..	$142_{7/2}$ —$5237_{7/2}$	−.09	--
30R	2620.344	38151.54	(.**118**) **1.816**.....	$217_{7/2}$ —$5992_{7/2}$	+.03	11
10	2621.144	38139.90		$164_{3/2}$ —$5446_{3/2}$	+.01	--
15	2621.975	38127.81	(.**510**).....	$151_{1/2}$ —$5329_{3/2}$	−.02	--
20	2623.285	38108.76	(**.185**, .**554**, .**919**)	$117_{9/2}$ —$4986_{7/2}$	+.06	--
8	2625.041	38083.28		$115_{5/2}$ —$4986_{3/2}$	+.09	--
3	2625.128	38082.02		$164_{3/2}$ —$5440_{3/2}$	−.08	--
7	2625.806	38072.19		$157_{3/2}$ —$5384_{3/2}$	+.08	--
1	2626.200	38066.48		$194_{5/2}$ —$5752_{3/2}$	+.06	--
5	2626.636	38060.16		$204_{3/2}$ —$5854_{1/2}$	+.01	--
1	2627.450	38048.36		$138_{3/2}$ —$5187_{3/2}$	+.05	--
8	2630.150	38009.31		$217_{7/2}$ —$5978_{7/2}$	+.04	--
7	2630.754	38000.59		$150_{7/2}$ —$5305_{5/2}$	+.04	--
20	2631.569	37988.81		$115_{5/2}$ —$4957_{5/2}$	−.36	--
10	2633.006	37968.08		$157_{3/2}$ —$5373_{7/2}$	+.04	--
20	2633.614	37959.32	(.**611**) .**555**.....	$151_{1/2}$ —$5312_{3/2}$	+.02	--
(2h)	2633.775	37957.00		$115_{5/2}$ —$4954_{5/2}$	.00	7
2	2634.908	37940.68		$164_{3/2}$ —$5426_{3/2}$	+.01	--
(1)	2635.29	37935.2		$166_{9/2}$ —$5455_{11/2}$	−.1	13
2	2636.019	37924.68		$244_{5/2}$ —$6235_{7/2}$	−.05	--
100R	2636.637	37915.79	(**.227**, .**691**) .**726**, **1.164**	$0_{3/2}$ —$3791_{3/2}$	−.08	--
10	2641.173	37850.68		$146_{5/2}$ —$5247_{7/2}$ $204_{3/2}$ —$5835_{5/2}$	−.17 −.01	-- --
60R	2642.752	37828.07	(.**754**, **1.217**, **1.679**, **2.144**) .**349**, .**821**, **1.293**, **1.765**, **2.237**	$117_{9/2}$ —$4958_{9/2}$	−.02	--
3	2643.092	37823.21		$150_{7/2}$ —$5288_{5/2}$	+.06	--
5	2644.768	37799.23		$150_{7/2}$ —$5285_{7/2}$	−.02	--
10	2645.804	37784.44		$142_{7/2}$ —$5200_{9/2}$	−.07	--
30R	2647.128	37765.54	(**.302**, .**905**, **1.508**)	$0_{3/2}$ —$3776_{7/2}$	−.11	--
2	2647.240	37763.95		$138_{3/2}$ —$5159_{5/2}$	−.01	--
7	2648.100	37751.67		$146_{5/2}$ —$5237_{7/2}$	+.01	--
50R	2649.050	37738.14	(.**564**, .**934**, **1.305**) .**640**, **1.009**, **1.379**, **1.749**, **2.118**	$142_{7/2}$ —$5195_{7/2}$	−.02	--
10	2649.584	37730.53		$172_{1/2}$ —$5496_{1/2}$	−.02	--
100R	2651.903	37697.55	(.**375**, **1.105**, **1.833**) .**128**, .**858**, **1.581**, **2.311**, **3.040**	$0_{3/2}$ —$3769_{5/2}$	−.11	--
20	2652.911	37683.22		$150_{7/2}$ —$5274_{9/2}$	+.11	--
40R	2654.120	37666.06	(**000**) **1.137**.....	$115_{5/2}$ —$4925_{3/2}$	.00	--
10	2654.773	37656.79		$146_{5/2}$ —$5227_{3/2}$	−.03	--
10	2655.178	37651.05		$138_{3/2}$ —$5147_{3/2}$	+.C2	--
15	2655.844	37641.61	(**0w**) **1.186**h	$163_{11/2}$—$5394_{11/2}$	+.03	10
2h	2656.486	37632.50		$194_{5/2}$ —$5709_{7/2}$	+.10	--
5	2656.950	37625.93		$247_{7/2}$ —$6235_{7/2}$	+.02	--
10	2657.449	37618.87		$217_{7/2}$ —$5939_{9/2}$	−.02	--
7	2658.688	37601.34	(.**318**).....	$164_{3/2}$ —$5392_{1/2}$	−.05	--
20	2659.024	37596.59	(.**135**) **1.058**h, **1.341**h	$146_{5/2}$ —$5221_{5/2}$	−.06	11
10	2659.792	37585.74	(.**120**).....	$263_{13/2}$—$6393_{13/2}$	−.06	--
2	2660.040	37582.22		$231_{5/2}$ —$6073_{5/2}$	−.25	--
2	2661.223	37565.52		$157_{3/2}$ —$5333_{7/2}$	.00	--
5	2661.760	37557.95		$166_{9/2}$ —$5417_{7/2}$	−.02	--
4	2662.196	37551.80		$150_{7/2}$ —$5261_{7/2}$	−.02	--
50	2663.633	37531.54	(**.235**, .**702**, **1.168**, **1.635**, **2.103**)	$117_{9/2}$ —$4928_{11/2}$	−.01	12
10	2664.215	37523.35	(**000**) **1.307**.....	$157_{5/2}$ —$5329_{3/2}$	+.05	--
15	2664.807	37515.02	(.**272**, **.818**).....	$164_{3/2}$ —$5384_{3/2}$	.00	--
1	2666.421	37492.30		$173_{7/2}$ —$5482_{5/2}$	+.10	--
20	2667.130	37482.34	(**0w**) **1.465** wC.	$173_{7/2}$ —$5481_{9/2}$	+.04	--
3	2668.194	37467.39		$166_{9/2}$ —$5408_{7/2}$	.00	--
5	2669.868	37443.89		$115_{5/2}$ —$4903_{7/2}$	.00	--
20	2670.236	37438.74	(.**316**, **.542**).....	$115_{5/2}$ —$4902_{3/2}$	−.07	--
30	2670.790	37430.97	(.**672**, **1.092**, **1.513**) .**919**, **1.344**, **1.769**	$142_{7/2}$ —$5164_{7/2}$	+.01	--
3	2671.329	37423.42		$263_{13/2}$—$6377_{13/2}$	−.02	--
40	2671.842	37416.24	(.**619**, **1.022**, **1.424**, **1.826**) .**527**, .**927**, **1.328**, **1.728**, **2.129**	$117_{9/2}$ —$4917_{9/2}$	.00	--
5	2672.420	37408.15		$194_{5/2}$ —$5686_{7/2}$	−.02	--
200R	2674.339	37381.30	(.**481**, **1.440**, **2.399**) .**490**, **1.458**, **2.423**, **3.383**	$0_{3/2}$ —$3738_{3/2}$	−.11	--
5	2674.917	37373.23		$142_{7/2}$ —$5159_{5/2}$	+.01	--
9	2676.088	37356.88		$138_{3/2}$ —$5118_{3/2}$	.00	--
15	2677.764	37333.49	(**000**) **1.281** D..	$146_{5/2}$ —$5195_{7/2}$	− 07	--
3	2678.054	37329.45		$166_{9/2}$ —$5394_{11/2}$	.00	--
20	2679.096	37314.93	(.**459**, .**784**, **1.108**)	$150_{7/2}$ —$5237_{7/2}$	.00	--

TABLE 2. *Classified lines of* Re I—Continued

Int.	λ_{vac}	σ_{vac}	Zeeman effect	Transition	O-C	Notes	Int.	λ_{vac}	σ_{vac}	Zeeman effect	Transition	O-C	Notes
	A	*K*						*A*	*K*				
30	2679.914	37303.55	(.524) 1.834	$151_{1/2}-5246_{1/2}$	−.01		30	2753.046	36312.66		$146_{5/2}-5093_{5/2}$	−.06	..
9	2681.010	37288.29	(.331)	$157_{5/2}-5305_{5/2}$	−.03	..	20	2755.212	36284.12		$138_{1/2}-5011_{3/2}$	−.04	..
(2)	2682.067	37273.60		$115_{3/2}-4885_{7/2}$	−.04	7	40r	2757.996	36247.49	(0w) 1.401h†	$146_{3/2}-5086_{7/2}$	−.05	..
5	2682.368	37269.41		$142_{7/2}-5148_{9/2}$	−.02	..	10h	2758.05	36246.7		$142_{7/2}-5046_{5/2}$	−.2	..
3	2683.030	37260.22		$142_{7/2}-5147_{7/2}$	−.07	..	10	2758.706	36238.17		$166_{9/2}-5285_{7/2}$	+.01	..
40	2683.558	37252.89	(0w) .959 D	$146_{5/2}-5187_{3/2}$	−.08	..	20	2761.926	36195.92	(0w) 1.156C	$115_{5/2}-4777_{3/2}$	−.03	..
3	2684.382	37241.46		$194_{3/2}-5669_{7/2}$	−.06	..	4	2762.786	36184.66		$157_{5/2}-5195_{7/2}$	+.06	..
3	2684.905	37234.21		$221_{9/2}-5939_{9/2}$	−.04	..	40	2763.295	36177.99	(.118, .342, .563)	$117_{9/2}-4793_{7/2}$	−.04	..
100	2688.528	37184.03	(0w) 1.456 B	$157_{5/2}-5296_{3/2}$	−.01	..							
20H	2690.247	37160.27		$163_{11/2}-5346_{11/2}$	−.15	..	40	2763.792	36171.49	(.246h) 1.166h	$150_{7/2}-5122_{7/2}$	+.04	..
4	2693.224	37119.20		$166_{9/2}-5373_{7/2}$	+.02	..	9	2766.051	36141.94		$164_{3/2}-5246_{1/2}$	.00	..
8	2693.719	37112.38		$151_{1/2}-5227_{1/2}$	−.01	..	30	2766.390	36137.52		$270_{13/2}-6326_{11/2}$	+.03	..
8	2693.822	37110.97		$157_{5/2}-5288_{3/2}$	+.05	..	7	2766.548	36135.45	(000) 1.256	$150_{7/2}-5119_{9/2}$	+.15	..
3	2694.034	37108.03		$138_{3/2}-5093_{3/2}$	−.03	..	5	2767.576	36122.03		$166_{9/2}-5274_{9/2}$	+.01	..
20	2694.394	37103.08	(.434, .726, 1.018, **1.309**) .202, .498, .793, 1.092	$117_{9/2}-4885_{7/2}$	.00	..	20	2767.744	36119.84	(**.095**, .283) **1.023**, 1.212, 1.400	$115_{5/2}-4770_{3/2}$	+.02	..
							6H	2768.282	36112.81		$247_{7/2}-6083_{5/2}$	−.07	..
15	2695.562	37087.00	(000) 1.268	$157_{5/2}-5285_{7/2}$	−.02	..	15	2768.851	36105.39	(.176, .515, .853, 1.192), **.337**, .000, .337, .675, 1.014	$117_{9/2}-4785_{11/2}$	−.02	..
2	2696.159	37078.79		$173_{7/2}-5440_{5/2}$	.00	..							
7	2696.640	37072.18		$163_{11/2}-5357_{9/2}$	−.02	..							
20	2697.265	37063.59	(.664) 1.284, **2.616**	$0_{3/2}-3706_{3/2}$	−.06	..							
3	2697.368	37062.18		$164_{3/2}-5338_{5/2}$	−.04	..	3	2768.954	36104.05		$157_{5/2}-5187_{3/2}$	+.04	..
15h	2698.794	37042.59	(**.131**, .402) 1.598	$204_{1/2}-5752_{3/2}$	+.01	..	4	2769.735	36093.87		$142_{7/2}-5031_{7/2}$	+.03	..
							70R	2770.417	36084.99	(0w) 1.021C	$115_{5/2}-4766_{7/2}$	−.06	..
15	2699.580	37031.81		$117_{9/2}-4878_{7/2}$	−.02	..	15	2771.609	36069.47		$138_{1/2}-4989_{1/2}$	+.02	..
3	2699.978	37026.35		$146_{5/2}-5164_{7/2}$	−.01	..	8	2772.421	36058.90		$173_{7/2}-5338_{5/2}$	−.01	..
8	2700.891	37013.84		$163_{11/2}-5332_{9/2}$	+.04	..	3	2772.687	36055.44		$172_{1/2}-5329_{1/2}$	+.02	..
2	2700.977	37012.66		$142_{7/2}-5122_{7/2}$	−.12	..	20	2773.109	36049.96	(.578) 1.950	$172_{1/2}-5328_{1/2}$	−.02	..
3	2704.179	36968.83		$146_{5/2}-5159_{3/2}$	+.21	..	2	2773.214	36048.59		$173_{7/2}-5337_{9/2}$	+.06	..
20	2704.369	36966.23	(.191, **.572**) 1.147, **1.522**, 1.896†	$164_{3/2}-5329_{3/2}$	+.02	..	10	2774.383	36033.41	(.530)†	$138_{1/2}-4985_{1/2}$	.00	..
							10	2775.126	36023.76		$273_{11/2}-6326_{11/2}$	+.01	..
							10	2775.126	36023.76		$273_{11/2}-6326_{11/2}$	+.01	..
6	2704.769	36960.77		$164_{1/2}-5328_{1/2}$	.00	..	2	2775.457	36019.47		$224_{1/2}-5844_{1/2}$	−.21	..
6	2705.076	36956.58		$146_{5/2}-5157_{3/2}$	−.01	..	15	2775.639	36017.11	(.457) 1.010	$151_{1/2}-5118_{3/2}$	.00	..
15	2706.056	36943.18	(**.101**, .307, .506, .705)	$150_{7/2}-5200_{9/2}$	.00	..	10	2775.948	36013.10		$247_{7/2}-6073_{5/2}$	+.04	..
							1	2776.560	36005.15		$173_{7/2}-5333_{7/2}$	+.03	..
5	2706.480	36937.40		$173_{7/2}-5426_{5/2}$	+.04	..	8	2777.223	35996.56		$194_{5/2}-5545_{7/2}$	−.03	..
10	2707.852	36918.69	(0w) .901h	$263_{13/2}-6326_{11/2}$	+.02	..	15	2777.71	35990.3		$173_{7/2}-5332_{9/2}$	+.2	..
2	2711.382	36870.62		$224_{1/2}-5929_{1/2}$	.00	..	10	2778.498	35980.04	(**.111**, .331, .550) **.537**, **.756**, .976	$142_{7/2}-5019_{9/2}$	−.04	..
20	2712.476	36855.76		$146_{5/2}-5147_{5/2}$	+.07	..							
15	2713.024	36848.31		$166_{9/2}-5346_{11/2}$	+.02	..							
10	2713.160	36846.47		$173_{7/2}-5417_{7/2}$	+.04	..	10	2779.082	35972.49		$231_{3/2}-5912_{1/2}$	.00	..
8	2713.664	36839.63		$157_{5/2}-5261_{7/2}$	+.04	..	15	2779.290	35969.79		$150_{7/2}-5102_{9/2}$	+.02	..
300R	2715.474	36815.06	(**.131**, .397, .659, .925, 1.197) **.070**, .336, .603, .869, 1.133	$117_{9/2}-4856_{11/2}$	−.05	..	15	2780.850	35949.61		$146_{5/2}-5057_{3/2}$	+.05	..
							30r	2781.434	35942.06	(**.072**, .217, .363) 1.894	$142_{7/2}-5015_{5/2}$	+.05	..
							7	2783.141	35920.03		$163_{11/2}-5222_{13/2}$	−.02	..
							60	2783.570	35914.49	(.164, .504, .844, 1.184), 2.614	$117_{9/2}-4766_{7\ 2}$	.00	..
30r	2715.770	36811.05		$142_{7/2}-5102_{9/2}$	−.05	..							
20	2716.246	36804.60		$270_{13/2}-6393_{13/2}$	−.02	..	50r	2785.206	35893.39	(**.085**, .256, .427) 1.179	$142_{7/2}-5011_{5/2}$	−.03	..
15	2716.754	36797.72	(.280, **.859**)	$164_{3/2}-5312_{3/2}$	+.04	..							
(3)	2718.659	36771.95		$231_{5/2}-5992_{7/2}$	−.15	7	10	2785.424	35890.58		$164_{3/2}-5221_{5/2}$	−.02	..
15	2719.536	36760.08	(.442) A	$166_{9/2}-5357_{9/2}$	+.01	..	9	2785.714	35886.85	(.689)	$172_{1/2}-5312_{3/2}$	−.04	..
9	2719.848	36755.86		$173_{7/2}-5408_{7/2}$	+.01	..	15	2786.138	35881.39	(0w) 1.300h	$217_{7/2}-5765_{7/2}$	−.06	..
2	2720.364	36748.89		$224_{3/2}-5917_{5/2}$	−.01	..	3	2786.450	35877.37		$157_{5/2}-5164_{7/2}$	−.03	..
10	2720.659	36744.91		$138_{3/2}-5057_{3/2}$	+.01	..	20r	2786.558	35875.98	(**.114**, .350, .575) **.580**, .810, 1.040, 1.270	$150_{7/2}-5093_{5/2}$	−.01	..
7	2721.675	36731.20		$164_{1/2}-5305_{3/2}$	−.03	..							
80	2722.702	36717.35	(**.100**, .286, .470)	$142_{7/2}-5093_{5/2}$	+.03	..							
10	2723.356	36708.52		$151_{1/2}-5187_{3/2}$	−.02	..	7	2789.173	35842.34		$146_{5/2}-5046_{5/2}$	.00	..
30	2723.836	36702.05		$157_{5/2}-5247_{3/2}$	+.16	..	15	2789.268	35841.12	(334h)	$138_{1/2}-4996_{3/2}$	+.09	..
5h	2724.437	36693.96		$197_{1/2}-5645_{1/2}$	.00	..	30	2790.939	35819.67	(.457, **.755**) .566, .867, **1.168**, 1.468, 1.771	$157_{5/2}-5159_{3/2}$	+.01	..
9	2724.686	36690.60		$172_{1/2}-5392_{1/2}$	.00	..							
3	2724.934	36687.27		$173_{7/2}-5401_{7/2}$	−.10	..							
20	2727.548	36652.10	(.456, .808, **1.159**)	$142_{7/2}-5086_{7/2}$	−.04	..							
							50r	2791.290	35815.16	(.398) .734C	$163_{11/2}-5212_{13/2}$	−.04	..
3h	2728.286	36642.19		$270_{13/2}-6377_{13/2}$	−.07	..	10	2791.626	35810.85		$150_{7/2}-5086_{7/2}$	+.04	..
10	2728.628	36637.60	(**.172**, .496)	$138_{3/2}-5046_{3\ 2}$	−.08	..	2	2792.940	35794.01		$263_{13/2}-6214_{11/2}$	.00	..
2	2729.209	36629.80		$231_{5/2}-5978_{7/2}$	−.06	..	3	2794.472	35774.38		$115_{5/2}-4735_{7/2}$	−.02	..
4	2729.427	36626.88		$164_{3/2}-5296_{1/2}$	−.07	..	10l	2796.078	35753.84		$166_{9/2}-5237_{7/2}$	.00	..
10	2729.635	36624.09		$164_{3/2}-5295_{3/2}$	+.01	..	2	2796.467	35748.87		$217_{7/2}-5752_{3/2}$	−.04	..
10	2730.826	36608.12		$146_{5/2}-5122_{7/2}$	−.06	..	9	2796.616	35746.96		$138_{3/2}-4957_{5/2}$	−.03	..
3h	2731.228	36602.73		$157_{5/2}-5237_{7/2}$	+.03	..	10	2798.104	35727.95	(0w) 1.385B	$173_{7/2}-5305_{3/2}$	+.03	..
2	2731.416	36600.20		$115_{5/2}-4818_{7/2}$	−.04	..	3	2799.245	35713.39	(.434) 2.198	$172_{1/2}-5295_{3/2}$	+.10	..
50R	2732.206	36589.62		$150_{7/2}-5164_{7/2}$	−.01	..	4	2800.746	35694.25		$163_{11/2}-5200_{9/2}$	+.03	..
10	2734.31	36561.5		$146_{5/2}-5118_{3/2}$	.0	..	3	2801.184	35688.66		$266_{5/2}-6235_{7/2}$	−.04	..
10	2734.886	36553.78		$164_{3/2}-5288_{3/2}$	−.05	..	5	2804.506	35646.40		$142_{7/2}-4986_{7/2}$	+.04	..
6	2736.522	36531.92		$150_{7/2}-5159_{3/2}$	+.03	..	4	2805.105	35638.78		$163_{11/2}-5194_{11/2}$	−.01	..
10	2736.767	36528.65		$273_{11/2}-6377_{13/2}$	+.13	..	7	2805.977	35627.71	(.496) .987?	$224_{3/2}-5805_{3/2}$	−.04	..
15	2738.323	36507.90	(0w) 1.148C	$151_{3/2}-5227_{3/2}$	+.04	..	20	2807.86	35603.8	(**.198**, .579, .960)	$117_{9/2}-4735_{7/2}$	.0	..
4	2738.625	36503.87		$217_{7/2}-5827_{9/2}$	−.04	..	4h	2808.456	35596.27		$217_{7/2}-5737_{7/2}$	−.08	..
4	2740.074	36484.56		$217_{7/2}-5826_{7/2}$	−.07	..	3	2809.109	35587.98		$115_{5/2}-4717_{3/2}$	−.1	..
15	2741.967	36459.38		$221_{9/2}-5861_{11/2}$	+.10	..	15	2812.073	35550.48	(**.104**, .306, .509) 1.153, 1.358, 1.562, **1.766**	$173_{7/2}-5288_{3/2}$	−.04	..
10	2742.856	36447.57		$157_{5/2}-5221_{3/2}$	−.12	..							
2	2743.122	36444.02		$194_{3/2}-5590_{3/2}$	−.10	..							
3	2743.650	36437.01		$138_{3/2}-5026_{3/2}$	−.09	..							
15	2743.874	36434.04		$163_{11/2}-5274_{9/2}$	−.11	..	20	2812.356	35546.91	(.208, **.626**) 1.085, **1.503**, 1.922	$164_{1/2}-5187_{3/2}$	−.01	..
20	2744.207	36429.62		$117_{9/2}-4818_{7/2}$	−.06	..							
2	2745.014	36418.91		$150_{7/2}-5147_{5/2}$	−.05	..							
5H	2745.564	36411.62		$244_{3/2}-6083_{5/2}$	−.08	..	15	2813.112	35537.34		$146_{5/2}-5015_{5/2}$	−.07	..
15	2745.867	36407.60	(.130) 1.210h	$173_{7/2}-5373_{7/2}$	−.04	..	20h	2813.964	35526.59	(.132) 1.277h	$173_{7/2}-5285_{7/2}$	−.03	..
20r	2747.438	36386.79	(.291) 1.233A	$115_{5/2}-4797_{3\ 2}$	−.07	..	40R	2814.676	35517.60	(.196, .587, .968) .309, .695, **1.081**, 1.467, 1.855	$115_{5/2}-4710_{3/2}$	−.05	..
1	2747.627	36384.28		$204_{3/2}-5686_{3/2}$	−.05	..							
6	2750.322	36348.63		$115_{5/2}-4793_{7/2}$	+.04	..							
3	2751.51	36333.0		$138_{3/2}-5015_{5/2}$	+.2	..							
15	2752.852	36315.22		$115_{5/2}-4789_{3/2}$	−.04	..	10	2815.640	35505.45		$217_{7/2}-5728_{9/2}$	−.01	..

TABLE 2. *Classified lines of* Re I—Continued

Int.	λ_{vac}	σ_{vac}	Zeeman effect	Transition	O–C	Notes
	A	*K*				
30	2816.319	35496.89	(.115) 1.191	$221_{9/2}-5765_{7/2}$	+.08	--
30	2816.954	35488.89	(.294, .879, **1.463**) .274, .858, **1.441**, 2.025, 2.609	$146_{5/2}-5011_{5/2}$	+.07	--
4	2819.528	35456.49		$239_{11/2}-5941_{11/2}$	+.03	--
50	2819.951	35451.17	(.699, 1.089, 1.528, **1.968**) .000, .441, .881, **1.313**, 1.745, 2.177, 2.610	$117_{9/2}-4720_{9/2}$	−.04	--
4	2820.976	35438.29		$239_{11/2}-5939_{9/2}$	.00	--
15	2822.123	35423.88	(.108, **.321**) 1.167, 1.376	$138_{9/2}-4925_{7/2}$	−.02	--
9	2822.407	35420.32		$115_{5/2}-4700_{7/2}$ $204_{3/2}-5590_{5/2}$	−.06 +.04	-- --
15	2823.193	35410.46		$173_{7/2}-5274_{9/2}$	−.02	--
2	2823.592	35405.46		$150_{7/2}-5046_{5/2}$	−.15	--
20	2824.245	35397.27	(.163) 1.202h	$217_{7/2}-5717_{7/2}$	−.03	--
20	2825.458	35382.07	(.483, .672, **.861**)	$166_{9/2}-5200_{9/2}$	−.02	--
3	2826.759	35365.79		$142_{7/2}-4958_{9/2}$	+.04	--
4	2826.812	35365.13		$194_{5/2}-5482_{5/2}$	.00	--
7	2827.284	35359.22		$244_{5/2}-5978_{7/2}$	−.05	--
30	2827.523	35356.24	(**.111**, .333, .553) 2.161	$142_{7/2}-4957_{5/2}$	−.01	--
7	2827.834	35352.35		$271_{7/2}-6249_{7/2}$	−.03	--
4	2829.164	35335.73	(0w) 1.160h	$166_{9/2}-5195_{7/2}$	−.01	--
10	2829.887	35326.71		$166_{9/2}-5194_{11/2}$	+.05	--
6	2830.096	35324.09		$142_{7/2}-4954_{5/2}$	−.01	--
9	2830.833	35314.89		$217_{7/2}-5709_{7/2}$	.00	--
2	2833.02	35287.7		$231_{5/2}-5844_{5/2}$	.0	--
40	2834.077	35274.47	(**.424**, 1.270) −**.124**, 725, 1.572	$146_{5/2}-4989_{7/2}$	+.36	12, 14
15	2834.608	35267.87		$0_{5/2}-3586_{5/2}$	+.07	--
5	2835.034	35262.57		$164_{3/2}-5159_{5/2}$	.00	11
3	2835.844	35252.50		$150_{7/2}-5031_{7/2}$	−.01	--
6	2836.005	35250.50		$164_{3/2}-5157_{3/2}$	−.04	--
7hs	2836.696	35241.91		$146_{5/2}-4986_{7/2}$	+.15	--
30	2837.547	35231.35	(000) 1.190	$221_{9/2}-5739_{11/2}$	−.05	--
8	2839.193	35210.92	(.168) 1.148†?	$197_{1/2}-5496_{1/2}$	−.02	--
50r	2840.348	35196.60	(000) 1.505	$138_{9/2}-4902_{5/2}$	−.05	--
3	2840.979	35188.79		$272_{9/2}-6235_{7/2}$	+.01	--
60r	2843.000	35163.77	(.159) 1.354A	$157_{5/2}-5093_{5/2}$	+.01	--
20	2844.162	35149.40	(**.293**, .879) **.406**, .992, 1.578	$115_{5/2}-4773_{3/2}$	−.02	--
8	2846.478	35120.80		$221_{9/2}-5728_{9/2}$	−.02	--
6	2847.744	35105.19		$231_{5/2}-5826_{7/2}$	−.03	--
2h	2848.112	35100.66		$150_{7/2}-5015_{5/2}$	−.02	--
3	2848.280	35098.59		$157_{5/2}-5086_{7/2}$	+.01	--
3	2848.400	35097.11		$151_{1/2}-5026_{3/2}$	−.22	--
60r	2850.975	35065.41	(.122) 1.302	$115_{5/2}-4864_{5/2}$	−.05	--
2	2851.744	35055.95		$194_{5/2}-5451_{7/2}$	.00	--
10	2852.054	35052.15		$150_{7/2}-5011_{5/2}$	+.06	--
20	2852.841	35042.48		$173_{7/2}-5237_{7/2}$	+.18	--
10	2855.528	35009.50	(000) 1.352	$194_{5/2}-5449_{3/2}$	−.01	--
4	2857.808	34981.58		$272_{9/2}-6214_{11/2}$	−.04	--
(4)	2857.985	34979.41		$275_{9/2}-6249_{7/2}$	+.21	7
20	2860.074	34953.86		$142_{7/2}-4917_{9/2}$	−.04	--
15	2860.254	34951.66		$194_{5/2}-5449_{3/2}$ $146_{5/2}-4957_{5/2}$	−.06 +.01	-- --
2	2862.009	34930.22		$221_{9/2}-5709_{7/2}$	−.03	--
15	2862.890	34919.48		$146_{5/2}-4954_{5/2}$	−.02	--
15	2864.563	34899.09		$273_{11/2}-6214_{11/2}$	.00	--
10	2864.831	34895.82		$231_{5/2}-5805_{5/2}$	+.05	--
3	2865.526	34887.37		$173_{7/2}-5221_{5/2}$	+.08	--
2	2865.612	34886.32		$163_{11/2}-5119_{9/2}$	−.02	--
30	2867.193	34867.07	(000) 1.166 C	$166_{9/2}-5148_{9/2}$	+.06	--
(5)	2868.151	34855.43	(375)	$164_{3/2}-5118_{3/2}$	−.06	3
3	2869.764	34835.84		$275_{9/2}-6235_{7/2}$	+.02	--
30	2871.82	34810.9	(.233) 1.543h†	$142_{7/2}-4903_{7/2}$	−.1	--
10	2872.304	34805.04	(000) 1.169	$150_{7/2}-4986_{7/2}$	+.01	--
10	2872.668	34800.63		$157_{5/2}-5057_{3/2}$	+.03	--
30	2875.282	34768.99	(000) 1.260	$115_{5/2}-4835_{7/2}$	−.04	--
1	2878.538	34729.66		$151_{1/2}-4989_{3/2}$	−.02	--
20	2879.271	34720.82		$163_{11/2}-5102_{9/2}$	+.01	--
3	2879.391	34719.37		$194_{5/2}-5417_{7/2}$	+.01	--
1	2880.212	34709.48		$197_{1/2}-5446_{3/2}$	−.01	--
6	2880.840	34701.91	(0w) .865 C	$244_{5/2}-5912_{5/2}$	+.01	--
10	2881.546	34693.41		$157_{5/2}-5046_{5/2}$	+.03	--
30	2883.444	34670.57	(0w) 1.694 B	$173_{7/2}-5200_{9/2}$	+.02	--
15	2884.045	34663.35		$239_{11/2}-5861_{11/2}$	+.03	--
4	2885.120	34650.44		$224_{3/2}-5707_{1/2}$	−.04	--
10	2885.930	34640.72		$142_{7/2}-4885_{7/2}$	−.02	--
4	2886.312	34636.13		$172_{1/2}-5187_{3/2}$	.00	--
15	2886.935	34628.66		$194_{5/2}-5408_{7/2}$ $275_{9/2}-6214_{11/2}$ $146_{5/2}-4925_{3/2}$	−.12 .00 +.10	-- -- --
15	2887.307	34624.19		$173_{7/2}-5195_{7/2}$	−.01	--
300R	2887.676	34619.76	(.383, .594, .805, **1.016**) .603, .815, 1.026, 1.239, **1.452**, 1.664, 1.877, 2.089, 2.301†.	$117_{9/2}-4637_{9/2}$	+.03	--
4	2888.456	34610.42		$166_{9/2}-5122_{7/2}$	+.06	--
20	2889.448	34598.54	(**.132**, .390, .678).	$117_{9/2}-4635_{7/2}$	+.07	--
20	2891.481	34574.21		$166_{9/2}-5119_{9/2}$	.00	--
30	2891.878	34569.46	(.137) 1.550h	$142_{7/2}-4878_{7/2}$	−.03	--
20	2892.634	34560.43	(0w)	$194_{5/2}-5401_{7/2}$	+.13	--
10	2894.322	34540.28	(**.081**, .245, .411) **.754**, .915, 1.076, 1.237.	$157_{5/2}-5031_{7/2}$	+.02	--
4H	2894.969	34532.56		$217_{7/2}-5830_{9/2}$	−.01	--
2	2895.328	34528.27		$115_{5/2}-4611_{5/2}$	−.01	--
15	2895.650	34524.43		$150_{7/2}-4958_{9/2}$	+.01	--
60R	2896.012	34520.12	(**.251**, .747, 1.240) **.220**, .715, 1.211, 1.696, 2.191.	$0_{5/2}-3452_{7/2}$	−.13	--
8	2896.446	34514.95		$150_{7/2}-4957_{5/2}$	+.03	--
10	2897.585	34501.38	(.550) .707†?	$151_{1/2}-4966_{3/2}$	+.12	--
10	2898.785	34487.11	(.071) 1.506	$204_{3/2}-5496_{1/2}$	−.01	--
3	2902.112	34447.57		$247_{7/2}-5917_{5/2}$	+.06	--
100	2902.48	34443.2	(0w) 1.186B	$224_{3/2}-5686_{3/2}$	.0	15
10	2905.393	34408.67		$166_{9/2}-5102_{9/2}$	−.01	--
30	2905.584	34406.41	(**.173**, 515, .858)†.	$146_{5/2}-4933_{7/2}$	+.02	--
15	2906.016	34401.29	(.881) .596, .956, **1.312**, 1.665, 2.018†.	$146_{5/2}-4902_{5/2}$	−.02	--
(2h)	2906.11	34400.2		$224_{3/2}-5682_{5/2}$	+.3	7
10	2907.100	34388.46	(.266) A	$157_{5/2}-5015_{5/2}$	+.01	--
2h	2907.434	34384.51		$194_{3/2}-5384_{1/2}$	−.13	--
2	2908.704	34369.50		$231_{5/2}-5752_{5/2}$	.00	--
60r	2909.829	34356.32	(.139) 1.234 A	$163_{11/2}-5066_{11/2}$	−.04	--
9	2910.084	34353.21	(000) 1.334	$115_{5/2}-4593_{7/2}$	−.01	--
2	2911.094	34341.28		$204_{3/2}-5482_{5/2}$	−.01	--
8	2911.232	34339.65		$172_{1/2}-5157_{3/2}$	−.10	--
3	2912.915	34319.82		$280_{5/2}-6235_{7/2}$	+.01	--
10	2913.154	34317.00	(.392) A	$173_{7/2}-5164_{7/2}$	.00	--
3	2915.246	34292.37		$115_{5/2}-4587_{3/2}$	−.01	--
3	2916.256	34280.50		$194_{3/2}-5375_{7/2}$	−.07	--
2	2918.052	34259.41		$173_{7/2}-5159_{5/2}$	+.15	--
1	2918.760	34251.10		$221_{9/2}-5641_{9/2}$	−.08	--
7	2918.877	34249.73		$166_{9/2}-5086_{7/2}$	+.01	--
20	2919.407	34243.50	(.372, **1.146**) .559, **1.307**, 2.057†?	$164_{3/2}-5037_{3/2}$	−.01	--
3	2921.676	34216.91		$231_{5/2}-5737_{7/2}$	−.03	--
20	2924.60	34182.7		$117_{9/2}-4593_{7/2}$	.0	--
20	2925.195	34175.75	(.214h) 1.242h	$266_{5/2}-6083_{5/2}$	+.08	--
2d	2925.606	34170.95		$197_{1/2}-5392_{1/2}$	−.04	--
1	2926.124	34164.90		$146_{5/2}-4878_{7/2}$	+.01	--
9	2926.934	34155.45		$173_{7/2}-5148_{9/2}$	−.02	--
40	2927.42	34149.7	(**.184**, .549, .912, 1.111, 1.302).	$117_{9/2}-4590_{11/2}$	.0	--
5	2927.714	34146.34		$173_{7/2}-5147_{5/2}$	+.01	--
2	2927.852	34144.73		$138_{5/2}-4797_{5/2}$	+.03	--
7	2928.576	34136.29	(**.282**, .854)	$164_{3/2}-5046_{5/2}$	.00	--
10	2929.48	34125.7		$217_{7/2}-5589_{7/2}$	−.1	--
10	2929.530	34125.18		$157_{5/2}-4989_{3/2}$	+.03	--
20	2930.610	34112.61	(0w) 1.110B	$150_{7/2}-4917_{9/2}$	+.04	--
4	2932.223	34093.84		$613_{11/2}-5040_{9/2}$	−.02	--
7	2932.317	34092.74		$157_{5/2}-4986_{7/2}$	−.06	--
5	2934.010	34073.08		$138_{5/2}-4789_{5/2}$	−.02	--
15	2936.500	34044.18	(0w) 1.408B	$166_{9/2}-5066_{11/2}$	−.05	--
8	2937.810	34029.01	(.253) .518	$224_{3/2}-5645_{1/2}$	−.03	--
5	2938.772	34017.87		$231_{5/2}-5717_{7/2}$	−.02	--
2	2938.841	34017.07		$244_{5/2}-5844_{3/2}$	−.04	--
9	2941.557	33985.66	(.127) 1.383h	$204_{3/2}-5446_{3/2}$	−.01	--
50r	2943.145	33967.32	(.160, .475, .800, **1.125**) .456, .775, 1.094, **1.411**, 1.730, 2.049, 2.368.	$142_{7/2}-4818_{7/2}$	−.02	--
10	2943.382	33964.58		$150_{7/2}-4902_{5/2}$	.00	--
8	2944.320	33953.77	(.168)	$138_{5/2}-4777_{3/2}$	.00	--
3	2945.106	33944.71		$172_{1/2}-5118_{3/2}$	+ 01	--
5	2945.886	33935.72	(.709)	$164_{3/2}-5026_{3/2}$	+.01	--
9	2946.572	33927.82	(.192, **.367**) **.447**, .865, 1.250.	$204_{3/2}-5440_{5/2}$	−.06	--
2h	2948.384	33906.97		$244_{5/2}-5833_{5/2}$	−.05	--
15	2949.088	33898.87	(0w) 1.246h	$173_{7/2}-5122_{7/2}$	+.05	--
7	2949.261	33896.89		$157_{5/2}-4966_{3/2}$	+.16	--
10	2949.880	33889.78		$163_{11/2}-5019_{9/2}$	−.01	--
10	2950.828	33878.89	(000) 1.331	$115_{5/2}-4546_{7/2}$	+.02	--
7	2950.920	33877.84		$194_{5/2}-5333_{7/2}$	−.19	--
15	2954.335	33838.68	(000) 1.478	$138_{5/2}-4765_{7/2}$	+.06	--
6	2954.580	33835.87		$194_{5/2}-5329_{3/2}$	+.04	--
5	2954.688	33834.63		$244_{5/2}-5826_{7/2}$	.00	--
2	2954.968	33831.43		$164_{3/2}-5015_{5/2}$	+.07	--
2	2957.762	33799.47		$150_{7/2}-4885_{7/2}$	+.06	--
7	2958.904	33786.43	(**.080**, .237)	$204_{3/2}-5426_{5/2}$	−.02	--
2h	2959.33	33781.5		$166_{9/2}-5040_{9/2}$	−.2	--
4	2960.296	33770.53		$157_{5/2}-4965_{3/2}$	−.01	--
20	2961.744	33754.03	(**.207**, .607)	$142_{7/2}-4797_{5/2}$	+.07	--
2	2961.880	33752.48		$221_{9/2}-5591_{9/2}$	+.10	--

Int.	λ_{vac}	σ_{vac}	Zeeman effect	Transition	O-C	Notes
	A	*K*				
30r	2962.266	33748.08	(.099, .294, .490) .787, .983, **1.179**, 1.374, 1.569.	$115_{9/2} - 4533_{3/2}$	+.01	..
15	2962.870	33741.20	(000) 1.142h....	$221_{9/2} - 5589_{7/2}$	+.04	..
2	2964.01	33728.2	.....	$150_{7/2} - 4878_{7/2}$	.0	..
80R	2965.112	33715.69	(.474, .809, **1.142**) 1.083, 1.408, **1.733**, 2.057, 2.382†.	$142_{7/2} - 4793_{7/2}$	.00	..
2	2965.502	33711.25	.....	$231_{5/2} - 5686_{3/2}$	.00	..
150R	2965.756	33708.37	(.119, .358, .596, .834) 2.440†.	$117_{9/2} - 4546_{7/}$	+.06	..
2	2966.416	33700.87	.....	$239_{11/2} - 5765_{9/2}$	+.02	..
2	2966.746	33697.12	.....	$173_{7/2} - 5102_{9/2}$	−.02	..
10	2967.246	33691.43	(000) 1.196....	$166_{9/2} - 5051_{7/2}$	+.01	..
20	2968.044	33682.38	(**.173**, .521, .870) 1.048, 1.395, 1.742, 2.089, **2.436**.	$142_{7/2} - 4789_{9/2}$	+.02	..
3	2968.330	33679.13	.....	$217_{7/2} - 5545_{7/2}$	+.05	..
8	2975.023	33603.37	.....	$173_{7/2} - 5093_{5/2}$	+.01	..
10	2975.250	33600.80	(.088, .263, **.438**) . . . , **1.273**, . . .	$194_{5/2} - 5305_{5/2}$	−.05	..
3	2975.658	33596.20	.....	$271_{7/2} - 6073_{5/2}$	+.05	..
40	2976.294	33589.02	{(**412**, .816), .535, .930, **1.333**.	$0_{5/2} - 5358_{3/2}$	−.10	..
9	2977.300	33577.67	(.760) A.....	$117_{9/2} - 4534_{9/2}$	−.03	..
20	2978.152	33568.07	(.432) 1.565, **1.852**, 2.138	$166_{9/2} - 5019_{9/2}$	+.01	..
1	2978.622	33562.77	.....	$164_{3/2} - 4989_{3/2}$	+.01	..
2	2980.244	33544.50	.....	$146_{3/2} - 4818_{7/2}$	+.03	..
20	2980.820	33538.02	.....	$231_{3/2} - 5669_{7/2}$	−.10	..
7	2981.010	33535.89	.....	$173_{7/2} - 5086_{7/2}$	−.16	..
2	2981.350	33532.06	.....	$115_{5/2} - 4512_{5/2}$	+.17	..
3	2981.495	33530.43	.....	$197_{1/2} - 5329_{3/2}$	+.08	..
4	2984.504	33496.62	.....	$247_{7/2} - 5826_{7/2}$	+.08	..
7	2984.750	33493.86	(.156) 1.594h†..	$164_{3/2} - 4985_{1/2}$	+.04	..
7d	2986.050	33479.29	(.502)†.....	$194_{3/2} - 5296_{3/2}$	+.03	..
20	2988.471	33452.16	(.190, .564, .929, **1.294**) .292, .643, 1.012, **1.377**, 1.742, 2.108.	$194_{3/2} - 5295_{1/2}$	+.16	..
4	2988.918	33447.16	.....	$224_{1/2} - 5590_{3/2}$	+.11	..
150R	2992.363	33408.65	(.223, .671, **1.120**) .830, 1.277, **1.727**, 2.174, 2.621.	$142_{7/2} - 4766_{7/2}$	+.01	..
8	2993.176	33399.58	.....	$204_{3/2} - 5392_{1/2}$	−.01	..
20	2995.395	33374.84	(0w) 1.065B...	$0_{3/2} - 5340_{3/2}$	−.08	..
2	2996.074	33367.27	.....	$194_{5/2} - 5285_{7/2}$	+.03	..
3	2996.533	33362.16	.....	$305_{11/2} - 6393_{13/2}$	−.01	..
9	2997.686	33349.34	(000) 1.149....	$197_{1/2} - 5312_{1/2}$	−.01	5
4	2997.902	33346.93	(.365) 1.093w†?	$115_{5/2} - 4494_{7/2}$	.00	..
5	2997.980	33346.07	.....	$146_{3/2} - 4797_{3/2}$	−.02	..
5	2998.550	33339.73	(.677).....	$138_{1/2} - 4718_{1/2}$	+.1	..
200R	2999.599	33328.06	(**.072**, .219, .366, .513), **.731**, .882. 1.032, 1.182, 1.332, 1.482.	$138_{1/2} - 4717_{1/2}$	+.1	..
			.....	$164_{1/2} - 4966_{1/2}$	+.09	..
			.....	$117_{9/2} - 4508_{11/2}$	−.05	..
4	3000.581	33317.16	.....	$115_{5/2} - 4490_{7/2}$	−.03	..
20r	3001.137	33310.99	(**.081**, .243, .406) 1.368, 1.533, **1.698**.	$146_{3/2} - 4793_{7/2}$	+.10	..
3	3002.633	33294.40	.....	$221_{9/2} - 5545_{7/2}$	−.04	..
20	3004.136	33277.73	(.170) 1.190A..	$146_{3/2} - 4789_{9/2}$	−.03	..
9	3004.342	33275.45	{(**.289**, .892) **600**, .590, 1.173.	$138_{3/2} - 4710_{3/2}$	−.03	..
			.....	$163_{11/2} - 4958_{9/2}$	−.01	..
4	3005.232	33265.60	.....	$266_{9/2} - 5992_{7/2}$	+.12	..
10	3005.975	33257.38	.....	$157_{5/2} - 4903_{7/2}$	−.05	..
20	3006.425	33252.40	(.467), .967, 1.142, **1.318**, 1.504, 1.693†.	$157_{3/2} - 4902_{3/2}$	+.05	..
7	3007.04	33245.6	(**.180**, .543).....	$164_{3/2} - 4957_{5/2}$	.0	..
4	3007.19	33243.9	(000) 1.192	$166_{9/2} - 4986_{7/2}$	.0	..
4	3011.48	33196.6	.....	$197_{1/2} - 5296_{3/2}$	.0	..
20	3011.92	33191.7	(**.318**, .967, 1.619).	$117_{9/2} - 4494_{7/2}$	+.01	..
15	3013.141	33178.29	(.105, **.310**) 1.174, **1.383**, 1.588.	$138_{3/2} - 4706_{3/2}$	+.07	..
6	3014.939	33158.51	(**.105**, .326).....	$146_{3/2} - 4777_{3/2}$	+.06	..
40	3016.015	33146.67	(0w) 2.635B...	$117_{9/2} - 4490_{7/2}$	+.04	..
20	3016.480	33141.56	(.218, .636, 1.059, **1.483**) .506, .932. **1.355**, 1.784, 2.213, 2.639.	$142_{7/2} - 4735_{7/2}$	+.06	..
6	3016.972	33136.16	.....	$115_{5/2} - 4472_{3/2}$	+.03	..
5	3017.891	33126.07	.....	$150_{7/2} - 4818_{7/2}$	+ 06	..
2	3018.150	33123.23	.....	$266_{9/2} - 5978_{7/2}$	−.01	..
15	3021.881	33082.33	(**.149**, .444) **.701**, .999, 1.299, 1.598.	$146_{3/2} - 4770_{3/2}$	+.01	..
15	3022.989	33070.21	(**.101**, .307, .514, .720).	$173_{7/2} - 5040_{9/2}$	+.02	..
5	3023.573	33063.81	.....	$221_{9/2} - 5582_{11/2}$	.00	..
9	3025.058	33047.59	{(000) 1.109†?...	$217_{7/2} - 5482_{5/2}$	−.03	..
1	3027.128	33024.99	.....	$146_{3/2} - 4766_{7/2}$	+.04	..
2	3027.958	33015.94	.....	$172_{1/2} - 5026_{3/2}$	+.07	..
2	3028.099	33014.40	.....	$157_{3/2} - 4878_{7/2}$	+.01	..
30	3030.446	32988.84	(**.231**, .697, 1.165, 1.631) **−.562**, −.086, 388, 869, 1.335, 1.807.	$194_{3/2} - 5247_{5/2}$	−.02	..
				$142_{7/2} - 4720_{9/2}$	−.03	..
6	3031.266	32979.90	(.343) 1.200A†?	$173_{7/2} - 5031_{7/2}$	+.02	..
2	3031.358	32978.90	(000) 1.195.....	$163_{11/2} - 4928_{11/2}$	−.02	..
9	3032.792	32963.32	(.538) A.....	$166_{9/2} - 4958_{9/2}$	−.01	..
20h	3034.552	32944.20	.....	$204_{7/2} - 5339_{7/2}$	.0	..
8	3035.622	32932.58	(**.085**, .256, .427).	$247_{7/2} - 5765_{9/2}$	−.05	..
9	3036.552	32922.50	(.218, **.659**) 1.033, **1.447**, 1.935.	$164_{3/2} - 4925_{3/2}$	−.01	..
1	3037.222	32915.24	.....	$194_{3/2} - 5237_{7/2}$	+.01	..
4	3037.463	32912.63	.....	$150_{7/2} - 4797_{3/2}$	.00	..
15	3037.960	32907.25	(.189, **.568**) 1.292, **1.672**, 2.054.	$138_{1/2} - 4673_{3/2}$	−.01	..
20	3040.033	32884.80	(**.338**, 1.017, 1.697) **1.226**, 1.905, 2.584.	$142_{7/2} - 4710_{3/2}$	+.05	..
10	3041.000	32874.35	(.550) A.....	$150_{7/2} - 4793_{7/2}$	−.01	..
7	3041.760	32866.14	.....	$173_{7/2} - 5019_{9/2}$	+.02	..
6	3041.993	32863.62	.....	$163_{11/2} - 4917_{9/2}$	+.01	+
10	3044.084	32841.04	(0w) 1.020 C...	$150_{7/2} - 4789_{5/2}$	+.01	..
3	3045.286	32828.08	.....	$173_{7/2} - 5015_{5/2}$	+.03	..
1	3045.732	32823.28	.....	$138_{3/2} - 4664_{5/2}$	−.02	..
5	3046.000	32820.39	.....	$194_{5/2} - 5227_{3/2}$	.00	..
30	3047.252	32806.91	(.246) 1.180 A † ?.	$280_{5/2} - 6083_{3/2}$	+.13	..
8	3049.802	32779.48	(**.239**, .720, 1.200).	$173_{7/2} - 5011_{5/2}$	+.02	..
4	3051.590	32760.27	(.372) A.....	$194_{5/2} - 5221_{5/2}$	+.05	..
3	3052.709	32747.29	.....	{$244_{5/2} - 5717_{7/2}$	−.01	..
			.....	{$231_{5/2} - 5590_{3/2}$	+.09	..
3	3052.884	32746.38	.....	$231_{3/2} - 5589_{7/2}$	−.01	..
10	3053.629	32738.40	(.362) A.....	$217_{7/2} - 5451_{7/2}$	−.04	..
3	3053.766	32736.93	.....	$146_{3/2} - 4735_{7/2}$	+.03	..
9	3054.899	32724.79	.....	$115_{5/2} - 4430_{3/2}$	+.02	..
2	3056.136	32711.54	.....	$197_{1/2} - 5246_{1/2}$	.00	..
10	3057.660	32695.24	(**.110**, .329, .548) **1.174**, 1.393 †.	$164_{3/2} - 4902_{5/2}$	−.02	..
6	3057.852	32693.18	(000) 1.174....	$298_{5/2} - 6249_{7/2}$	+.05	..
20	3058.780	32683.27	(0w) 1.288 C...	$138_{3/2} - 4650_{3/2}$	−.01	..
9	3060.319	32666.83	.....	$166_{9/2} - 4928_{11/2}$	+.04	..
4	3061.218	32657.24	(.270).....	$172_{1/2} - 4989_{3/2}$	−.03	..
9	3061.608	32653.08	(.130) 1.184 h †	$221_{9/2} - 5481_{9/2}$	.00	..
3	3062.500	32643.57	.....	{$271_{7/2} - 5978_{7/2}$	+.03	..
			.....	{$204_{3/2} - 5512_{3/2}$	+.11	..
3	3063.383	32634.15	.....	$217_{7/2} - 5440_{5/2}$	−.06	..
1	3064.499	32622.27	(1.063) 1.446 h..	$306_{9/2} - 6326_{11/2}$	−.03	..
7	3064.597	32621.23	.....	$172_{1/2} - 4985_{1/2}$	.00	..
5	3065.279	32613.97	(.502).....	$151_{1/2} - 4777_{1/2}$	−.05	..
5	3065.576	32610.81	.....	$150_{7/2} - 4766_{7/2}$	−.01	..
200r	3067.398	32591.44	(**.093**, .280) 1.866, 2.044, **2.231**.	$0_{3/2} - 3259_{3/2}$	−.19	..
60r	3069.942	32564.44	(**.150**, .446) .836, 1.134, 1.432, 1.726.	$115_{5/2} - 4414_{3/2}$	−.05	..
2	3070.679	32556.62	.....	$247_{7/2} - 5728_{9/2}$	−.02	..
20	3071.164	32551.47	(.166) 1.149 h..	$166_{9/2} - 4917_{9/2}$	−.01	..
3	3072.452	32537.83	.....	$151_{1/2} - 4770_{3/2}$	−.06	..
20	3072.965	32532.40	(.284) 1.227 A..	$173_{7/2} - 4986_{7/2}$	.00	..
3	3074.102	32520.37	.....	$197_{1/2} - 5287_{3/2}$	.00	..
8H	3075.02	32510.7	.....	$266_{9/2} - 5917_{5/2}$	+.3	..
10	3076.142	32498.80	(.428) 1.936....	$151_{1/2} - 4765_{1/2}$	−.05	..
5	3076.304	32497.09	.....	$194_{3/2} - 51957_{7/2}$	−.04	..
3	3076.716	32492.74	.....	$217_{7/2} - 5426_{5/2}$	−.04	..
5	3077.908	32480.16	.....	$146_{3/2} - 4710_{5/2}$	+.01	..
15	3078.864	32470.08	.....	$117_{9/2} - 4428_{9/2}$	+.02	..
1	3079.263	32465.86	.....	$266_{9/2} - 5912_{3/2}$	−.01	..
7	3080.922	32448.39	.....	$247_{7/2} - 5717_{7/2}$	−.09	..
2	3081.656	32440.66	.....	$244_{5/2} - 5686_{3/2}$	.00	..
50	3082.426	32432.56	(**.121**, .362, .603) 1.026, 1.266, 1.505, 1.745, 1.904, **2.224**.	$142_{7/2} - 4664_{5/2}$	.00	..
3	3082.772	32428.92	.....	$172_{1/2} - 4966_{3/2}$	−.03	..
15	3084.210	32413.79	(0w) 1.146 W...	$157_{5/2} - 4818_{7/2}$	+.01	..
4	3085.344	32401.88	.....	$217_{7/2} - 5417_{7/2}$	+.03	..
3	3085.528	32399.95	.....	$224_{1/2} - 5482_{3/2}$	−.24	..
3	3086.03	32394.6	.....	$221_{9/2} - 5455_{11/2}$	.0	..
10	3087.154	32382.88	.....	$146_{5/2} - 4700_{3/2}$	.00	..
30r	3088.762	32366.03	{(.243) 1.336 A..	$247_{7/2} - 5709_{7/2}$	−.04	..
				$115_{5/2} - 4394_{3/2}$	+.01	..

TABLE 2. *Classified lines of* Re I—Continued

Int.	λ_{vac}	σ_{vac}	Zeeman effect	Transition	O–C	Notes
	A	*K*				
10	3089.932	32353.77	(000) 1.157	$221_{9/2}-5451_{7/2}$	−.03	--
20	3093.636	32315.04	(.384) 1.099, **1.869.**	$138_{3/2}-4614_{1/2}$	+.05	--
4	3093.994	32311.30		$217_{7/2}-5408_{7/2}$	+.03	--
10	3095.060	32300.16	(000) 1.152	$150_{7/2}-4735_{7/2}$	−.01	--
20	3095.788	32292.57		$142_{7/2}-4650_{9/2}$	+.03	--
7	3096.414	32286.04		$138_{3/2}-4611_{5/2}$	−.08	--
4	3097.922	32270.33		$275_{9/2}-5978_{7/2}$	−.03	--
				$263_{13/2}-5861_{11/2}$	−.03	--
2	3098.674	32262.50		$163_{11/2}-4856_{11/2}$	+.02	--
(1H)	3099.69	32251.9		$173_{7/2}-4958_{9/2}$	+.1	13
3	3099.765	32251.14		$272_{9/2}-5941_{11/2}$	+.03	--
40R	3100.672	32241.71	(**.136**, .407, .677, .948, 1.219) **.047**, .317, .589, .862, 1.133, 1.404, 1.676, 1.936.	$117_{9/2}-4399_{11/2}$	−.07	--
7	3100.998	32238.32		$166_{9/2}-4885_{7/2}$	.00	--
3	3101.700	32231.03		$115_{5/2}-4381_{7/2}$	−.02	--
2	3103.709	32210.16		$173_{7/2}-4965_{5/2}$	+.02	--
10	3104.647	32200.43		$157_{5/2}-4797_{3/2}$	+.03	--
2	3105.660	32189.93		$194_{5/2}-5164_{7/2}$	.00	--
5	3107.864	32167.10		$166_{9/2}-4878_{7/2}$	+.03	--
100R	3108.808	32157.33	(**.142**, .378, .613, .849) **.468**, .715, .972, 1.218, 1.461, 1.707, 1.953 †.	$142_{7/2}-4637_{9/2}$	−.06	--
4	3109.478	32150.41		$273_{11/2}-5939_{9/2}$	.00	--
8	3109.756	32147.53		$150_{7/2}-4780_{9/2}$	−.01	--
40r	3110.860	32136.13	(.447, .611, **1.049**) .526, .821, 1.116, **1.413**, 1.710, 2.002, 2.301†.	$142_{7/2}$ $4635_{7/2}$	.00	--
2	3111.236	32132.24		$194_{3/2}-5159_{3/2}$	+.05	--
9	3111.564	32128.85	(.256) A	$157_{3/2}-4789_{5/2}$	+.05	--
2	3112.404	32120.18		$194_{5/2}-5157_{3/2}$	+.02	--
1	3112.594	32118.22		$115_{5/2}-4370_{3/2}$	−.02	--
7	3113.205	32111.92	(**.352**, 1.057)	$146_{5/2}-4673_{1/2}$	.00	--
40	3118.192	32060.57	(0w) 2.195 B	$117_{9/2}-4381_{7/2}$	+.08	--
4	3119.192	32050.28		$138_{3/2}-4587_{3/2}$	+.06	--
2	3119.744	32044.61		$224_{3/2}-5446_{3/2}$	+.04	--
3	3119.854	32043.48		$150_{7/2}-4710_{5/2}$	+.06	--
30	3121.360	32028.03	(.478) A	$146_{5/2}-4664_{3/2}$	+.07	--
3	3122.206	32019.35		$194_{5/2}-5147_{3/2}$	+.09	--
1h	3122.411	32017.25		$221_{9/2}-5417_{7/2}$	+.04	--
9	3123.161	32009.55	(0w) 1.271	$157_{5/2}-4777_{3/2}$	+.06	--
3	3123.413	32006.97		$151_{1/2}-4718_{1/2}$	.0	--
1	3124.956	31991.17		$138_{3/2}-4581_{1/2}$	+.03	--
2	3125.288	31987.77		$204_{1/2}-5246_{1/2}$	+.05	--
1	3125.384	31986.79		$224_{1/2}-5440_{3/2}$	+.01	--
10	3125.518	31985.42	(.337, **.559**) .932, **1.157**, 1.383.	$115_{5/2}-4356_{5/2}$	+.02	12
3	3128.353	31956.43		$239_{11/2}-5591_{9/2}$	+.01	--
40	3128.944	31950.40	(0w) 1.700B†?	$166_{9/2}-4856_{11/2}$	+.05	--
1	3130.608	31933.42		$157_{5/2}-4770_{3/2}$	+.06	--
3	3131.270	31926.66		$221_{9/2}-5408_{7/2}$	+.03	--
2	3132.013	31919.09		$261_{3/2}-5805_{3/2}$	+.08	--
10	3134.022	31898.63	(0w) .883C	$157_{5/2}-4766_{7/2}$	+.04	--
2	3134.344	31895.23		$142_{7/2}-4611_{5/2}$	−.02	--
10	3135.068	31887.98		$146_{5/2}-4650_{5/2}$	+.04	--
3	3138.026	31857.93		$221_{9/2}-5401_{7/2}$	−.22	--
5	3139.263	31845.37		$224_{3/2}-5426_{5/2}$	+.02	--
10	3139.792	31840.01		$173_{7/2}-4917_{9/2}$	+.07	--
9	3139.945	31838.46	(.545) .741	$151_{1/2}-4700_{3/2}$	+.01	--
4	3141.254	31825.20		$115_{5/2}-4341_{5/2}$	+.05	--
10	3141.381	31823.91	(000) 1.522B	$115_{5/2}-4340_{7/2}$	.00	--
3	3141.718	31820.50		$239_{11/2}-5577_{13/2}$	−.01	--
1	3144.86	31788.7		$221_{9/2}-5394_{11/2}$	.0	--
4	3145.616	31781.07		$266_{5/2}-5844_{3/2}$	−.01	--
10	3146.536	31771.78	(0w) .935 D	$194_{5/2}-5122_{7/2}$	+.03	--
3	3147.911	31757.89		$115_{5/2}-4334_{3/2}$	.00	--
4	3150.047	31736.36		$204_{3/2}-5221_{5/2}$	−.02	--
6	3150.529	31731.51		$146_{5/2}-4635_{7/2}$	−.02	--
10	3151.162	31725.13		$194_{5/2}-5118_{3/2}$	+.02	--
40	3151.636	31720.36	(.610, .890) .603, .887, 1.167, **1.420**, 1.701, 1.994†?	$142_{7/2}-4593_{7/2}$	+.04	--
40r	3153.79	31698.7	(.253, .462, .672, **.881**) .660, .856, **1.051**, 1.247, 1.441†?	$117_{9/2}-4345_{9/2}$	−.1	--
2	3156.552	31670.96		$266_{5/2}-5833_{5/2}$	−.03	--
4	3156.827	31668.20		$231_{3/2}-5482_{3/2}$	−.01	--
50	3158.306	31653.38		$117_{9/2}-4340_{7/2}$	+.03	--
6	3159.312	31643.29	(**.275** . . .)	$164_{3/2}-4797_{3/2}$	−.02	--
2	3162.208	31614.32		$217_{7/2}-5338_{5/2}$	−.01	--
4	3163.243	31603.97		$217_{7/2}-5337_{9/2}$	+.02	--
10	3164.520	31591.22	(.084, .270, .453) .708, .888, 1.068, 1.248.	$150_{7/2}-4664_{5/2}$	−.01	--
7	3164.864	31587.79		$157_{5/2}-4735_{7/2}$	−.15	--
7	3165.802	31578.43	(0w) 1.278w	$221_{9/2}-5373_{7/2}$	+.01	--
7	3166.476	31571.71		$164_{3/2}-4789_{5/2}$	.00	--
7	3166.904	31567.45		$151_{1/2}-4673_{3/2}$	−.04	--
10	3167.155	31564.93		$166_{9/2}-4818_{7/2}$	+.01	--
5	3167.594	31560.56	(.544) A	$217_{7/2}-5333_{7/2}$	+.02	--
50	3168.374	31552.79	(.248) 1.259A	$163_{11/2}-4785_{11/2}$	+.01	--
2	3169.097	31545.60		$217_{7/2}-5332_{9/2}$	+.05	--
10	3170.992	31526.75	(000) 1.246w †?	$173_{7/2}-4885_{7/2}$	−.03	--
9	3173.094	31505.86	(**.198**, .597) **.495**, .890, 1.289, 1.690.	$138_{3/2}-4533_{3/2}$	−.05	--
20	3174.610	31490.82	(.369, **.639**) .743, 1.014, **1.284**, 1.552, 1.810 †?	$146_{3/2}-4611_{3/2}$	+.04	--
20	3174.776	31489.18	(.0w) 1.430h	$270_{13/2}-5861_{11/2}$	.00	--
2	3176.084	31476.20		$194_{5/2}-5093_{3/2}$	−.09	--
30r	3177.714	31460.06	(.085, .256, **.425**) 1.029, 1.196, **1.362**, 1.529, 1.696.	$115_{5/2}-4304_{5/2}$	.00	--
2	3177.934	31457.88		$272_{9/2}-5861_{11/2}$	−.09	--
2	3178.176	31455.49		$173_{7/2}-4878_{7/2}$	−.04	--
6	3178.488	31452.40	(.495)	$164_{3/2}-4777_{3/2}$	.00	--
15	3178.612	31451.17	(**.111**, .334, .556) **.593**, .817. . .	$150_{7/2}-4650_{3/2}$	−.04	--
3h	3181.258	31425.01		$197_{1/2}-5118_{3/2}$	−.08	--
1	3181.792	31419.74		$224_{3/2}-5384_{3/2}$	+.04	--
7	3182.664	31411.13	(.623)	$194_{5/2}-5086_{7/2}$	+.02	10
100R	3182.869	31409.11	(.466, .925) **.632**, 1.110, 1.588†?	$1895_{5/2}-5035_{7/2}$	.0	--
200R	3184.760	31390.46		$1895_{5/2}-5034_{5/2}$	.0	--
250R	3185.574	31382.44		$1895_{5/2}-5033_{3/2}$	−.1	--
1	3186.198	31376.29		$164_{3/2}-4770_{5/2}$	+.02	--
10	3186.292	31375.37	(0w) 1.155	$273_{11/2}-5861_{11/2}$	−.07	--
3	3187.956	31358.99		$231_{5/2}-5451_{7/2}$	−.04	--
20	3190.170	31337.23	(.104) 1.819	$164_{3/2}-4765_{1/2}$	.00	--
20	3190.782	31331.22	(.211, .634, **1.057**) .263, .684, **1.105**, 1.526, 1.948.	$157_{5/2}-4710_{5/2}$	+.03	--
20	3192.362	31315.71	(.083, .249) 1.068.	$146_{5/2}-4593_{7/2}$	−.01	--
(3)	3192.608	31313.30		$166_{9/2}-4793_{7/2}$	+.03	7
4	3192.682	31312.57		$231_{5/2}-5446_{3/2}$	−.02	--
10	3193.199	31307.50	(000) 1.165	$221_{9/2}-5346_{11/2}$	−.03	--
				$311_{5/2}-6249_{7/2}$	+.07	16
1	3193.979	31299.86		$278_{3/2}-5912_{5/2}$	+.21	--
30	3194.497	31294.79	(.385) 1.212A	$150_{7/2}-4635_{7/2}$	−.01	--
3	3195.666	31283.33		$217_{7/2}-5305_{5/2}$	−.01	--
3	3197.248	31267.86	(.537, 692, .846) A†?	$239_{11/2}-5522_{11/2}$	+.01	--
15	3198.578	31254.86		$146_{5/2}-4587_{3/2}$	−.02	--
				$231_{5/2}-5440_{5/2}$	+.06	--
8	3199.486	31245.98		$142_{7/2}-4546_{7/2}$	+.01	--
20	3200.035	31240.62	(0w) 1.185C	$166_{9/2}-4785_{11/2}$	−.03	--
10	3200.725	31233.89	(000) 1.344	$157_{5/2}-4700_{5/2}$	−.03	--
6	3202.224	31219.27		$221_{9/2}-5337_{9/2}$	−.04	--
100	3204.245	31199.58	(0w) 1.292B	$163_{11/2}-4750_{13/2}$	−.06	--
15	3205.420	31188.15	(0w) .959D	$247_{7/2}-5591_{9/2}$	−.05	--
9	3208.222	31160.90	(.237, .400, .563, .727).	$221_{9/2}-5332_{9/2}$	−.01	--
1	3208.582	31157.41		$273'_{1/2}-5854_{1/2}$	−.07	--
1	3208.662	31156.63		$273_{1/2}-5854_{1/2}$	−.05	--
2	3210.564	31138.17		$271_{7/2}-5827_{9/2}$	−.01	--
20	3211.752	31126.06	(**.221**, .650, 1.083) **000**, .436, .870, 1.302.	$142_{7/2}-4534_{9/2}$	−.05	--
15	3212.938	31115.17	(**.242**, .713, 1.171, 1.637).	$142_{7/2}-4533_{5/2}$	.00	--
2	3213.152	31113.10		$194_{5/2}-5057_{3/2}$	−.03	--
3	3213.646	31108.32		$204_{3/2}-5159_{3/2}$	−.03	--
3	3213.890	31105.95		$217_{7/2}-5288_{5/2}$	+.01	--
9	3214.110	31103.82	(0w) 1.099	$263_{13/2}-5745_{13/2}$	−.05	--
2	3214.646	31098.63		$272_{9/2}-5826_{7/2}$	−.05	--
4	3214.818	31096.97		$280_{5/2}-5912_{3/2}$	−.01	--
2	3219.712	31049.70		$166_{9/2}-4766_{7/2}$	−.03	--
2	3220.466	31042.44		$263_{13/2}-5739_{11/2}$	−.04	--
2	3221.194	31035.42		$273_{11/2}-5827_{9/2}$	−.01	--
2	3221.860	31029.01		$244_{5/2}-5545_{7/2}$	−.07	--
1	3222.549	31022.37		$231_{3/2}-5417_{7/2}$	−.07	--
2	3224.260	31005.91		$194_{5/2}-5046_{3/2}$	.00	--
8	3227.45	30975.3	(.807) 1.541	$151_{1/2}-4614_{1/2}$	+.1	--
8	3227.48	30975.0		$288_{7/2}-5978_{7/2}$	+.2	--
6	3228.329	30966.83		$224_{3/2}-5338_{5/2}$	−.07	--
3	3228.428	30965.88		$217_{7/2}-5274_{9/2}$	−.02	--
15	3228.734	30962.95	(**.271**, .808) **.483**, 1.027, 1.571, 2.119	$157_{3/2}-4673_{3/2}$	−.01	--
2	3230.954	30941.67		$261_{3/2}-5707_{1/2}$	−.07	--
1	3231.454	30936.88		$208_{5/2}-6073_{5/2}$	−.02	--
1	3231.983	30931.82		$231_{5/2}-5408_{7/2}$	−.04	--

TABLE 2. *Classified lines of* Re I—Continued

Int.	λ_{vac}	σ_{vac}	Zeeman effect	Transition	O–C	Notes
	A	*K*				
30	3235.944	30893.96	(.077, .239) 1.235, **1.407**, 1.571	$138_{1/2} - 4472_{3/2}$	−.01	..
10	3237.513	30878.99	(000) 1.325 (.216, .368, **.520**)	$157_{5/2} - 4664_{5/2}$ $150_{7/2} - 4593_{7/2}$	−.01 .00	.. ..
4	3238.363	30870.88		$224_{3/2} - 5329_{3/2}$	−.01	..
2	3238.938	30865.40		$224_{3/2} - 5328_{1/2}$	−.05	..
4	3239.156	30863.33	(000) 1.1922h	$231_{5/2} - 5401_{7/2}$	−.05	..
1	3239.807	30857.13		$239_{11/2} - 5481_{9/2}$	+.01	..
4	3240.331	30852.14		$285_{7/2} - 5939_{9/2}$	−.02	..
1	3241.023	30845.55		$164_{3/2} - 4718_{1/2}$	+.2	..
1	3241.112	30844.71		$164_{3/2} - 4717_{3/2}$	+.1	..
10	3241.466	30841.34	(.077, .232, .382) 1.371, 1.526, **1.681**	$146_{5/2} - 4546_{7/2}$	−.03	..
2	3242.174	30834.60		$217_{7/2} - 5261_{7/2}$	−.01	..
10	3248.547	30774.11	(**.408**, 1.221)	$164_{3/2} - 4710_{5/2}$	+.01	..
2	3251.548	30745.71		$275_{9/2} - 5826_{7/2}$	−.01	..
20	3252.259	30738.99	(.137) 1.343	$166_{9/2} - 4735_{7/2}$ $157_{5/2} - 4650_{5/2}$	−.09 +.01	.. ..
2	3252.736	30734.48		$261_{3/2} - 5686_{3/2}$	−.01	..
10	3253.186	30730.23		$247_{7/2} - 5545_{7/2}$	−.03	..
2	3254.886	30714.24		$278_{9/2} - 5854_{11/2}$	+.01	..
3	3255.292	30710.41		$146_{5/2} - 4533_{5/2}$ $151_{1/2} - 4587_{3/2}$ $266_{3/2} - 5737_{7/2}$	−.16 −.04 +.09	.. .. ..
8	3256.286	30700.98		$194_{5/2} - 5015_{3/2}$	.00	..
2	3256.666	30697.39		$221_{9/2} - 5285_{7/2}$	−.01	..
7	3258.055	30684.30		$142_{7/2} - 4490_{7/2}$	+.01	..
40r	3258.848	30676.84	(.218, **.651**,) 1.074, **1.501**, 1.928.	$164_{3/2} - 4700_{3/2}$	+.01	..
50r	3259.550	30670.23	(**.149**, .450), **.828**, 1.127, 1.426, 1.726.	$115_{5/2} - 4225_{11/2}$	.00	..
1	3260.052	30665.51		$273_{1/2} - 5805_{3/2}$	+.13	..
20	3261.559	30651.35	(0*w*) 2.276	$151_{1/2} - 4581_{1/2}$	−.02	..
10	3262.768	30639.98	(0*w*) 1.453B	$173_{7/2} - 4797_{5/2}$	−.02	..
1	3263.877	30629.57		$285_{7/2} - 5917_{5/2}$	−.03	..
15	3266.851	30601.69	(.154) 1.247A	$173_{7/2} - 4793_{7/2}$	−.04	..
15	3268.077	30590.21		$138_{3/2} - 4441_{1/2}$	.00	..
10	3268.480	30586.44	(.305) 1.154A	$166_{9/2} - 4720_{9/2}$	−.01	..
1	3268.782	30583.62		$231_{5/2} - 5373_{7/2}$	−.03	..
15	3268.894	30582.57		$157_{5/2} - 4635_{7/2}$	.00	..
15	3269.033	30581.27		$221_{9/2} - 5274_{9/2}$	+.01	..
(1)	3270.42	30568.3		$173_{7/2} - 4789_{5/2}$	−.1	13
2	3272.780	30546.26		$20444_{7/2} - 50998_{9/2}$	−.1	..
4	3273.282	30541.57		$172_{1/2} - 4777_{3/2}$	−.04	..
1	3274.354	30531.57		$224_{3/2} - 5295_{3/2}$	−.06	..
3	3274.658	30528.73		$224_{3/2} - 5295_{3/2}$	−.03	..
8	3276.060	30515.67		$271_{7/2} - 5765_{9/2}$	−.05	..
4	3276.544	30511.17		$266_{5/2} - 5717_{7/2}$	−.10	..
4	3277.18	30505.2		$197_{1/2} - 5026_{3/2}$	−.1	..
20	3277.710	30500.31		$146_{5/2} - 4518_{3/2}$	−.04	..
2	3281.457	30465.48		$172_{1/2} - 4770_{3/2}$	.00	..
4	3282.863	30452.44		$204_{3/2} - 5093_{5/2}$	−.01	..
4	3283.124	30450.02		$221_{9/2} - 5261_{7/2}$	+.05	..
5	3283.907	30442.76		$217_{7/2} - 5221_{5/2}$	+.05	..
3	3284.454	30437.69		$194_{5/2} - 4989_{9/2}$	+.01	..
8	3285.638	30426.71	(.513) 2.039	$172_{1/2} - 4765_{1/2}$	+.27	..
10	3287.127	30412.94	(000) 1.150B	$273_{11/2} - 5765_{9/2}$	−.03	..
3	3287.92	30405.6		$164_{3/2} - 4673_{3/2}$	−.3	..
6	3290.093	30385.52		$117_{9/2} - 4214_{9/2}$	−.02	..
3	3292.088	30367.11		$319_{7/2} - 6235_{7/2}$	−.03	..
2	3292.65	30361.9		$288_{7/2} - 5917_{5/2}$	.0	..
10	3294.834	30341.80	(.229) 1.353A	$157_{5/2} - 4611_{5/2}$	−.02	..
15	3296.696	30324.67		$146_{5/2} - 4494_{7/2}$	+.01	..
10	3296.992	30321.94		$164_{3/2} - 4664_{5/2}$	+.03	..
2	3299.143	30302.17		$280_{5/2} - 5833_{5/2}$	+.07	..
10	3300.972	30285.39		$150_{7/2} - 4534_{9/2}$	+.01	..
15	3301.595	30279.66	(000) 1.502B	$146_{5/2} - 4490_{7/2}$	−.03	..
10	3302.230	30273.84		$150_{7/2} - 4533_{5/2}$	.00	..
6	3303.595	30261.34		$270_{13/2} - 5739_{11/2}$	+.04	..
15	3303.754	30259.88	(000) 1.033C	$115_{5/2} - 4184_{7/2}$	−.01	..
3	3306.484	30234.90		$231_{5/2} - 5338_{5/2}$	−.02	..
10	3307.007	30230.12	(**.064**, .192, .320, .447, .575).	$272_{9/2} - 5739_{11/2}$	+.03	..
1	3307.454	30226.03		$217_{7/2} - 5200_{9/2}$	+.06	..
8	3308.872	30213.08		$221_{9/2} - 5237_{7/2}$	.00	..
1	3309.164	30210.41		$272_{9/2} - 5737_{7/2}$	+.01	..
7	3309.324	30208.95		$273_{11/2} - 5745_{13/2}$	.00	..
1	3309.795	30204.65		$266_{5/2} - 5698_{7/2}$	+.02	..
9	3312.288	30181.92	(**.166**, .498) **.875**, 1.210. 1.545.	$164_{3/2} - 4650_{3/2}$	+.03	..
2	3313.105	30174.47		$263_{13/2} - 5652_{13/2}$	+.02	..
15	3313.948	30166.80	(000) 1.274	$157_{5/2} - 4593_{7/2}$	+.04	..
2h	3314.52	30161.6		$266_{5/2} - 5682_{5/2}$	+.3	..
6	3316.062	31047.57		$273_{11/2} - 5739_{11/2}$	+.01	..
1	3316.612	30142.58		$275_{9/2} - 5765_{9/2}$	+.04	..
5	3317.013	30138.92		$231_{5/2} - 5329_{3/2}$	+.01	..
2	3317.152	30137.66		$197_{1/2} - 4989_{3/2}$	.00	..
10	3318.671	30123.87		$138_{3/2} - 4394_{5/2}$	+.01	..
1h	3319.146	30119.56		$272_{9/2} - 5728_{9/2}$	+.05	..
1	3319.622	30115.24		$194_{5/2} - 4957_{3/2}$	+.02	..
2	3329.647	30105.95		$157_{5/2} - 4587_{3/2}$	+.03	..
1	3321.124	30101.62		$197_{1/2} - 4985_{1/2}$	.00	..
6	3321.450	30098.66	(**.089**, .265)	$247_{7/2} - 5482_{5/2}$ $146_{5/2} - 4472_{3/2}$	−.14 +.03	.. ..
9	3322.196	30091.91		$142_{7/2} - 4430_{5/2}$	+.04	..
10	3322.478	30089.35	(**.167**, .500, .832, 1.164) .707, 1.041, 1.376, 1.712, 2.048, 2.389, **2.729.**†	$117_{9/2} - 4184_{7/2}$	+.02	..
4	3324.930	30067.17		$204_{3/2} - 5057_{3/2}$	+.06	22
5	3326.896	30049.40		$163_{11/2} - 4637_{9/2}$	+.10	..
5	3327.204	30046.62	(.276) .521	$224_{3/2} - 5247_{5/2}$	−.08	..
9	3327.712	30042.03		$224_{3/2} - 5246_{1/2}$	.00	..
4	3328.172	30037.88		$244_{5/2} - 5446_{3/2}$	+.03	..
3	3328.874	30031.55		$266_{5/2} - 5669_{7/2}$	−.10	..
2	3329.319	30027.53		$271_{7/2} - 5717_{7/2}$	−.02	..
2	3330.116	30020.34		$173_{7/2} - 4735_{7/2}$	−.01	..
15	3331.520	30007.69	(**.157**, .471, .786, 1.100) **.156**, .472, .789, 1.105, 1.408.	$280_{5/2} - 5805_{3/2}$	+.08	..
20	3335.364	29973.11	(**.188**, .565) **.699**, 1.081, 1.466, 1.853†.	$142_{7/2} - 4422_{9/2}$	−.03	..
2	3337.250	29956.17		$115_{5/2} - 4155_{3/2}$	−.01	..
300R	3338.178	29947.84	(**.104**, .323, .548, .772) **.920**, 1.135†.	$151_{1/2} - 4512_{3/2}$ $20447_{7/2} - 50399_{9/2}$	+.25 −.1	.. ..
15	3339.685	29934.33	(.155) 2.361	$172_{1/2} - 4718_{1/2}$	−.3	..
3	3340.304	29928.78		$272_{9/2} - 5709_{7/2}$	−.16	..
250R	3342.245	29911.40	(.376) 1.877h†	$20447_{7/2} - 50357_{7/2}$	.0	..
1	3343.092	29903.83		$231_{5/2} - 5395_{5/2}$	−.10	..
100	3344.322	29892.82	(.156, .484) 1.572†.	$20447_{7/2} - 50345_{7/2}$	.0	10, 18
40	3346.199	29876.06	(.239, **.722**) 1.252, **1.727**, 2.199.	$138_{3/2} - 4370_{3/2}$	−.02	..
4	3346.606	29872.43		$217_{7/2} - 5164_{7/2}$	+.01	..
2	3348.292	29857.38		$275_{9/2} - 5737_{7/2}$	−.06	..
1	3348.508	29855.46		$224_{3/2} - 5227_{3/2}$	+.01	..
8	3349.916	29842.91		$150_{7/2} - 4490_{7/2}$ $244_{5/2} - 5426_{5/2}$	−.05 +.13	.. ..
4	3350.094	29841.33		$221_{9/2} - 5260_{9/2}$	.00	..
20	3353.208	29813.61	(.497) 1.203, **2.200.**	$164_{3/2} - 4614_{1/2}$	+.01	..
30	3355.288	29795.14		$224_{3/2} - 5221_{5/2}$ $221_{9/2} - 5195_{7/2}$	−.14 +.16	.. ..
4	3355.626	29792.14		$194_{5/2} - 4925_{3/2}$	+.01	..
10	3355.903	29789.68		$247_{7/2} - 5451_{7/2}$	+.06	..
10	3356.328	29785.90		$221_{9/2} - 5194_{11/2}$	.00	..
9	3356.462	29784.71	(**.149**, .452)	$164_{3/2} - 4611_{3/2}$	−.02	..
4	3356.821	29781.52		$204_{3/2} - 5026_{3/2}$	+.03	..
10	3358.021	29770.88	(**.180**, .539, .897) 1.077, 1.437, 1.796, **2.159.**	$173_{7/2} - 4710_{5/2}$	+.09	..
6	3358.56	29766.1		$172_{1/2} - 4700_{3/2}$	+.1	..
10h	3359.22	29760.2		$20635_{7/2} - 53397_{7/2}$	.0	..
10	3359.818	29754.97		$166_{9/2} - 4637_{9/2}$	.00	..
4	3360.177	29751.78		$244_{5/2} - 5417_{7/2}$	−.07	..
10	3361.145	29743.21	(000) 1.524	$138_{3/2} - 4356_{5/2}$	−.03	..
3	3361.828	29737.17		$285_{7/2} - 5827_{9/2}$	−.01	..
2	3362.284	29733.14		$142_{7/2} - 4394_{5/2}$	+.02	..
15	3362.745	29729.07	(000) 1.280	$117_{9/2} - 4131_{5/2}$	+.01	..
6	3363.025	29726.59		$231_{5/2} - 5288_{5/2}$	+.06	..
9	3365.732	29702.68		$231_{5/2} - 5285_{7/2}$	+.05	..
8	3366.189	29698.73		$117_{9/2} - 4145_{9/2}$	+.07	..
2	3366.418	29696.63		$278_{9/2} - 5752_{3/2}$	−.03	..
3	3366.892	29692.45		$157_{5/2} - 4546_{7/2}$	+.04	..
1	3367.298	29688.87		$273'_{1/2} - 5707_{1/2}$	−.04	..
1	3367.384	29688.11		$273''_{1/2} - 5707_{1/2}$	.00	..
6	3367.482	29687.25		$146_{5/2} - 4439_{5/2}$	−.02	..
5	3367.677	29685.53	(000) 1.023	$247_{7/2} - 5449_{5/2}$	+.14	..
2h	3368.132	29681.51		$271_{7/2} - 5682_{5/2}$	−.11	..
8	3368.605	29677.35		$204_{3/2} - 5015_{3/2}$	+.21	..
2	3370.764	29658.34		$275_{9/2} - 5717_{9/2}$	−.05	..
8	3377.619	29598.15		$142_{7/2} - 4381_{7/2}$	.00	..
10	3377.743	29597.06	(.391) 1.251A	$163_{11/2} - 4590_{11/2}$	−.04	..
20	3379.700	29579.93		$115_{5/2} - 4116_{7/2}$	−.02	..
9	3381.424	29564.84		$194_{5/2} - 4992_{5/2}$	−.04	..
5	3381.794	29561.61		$157_{5/2} - 4533_{5/2}$	.00	..
3	3382.646	29554.17		$151_{1/2} - 4472_{3/2}$	−.03	..
2	3383.259	29548.81		$164_{3/2} - 4587_{3/2}$	−.02	..
1	3383.814	29543.96		$247_{7/2} - 5426_{5/2}$	.00	..
30	3384.452	29538.39		$272_{9/2} - 5669_{7/2}$	+.33	..
40	3385.757	29527.01	(**.214**, .644)	$146_{5/2} - 4414_{5/2}$	+.02	..
2	3386.264	29522.59		$288_{7/2} - 5833_{5/2}$	+.04	..
2	3387.053	29515.71		$138_{3/2} - 4334_{3/2}$	−.02	..
20	3389.428	29495.03	(.333) **1.528**, 2.195.	$172_{1/2} - 4673_{3/2}$	−.05	..
8	3389.767	29492.08	(.141) 1.407	$197_{1/2} - 4925_{3/2}$	−.03	..
4	3390.032	29489.78		$164_{3/2} - 4581_{1/2}$	+.03	..
30	3390.254	29487.85	(0*w*) 1.396w	$221_{9/2} - 5164_{7/2}$	+.07	..
1	3390.970	29481.62		$273'_{1/2} - 5686_{3/2}$	−.04	5
1	3391.052	29480.90		$273''_{1/2} - 5686_{3/2}$	+.04	..
5h	3391.256	29479.13		$20887_{7/2} - 58369_{9/2}$	−.1	..
8	3392.376	29469.40	(**.068**, .200, .332, .464).	$288_{7/2} - 5827_{9/2}$	−.04	..
8	3394.122	29454.24	(.296) 1.223A†	$217_{7/2} - 5122_{7/2}$	.00	..
1	3394.430	29451.57		$224_{3/2} - 5187_{3/2}$	−.03	..

TABLE 2. *Classified lines of* Re I—Continued

Int.	λ_{vac}	σ_{vac}	Zeeman effect	Transition	O-C	Notes
	A	*K*				
9	3397.210	29427.47	(.277) 1.076A	$263_{13/2}-5577_{13/2}$	−.08	--
5	3397.686	29423.35	(0w) D	$239_{11/2}-5357_{9/2}$	.00	--
3	3398.404	29417.13		$244_{5/2}-5384_{3/2}$	.00	--
8	3398.793	29413.77		$204_{3/2}-4989_{3/2}$	−.07	--
400R	3399.302	29409.36	(**.108**, .324, .539, .769) 1.218, 1.429, 1.641, 1.853, 2.066, **2.280.**	$117_{9/2}-4116_{7/2}$	−.03	--
1	3402.97	29377.6		$204_{3/2}-4985_{1/2}$	−.2	--
1	3404.438	29364.99		$239_{11/2}-5332_{9/2}$	+.04	--
80R	3404.724	29362.53	(**.127**, .384, .635) .826, 1.119, 1.400, 1.667, 1.933, **2.171.**	$115_{9/2}-4094_{7/2}$	−.04	--
				$247_{7/2}-5408_{7/2}$	+.08	--
60	3405.888	29352.49	(0w) 1.685B	$142_{7/2}-4356_{5/2}$	−.01	--
30	3408.673	29328.51	(.109, .344, .580) 1.034, **1.270**, 1.505, 1.730.	$146_{5/2}-4394_{3/2}$	−.01	--
				$194_{5/2}-4878_{7/2}$	+.05	--
15	3409.831	29318.55	(0w) 1.069C	$173_{7/2}-4664_{5/2}$	−.05	--
2	3409.960	29317.44		$231_{5/2}-5247_{3/2}$	−.06	--
5	3412.701	29293.89		$247_{7/2}-5401_{7/2}$	−.08	--
10	3413.744	29284.95	(000) 1.178	$166_{9/2}-4590_{11/2}$	−.02	--
2	3414.380	29279.49		$273_{11/2}-5652_{13/2}$	−.04	--
40	3417.767	29250.48	(0w) 1.018 (1.110) 1.265	$150_{7/2}-4430_{5/2}$	−.06	--
1	3418.330	29245.66		$278_{9/2}-5707_{1/2}$	.00	--
2	3418.933	29240.50		$266_{9/2}-5590_{9/2}$	−.08	--
5	3419.242	29237.85		$115_{5/2}-4082_{5/2}$	−.02	--
60r	3419.410	29236.42	(**.113**, .341, .568, .794) **.529**, .762, .994, 1.226, 1.456, 1.687.	$142_{7/2}-4345_{9/2}$	−.02	--
20	3420.754	29224.93	(.117) 1.158	$115_{5/2}-4089_{5/2}$	+.04	17
5	3421.582	29217.86	(000) 1.403	$138_{9/2}-4304_{5/2}$	−.04	--
1h	3422.923	29206.42		$2885_{5/2}-5806_{7/2}$	−.04	--
600R	3424.620	29191.94	(000) 1.522	$117_{9/2}-4094_{7/2}$	−.07	--
3	3425.412	29185.20		$275_{9/2}-5669_{7/2}$	+.10	--
40r	3426.189	29178.57	(**.062**, .186, .310) **.943**, 1.065, 1.186, 1.311, 1.437.	$173_{7/2}-4650_{5/2}$	−.01	--
2	3426.527	29175.69		$157_{5/2}-4494_{7/2}$	−.01	--
50	3427.61	29166.5	(000) 1.434 D†	$150_{7/2}-4422_{9/2}$	+.1	--
7	3428.513	29158.80	(**.125**, .378, .631).	$217_{7/2}-5093_{5/2}$	+.02	--
1	3430.44	29142.5		$280_{5/2}-5717_{7/2}$	+.1	--
1	3430.80	29139.4		$306_{9/2}-5978_{7/2}$	+.1	--
4	3431.818	29130.72		$157_{5/2}-4490_{7/2}$	−.01	--
5	3432.668	29123.51	(**.133**, .395)	$231_{5/2}-5227_{3/2}$	+.04	--
(3)	3433.728	29114.52		$285_{7/2}-5765_{9/2}$	−.20	3
3	3436.193	29093.63	(.310) 1.133hA	$217_{7/2}-5086_{7/2}$	+.03	--
50	3437.714	29080.76	(**.409**, 1.224) −.077, .740, 1.559, 2.379.	$146_{5/2}-4379_{3/2}$	+.02	--
4	3438.589	29073.35		$341_{9/2}-6326_{11/2}$	−.01	--
2	3439.027	29069.65		$221_{9/2}-5122_{7/2}$	+.05	--
1	3439.168	29068.46		$332_{5/2}-6235_{7/2}$	−.02	--
2h	3439.67	29064.2		$273_{11/2}-5639_{9/2}$	+.1	--
3	3439.776	29063.32		$231_{5/2}-5221_{3/2}$	+.02	--
2h	3440.173	29059.97		$280_{5/2}-5709_{7/2}$	.00	--
5	3440.843	29054.31	(.092)	$224_{7/2}-5147_{5/2}$	−.01	--
4	3442.13	29043.4		$173_{7/2}-4637_{9/2}$	.0	--
5h	3442.722	29038.45		$278_{9/2}-5686_{5/2}$	+.04	--
10	3442.967	29036.39	(**.058**, .169, .279, .390, .500).	$165_{11/2}-4534_{9/2}$	−.03	--
1	3446.743	29004.58		$164_{3/2}-4533_{5/2}$	+.06	--
1h	3447.801	28995.68		$301_{1/2}-5912_{3/2}$	−.05	--
15	3449.333	28982.81	(.397) 1.166, 1.965.	$151_{1/2}-4414_{3/2}$	+.25	--
15	3449.407	28982.18		$285_{7/2}-5752_{5/2}$	.00	--
400R	3451.880	28961.42	(**.191**, .578) **1.376**, 1.761, 2.143, 2.525.	$0_{3/2}-2896_{3/2}$	−.13	--
15	3453.280	28949.68		$157_{5/2}-4472_{3/2}$	+.01	--
50	3453.495	28947.88	(.178, .560, **.884**) 1.002, **1.349**, 1.695, 2.043†.	$146_{5/2}-4356_{3/2}$	−.02	--
1	3457.956	28910.54		$244_{5/2}-5333_{7/2}$	.00	--
15	3458.881	28902.80	(.903) 1.611	$172_{1/2}-4614_{3/2}$	−.01	--
1000R	3460.465	28889.57	(**.119**, .360, .594) **1.121**, 1.361, 1.599, 1.831, 2.068, 2.309.	$0_{3/2}-2888_{1/2}$	−.15	--
2	3463.653	28867.98		$221_{9/2}-5102_{9/2}$	+.06	--
7000R	3464.726	28854.04	(0w) 1.973A	$0_{3/2}-2885_{5/2}$	−.14	--
10	3465.988	28843.53		$166_{9/2}-4546_{7/2}$	−.02	--
1	3467.093	28834.34		$305_{11/2}-5939_{9/2}$	−.04	--
1h	3467.656	28829.66		$285_{7/2}-5737_{7/2}$	+.04	--
80	3467.960	28827.14	(**.071**, .212, .354) 1.886B,	$142_{7/2}-4304_{5/2}$	−.02	--
6	3471.923	28794.23		$164_{1/2}-4512_{3/2}$	−.07	--
(10h)	3471.994	28793.65		$275_{9/2}-5630_{9/2}$	−.01	3
8	3472.071	28793.01		$266_{5/2}-5545_{7/2}$	−.04	--
30	3472.723	28787.60		$146_{5/2}-4341_{3/2}$	−.05	--
7	3472.875	28786.34		$146_{5/2}-4340_{7/2}$	−.07	--
2	3473.000	28785.30		$239_{11/2}-5274_{9/2}$	.00	--
6	3473.467	28781.43		$173_{7/2}-4611_{5/2}$	+.01	--
10	3474.183	28775.50		$163_{11/2}-4508_{11/2}$	+.02	--
5	3474.700	28771.22		$271_{7/2}-5591_{9/2}$	−.07	--
5	3475.201	28767.07		$306_{9/2}-5941_{11/2}$	−.06	--
4	3476.031	28760.21		$224_{3/2}-5118_{1/2}$ $271_{7/2}-5589_{7/2}$	+.04 +.14	-- --
30	3476.442	28756.81	(.099, .290, .486, **.682**) .666, .861, 1.056, **1.251**, 1.447, 1.641, 1.835.	$150_{7/2}-4381_{7/2}$	−.01	--
8	3477.143	28751.00	(.323) 1.063A	$272_{9/2}-5591_{9/2}$	−.07	--
3	3478.491	28739.86		$272_{9/2}-5589_{7/2}$	+.01	--
4	3478.629	28738.72		$285_{7/2}-5728_{5/2}$	−.01	--
30	3480.381	28724.26	(.158) 1.154A	$166_{9/2}-4534_{9/2}$	−.03	--
40	3480.852	28720.38	(**.089**, .267) .871, 1.051, 1.231, **1.418.**	$146_{5/2}-4334_{3/2}$	−.01	--
40	3482.233	28708.98	(0w) 1.208w	$221_{9/2}-5086_{7/2}$	+.02	--
2	3482.853	28703.87		$2896_{3/2}-5766_{3/2}$	−.01	--
5	3484.365	28691.42	(.261)	$261_{3/2}-5482_{5/2}$	−.03	--
5	3484.728	28688.43	(000) 1.138	$217_{7/2}-5046_{5/2}$	+.03	--
4	3487.521	28665.53		$247_{7/2}-5338_{5/2}$	+.02	--
4	3488.77	28655.2		$247_{7/2}-5337_{9/2}$	+.1	--
5	3489.850	28646.32		$270_{13/2}-5577_{13/2}$	−.05	--
10	3490.860	28638.04	(.577) .813	$172_{1/2}-4587_{3/2}$	.00	--
4	3491.433	28633.34		$244_{5/2}-5305_{5/2}$	.00	--
2	3491.772	28630.56		$285_{7/2}-5717_{7/2}$	−.01	--
2	3492.372	28625.64		$217_{7/2}-5040_{9/2}$	+.03	--
2	3492.545	28624.22		$278_{5/2}-5645_{1/2}$	.00	--
2	3494.06	28611.8		$247_{7/2}-5333_{7/2}$	+.1	--
10	3494.725	28606.36	(.140) 1.280hw	$173_{7/2}-4593_{7/2}$	.00	--
1	3495.415	28600.72		$304_{3/2}-5912_{3/2}$	+.02	--
9	3502.727	28541.02		$204_{3/2}-4902_{5/2}$	−.02	--
40	3503.056	28538.34	(.234) 1.266A	$157_{5/2}-4430_{3/2}$	+.03	--
4	3503.305	28536.31		$151_{1/2}-4370_{3/2}$	.00	--
5	3503.748	28532.70		$273_{11/2}-5577_{13/2}$	+.07	--
(2h)	3505.68	28517.0		$273''_{1/2}-5590_{9/2}$	+.2	7
3	3506.177	28512.93		$194_{5/2}-4797_{5/2}$	.00	--
10	3506.390	28511.20	(**.173**, .522)	$224_{3/2}-5093_{5/2}$ $150_{7/2}-4356_{3/2}$	−.15 +.03	-- --
3	3507.334	28503.53		$221_{9/2}-5066_{11/2}$	+.06	--
1	3508.626	28493.03		$231_{5/2}-5164_{7/2}$	+.02	--
10	3510.889	28474.67		$194_{5/2}-4793_{7/2}$	+.01	--
4	3511.343	28470.99	(.117, .351)	$288_{7/2}-5728_{9/2}$	.00	--
20	3512.280	28463.38	(**.105**, .320, .534, . . .)	$166_{9/2}-4508_{11/2}$	+.03	--
5	3515.01	28441.2	(.418)†?	$194_{5/2}-4789_{3/2}$	−.1	--
5	3515.756	28435.25	(.421)	$231_{5/2}-5159_{3/2}$	−.02	--
5	3516.146	28432.09		$244_{5/2}-5285_{7/2}$	+.05	--
40	3516.646	28428.05	(.137) 1.522A	$138_{3/2}-4225_{3/2}$	−.02	--
60	3517.326	28422.55	(.146, .439, **.732**) .704, .997, **1.290**, 1.583, 1.874	$146_{5/2}-4304_{3/2}$	−.01	--
15	3520.723	28395.13		$150_{7/2}-4345_{9/2}$	+.02	--
1	3521.041	28392.57		$164_{3/2}-4472_{3/2}$	−.01	--
4	3521.746	28386.88		$275_{9/2}-5589_{7/2}$	−.01	--
6	3522.171	28383.46		$217_{7/2}-5015_{5/2}$	−.01	--
4	3522.528	28380.58		$263_{13/2}-5472_{13/2}$	+.02	--
3	3524.736	28362.80		$288_{7/2}-5717_{7/2}$	−.03	--
2	3526.21	28350.95		$150_{7/2}-4341_{5/2}$	+.03	--
3	3526.368	28349.68		$150_{7/2}-4340_{7/2}$	.00	--
2	3527.229	28342.76		$115_{5/2}-3992_{3/2}$	−.03	--
4	3528.214	28334.84		$217_{7/2}-5011_{3/2}$	−.04	--
15	3529.213	28326.83	(**.132**, .397, .663)	$166_{9/2}-4494_{7/2}$	−.01	--
4	3529.74	28322.6		$231_{5/2}-5147_{3/2}$	+.3	--
5	3529.81	28322.0		$194_{5/2}-4777_{3/2}$	.0	--
4	3530.893	28313.35		$271_{7/2}-5545_{7/2}$	.00	--
2H	3532.69	28299.0		$341_{9/2}-6249_{7/2}$	−.2	--
2	3533.412	28293.16		$272_{9/2}-5545_{7/2}$	+.03	--
20	3534.822	28281.88	(0w) .908C	$166_{9/2}-4490_{7/2}$	+.01	--
1	3535.30	28278.1		$261_{3/2}-5440_{5/2}$	+.1	--
5	3536.157	28271.20		$239_{11/2}-5222_{13/2}$	.00	--
50	3537.462	28260.77	(0w) 1.167B	$115_{5/2}-3984_{7/2}$	−.02	--
2	3538.784	28250.22		$298_{5/2}-5805_{3/2}$	+.02	--
20	3539.329	28245.86	(0w) 1.221C	$194_{5/2}-4770_{3/2}$	−.03	--
10	3539.944	28240.96		$221_{9/2}-5040_{9/2}$	−.01	--
5	3543.688	28211.12		$194_{5/2}-4766_{7/2}$	.00	--
4	3544.370	28205.69		$263_{13/2}-5455_{11/2}$	+.04	--
3	3547.024	28184.59		$244_{5/2}-5261_{7/2}$	−.02	--
8	3548.106	28175.99		$151_{1/2}-4334_{3/2}$	+.03	--
5	3549.319	28166.37		$239_{11/2}-5212_{13/2}$	+.02	--
50	3549.891	28161.83	(**.115**, .342, .569, .794, 1.030) **.282**, .508, .720, .928, 1.154	$117_{9/2}-3991_{11/2}$	−.04	--
2	3550.644	28155.86		$341_{9/2}-6235_{7/2}$	.00	5
40	3551.294	28150.70	(0w) 1.292C	$221_{9/2}-5031_{7/2}$	+.04	--
2	3553.078	28136.57		$261_{3/2}-5426_{3/2}$	−.04	--

Int.	λ_{vac}	σ_{vac}	Zeeman effect	Transition	O–C	Notes
	A	*K*				
3	3553.50	28133.2		$247_{7/2}-5285_{7/2}$	.0	--
20	3553.650	28132.04	(137) 1.249A?..	$173_{7/2}-4546_{7/2}$	+.03	--
30	3558.935	28090.27	**(.161, .477, .788, 1.104)**	$117_{9/2}-3984_{7/2}$	+.04	--
1	3559.239	28087.86		$217_{7/2}-4986_{7/2}$	+.04	--
6	3559.407	28086.54		$115_{5/2}-3967_{5/2}$	-.02	--
10	3562.454	28062.52		$272_{9/2}-5522_{11/2}$	+.02	--
20	3564.732	28044.59	(000) 1.403.....	$157_{5/2}-4381_{7/2}$	.00	--
5	3565.195	28040.94		$224_{5/2}-5046_{5/2}$	-.03	--
1	3565.706	28036.93		$221_{9/2}-5019_{9/2}$	+.03	--
4	3566.816	28028.20		$231_{5/2}-5118_{5/2}$	+.01	--
1	3567.600	28022.04		$197_{1/2}-4777_{1/2}$	+.04	--
30	3568.234	28017.06	**(.071, .227, .382)**	$247_{7/2}-5274_{9/2}$	-.02	--
2	3568.780	28012.78		$288_{7/2}-5682_{5/2}$ $173_{7/2}-4534_{9/2}$	-.10 +.03	--
30	3570.255	28001.20	**(.087, .259, .431) .997, 1.169, 1.338, 1.506, 1.675**	$173_{7/2}-4535_{5/2}$	-.01	--
2	3571.052	27994.95		$313_{9/2}-5939_{9/2}$	-.04	--
8	3571.694	27989.92		$239_{11/2}-5194_{11/2}$	+.01	--
2	3572.213	27985.86		$150_{7/2}-4304_{5/2}$	+.03	--
8	3572.804	27981.23		$164_{3/2}-4430_{5/2}$	+.01	--
2	3572.961	27980.00		$273_{11/2}-5522_{11/2}$	+.01	--
3	3573.730	27973.98		$306_{9/2}-5861_{11/2}$	-.01	--
1	3577.09	27947.7		$244_{5/2}-5237_{7/2}$	.0	--
6	3577.325	27945.87	(.233).....	$197_{1/2}-4770_{3/2}$	.00	--
1	3577.923	27941.20		$311_{5/2}-5912_{3/2}$	-.02	--
2	3578.054	27940.17		$275_{9/2}-5545_{7/2}$	.00	--
60	3579.125	27931.81	**(.322,** .973) **.330, .990,** 1.643	$157_{5/2}-4370_{5/2}$	+.03	--
50	3580.970	27917.42	(0w) 1.226.....	$163_{11/2}-4422_{9/2}$	-.01	--
80	3583.02	27901.5	(.303) 1.488A	$117_{9/2}-3965_{9/2}$	.0	--
7	3583.146	27900.47	(0w) **.609,** .825, 1.041	$194_{3/2}-4735_{7/2}$	.00	--
15	3585.030	27885.81		$247_{7/2}-5261_{7/2}$	+.02	--
10d	3585.329	27883.48	(.927) **.252,** .565	$172_{1/2}-4512_{3/2}$	-.03	--
1	3586.842	27871.72		$280_{5/2}-5590_{3/2}$	+.03	--
2	3589.264	27852.91		$244_{3/2}-5227_{3/2}$	+.03	--
10	3590.878	27840.39	(.240) .532, **1.010**	$224_{3/2}-5026_{3/2}$	.00	19
1	3591.86	27832.7		$314_{3/2}-5929_{3/2}$	-.1	--
10	3593.388	27820.95		$164_{3/2}-4414_{3/2}$	+.01	--
15	3595.164	27807.20	(0w) 1.507C...	$217_{7/2}-4958_{9/2}$	-.01	--
2h	3595.32	27806.0		$266_{5/2}-5446_{3/2}$ $304_{3/2}-5835_{3/2}$	.0 +.2	--
2	3595.887	27801.61		$319_{7/2}-5978_{7/2}$	-.07	--
10	3596.230	27798.96		$157_{5/2}-4356_{3/2}$	+.02	--
20	3596.392	27797.71	**(.106,** .315, .531) **.621,** .831, 1.041, 1.245	$217_{7/2}-4957_{5/2}$	.00	--
3	3597.039	27792.71		$244_{5/2}-5221_{5/2}$	.00	--
15	3598.767	27779.36	(.313, **.517**) .877, 1.081, **1.286,** 1.490, 1.694.	$231_{3/2}-5093_{3/2}$	-.01	--
15	3604.394	27736.00	**(.326,** .978) 1.101, 1.752, **2.404.**	$224_{3/2}-5015_{5/2}$	-.04	--
2	3605.971	27723.87		$298_{5/2}-5752_{5/2}$	-.06	--
4	3606.558	27719.35		$305_{11/2}-5827_{9/2}$	-.05	--
10	3607.232	27714.18	(0w) 1.325.....	$231_{5/2}-5086_{7/2}$ $194_{5/2}-4717_{3/2}$	-.91 -.0	--
2	3607.833	27709.56		$275_{9/2}-5522_{11/2}$	+.02	--
10	3608.661	27703.20		$221_{9/2}-4986_{7/2}$	+.02	--
30	3610.492	27689.15	(0w) 1.234A...	$163_{11/2}-4399_{11/2}$	.00	--
2	3611.437	27681.91		$271_{7/2}-5482_{5/2}$	+.02	--
(2H)	3613.41	27666.8		$314_{3/2}-5912_{3/2}$	+.1	7
8	3615.372	27651.78		$272_{9/2}-5481_{9/2}$	+.01	--
3	3616.427	27643.72		$194_{3/2}-4710_{3/2}$	.00	--
80	3617.085	27638.68	(.777) 1.103, **1.315,** 1.526†.	$157_{5/2}-4341_{3/2}$	-.01	19
20	3617.252	27637.41		$157_{5/2}-4340_{7/2}$	-.04	--
20	3617.859	27632.77	**(.209,** .621).....	$146_{5/2}-4225_{3/2}$	+.04	--
1	3619.203	27622.51		$164_{3/2}-4394_{5/2}$	+.04	--
2	3620.145	27615.33		$173_{7/2}-4494_{11/2}$	+.03	--
2	3620.230	27614.68		$306_{9/2}-5826_{7/2}$	-.02	--
30	3621.460	27605.29	(.328, 1.205)A...	$166_{5/2}-4422_{9/2}$	-.01	--
10	3622.183	27599.78		$263_{13/2}-5394_{11/2}$	+.01	--
2	3622.265	27599.16		$270_{13/2}-5472_{13/2}$	-.22	--
20	3625.908	27571.43	**(.167,** .569) 1.154, 1.489, **1.823†**	$157_{5/2}-4334_{3/2}$ $298_{5/2}-5737_{7/2}$	-.00 +.06	--
8	3626.053	27570.33	(000) 1.242.....	$173_{7/2}-4499_{7/2}$	.00	--
20	3629.200	27546.42	(0w) 1.455B...	$194_{5/2}-4700_{3/2}$	-.03	--
2	3632.154	27524.02		$304_{3/2}-5805_{3/2}$	+.04	--
4	3636.772	27489.07	**(.135,** .396)...	$204_{3/2}-4797_{5/2}$	-.02	--
40	3637.064	27486.86	**(.102,** .304) **.969,** 1.175, 1.379.	$148_{3/2}-4131_{3/2}$	-.04	--
10	3637.228	27485.62		$273_{11/2}-5472_{13/2}$	-.02	--
15	3637.732	27481.82	(.601) .727...	$172_{1/2}-4478_{1/2}$	+.03	--
60	3637.848	27480.94	(.171) 1.304A...	$115_{5/2}-3966_{3/2}$	-.02	--
2	3641.202	27455.63		$332_{1/2}-6073_{3/2}$	.00	--
15	3642.986	27442.19	**(.068,** .201, .335).	$117_{9/2}-3919_{11/2}$	-.03	--
4	3643.712	27436.72	(.185) .948.....	$224_{3/2}-4985_{1/2}$	+.02	--
5	3645.33	27424.5		$270_{13/2}-5455_{11/2}$	.0	--
8	3645.590	27422.58		$221_{9/2}-4958_{9/2}$	+.01	--
5	3646.636	27414.72	(.617) 1.602...	$197_{1/2}-4718_{1/2}$	-.3	--
1	3646.69	27414.3		$195_{1/2}-4717_{3/2}$	+.1	--
2	3649.210	27395.38		$217_{7/2}-4917_{9/2}$	+.02	--
6	3649.47	27393.4		$272_{9/2}-5455_{11/2}$	+.1	--
20	3651.656	27377.03		$166_{9/2}-4399_{11/2}$	+.01	--
80	3651.972	27374.67	(.127, **.384**) 1.585, **1.835,** 2.093.	$164_{3/2}-4370_{3/2}$	-.02	--
2	3652.29	27372.3		$298_{5/2}-5717_{7/2}$	.0	--
2	3652.563	27370.23		$285_{7/2}-5591_{9/2}$	-.06	--
15	3653.621	27362.31		$236_{9/2}-5099_{7/2}$	-.02	--
4	3654.366	27356.73		$266_{5/2}-5401_{7/2}$ $236_{9/2}-5098_{7/2}$	-.03 +.08	--
8	3654.935	27352.47	**(.084,** .248, .410).	$272_{9/2}-5451_{7/2}$	-.02	--
20	3660.515	27310.77	(0w) 1.193†?	$273_{11/2}-5455_{11/2}$	+.04	--
10	3662.126	27298.76	(.200) 1.171A...	$275_{9/2}-5481_{9/2}$	-.05	--
2	3665.251	27275.49		$194_{3/2}-4673_{3/2}$	.00	--
2	3665.522	27273.47		$157_{5/2}-4304_{5/2}$	-.13	--
3	3669.159	27246.44		$197_{1/2}-4700_{3/2}$	+.01	--
8	3669.436	27244.38	(.748).....	$224_{3/2}-4966_{3/2}$	-.04	--
40	3669.778	27241.81	**(.103,** .399) **1.190,** 1.396.	$164_{3/2}-4356_{3/2}$	-.01	--
7	3669.993	27240.25		$117_{9/2}-3899_{9/2}$	+.04	--
10	3670.358	27237.54		$239_{11/2}-5119_{9/2}$	+.05	--
50	3670.528	27236.28	**(.108,** .314, .521, .728) **.635,** .842, 1.049, 1.258.	$142_{7/2}-4145_{9/2}$	-.04	--
(1)	3671.24	27231.0		$247_{7/2}-5195_{7/2}$	+.2	13
20	3672.407	27222.34	(0w) 1.314B...	$241_{5/2}-5164_{7/2}$ $146_{5/2}-4184_{7/2}$	-.08 -.05	--
15	3676.000	27195.73	(.088, .265, .443, .620) **.555,** .733.	$166_{9/2}-4381_{7/2}$	.00	--
4	3676.570	27191.52	(.053) 1.359h...	$194_{5/2}-4664_{5/2}$	-.01	--
2	3677.722	27183.09		$204_{3/2}-4765_{1/2}$	-.01	--
6	3678.392	27178.05		$172_{1/2}-4441_{1/2}$	+.02	--
10	3680.206	27164.65	(.117) 1.114A...	$244_{3/2}-5159_{3/2}$	-.03	--
8	3681.284	27156.70	(.360) .290.....	$261_{3/2}-5328_{1/2}$	-.01	--
2	3681.407	27155.79		$231_{5/2}-5031_{7/2}$	-.10	--
4	3681.834	27152.64		$244_{5/2}-5157_{7/2}$	-.01	--
5	3682.155	27150.28		$224_{3/2}-4957_{5/2}$	.00	--
8	3682.714	27146.16		$163_{11/2}-4345_{9/2}$	+.01	--
1	3685.303	27127.08		$271_{7/2}-5426_{5/2}$	+.03	--
2	3685.444	27126.05		$221_{9/2}-4928_{11/2}$	+.02	--
3	3686.452	27118.63		$263_{13/2}-5346_{11/2}$	+.02	--
6	3688.646	27102.50		$288_{7/2}-5591_{9/2}$	-.1	--
150	3689.504	27096.20	**(.147,** .439, .732) 1.144, 1.429, 1.715, **1.991.**	$142_{7/2}-4131_{7/2}$	+.04	12
(1)	3690.16	27091.4		$288_{7/2}-5589_{7/2}$	+.1	13
1	3690.547	27088.54		$151_{7/2}-4225_{7/2}$	+.24	--
20	3691.385	27082.39		$273_{11/2}-5446_{7/2}$ $217_{7/2}-4885_{7/2}$	+.19 +.19	--
200	3691.48	27081.7		$150_{7/2}-4214_{9/2}$ $164_{3/2}-4343_{3/2}$	-.2 +.1	--
10	3692.115	27077.03		$266_{5/2}-5373_{7/2}$	.00	--
2	3692.808	27071.95		$239_{11/2}-5102_{9/2}$	-.01	--
2	3693.664	27065.68		$298_{5/2}-5686_{5/2}$	.00	--
3	3695.600	27051.50		$194_{5/2}-4650_{3/2}$	-.01	--
2	3697.124	27040.35		$275_{9/2}-5455_{11/2}$	+.05	--
20	3697.710	27036.07		$271_{7/2}-5417_{7/2}$	-.05	--
2d	3700.684	27014.34		$164_{3/2}-4324_{5/2}$	.00	--
4	3701.184	27010.69	(000) 1.188.....	$221_{9/2}-4917_{9/2}$	-.03	--
5	3702.098	27004.02	(.370, **.613**).....	$231_{5/2}-5015_{5/2}$	-.04	--
(2h)	3702.74	26999.4		$275_{9/2}-5451_{7/2}$	-.1	7
100	3703.243	26995.67	**(.180,** .540) **.588,** .947, 1.306, 1.665.	$138_{3/2}-4082_{3/2}$	-.04	--
1	3703.53	26993.6		$261_{3/2}-5312_{3/2}$	.0	--
10	3704.842	26984.02		$138_{3/2}-4081_{3/2}$	-.03	--
20	3705.02	26982.8		$138_{3/2}-4080_{1/2}$	+.1	--
8	3705.686	26977.88		$173_{7/2}-4430_{5/2}$	-.03	--
6h	3708.774	26955.42		$231_{5/2}-5011_{5/2}$	-.05	--
60	3709.930	26947.02	(.382, .629, .875) .698, .948, 1.198, **1.447,** 1.697, 1.947, 2.196.	$142_{7/2}-4116_{7/2}$	-.03	--
2	3710.64	26941.8		$301_{1/2}-5707_{1/2}$	+.1	--
5	3711.46	26935.9	(.258).....	$146_{5/2}-4155_{3/2}$	+.3	--
5h	3712.920	26925.32		$272_{9/2}-5408_{7/2}$	.00	--
10	3713.160	26923.58		$247_{7/2}-5164_{7/2}$	-.02	--
1	3714.530	26913.64		$338_{7/2}-6073_{3/2}$	-.10	--
1	3714.712	26912.32		$285_{7/2}-5545_{7/2}$	-.03	--
5	3714.995	26910.28	(.479) **1.088,** 2.040.	$172_{1/2}-4414_{3/2}$	+.13	--
100	3717.285	26893.70	(000) 1.257w...	$173_{7/2}-4422_{5}$	-.06	--
20	3717.44	26892.6		$305_{11/2}-5745_{13/2}$	-.2	--
2h	3720.860	26867.86		$221_{9/2}-4963_{7/2}$	+.05	--
4	3721.146	26865.79		$247_{7/2}-5159_{5/2}$	-.07	--
(3)	3722.22	26858.1		$324_{5/2}-5929_{3/2}$	-.2	13

Int.	λvac	σvac	Zeeman effect	Transition	O–C	Notes
	A	*K*				
2000R	3725.760	26832.52	(**.073**. **.218**, .373, **.413**, .653) **.981**. . .	$^{2363}9/_2 - ^{5047}11/_2$	.00	--
8	3726.502	26827.18		$^{224}3/_2 - ^{4925}5/_2$	−.01	--
4	3726.68	26825.9		$^{151}1/_2 - ^{4199}1/_2$	+.2	--
7	3727.498	26820.01	(.056) .704.	$^{261}3/_2 - ^{5295}5/_2$	−.01	--
1h	3729.684	26804.29		$^{244}5/_2 - ^{5122}7/_2$	+.05	--
20	3731.870	26788.60	(.118, **.557**) .809†.	$^{166}9/_2 - ^{4340}7/_2$	+.01	19
(5H)	3732.058	26787.25		$^{272}9/_2 - ^{5394}11/_2$	−.13	7
40	3732.278	26785.67	(.152w) 1.176A. .	$^{150}7/_2 - ^{4184}7/_2$	+.01	--
20	3735.01	26766.1		$^{117}9/_2 - ^{3852}7/_2$	−.1	--
1000	3735.314	26763.90	(.413) 1.712A . .	$^{2363}9/_2 - ^{5039}9/_2$	.00	--
4h	3736.193	26757.60		$^{244}5/_2 - ^{5118}9/_2$	.00	--
10	3736.838	26752.98		$^{247}7/_2 - ^{5147}5/_2$	+.05	--
1	3737.806	26746.05		$^{306}9/_2 - ^{5739}11/_2$	−.06	--
1	3738.538	26740.82		$^{231}5/_2 - ^{4989}9/_2$	+.06	--
200	3740.10	26729.7	(0w) 1.485C. . .	$^{142}7/_2 - ^{4094}7/_2$	.0	19
30	3740.414	26727.41		$^{2363}9/_2 - ^{5035}7/_2$	.00	--
2	3743.072	26708.43		$^{231}5/_2 - ^{4986}7/_2$	+.02	--
1	3743.194	26707.56		$^{239}11/_2 - ^{5066}11/_2$	+.05	--
2	3743.572	26704.86		$^{273}11/_2 - ^{5394}11/_2$	+.01	--
80	3745.436	26691.57	(000) 1.065, **1.206**, **1.341**, 1.472.	$^{146}9/_2 - ^{4131}5/_2$	+.01	--
5	3750.666	26654.35		$^{194}5/_2 - ^{4611}5/_2$	.00	--
2	3752.718	26639.77		$^{278}3/_2 - ^{5446}3/_2$	+.02	--
1	3753.316	26635.53		$^{306}3/_2 - ^{5728}9/_2$	.00	--
2	3753.770	26632.31		$^{266}5/_2 - ^{5329}5/_2$	+.02	--
15	3755.624	26619.17	(**.063**, **.188**, **.313**) **.945**, 1.069, 1.194.	$^{173}7/_2 - ^{4394}5/_2$	+.01	--
15	3757.622	26605.01	(**.223**, .668)	$^{142}7/_2 - ^{4082}5/_2$	+.04	--
2	3759.749	26589.96		$^{314}3/_2 - ^{5805}3/_2$	.00	--
2	3765.878	26546.68		$^{304}3/_2 - ^{5707}1/_2$	−.03	--
15	3766.480	26542.44	(**.082**, .247, .413) 1.424, 1.576, **1.740**.	$^{146}9/_2 - ^{4116}7/_2$	−.01	--
5d	3769.297	26522.60	(.249)	$^{204}3/_2 - ^{4700}3/_2$	−.01	--
8	3770.738	26512.47		$^{231}5/_2 - ^{4966}3/_2$	+.03	--
2h	3771.252	26508.86		$^{244}5/_2 - ^{5085}3/_2$	+.08	--
2	3774.83	26483.8		$^{157}5/_2 - ^{4225}5/_2$	.0	--
3	3775.460	26479.31		$^{194}5/_2 - ^{4593}7/_2$	+.02	--
30	3777.69	26463.7	(.284) 1.241, **1.680**†.	$^{172}1/_2 - ^{4370}3/_2$	−.2	--
2	3778.535	26457.77		$^{273'}1/_2 - ^{5384}3/_2$ $^{273''}1/_2 - ^{5384}3/_2$	−.36 +.44	-- --
15	3780.357	26445.01		$^{239}11/_2 - ^{5040}9/_2$ $^{306}9/_2 - ^{5709}7/_2$	.00 +.05	-- --
2	3780.54	26443.8		$^{244}5/_2 - ^{5086}7/_2$	+.2	--
4	3781.864	26434.48		$^{275}9/_2 - ^{5394}11/_2$	+.06	--
15	3784.179	26418.30	(.254, .423) 1.256.	$^{194}5/_2 - ^{4587}3/_2$ $^{231}3/_2 - ^{4957}3/_2$	−.15 .00	-- --
(6)	3785.40	26409.8		$^{221}9/_2 - ^{4856}11/_2$	+.2	13
2	3785.535	26408.84		$^{217}1/_2 - ^{4818}1/_2$	+.04	--
10	3787.192	26397.28		$^{266}5/_2 - ^{5305}3/_2$	−.03	--
150	3787.520	26395.00	(**.102**, .308, .514, .720) .638, .844, 1.050, 1.254, 1.459, 1.666, 1.872, **2.084**.	$^{150}7/_2 - ^{4145}9/_2$	+.01	--
4	3789.212	26383.21		$^{197}1/_2 - ^{4614}1/_2$	+.01	--
4	3789.771	26379.32		$^{280}5/_2 - ^{5440}5/_2$	+.03	--
3	3795.505	26339.47		$^{304}3/_2 - ^{5686}3/_2$	+.01	--
10	3795.800	26337.42	(0w) D.	$^{270}3/_2 - ^{5346}11/_2$	−.01	--
50	3796.590	26331.94	(**.108**, .319) . .	$^{115}5/_2 - ^{3791}3/_2$	+.03	--
50	3797.586	26325.04	(**.192**, .574, .955) 2.103.	$^{146}3/_2 - ^{4094}7/_2$	−.03	--
3	3798.252	26320.42		$^{301}1/_2 - ^{5645}1/_2$	+.11	--
3	3801.742	26296.26		$^{319}7/_2 - ^{5827}9/_2$ $^{304}3/_2 - ^{5688}5/_2$	−.06 +.11	-- --
2	3802.21	26293.0		$^{266}5/_2 - ^{5296}3/_2$	.0	--
2	3804.527	26277.01		$^{319}7/_2 - ^{5829}7/_2$	−.03	--
5	3805.41	26270.9		$^{285}7/_2 - ^{5481}9/_2$	−.1	--
40	3807.742	26254.82	(**.064**, .192, .318) **.830**, .957, 1.084.	$^{150}7/_2 - ^{4131}5/_2$	−.01	--
10d	3808.200	26251.67		$^{204}3/_2 - ^{4673}3/_2$	+.02	--
2	3808.640	26248.64		$^{271}7/_2 - ^{5338}5/_2$	+.04	--
3	3809.752	26240.98		$^{239}11/_2 - ^{5019}9/_2$	+.04	--
20	3810.098	26238.59		$^{173}7/_2 - ^{4359}5/_2$	+.05	--
20	3812.259	26223.72	(.160) 1.102A . .	$^{273}11/_2 - ^{5345}11/_2$	+.03	--
7	3812.812	26219.92		$^{266}5/_2 - ^{5288}5/_2$	+.01	--
(1H)	3814.24	26210.1		$^{247}7/_2 - ^{5083}5/_2$	+.1	7
40	3815.655	26200.38	(0w) 1.107C. . . .	$^{146}5/_2 - ^{4082}5/_2$	+.01	19
2	3816.294	26195.99		$^{266}5/_2 - ^{5285}7/_2$	−.02	--
30	3817.539	26187.45	(**.183**, .549)	$^{146}5/_2 - ^{4083}5/_2$	+.06	--
5	3818.655	26179.79		$^{271}7/_2 - ^{5332}9/_2$	−.03	--
(8)	3820.45	26167.5		$^{204}3/_2 - ^{4644}5/_2$	−.2	13
3	3821.598	26159.64		$^{272}9/_2 - ^{5332}9/_2$	+.04	--
2h	3821.962	26157.15		$^{217}7/_2 - ^{4793}7/_2$	.00	--
3	3823.478	26146.77		$^{280}5/_2 - ^{5417}7/_2$ $^{261}3/_2 - ^{5227}3/_2$	−.16 +.06	-- --
10	3823.772	26144.76		$^{247}7/_2 - ^{5086}7/_2$	−.02	--
15	3827.04	26122.4		$^{173}7/_2 - ^{4345}9/_2$	−.1	--
9	3827.625	26118.45	(.201)	$^{197}1/_2 - ^{4587}1/_2$	+.02	--
50	3828.325	26113.67	(.149) 1.245A . .	$^{115}5/_2 - ^{3769}5/_2$	−.03	--
20	3829.80	26103.6	(.776) .196.	$^{172}1/_2 - ^{4334}5/_2$	.0	--
10	3829.83	26103.4		$^{338}7/_2 - ^{5992}7/_2$	+.1	--
2	3830.098	26101.58		$^{298}3/_2 - ^{5590}3/_2$	−.05	--
3	3831.028	26095.25		$^{231}3/_2 - ^{4926}1/_2$	+.04	--
70	3833.702	26077.04	(.343) 1.033, 1.183, **1.333**, 1.488, 1.652†?	$^{273}11/_2 - ^{5332}9/_2$ $^{173}7/_2 - ^{4340}7/_2$	−.03 −.01	-- --
100	3834.235	26073.42	(**.059**, .177, .296) **.894**, 1.024, 1.145, 1.264.	$^{157}5/_2 - ^{4184}7/_2$	−.01	--
70	3836.305	26059.35	(.607) 1.587.	$^{197}1/_2 - ^{4581}1/_2$	.00	--
1h	3837.088	26054.03		$^{306}9/_2 - ^{5669}7/_2$	−.05	--
10	3841.498	26024.12	(0w) 1.123b. . . .	$^{221}9/_2 - ^{4818}7/_2$	−.04	--
60	3843.415	26011.15	(**.097**, .292 . . .)	$^{117}9/_2 - ^{3776}7/_2$	+.02	--
(3)	3844.35	26004.8		$^{194}5/_2 - ^{4546}7/_2$	−.1	13
7	3846.857	25987.87		$^{280}5/_2 - ^{5401}7/_2$	.00	--
15	3851.988	25953.26	(0w) 1.459B. . .	$^{275}5/_2 - ^{5346}11/_2$	.00	--
5	3852.689	25948.53		$^{266}5/_2 - ^{5291}7/_2$	−.05	--
30	3855.936	25926.69	(.202) 1.512, 1.643.	$^{164}5/_2 - ^{4285}5/_2$	+.01	--
1	3858.584	25908.89		$^{273'}1/_2 - ^{5329}3/_2$ $^{273''}1/_2 - ^{5329}3/_2$	−.43 +.37	-- --
2	3859.328	25903.90		$^{273'}1/_2 - ^{5328}1/_2$ $^{273''}1/_2 - ^{5328}1/_2$	+.02 .00	-- --
2	3859.450	25903.08		$^{217}7/_2 - ^{4766}7/_2$	−.01	--
9	3860.862	25893.60		$^{150}7/_2 - ^{4094}7/_2$	.00	--
6	3861.647	25888.34		$^{244}5/_2 - ^{5031}7/_2$	−.02	--
6	3862.103	25885.28		$^{263}13/_2 - ^{5222}13/_2$	+.01	--
5	3863.153	25878.25		$^{194}5/_2 - ^{4533}5/_2$	−.01	--
15	3863.768	25874.13		$^{231}5/_2 - ^{4903}7/_2$	.00	--
4	3863.932	25873.04		$^{285}7/_2 - ^{5440}5/_2$	−.03	--
4	3864.766	25867.45		$^{275}9/_2 - ^{5337}9/_2$	.00	--
1	3865.126	25865.04		$^{3340}5/_2 - ^{5926}5/_2$	−.03	--
2h	3865.875	25860.03		$^{305}11/_2 - ^{5641}9/_2$	−.2	--
2	3867.21	25851.1		$^{138}9/_2 - ^{3967}3/_2$	−.07	--
2	3868.213	25844.33		$^{163}11/_2 - ^{4214}9/_2$	−.07	--
100	3869.944	25832.84	(0w) 1.306C. . .	$^{280}5/_2 - ^{5384}3/_2$	.00	--
3	3873.037	25812.21		$^{275}9/_2 - ^{5332}9/_2$	+.02	--
4	3873.870	25806.66		$^{115}5/_2 - ^{3738}3/_2$	−.1	--
100	3875.26	25797.4	(.436, .723) .852, **1.134**, 1.413.			
150	3876.861	25786.75	(**.171**, .512) **.797**, 1.139, 1.480.	$^{157}5/_2 - ^{4155}3/_2$	+.09	--
20	3878.868	25773.41		$^{313}9/_2 - ^{5717}1/_2$ $^{263}13/_2 - ^{5212}13/_2$	+.01 +.02	-- --
10	3879.016	25772.42		$^{221}9/_2 - ^{4793}7/_2$	−.09	--
2	3880.336	25763.66		$^{150}7/_2 - ^{4082}5/_2$	+.02	--
40	3881.89	25753.3		$^{1895}5/_2 - ^{4470}5/_2$	.0	--
5	3883.958	25739.63		$^{247}7/_2 - ^{5046}5/_2$	+.05	--
2h	3884.888	25733.47		$^{244}5/_2 - ^{5015}5/_2$	.00	--
40	3887.488	25716.26		$^{271}7/_2 - ^{5285}7/_2$	−.05	--
40	3887.950	25713.20	(.095, 285, **.476**.)	$^{173}7/_2 - ^{4304}5/_2$	.00	--
2	3889.36	25703.9		$^{288}7/_2 - ^{5451}7/_2$	−.1	--
40	3889.962	25699.91	(000) 1.123w. . .	$^{221}9/_2 - ^{4785}11/_2$	+.02	--
1	3890.54	25696.1		$^{272}9/_2 - ^{5285}7/_2$	.0	--
5	3893.48	25676.7		$^{247}7/_2 - ^{5040}9/_2$	−.1	--
5	3893.914	25673.82		$^{319}7/_2 - ^{5765}9/_2$	−.04	--
4	3895.41	25664.0		$^{164}3/_2 - ^{4199}1/_2$ $^{194}3/_2 - ^{4512}3/_2$	−.1 +.1	-- --
30	3896.110	25659.35	(.366) 1.080, **1.811**.	$^{204}3/_2 - ^{4614}1/_2$	−.03	--
2	3898.41	25644.2		$^{151}1/_2 - ^{4081}1/_2$	−.1	--
2	3900.34	25631.5		$^{231}5/_2 - ^{4878}7/_2$	.0	--
3	3900.50	25630.4		$^{204}3/_2 - ^{4611}5/_2$	−.1	--
30	3900.907	25627.80	(.534, .883, **1.235**.)	$^{142}7/_2 - ^{3984}7/_2$	−.09	--
20	3901.092	25626.58		$^{239}11/_2 - ^{4958}9/_2$	−.03	--
5	3902.580	25616.81		$^{266}5/_2 - ^{5227}3/_2$	−.04	--
3	3902.82	25615.2		$^{324}5/_2 - ^{5805}3/_2$	−.2	--
10	3905.12	25600.1	(000) 1.190B. . .	$^{271}7/_2 - ^{5274}9/_2$	−.1	--
(5)	3905.56	25597.3		$^{263}13/_2 - ^{5194}11/_2$	+.3	13
3	3907.20	25586.5		$^{247}7/_2 - ^{5031}7/_2$	.0	--
3	3907.74	25583.0		$^{217}7/_2 - ^{4735}7/_2$	.0	--
40	3908.210	25579.91	(.155, .257, .360, **.453**) 1.152.	$^{272}9/_2 - ^{5274}9/_2$	−.04	--
1	3909.84	25569.23		$^{273''}1/_2 - ^{5296}3/_2$	−.03	--
2	3910.157	25567.18		$^{273'}1/_2 - ^{5295}3/_2$	−.01	--
2	3910.272	25566.42		$^{273''}1/_2 - ^{5295}3/_2$	+.03	--
2	3911.76	25556.7		$^{266}9/_2 - ^{5221}3/_2$	.0	--
60	3913.924	25542.57	(.089) 1.291A. .	$^{157}5/_2 - ^{4131}5/_2$	−.03	--
200	3917.270	25520.75	(.141w) 1.142C	$^{166}9/_2 - ^{4214}9/_2$	−.03	--
10	3919.076	25508.99		$^{221}9/_2 - ^{4766}7/_2$	+.02	--
20	3920.85	25497.5	(0w) 1.189B. . .	$^{273}11/_2 - ^{5274}9/_2$	+.1	--
10	3922.274	25488.19	(**.226**, .682) **.226**, .682.	$^{194}3/_2 - ^{4494}7/_2$	−.04	--
5	3923.58	25479.7		$^{115}5/_2 - ^{3706}3/_2$	.0	--
10	3924.090	25476.40	(.224)	$^{224}3/_2 - ^{4789}3/_2$	+.01	--
4	3924.67	25472.6		$^{247}7/_2 - ^{5019}9/_2$	−.1	--
2	3925.038	25470.24		$^{244}5/_2 - ^{4989}9/_2$	+.07	--
2	3925.63	25466.4		$^{278}9/_2 - ^{5329}3/_2$	+.3	--
10	3926.522	25460.62	(.238)	$^{278}9/_2 - ^{5328}1/_2$	−.01	--
4	3926.85	25458.5	(.188)	$^{261}3/_2 - ^{5159}9/_2$ $^{288}7/_2 - ^{5429}1/_2$	.0 +.2	-- --
30	3927.59	25453.7	(**.227**, .693)	$^{142}7/_2 - ^{3967}5/_2$	.0	--

Int.	λ_{vac}	σ_{vac}	Zeeman effect	Transition	O–C	Notes
	A	*K*				
2	3928.364	25448.68		$272_{9/2} - 5261_{7/2}$	+.02	--
15	3928.704	25446.48	(.130, **.395**)	$261_{3/2} - 5157_{3/2}$	.00	--
6	3929.198	25443.27		$194_{5/2} - 4490_{7/2}$	+.01	--
200	3929.847	25439.07	(**.067**, .202, .338, .474) **.968**, 1.103, 1.239, 1.374.	$142_{7/2} - 5965_{9/2}$	−.06	--
6	3930.53	25434.7		$247_{7/2} - 5015_{5/2}$	.0	--
20	3931.201	25430.31	(0w) .972C	$217_{7/2} - 4780_{9/2}$	−.02	--
2	3936.70	25394.8		$204_{3/2} - 4587_{3/2}$	+.2	--
100	3936.899	25393.51	(000) 1.321	$157_{5/2} - 4116_{7/2}$	+.02	--
2h	3937.628	25388.81		$319_{7/2} - 5737_{7/2}$	+.05	--
6	3941.468	25364.07	(.156) **.520**, .828.	$197_{1/2} - 4512_{3/2}$	+.17	--
(2)	3942.22	25359.2		$280_{3/2} - 5338_{5/2}$	−.2	13
10	3942.562	25357.03		$224_{5/2} - 4777_{3/2}$	−.05	--
15	3944.344	25345.58		$261_{3/2} - 5147_{5/2}$	.00	--
50	3944.718	25343.17	(**.075**, .226)	$275_{9/2} - 5285_{7/2}$	+.04	--
150	3945.906	25335.55	(.374) **1.068**, 1.815.	$204_{3/2} - 4581_{1/2}$	+.02	--
2	3946.75	25330.1		$239_{11/2} - 4928_{11/2}$	.0	--
15	3950.570	25305.64	(**.204**, .611) 1.377.	$280_{5/2} - 5333_{7/2}$	+.02	--
10	3950.64	25305.2		$146_{3/2} - 3962_{3/2}$	−.1	--
2	3951.45	25300.0		$313_{9/2} - 5669_{7/2}$	−.1	--
2	3951.836	25297.53		$278_{5/2} - 5312_{3/2}$	−.01	--
15	3954.428	25280.95	(1.017) .438, **1.104**, 1.767.	$224_{3/2} - 4770_{3/2}$	.00	--
2	3956.60	25267.1		$306_{9/2} - 5591_{9/2}$	.0	--
3	3957.173	25263.41		$280_{5/2} - 5329_{7/2}$	+.01	--
10	3957.363	25262.20	(000) 1.385	$194_{3/2} - 4472_{3/2}$	.00	--
7	3958.357	25255.86		$306_{9/2} - 5589_{7/2}$	−.01	--
15	3960.552	25241.86	{	$224_{3/2} - 4765_{1/2}$	−.07	--
			(.095)	$244_{3/2} - 4966_{5/2}$	+.01	--
150	3961.036	25238.77	(**.073**, .220) **1.120**, 1.267, 1.414, 1.562.	$138_{3/2} - 3906_{5/2}$	−.03	--
300	3962.484	25229.55	(0w) 1.781W	$164_{5/2} - 4155_{3/2}$	−.02	--
40	3963.267	25224.57	(0w) 1.099h	$166_{9/2} - 4184_{7/2}$	.00	--
7	3963.707	25221.77		$52441_{7/2} - 5766_{9/2}$	−.05	--
5	3964.279	25218.13		$341_{9/2} - 5941_{11/2}$	−.06	--
2	3964.53	25216.5		$305_{11/2} - 5577_{13/2}$	−.1	--
15	3964.810	25214.75	(**.070**, .209, .348, .487, .626) **.365** . . .	$239_{11/2} - 4917_{9/2}$	−.01	--
1	3965.27	25211.8		$272_{9/2} - 5237_{7/2}$	.0	--
30	3967.39	25198.4	(0w) .140w	$221_{9/2} - 4735_{7/2}$	+.1	--
2	3967.707	25196.34		$285_{7/2} - 5373_{7/2}$	+.01	--
(1h)	3970.93	25175.9		$157_{5/2} - 4094_{3/2}$	−.2	7
3	3975.374	25147.75		$244_{3/2} - 4957_{5/2}$	+.03	--
20	3975.648	25146.01		$163_{11/2} - 4145_{9/2}$	−.02	--
4	3976.759	25138.99		$247_{7/2} - 4986_{7/2}$	−.01	--
7	3982.286	25104.10		$1895_{5/2} - 4405_{3/2}$	.0	--
10	3983.41	25097.0		$270_{13/2} - 5222_{13/2}$	−.1	--
1	3985.31	25085.0		$273'_{1/2} - 5246_{1/2}$	−.1	--
1	3985.42	25084.3		$273''_{1/2} - 5246_{1/2}$	.0	--
5h	3987.086	25073.88		$3259_{9/2} - 5766_{9/2}$	+.08	--
15	3990.660	25051.42	{	$261_{3/2} - 5118_{3/2}$	−.01	--
			{	$157_{3/2} - 4982_{5/2}$	+.01	--
30	3991.033	25049.08	(.130) 1.012, 1.212.†	$146_{5/2} - 3967_{3/2}$	+.02	11
10	3991.571	25045.70		$221_{9/2} - 4780_{9/2}$	+.01	--
10	3992.72	25038.5		$157_{3/2} - 4080_{3/2}$	+.1	--
4d	3994.154	25029.50		$231_{5/2} - 4818_{7/2}$	+.11	--
3	3996.987	25011.77		$313_{9/2} - 5641_{9/2}$	−.15	--
3	4000.122	24992.17		$270_{13/2} - 5212_{13/2}$	−.02	--
3	4001.19	24985.5		$197_{1/2} - 4472_{3/2}$	−.02	--
70	4004.930	24962.16	(.174) 1.157, **1.303**.	$164_{3/2} - 4131_{3/2}$	.0	--
3	4010.322	24928.60	{	$266_{9/2} - 5159_{9/2}$	−.05	--
			{	$288_{7/2} - 5373_{7/2}$	+.01	--
(35)	4011.514	24921.19		$280_{5/2} - 5295_{3/2}$	−.08	3
15	4012.26	24916.6		$266_{9/2} - 5157_{3/2}$	.0	--
20	4018.40	24878.5	(000) 1.160	$273_{11/2} - 5212_{13/2}$	.0	--
6	4019.124	24874.01		$217_{7/2} - 4664_{9/2}$	−.01	--
10	4022.86	24850.9	{	$280_{5/2} - 5288_{5/2}$	−.1	--
			{	$194_{3/2} - 4479_{3/2}$	+.1	--
60	4022.965	24850.26	(**.176**, .525) **.553**, .907, 1.260.	$204_{3/2} - 4553_{3/2}$	−.04	--
40	4023.313	24848.11		$142_{7/2} - 3906_{5/2}$	+.05	--
3d	4025.07	24837.3	{	$301_{1/2} - 5496_{1/2}$	.0	--
			{	$285_{7/2} - 5337_{9/2}$	+.1	--
9	4025.614	24833.91		$166_{9/2} - 4145_{9/2}$	+.01	--
3	4026.707	24827.17		$280_{5/2} - 5285_{7/2}$	+.05	--
4	4027.124	24824.60	(**.102**, .304)	$244_{5/2} - 4925_{3/2}$	−.02	--
30	4028.53	24815.9	(0w) 1.168	$231_{5/2} - 4797_{3/2}$	−.1	22
60	4029.63	24809.2	(0w) 1.212B	$270_{13/2} - 5194_{11/2}$	+.1	
				$173_{7/2} - 4214_{9/2}$	.0	--
8	4032.143	24793.70		$306_{9/2} - 5545_{7/2}$	.0	--
				$285_{7/2} - 5333_{7/2}$	−.11	--
100	4033.31	24786.5	(.208w) 1.152A	$272_{9/2} - 5195_{7/2}$	+.03	--
10	4033.63	24784.6		$150_{7/2} - 3984_{7/2}$	−.1	--
1h	4034.74	24777.7		$272_{9/2} - 5194_{11/2}$	.0	--
50	4037.49	24760.9	(.813) **.073**, 1.559.	$142_{7/2} - 3896_{9/2}$	−.2	--
				$231_{3/2} - 4793_{7/2}$	.0	--
				$151_{1/2} - 3992_{3/2}$	.0	--
2h	4039.52	24748.4		$3452_{7/2} - 5926_{5/2}$	−.1	--
10	4040.178	24744.39	(.080) 1.211h	$231_{5/2} - 4789_{5/2}$	−.02	--
3	4041.305	24737.49		$324_{5/2} - 5717_{7/2}$	−.07	--
3	4044.798	24716.12		$311_{3/2} - 5590_{7/2}$	+.19	--
4	4045.237	24713.44		$298_{5/2} - 5451_{7/2}$	−.02	--
2	4047.106	24702.03		$273_{11/2} - 5194_{11/2}$	−.03	--
80	4048.99	24690.6	(**.106**, .322) **1.036**, 1.249, 1.462, 1.676.	$194_{5/2} - 4414_{3/2}$	.0	--
10	4050.926	24678.74	(**.058**, .174) 1.073.	$224_{3/2} - 4716_{5/2}$	−.04	--
3	4052.852	24667.01		$298_{5/2} - 5446_{3/2}$	−.01	--
3	4053.36	24663.9		$305_{11/2} - 5522_{11/2}$	.0	--
15	4054.265	24658.41		$197_{1/2} - 4441_{1/2}$	−.01	--
20H	4055.330	24651.93		$3340_{5/2} - 5806_{7/2}$	+.02	--
10	4057.601	24641.78	(.213) .668	$278_{5/2} - 5246_{1/2}$	−.02	--
2	4059.753	24625.08		$231_{5/2} - 4777_{3/2}$	−.02	--
3	4061.643	24613.62		$239_{11/2} - 4856_{11/2}$	−.01	--
30	4061.856	24612.33	(0w) .1.241B	$150_{7/2} - 3967_{5/2}$	.00	--
(4h)	4062.40	24609.0		$298_{5/2} - 5440_{5/2}$	−.2	7
15h	4064.328	24597.36		$244_{5/2} - 4902_{5/2}$	−.01	--
2	4066.94	24581.6		$224_{3/2} - 4700_{3/2}$	+.1	--
2	4067.246	24579.71	{	$288_{7/2} - 5338_{5/2}$	−.15	--
			{	$280_{5/2} - 5261_{7/2}$	+.02	--
1	4067.44	24578.5		$306_{9/2} - 5522_{11/2}$	.0	--
10	4069.16	24568.2		$266_{5/2} - 5122_{7/2}$	.0	--
1	4072.36	24548.9		$231_{5/2} - 4770_{3/2}$	−.1	--
4	4073.060	24544.63		$166_{9/2} - 4116_{7/2}$	.00	--
8	4078.120	24514.17	(000) 1.231	$231_{3/2} - 4766_{1/2}$	−.03	--
10	4079.364	24506.70	(.160)	$271_{7/2} - 5164_{5/2}$	+.01	--
80	4081.432	24494.29	(**.291**, .874) **.259**, .831, 1.413.	$164_{5/2} - 4082_{5/2}$	−.03	--
2	4082.65	24487.0		$275_{9/2} - 5200_{9/2}$	−.1	--
20	4083.365	24482.69	(.271) 1.970	$164_{3/2} - 4081_{1/2}$	+.03	17
20	4083.584	24481.38		$164_{3/2} - 4080_{3/2}$	+.04	17
4	4087.89	24455.6		$338_{7/2} - 5827_{9/2}$	−.1	--
4	4088.10	24454.4		$2044_{7/2} - 4491_{5/2}$	−.4	--
1	4088.69	24450.8		$278_{5/2} - 5227_{3/2}$	+.2	5
5	4089.01	24448.9		$271_{7/2} - 5159_{5/2}$	−.1	--
4	4089.407	24446.52		$247_{7/2} - 4917_{9/2}$	−.02	--
30	4089.919	24443.46	(.442) **1.247**, 1.435.	$146_{5/2} - 3906_{5/2}$	.00	--
2	4090.59	24439.4		$261_{3/2} - 5057_{3/2}$	−.1	--
4	4091.12	24436.3		$338_{7/2} - 5826_{7/2}$	.0	--
(5h)	4093.02	24424.9		$341_{9/2} - 5861_{11/2}$	−.2	13
2h	4099.31	24387.4		$324_{5/2} - 5682_{5/2}$	−.2	--
3h	4103.763	24361.00		$244_{5/2} - 4878_{7/2}$	+.05	--
70	4104.422	24357.09	(000) 1.330	$194_{5/2} - 4581_{7/2}$	−.03	--
10	4106.440	24345.12	(000) 1.188h	$271_{7/2} - 5148_{9/2}$	−.04	--
5h	4106.829	24342.81		$280_{5/2} - 5237_{7/2}$	+.01	--
2h	4107.431	24339.25	{	$333_{11/2} - 5765_{9/2}$	−.03	--
			{	$285_{7/2} - 5288_{5/2}$	+.04	--
1	4107.832	24336.87		$217_{7/2} - 4611_{5/2}$	+.03	--
3	4107.973	24336.03		$271_{7/2} - 5147_{5/2}$	+.01	--
10	4108.618	24332.22	(**.241**, .744) **1.408**, **1.884**.	$261_{3/2} - 5046_{5/2}$	−.01	--
1	4109.451	24327.28		$166_{9/2} - 4094_{7/2}$	+.03	--
100	4110.894	24318.74	(.435) **1.219**, 2.091.	$172_{1/2} - 4155_{3/2}$	−.04	--
5	4111.598	24314.58		$263_{13/2} - 5066_{11/2}$	+.03	--
3	4112.275	24310.58		$224_{3/2} - 4673_{3/2}$	+.03	--
30	4113.402	24303.91	(.184, .545, .905, **1.266**) .684, 1.034, **1.383**, 1.727.	$142_{7/2} - 3852_{7/2}$	+.03	--
3	4114.676	24296.39	(**.129**, .389)	$304_{3/2} - 5482_{5/2}$	−.03	--
10	4121.548	24255.88	{		+.3	--
30	4121.635	24255.37	(0w) 2.010B	$2044_{7/2} - 4470_{5/2}$	−.2	27
8	4122.738	24248.88	(**.132**, .399)	$288_{7/2} - 5305_{5/2}$	+.01	--
2	4122.896	24247.95		$280_{5/2} - 5227_{3/2}$	−.01	--
2	4123.507	24244.36		$194_{5/2} - 4370_{3/2}$	+.05	--
2	4123.82	24242.5		$273_{11/2} - 5148_{9/2}$	+.1	--
2	4128.002	24217.95		$298_{5/2} - 5401_{7/2}$	+.14	--
8	4130.458	24203.56	(0w) 1.084	$231_{5/2} - 4735_{7/2}$	+.01	--
10	4132.277	24192.90	{	$221_{9/2} - 4635_{7/2}$	−.05	22
			{	$273''_{1/2} - 5157_{3/2}$	+.05	--
100	4133.425	24186.18	(**.061**, .183, .305, .426, .548, .669) **1.151**, . . . 2.049.	$163_{11/2} - 4049_{13/2}$	−.01	--
200	4136.45	24168.5	(.464) 1.516A	$117_{9/2} - 3592_{9/2}$	.0	--
20	4137.603	24161.76	(.235, .387, **.545**) 1.077, **1.223**, 1.383.	$217_{7/2} - 4593_{7/2}$	−.02	--
3	4138.532	24156.34		$157_{5/2} - 3992_{3/2}$	+.01	--
(1h)	4142.44	24133.6		$275_{9/2} - 5164_{7/2}$	+.1	23
4	4142.767	24131.65		$261_{3/2} - 5026_{3/2}$	.00	--
200	4144.363	24122.35	(**.061**, .183, .306, .428) 1.195, 1.319, 1.442, 1.566, 1.689, **1.811**.	$173_{7/2} - 4145_{9/2}$	−.01	--
10	4146.233	24111.47	(.074, .223, **.370**).	$194_{5/2} - 4356_{5/2}$	.00	--
50	4149.96	24089.8	(0w) 1.484A	$138_{3/2} - 3791_{3/2}$	.0	--
10	4150.527	24086.53		$224_{3/2} - 4650_{5/2}$	−.04	--
2	4150.790	24085.01		$341_{9/2} - 5827_{9/2}$	−.03	--
10h	4152.29	24076.3		$3358_{3/2} - 5766_{9/2}$	.0	--

Int.	λ_{vac}	σ_{vac}	Zeeman effect	Transition	O–C	Notes
	A	*K*				
30	4152.632	24074.32		$157_{5/2}-3984_{7/2}$	−.01	--
3	4157.252	24047.57		$288_{7/2}-5285_{7/2}$	.00	--
20	4159.925	24032.11	(0w) .746C	$272_{9/2}-5119_{9/2}$	−.03	10
5	4160.773	24027.22		$261_{1/2}-5015_{3/2}$	−.08	--
1	4164.32	24006.8		$150_{7/2}-3906_{5/2}$	+.1	--
10	4166.408	23994.72		$305_{11/2}-5455_{11/2}$	+.02	--
15	4168.588	23982.17	(0w) 1.220h	$173_{7/2}-4131_{5/2}$	−.03	--
100d	4170.395	23971.78	(.569) **.915,** 2.051.	$275_{9/2}-5148_{9/2}$ $138_{5/2}-3779_{1/2}$	−.20 −.05	9
10	4173.978	23951.21		$194_{5/2}-4341_{5/2}$	−.01	--
10	4175.186	23944.27	(.495)	$197_{1/2}-4370_{3/2}$	−.02	--
10	4176.540	23936.51		$150_{7/2}-3899_{9/2}$	−.03	--
6	4176.867	23934.64		$204_{3/2}-4441_{1/2}$	+.04	--
2	4177.419	23931.48		$288_{7/2}-5274_{9/2}$	+.05	--
3	4178.599	23924.72		$280_{5/2}-5195_{7/2}$	+.02	--
3	4179.73	23918.2		$319_{7/2}-5589_{7/2}$	.0	--
2	4181.29	23909.3		$306_{9/2}-5455_{11/2}$	.0	--
(1)	4182.22	23904.0		$239_{11/2}-4785_{11/2}$	+.1	23
100	4182.902	23900.11	(.106, .316 **.522**) .795, 1.002, **1.212,** 1.410, 1.613.	$157_{5/2}-3967_{5/2}$	+.01	--
100	4183.056	23899.23	(0w) 1.304w	$146_{5/2}-3852_{7/2}$	−.05	--
2h	4184.48	23891.1		$332_{5/2}-5717_{7/2}$	.0	--
2h	4185.72	23884.0		$194_{5/2}-4334_{3/2}$	.0	--
5	4187.909	23871.53		$138_{5/2}-3769_{3/2}$	−.01	--
2	4188.441	23868.50		$306_{9/2}-5451_{7/2}$	−.01	--
3Hl	4191.92	23848.7		$3452_{7/2}-5836_{9/2}$	.0	--
50	4194.668	23833.07	(.132) 1.258A	$173_{7/2}-4116_{7/2}$	−.02	--
10	4195.741	23826.97	(.**108,** .323) **.885,** 1.100, 1.315.	$204_{3/2}-4490_{3/2}$	−.03	--
7	4203.308	23784.08		$273_{11/2}-5102_{9/2}$	.00	--
30	4204.525	23777.19	(w) 1.058B	$221_{9/2}-4593_{7/2}$	+.05	--
30	4213.266	23727.87	(w) 1.293h	$261_{3/2}-4985_{1/2}$ $271_{7/2}-5086_{7/2}$	−.09 .00	9
2	4214.974	23718.25		$224_{1/2}-4614_{1/2}$	−.03	--
15	4215.500	23715.30		$275_{9/2}-5122_{7/2}$	−.03	--
200	4221.079	23683.95	(.277) 1.130, 1.238, **1.344,** 1.452, 1.560.	$115_{5/2}-3526_{5/2}$	−.03	--
2	4222.500	23675.98		$285_{7/2}-5221_{5/2}$	.00	--
15	4224.163	23666.66		$204_{3/2}-4414_{3/2}$	−.06	--
2000	4227.46	23648.2	(**.133,** .394, .657) **1.292,** 1.526, 1.855, 2.114, 2.372, 2.626.	$1895_{5/2}-4259_{7/2}$	.0	--
20	4232.956	23617.50	(**.054,** .162, .270).	$280_{5/2}-516_{4}{}_{7/2}$	.00	--
10	4233.275	23615.72		$173_{7/2}-4094_{7/2}$	+.01	--
6	4234.43	23609.3		$163_{11/2}-3991_{11/2}$	+.1	--
10	4234.95	23606.4		$2044_{7/2}-4405_{5/2}$	.0	--
20	4236.237	23599.20	(1.448) .252, **1.227.**	$164_{3/2}-3992_{1/2}$	−.04	--
7	4238.016	23589.30	(.074)	$298_{1/2}-5338_{3/2}$	−.05	--
15	4238.586	23586.13	(.213)	$194_{5/2}-4394_{3/2}$	.00	--
2	4239.956	23578.51		$231_{3/2}-4672_{3/2}$	−.06	--
40	4241.16	23571.8	(?) .964	$172_{1/2}-4081_{1/2}$	−.1	17
50	4241.42	23570.4	(?) .766	$172_{1/2}-4080_{7/2}$	−.2	17
2	4241.806	23568.23		$217_{7/2}-4534_{9/2}$	+.06	--
2	4243.85	23556.8		$217_{7/2}-4533_{5/2}$	+.2	--
20	4244.12	23555.4	(.248)	$138_{5/2}-3738_{5/2}$	+.1	--
40hl	4246.820	23540.40	(.418)	$3452_{7/2}-5806_{7/2}$	+.01	--
4h	4247.679	23535.64		$261_{3/2}-4966_{3/2}$ $298_{1/2}-5337_{7/2}$	−.04 +.08	--
2	4248.357	23531.88		$306_{9/2}-5417_{7/2}$	−.04	--
2	4255.10	23494.6		$231_{3/2}-4664_{5/2}$	.0	--
2	4255.33	23493.3		$298_{1/2}-5329_{3/2}$	.0	--
20	4255.749	23491.01		$173_{7/2}-4082_{5/2}$	.00	--
200	4257.60	23480.8	(**.176,** .525, .875) 1.043, 1.393, 1.745, 2.096, **2.447.**	$142_{7/2}-3769_{5/2}$	.0	--
(1)	4258.88	23473.8		$244_{3/2}-4789_{1/2}$	.0	23
3	4259.880	23468.23		$204_{3/2}-4394_{5/2}$	−.02	--
6	4260.91	23462.6		$150_{7/2}-3852_{7/2}$ $341_{9/2}-5765_{9/2}$	.0 .0	--
3	4261.86	23457.3		$338_{7/2}-5728_{9/2}$	+.1	--
3	4263.35	23449.1		$266_{5/2}-5011_{5/2}$	+.2	--
3	4263.76	23446.9		$280_{5/2}-5147_{5/2}$	+.1	--
2h	4264.73	23441.5		$261_{3/2}-4957_{3/2}$	.0	--
5	4268.71	23419.7		$273_{11/2}-5066_{11/2}$	+.1	--
3	4269.79	23413.8		$313_{9/2}-5481_{9/2}$	.0	--
20	4269.94	23413.0		$285_{7/2}-5195_{7/2}$	+.1	--
10	4274.34	23388.9		$305_{11/2}-5594_{11/2}$	+.1	--
3	4279.185	23362.36		$314_{5/2}-5482_{5/2}$	−.04	--
6	4280.59	23354.7		$275_{9/2}-5086_{7/2}$ $231_{3/2}-4650_{5/2}$ $244_{5/2}-4777_{3/2}$	.0 +.1 +.2	--
2	4281.664	23348.83		$163_{11/2}-3965_{9/2}$	−.01	--
10	4282.734	23343.00		$164_{3/2}-3967_{3/2}$	−.01	--
1h	4285.55	23327.6		$311_{3/2}-5451_{7/2}$	−.2	--
10	4286.463	23322.69	(?) 1.267h	$271_{7/2}-5046_{3/2}$	+.02	--
100	4291.17	23297.1	(**.068,** .208) 1.420, 1.579, **1.740.**	$166_{9/2}-3991_{11/2}$	.0	--
30	4291.654	23294.48		$157_{5/2}-3906_{5/2}$ $146_{5/2}-3791_{1/2}$	−.02 +.07	--
2	4294.62	23278.4		$244_{5/2}-4770_{3/2}$	.0	--
20	4299.917	23249.72		$239_{11/2}-4720_{9/2}$	−.01	--
4	4301.052	23243.58		$244_{5/2}-4766_{7/2}$	−.03	--
4	4301.774	23239.68		$272_{9/2}-5040_{9/2}$	+.02	--
3d	4302.11	23237.9		$138_{5/2}-3706_{3/2}$	+.4	--
100	4304.404	23225.48	(0w) 1.110B	$166_{9/2}-3984_{7/2}$	+.01	--
2	4304.78	23223.5		$311_{5/2}-5440_{5/2}$	.0	--
15	4305.334	23220.47	(.261, .783)	$204_{3/2}-4370_{3/2}$	.00	--
4	4308.802	23201.78		$266_{5/2}-4986_{7/2}$	−.01	--
9	4309.474	23198.16		$231_{5/2}-4635_{7/2}$	−.02	--
2h	4313.31	23177.5		$341_{9/2}-5737_{7/2}$	.0	--
15	4314.578	23170.72	(.121, .359, .596, **.833**).	$217_{7/2}-4494_{7/2}$	.00	--
20	4315.71	23164.7	(.293)	$142_{7/2}-3738_{5/2}$	+.1	--
4	4316.18	23162.1		$301_{1/2}-5329_{3/2}$	−.1	--
5	4317.11	23157.2		$273_{11/2}-5040_{9/2}$	+.1	--
2h	4317.68	23154.1		$298_{5/2}-5296_{3/2}$	.0	--
2h	4317.93	23152.8		$280_{5/2}-5118_{3/2}$	+.1	--
10	4318.585	23149.21		$272_{9/2}-5031_{7/2}$ $275_{9/2}-5066_{11/2}$	−.14 +.01	--
15	4319.531	23144.15	(**.093,** .279, .464).	$146_{5/2}-3776_{7/2}$	−.04	--
3	4324.33	23118.4		$261_{3/2}-4925_{7/2}$	−.1	--
3	4329.076	23093.12		$309_{9/2}-5373_{7/2}$	−.01	--
2h	4331.14	23082.1		$311_{5/2}-5426_{3/2}$	.0	--
3	4331.365	23080.91		$298_{5/2}-5288_{5/2}$	−.05	--
80	4332.25	23076.2	(.106) 1.208D	$146_{5/2}-3769_{5/2}$	.0	19
9	4335.860	23056.99	(**.037,** .112, .187) 1.478B.	$298_{5/2}-5285_{7/2}$	−.07	--
8	4339.68	23036.7		$166_{9/2}-3965_{9/2}$	.0	--
1	4345.32	23006.8		$314_{5/2}-5446_{7/2}$	.0	--
2	4345.505	23005.81		$266_{5/2}-4966_{3/2}$	−.01	--
4	4352.46	22969.1		$271_{7/2}-5011_{5/2}$	−.1	--
10	4357.06	22944.8		$247_{7/2}-4766_{7/2}$	.0	--
100	4358.69	22936.2	(**.088,** .262, .437) 1.188, 1.363, 1.533, 1.707, **1.880.**	$115_{5/2}-3452_{7/2}$	−.1	--
7	4359.310	22932.96		$244_{5/2}-4735_{7/2}$	.00	--
10	4360.375	22927.36		$204_{3/2}-4341_{5/2}$	−.02	--
4	4361.26	22922.7		$221_{9/2}-4598_{11/2}$	+.1	--
6	4363.37	22911.6		$266_{5/2}-4957_{5/2}$	−.1	--
10	4364.13	22907.6	(.333w)	$305_{11/2}-5346_{11/2}$	.0	--
9	4364.851	22903.85	(.070, .209, **.347**.)	$280_{5/2}-5093_{5/2}$	−.01	--
1	4366.35	22896.0		$341_{9/2}-5709_{7/2}$	.0	--
100	4367.58	22889.5	(.621, .776, **.929**) .862, 1.014, **1.168,** 1.323, 1.476.	$163_{11/2}-3919_{11/2}$	−.1	--
2	4369.64	22878.7	(.581w)	$273'_{1/2}-5026_{3/2}$ $273''_{1/2}-5026_{3/2}$	−.1 +.1	20
4	4369.77	22878.1				
5	4373.202	22860.11	(.720)	$204_{3/2}-4334_{3/2}$	−.01	--
2	4377.056	22839.98		$319_{7/2}-5482_{5/2}$	−.05	--
3	4377.44	22838.0		$288_{7/2}-5164_{7/2}$	.0	--
1	4380.45	22822.3		$306_{9/2}-5346_{11/2}$	+.1	--
(10)	4381.00	22819.4		$305_{11/2}-5337_{9/2}$	.0	7
10	4385.443	22796.30	(**.108,** .324)	$275_{9/2}-5051_{7/2}$ $194_{5/2}-4225_{7/2}$	−.10 .00	--
2	4386.14	22792.7		$3526_{5/2}-5806_{7/2}$	.0	--
10	4387.404	22786.11	(**.160,** .428)	$221_{9/2}-4494_{7/2}$	+.03	--
(2)	4388.52	22780.3		$288_{7/2}-5159_{5/2}$	+.1	13
100	4391.342	22765.68	(**.045,** .134, .224) 1.747	$117_{9/2}-3452_{7/2}$	−.05	--
3	4392.122	22761.64		$304_{3/2}-5328_{1/2}$	−.04	--
40	4392.45	22760.0	(?) .988, **1.075**	$146_{5/2}-3738_{5/2}$	.0	--
80	4394.30	22750.3	(.437) **1.053,** 1.928	$151_{1/2}-3791_{3/2}$	+.3 −.5	24
50	4394.46	22749.5				
10	4396.089	22741.10		$221_{9/2}-4490_{7/2}$	−.01	--
30	4396.802	22737.41	(**.184,** .550) **.784,** 1.151	$164_{3/2}-3906_{5/2}$	.00	--
8	4399.80	22721.9		$271_{7/2}-4986_{7/2}$	−.2	--
40	4402.600	22707.47	(.662) .700, .881, **1.062,** 1.243, 1.424.	$150_{7/2}-3776_{7/2}$	+.01	--
5	4403.683	22701.88		$272_{9/2}-4986_{7/2}$	+.01	--
1	4404.27	22698.8		$224_{1/2}-4512_{3/2}$	−.2	--
20	4406.30	22688.4	(.883) .150	$172_{1/2}-3992_{1/2}$	−.1	--
30	4406.47	22687.5	(000) 1.251	$163_{11/2}-3899_{9/2}$ $285_{7/2}-5122_{7/2}$	−.1 .0	--
3	4408.64	22676.4		$288_{7/2}-5148_{9/2}$ $244_{5/2}-4710_{3/2}$	.0 +.2	--
2h	4410.39	22667.4		$288_{7/2}-5147_{5/2}$	+.1	--
(1)	4412.52	22656.4		$311_{5/2}-5384_{3/2}$	−.1	23
1	4413.500	22651.39		$285_{7/2}-5119_{9/2}$	+.03	5
80	4415.822	22639.48	(0w) .987C†	$150_{7/2}-3769_{5/2}$	+.01	--
8	4417.22	22632.3		$151_{1/2}-3779_{1/2}$	+.2 −.3	24
10	4417.33	22631.8				
2h	4419.86	22618.8		$313_{9/2}-5401_{7/2}$	−.1	--
2	4423.810	22598.60		$304_{3/2}-5312_{7/2}$	+.01	--
2	4425.762	22588.63		$266_{5/2}-4925_{3/2}$	+.04	--
(4)	4425.95	22587.7		$338_{7/2}-5641_{9/2}$	+.1	13
2	4427.67	22578.9		$244_{5/2}-4700_{3/2}$	.0	--
7	4427.951	22577.47		$166_{9/2}-3919_{11/2}$	+.01	--
2h	4428.864	22572.81		$298_{5/2}-5297_{7/2}$	+.07	--
41	4432.846	22552.53		$311_{5/2}-5373_{7/2}$	+.15	--

TABLE 2. *Classified lines of* Re I—Continued

Int.	λ_{vac}	σ_{vac}	Zeeman effect	Transition	O–C	Notes
	A	*K*				
3	4436.614	22533.38		$217_{7/2}-4430_{5/2}$	+.05	..
20	4440.44	22514.0	(?) 1.255	$173_{7/2}-3984_{7/2}$	+.1	..
2h	4445.97	22486.0		$285_{7/2}-5102_{9/2}$	+.2	..
2	4448.115	22475.12		$273'_{1/2}-4985_{1/2}$	−.01	..
2	4448.259	22474.39		$273''_{1/2}-4985_{1/2}$	+.06	..
2	4453.26	22449.2		$217_{7/2}-4428_{7/2}$	.0	..
20	4453.92	22445.8		$3592_{9/2}-5836_{9/2}$	−.1	..
70	4454.62	22442.3	(.257) .893, 1.415, **1.933.**	$146_{5/2}-3706_{3/2}$	+.1	..
3	4456.370	22433.49		$280_{5/2}-5046_{5/2}$	+.01	..
6	4456.668	22431.99		$271_{7/2}-4957_{5/2}$	+.01	..
2	4457.47	22428.0		$304_{3/2}-5296_{1/2}$	+.1	..
3	4459.405	22418.22		$239_{11/2}-4637_{9/2}$	−.03	..
2	4464.627	22392.00		$285_{7/2}-5093_{5/2}$	−.05	..
5	4465.834	22385.95		$194_{5/2}-4184_{7/2}$	−.01	..
15	4467.544	22377.38		$247_{7/2}-4710_{5/2}$	−.01	..
40	4467.924	22375.47		$166_{9/2}-3899_{9/2}$	+.02	..
2	4472.06	22354.8		$304_{3/2}-5288_{5/2}$	+.1	..
4	4473.23	22348.9		$275_{9/2}-4986_{7/2}$	.0	..
80	4475.082	22339.68	(.073, .217, .362) 1.328, 1.475, **1.621.**	$173_{7/2}-3967_{3/2}$	−.02	..
6	4476.78	22331.2		$278_{3/2}-5015_{5/2}$	.0	..
3	4477.642	22326.92		$285_{7/2}-5086_{7/2}$	+.05	..
30	4477.986	22325.20	(.091)	$173_{7/2}-3965_{9/2}$	+.03	..
60	4478.386	22323.20	(.079, .242) 1.068, 1.232, 1.375, **1.557.**	$150_{7/2}-3738_{5/2}$	−.02	..
10	4481.443	22307.98		$231_{5/2}-4546_{7/2}$ $244_{3/2}-4673_{3/2}$	−.04 .00	.. ..
3h	4486.58	22282.4		$278_{3/2}-5011_{5/2}$	−.2	..
5	4486.991	22280.39		$280_{5/2}-5031_{7/2}$	+.01	..
15	4496.432	22233.62	(?) .796	$197_{1/2}-4199_{1/2}$	−.03	..
10	4498.378	22224.00		$244_{5/2}-4664_{5/2}$	−.02	..
3	4499.04	22220.7		$263_{11/2}-4856_{11/2}$	.0	..
4	4502.52	22203.6		$311_{5/2}-5338_{5/2}$	−.1	..
4	4504.41	22194.3		$319_{7/2}-5417_{7/2}$	.5	..
100	4507.035	22181.31	(.814) .186† ..	$2885_{5/2}-5104_{3/2}$ $305_{11/2}-5274_{9/2}$	−.07 .00	21 25
60	4508.007	22176.52	(?) .121, .418†	$2885_{5/2}-5103_{1/2}$	−.03	21
1	4508.39	22174.6		$217_{7/2}-4394_{5/2}$	.0	..
500	4513.31	22150.5	(.350) 1.967A..	$2044_{7/2}-4259_{7/2}$	.0	..
20	4514.26	22145.8		$2888_{7/2}-5104_{5/2}$	.0	..
200	4516.638	22134.15	(.151, .475, .800)†,	$2885_{5/2}-5098_{7/2}$	−.14	..
1	4517.774	22128.58		$280_{5/2}-5015_{5/2}$	+.03	..
3	4518.570	22124.60		$272_{9/2}-4988_{11/2}$	−.03	..
80	4519.762	22118.85	(.975) .804, 1.291, **1.684** . . . †	$2885_{5/2}-5097_{5/2}$	−.14	..
400	4522.73	22104.3	P–B	$2888_{7/2}-5099_{9/2}$	−.1	
100	4523.878	22098.72	P–B	$2888_{7/2}-5098_{7/2}$	−.03	26
80	4526.009	22088.32	P–B	$2896_{1/2}-5105_{1/2}$	.00	
10	4526.98	22083.6		$2888_{7/2}-5097_{5/2}$	+.1	..
60	4528.966	22073.90	P–B	$298_{5/2}-5187_{1/2}$ $2896_{1/2}-5104_{5/2}$	−.15 −.11	.. 26
150	4529.950	22069.11	P–B	$2896_{1/2}-5103_{3/2}$	−.07	
30	4530.889	22064.53		$221_{9/2}-4422_{9/2}$	−.01	..
40	4536.014	22039.60	(.512, .713) 1.246, **1.452,** 1.699.	$217_{7/2}-4381_{7/2}$	−.01	..
3	4537.54	22032.2		$324_{5/2}-5446_{3/2}$ $278_{3/2}-4985_{1/2}$	−.1 +.3	.. ..
50	4541.80	22011.5		$2896_{3/2}-5097_{5/2}$	−.1	..
100	4545.174	21995.19	(0w) 1.356	$157_{5/2}-3776_{7/2}$	−.04	..
10	4545.53	21993.5		$224_{3/2}-4441_{1/2}$	.0	..
4	4551.502	21964.61		$306_{9/2}-5261_{7/2}$	−.07	..
3	4556.025	21942.80		$304_{3/2}-5246_{1/2}$	−.05	..
4	4557.33	21936.5		$313_{9/2}-5333_{7/2}$	.0	..
50	4559.268	21927.19		$157_{5/2}-3769_{5/2}$	−.05	..
50	4559.682	21925.20	(.129) .616, **.874.**	$247_{7/2}-4664_{3/2}$	.00	..
7	4563.63	21906.2		$333_{11/2}-5522_{11/2}$	−.01	..
4	4564.633	21901.42		$166_{9/2}-3852_{7/2}$	−.04	..
50	4565.30	21898.2		$151_{1/2}-3706_{3/2}$	+.4	27
60	4565.51	21897.2			−.6	
2h	4568.748	21881.70		$271_{7/2}-4902_{5/2}$	+.06	..
(1)	4571.91	21866.6		$272_{9/2}-4903_{7/2}$	+.1	23
4	4572.195	21865.20		$280_{5/2}-4989_{3/2}$	−.05	..
2	4575.935	21847.33		$298_{5/2}-5164_{7/2}$	−.11	..
3	4577.550	21839.62		$278_{3/2}-4966_{3/2}$	+.02	..
4	4578.251	21836.28		$221_{9/2}-4399_{11/2}$	+.02	..
3h	4578.93	21833.1		$314_{3/2}-5329_{3/2}$ $324_{5/2}-5486_{5/2}$ $280_{5/2}-4986_{7/2}$	.0 +.1 +.2	.. .. ..
100	4580.68	21824.7	(.341, .562) 1.177, **1.394,** 1.611.	$115_{5/2}-3340_{5/2}$	−.1	..
3	4586.06	21799.1		$197_{1/2}-4155_{3/2}$	−.1	..
8	4587.141	21793.96		$217_{7/2}-4356_{5/2}$	.00	..
(2)	4588.95	21785.4		$247_{7/2}-4550_{5/2}$	+.2	23
3	4590.540	21777.82		$298_{5/2}-5157_{3/2}$	+.15	..
20	4591.682	21772.40		$204_{3/2}-4225_{3/2}$	−.06	..
4	4592.53	21768.4		$285_{7/2}-5031_{7/2}$ $311_{5/2}-5296_{3/2}$	−.2 .0	.. ..
4	4595.263	21755.44		$319_{7/2}-5373_{7/2}$	−.03	..
5	4597.32	21745.7		$278_{3/2}-4957_{5/2}$	+.2	..
1	4599.764	21734.15		$173_{7/2}-3906_{5/2}$	+.05	..
1h	4601.13	21727.7		$306_{9/2}-5237_{7/2}$	−.1	..
200	4605.73	21706.0	(0w) 1.312B...	$194_{5/2}-4116_{7/2}$	.0	..
3	4607.80	21696.3		$272_{9/2}-4885_{7/2}$	.0	..
4	4608.802	21691.53		$304_{3/2}-5221_{5/2}$	+.02	..
1h	4609.81	21686.8		$244_{5/2}-4611_{5/2}$	.0	..
5	4613.95	21667.3		$305_{11/2}-5222_{13/2}$	.0	..
50	4614.66	21664.0	(.000) 1.248h...	$173_{7/2}-3899_{9/2}$	+.1	..
30	4616.57	21655.1		$221_{9/2}-4381_{7/2}$	+.1	..
80	4621.38	21632.5	(.439, .724) 1.003, **1.274,** 1.553†.	$217_{7/2}-4340_{7/2}$	.0	26
(1h)	4624.73	21616.8		$285_{7/2}-5015_{5/2}$	+.1	23
30	4625.96	21611.1		$157_{5/2}-3738_{5/2}$	+.1	..
1	4628.76	21598.0		$314_{3/2}-5305_{3/2}$	−.1	..
7	4630.24	21591.1		$288_{7/2}-5040_{9/2}$	.0	..
80	4630.82	21588.4	(?) 1.594	$164_{3/2}-3791_{3/2}$	.0	..
3	4635.78	21565.3		$231_{5/2}-4472_{3/2}$	.0	..
1h	4640.63	21542.8		$280_{5/2}-4957_{5/2}$	.0	..
1h	4640.94	21541.3		$332_{5/2}-5482_{5/2}$	−.1	..
2	4642.68	21533.3		$261_{3/2}-4765_{1/2}$	+.2	..
20	4644.95	21522.7		$266_{5/2}-4818_{7/2}$	−.1	..
10	4647.46	21511.1		$263_{13/2}-4785_{11/2}$	+.1	..
4	4648.56	21506.0		$2888_{7/2}-5039_{9/2}$	.0	..
1h	4649.19	21503.1		$3776_{7/2}-5926_{5/2}$	.0	..
3	4649.70	21500.8		$288_{7/2}-5031_{7/2}$	.0	..
3h	4650.825	21495.54		$333_{11/2}-5481_{9/2}$	−.01	..
1h	4651.20	21493.8		$314_{3/2}-5296_{3/2}$	.0	..
4	4651.82	21491.0		$314_{3/2}-5295_{3/2}$	.0	..
100	4652.33	21488.6	(.087, .254) 1.447, 1.630, 1.796, **1.963.**	$194_{5/2}-4094_{7/2}$	.0	..
2	4652.77	21486.6		$2885_{5/2}-5034_{5/2}$	+.2	..
10	4654.53	21478.4		$2885_{5/2}-5033_{3/2}$	.0	..
2h	4656.29	21470.3		$164_{3/2}-3779_{1/2}$	−.1	..
10	4656.47	21469.5		$2888_{7/2}-5035_{7/2}$	.0	..
10	4660.51	21450.8		$2888_{7/2}-5034_{5/2}$ $244_{5/2}-4587_{5/2}$	−.1 −.1	.. ..
9	4661.483	21446.39		$301_{1/2}-5157_{3/2}$	−.09	5
60	4662.493	21441.75		$138_{3/2}-3526_{5/2}$	−.07	..
8	4662.99	21439.4		$270_{13/2}-4856_{11/2}$	−.1	..
5	4665.217	21429.23		$298_{5/2}-5122_{7/2}$	−.03	..
6	4666.713	21422.36		$278_{3/2}-4925_{3/2}$	−.01	..
2	4669.81	21408.1		$272_{9/2}-4856_{11/2}$	−.2	..
9	4674.304	21387.57		$239_{11/2}-4534_{9/2}$	.00	..
2	4675.38	21382.6		$298_{5/2}-5118_{5/2}$	.0	..
15	4679.476	21363.93		$194_{5/2}-4082_{5/2}$	−.01	..
2h	4681.89	21352.9		$319_{7/2}-5333_{7/2}$ $3791_{3/2}-5926_{5/2}$	−.1 .0	.. ..
60	4682.319	21350.96		$194_{5/2}-4080_{3/2}$	.00	..
(5h)	4684.02	21343.2		$275_{9/2}-4885_{7/2}$	−.1	7
1h	4685.20	21337.8		$319_{7/2}-5332_{9/2}$	−.2	..
(15)	4687.858	21325.74		$273_{11/2}-4856_{11/2}$	−.01	3
1h	4688.87	21321.1		$285_{7/2}-4986_{7/2}$	.0	..
4h	4691.45	21309.4		$266_{5/2}-4797_{5/2}$	.0	..
1	4692.80	21303.3		$324_{5/2}-5373_{7/2}$	.0	..
8	4693.38	21300.7		$306_{9/2}-5194_{11/2}$	+.1	..
30	4694.99	21293.6		$221_{9/2}-4345_{9/2}$ $157_{5/2}-3706_{3/2}$	+.1 +.2	.. ..
2h	4698.08	21279.3		$224_{3/2}-4370_{5/2}$	−.1	..
4	4699.69	21272.0		$275_{9/2}-4878_{7/2}$	.0	..
50	4700.440	21268.65		$217_{7/2}-4304_{5/2}$	+.03	..
60	4705.04	21247.8		$221_{9/2}-4347_{7/2}$	.0	..
2	4711.22	21220.0		$280_{5/2}-4925_{5/2}$	+.3	..
20	4712.76	21213.0		$247_{7/2}-4593_{7/2}$	.0	..
4	4725.02	21158.0		$263_{13/2}-4750_{11/2}$	+.2	..
20	4725.93	21153.9		$231_{5/2}-4430_{5/2}$	.0	..
80	4727.60	21146.5		$224_{3/2}-4356_{3/2}$ $166_{9/2}-3776_{7/2}$	.0 +.1	.. ..
2h	4730.43	21133.8		$298_{5/2}-5293_{5/2}$	.0	..
4	4733.87	21118.5		$266_{5/2}-4777_{5/2}$	.0	5
4	4743.46	21075.7		$319_{7/2}-5305_{5/2}$	−.1	..
5	4746–24	21063.4		$304_{3/2}-5159_{5/2}$	−.1	..
8	4748.06	21055.3		$275_{9/2}-4856_{11/2}$	.0	..
80	4748.38	21053.9		$164_{3/2}-3738_{5/2}$	.0	..
40	4749.03	21051.0		$142_{7/2}-3526_{5/2}$ $197_{1/2}-4089_{1/2}$	−.1 +.1	.. ..
5	4750.99	21042.4		$266_{5/2}-4770_{3/2}$	.0	..
1	4751.23	21041.3		$261_{3/2}-4718_{1/2}$	.0	..
10	4751.345	21040.78		$261_{3/2}-4717_{3/2}$	+.1	..
4	4752.10	21037.4		$244_{5/2}-4542_{7/2}$	.0	..
40	4758.833	21007.67		$115_{5/2}-3259_{1/2}$ $266_{5/2}-4769_{7/2}$	.00 +.09	.. ..
20	4763.672	20986.34		$224_{3/2}-4341_{5/2}$	+.06	..
4	4771.807	20950.56		$304_{3/2}-5147_{3/2}$	+.01	..
4h	4778.99	20919.1		$224_{3/2}-4334_{3/2}$	+.1	..
2h	4781.83	20906.6		$244_{5/2}-4533_{3/2}$	.0	..
10	4789.206	20874.45		$319_{7/2}-5285_{7/2}$	.00	..
3	4789.60	20872.7		$261_{3/2}-4700_{3/2}$	−.1	..
200	4791.418	20864.81	(.149, .446) 1.310, 1.599, 1.887, 2.178, **2.468.**	$150_{7/2}-3592_{9/2}$	−.02	..
4	4796.895	20840.99		$306_{9/2}-5148_{9/2}$	+.03	..
15	4799.127	20831.29		$204_{3/2}-4131_{5/2}$	.00	..
9	4799.49	20829.7		$271_{7/2}-4797_{5/2}$	.0	..
1	4802.28	20817.6		$314_{3/2}-5227_{1/2}$	−.1	..
3	4813.139	20770.65		$298_{5/2}-5057_{3/2}$	+.01	..
2	4814.92	20763.0		$288_{7/2}-4957_{5/2}$	−.2	..
2	4816.03	20758.2		$319_{7/2}-5274_{9/2}$ $271_{7/2}-4789_{5/2}$	−.1 +.1	.. ..

TABLE 2. *Classified lines of* Re I—Continued

Int.	λ_{vac}	σ_{vac}	Zeeman effect	Transition	O-C	Notes
	A	*K*				
(1)	4818.40	20748.0		$3852_{7/2} - 5926_{3/2}$	−.1	23
20	4820.57	20738.6		$247_{7/2} - 4549_{7/2}$	.0	--
2	4822.65	20729.7		$270_{13/2} - 4785_{11/2}$	−.1	--
6	4829.87	20698.7		$272_{9/2} - 4785_{11/2}$	+.1	--
9	4834.79	20677.6		$172_{1/2} - 3791_{3/2}$	.0	--
(1)	4838.83	20660.4		$231_{5/2} - 4381_{7/2}$	+.2	23
3	4845.67	20631.2		$333_{11/2} - 5394_{11/2}$	.0	--
3	4846.26	20628.7		$285_{7/2} - 4917_{9/2}$	+.1	--
20	4848.45	20619.4		$247_{7/2} - 4534_{9/2}$	.0	--
1	4849.23	20616.0		$273_{11/2} - 4785_{11/2}$	−.1	--
				$313_{9/2} - 5200_{9/2}$	−.2	--
7	4852.57	20601.9		$261_{3/2} - 4673_{3/2}$	+.1	--
				$3706_{3/2} - 5766_{3/2}$	+.1	--
				$306_{9/2} - 5122_{7/2}$	.0	--
1h	4856.70	20584.3		$172_{1/2} - 3779_{1/2}$	−.01	--
5	4862.539	20559.64		$271_{7/2} - 4766_{7/2}$	+.1	--
3	4870.03	20528.0		$261_{3/2} - 4664_{5/2}$	.0	--
2	4872.43	20517.9		$298_{5/2} - 5031_{7/2}$	−.02	--
2	4874.237	20510.30		$272_{9/2} - 4766_{7/2}$	.0	--
10	4874.85	20507.7		$285_{7/2} - 4902_{5/2}$	+.07	--
3	4881.278	20480.71		$244_{5/2} - 4490_{7/2}$	.0	--
3	4882.45	20475.8		$194_{3/2} - 3992_{3/2}$	.0	--
3	4884.10	20468.9		$311_{5/2} - 5164_{7/2}$	+.1	--
2	4885.80	20461.8		$0_{3/2} - 2044_{5/2}$	.0	--
200	4889.14	20447.8		$173_{7/2} - 3776_{7/2}$	+.07	--
4	4892.222	20434.90		$275_{9/2} - 4793_{7/2}$	+.19	--
10	4896.167	20418.43		$311_{5/2} - 5159_{5/2}$	−.01	--
6	4899.634	20403.99		$194_{5/2} - 3984_{7/2}$	.0	--
15	4903.73	20386.9		$306_{9/2} - 5102_{9/2}$	+.1	--
2	4904.75	20382.7		$261_{3/2} - 4650_{5/2}$	.0	--
1	4905.93	20377.8		$270_{13/2} - 4750_{13/2}$	.00	--
30	4906.208	20376.65		$173_{7/2} - 3769_{5/2}$	+.04	--
20	4908.562	20366.88		$217_{7/2} - 4214_{9/2}$	+.12	--
4	4909.066	20364.78		$265_{9/2} - 4700_{7/2}$	.0	--
4	4914.34	20342.9		$204_{3/2} - 4082_{5/2}$	+.01	--
100	4915.020	20340.11	(**.160**, .481) **.645**, .965, 1.285.			
6	4917.84	20328.5		$204_{3/2} - 4081_{1/2}$	+.1	--
(2)	4922.366	20309.76		$298_{5/2} - 5011_{5/2}$	−.14	3
200	4923.903	20303.42	(.183, .297, **.409**) 1.276, **1.390**, 1.505.	$142_{7/2} - 3458_{7/2}$	+.03	--
2h	4925.99	20294.8		$244_{5/2} - 4478_{3/2}$	+.1	--
4	4926.893	20291.10		$311_{5/2} - 5147_{5/2}$	+.03	--
3	4928.585	20284.13		$3738_{3/2} - 5766_{3/2}$	+.11	--
2	4932.359	20268.65		$239_{11/2} - 4428_{9/2}$	+.07	--
				$338_{7/2} - 5498_{7/2}$	−.05	--
30	4932.734	20262.96		$273_{11/2} - 4750_{13/2}$	+.05	--
15	4935.842	20254.31		$231_{5/2} - 4341_{3/2}$	+.01	--
2h	4940.53	20235.1		$319_{7/2} - 5221_{5/2}$	.0	--
8	4943.73	20222.0		$247_{7/2} - 4494_{7/2}$	+.1	--
7	4944.867	20217.34		$271_{7/2} - 4735_{7/2}$	+.11	--
150	4946.72	20209.8		$150_{3/2} - 3526_{5/2}$	.0	--
20	4949.82	20197.1		$272_{9/2} - 4735_{7/2}$	+.1	--
2	4952.270	20187.12		$231_{5/2} - 4334_{3/2}$	+.08	--
3	4955.286	20174.83		$324_{5/2} - 5861_{7/2}$	−.04	--
100	4956.765	20168.82	(?) .170	$197_{1/2} - 3992_{3/2}$	−.02	--
2h	4960.42	20154.0		$280_{5/2} - 4818_{7/2}$	+.1	--
10	4961.383	20150.04		$333_{11/2} - 5340_{11/2}$	+.04	--
10	4963.065	20143.21		$278_{5/2} - 4797_{5/2}$	+.04	--
10	4969.435	20117.39		$314_{1/2} - 5157_{3/2}$	−.04	--
8	4972.836	20103.64		$305_{11/2} - 5066_{11/2}$	+.04	--
2	4976.932	20087.09		$313_{9/2} - 5148_{9/2}$	+.10	--
7	4980.677	20071.99		$266_{9/2} - 4673_{3/2}$	+.04	--
20	4981.544	20068.49		$217_{7/2} - 4184_{7/2}$	+.06	--
200	4985.978	20050.65		$173_{7/2} - 3738_{5/2}$	+.03	--
				$304_{5/2} - 5057_{3/2}$	+.07	--
5	4987.521	20044.45		$272_{9/2} - 4720_{9/2}$	.0	--
3	4994.02	20018.4		$319_{7/2} - 5220_{9/2}$	.0	--
1	4994.48	20016.5		$314_{3/2} - 5147_{5/2}$	+.1	--
1	4996.22	20009.6		$261_{3/2} - 4654_{1/2}$	+.1	--
4	4997.74	20003.5		$333_{11/2} - 5352_{9/2}$	.0	23
(2)	4999.39	19996.9		$311_{5/2} - 5118_{5/2}$	.0	--
10	5003.60	19980.6		$221_{9/2} - 4814_{5/2}$	−.1	--
1	5006.68	19967.7		$3769_{5/2} - 5746_{3/2}$	.0	--
6	5008.14	19961.9		$273_{11/2} - 4789_{9/2}$	.0	--
4	5010.56	19952.3		$278_{5/2} - 4777_{3/2}$	.0	--
1	5014.35	19937.2		$304_{3/2} - 5046_{5/2}$	+.03	--
2	5024.022	19898.82		$146_{5/2} - 3452_{7/2}$	−.01	--
20	5026.452	19889.20		$231_{5/2} - 4304_{5/2}$	−.03	--
15	5027.943	19883.30		$244_{5/2} - 4490_{5/2}$	+.1	--
2	5029.75	19876.2		$278_{5/2} - 4770_{3/2}$	+.1	--
1h	5031.57	19869.0		$280_{5/2} - 4789_{3/2}$	.0	--
2h	5031.94	19867.5		$3779_{1/2} - 5766_{3/2}$	.0	--
1h	5039.88	19848.0		$266_{5/2} - 4650_{5/2}$	−.1	--
3H	5041.40	19830.2		$313_{9/2} - 5122_{7/2}$	+.03	--
7	5042.631	19825.38		$172_{1/2} - 3706_{3/2}$	+.1	--
				$(273'')_{1/2} - 4718_{1/2}$	+.1	--
2	5052.20	19787.8		$(273')_{1/2} - 4717_{3/2}$	+.3	--
1	5052.365	19787.19		$273''_{1/2} - 4717_{3/2}$	.0	--
1h	5054.95	19777.1		$332_{5/2} - 5305_{3/2}$	−.01	--
10	5056.083	19772.72		$298_{5/2} - 4957_{5/2}$	−.03	--
100	5058.557	19762.97		$138_{3/2} - 3358_{3/2}$	−.02	--
5	5060.427	19755.66		$306_{9/2} - 5046_{9/2}$	.0	--
3	5065.31	19736.6		$304_{3/2} - 5026_{3/2}$	−.04	--
2	5067.544	19727.92		$301_{1/2} - 4985_{1/2}$	−.2	--
4	5068.85	19722.9		$244_{5/2} - 4414_{3/2}$	−.03	--
6	5078.423	19685.66		$261_{3/2} - 4581_{1/2}$	.00	--
1	5081.573	19673.46		$280_{5/2} - 4770_{3/2}$		

Int.	λ_{vac}	σ_{vac}	Zeeman effect	Transition	O-C	Notes
	A	*K*				
6	5090.57	19638.7		$280_{3/2} - 4766_{7/2}$	.0	--
3	5093.19	19628.6		$313_{9/2} - 5102_{9/2}$	−.1	--
150	5096.50	19615.8		$163_{11/2} - 3592_{9/2}$	−.1	--
2	5098.782	19607.06		$319_{7/2} - 5159_{5/2}$	−.03	--
2	5100.70	19599.7		$332_{5/2} - 5288_{5/2}$	.0	--
20	5104.66	19584.5		$247_{7/2} - 4430_{5/2}$	.0	--
10	5105.15	19582.6		$138_{3/2} - 3340_{5/2}$	.0	--
10	5108.78	19568.7	(?) .585	$224_{3/2} - 4199_{1/2}$	.0	19
15	5112.265	19555.35		$263_{13/2} - 4590_{11/2}$	+.06	--
1	5113.25	19551.6		$306_{9/2} - 5019_{9/2}$	.0	--
1	5115.18	19544.2		$341_{9/2} - 5373_{7/2}$	.0	--
2	5116.90	19537.6		$217_{7/2} - 4131_{5/2}$	.0	--
2	5117.42	19535.6		$301_{1/2} - 4966_{3/2}$	−.1	--
30	5120.32	19524.6		$244_{5/2} - 4394_{5/2}$	.0	--
9	5124.597	19508.29		$271_{7/2} - 4664_{5/2}$	.00	--
20	5126.70	19500.3		$247_{7/2} - 4422_{9/2}$	−.1	--
4	5140.058	19449.61		$298_{5/2} - 4925_{3/2}$	−.03	--
3	5141.288	19444.96		$204_{3/2} - 3992_{3/2}$	−.06	--
6	5145.593	19428.69		$285_{7/2} - 4797_{5/2}$	.00	--
				$3984_{7/2} - 5926_{5/2}$	−.2	--
15	5146.89	19423.8		$333_{11/2} - 5274_{9/2}$	+.1	--
15	5156.248	19388.54		$217_{7/2} - 4116_{7/2}$	+.03	--
30	5161.650	19368.25		$271_{7/2} - 4650_{5/2}$	−.02	--
2	5167.860	19344.98		$278_{3/2} - 4718_{1/2}$	−.2	--
2	5172.370	19328.11		$280_{5/2} - 4785_{7/2}$	+.07	--
80	5178.891	19303.77		$166_{9/2} - 3592_{9/2}$	+.03	--
20	5181.741	19293.16		$221_{9/2} - 4145_{9/2}$	+.02	--
3	5185.896	19277.70		$311_{5/2} - 5046_{5/2}$	−.02	--
2	5186.149	19276.76		$244_{5/2} - 4370_{3/2}$	−.04	--
1	5186.423	19275.74		$266_{5/2} - 4593_{7/2}$	−.01	--
8	5199.89	19225.8		$247_{7/2} - 4394_{5/2}$	.0	--
4	5200.82	19222.4		$298_{5/2} - 4902_{5/2}$	.0	--
1	5202.83	19215.0		$266_{5/2} - 4587_{5/2}$	+.1	--
2	5203.46	19212.6		$324_{5/2} - 5164_{7/2}$	−.1	--
1h	5206.74	19200.5		$261_{3/2} - 4533_{5/2}$	.0	--
200	5209.08	19191.9		$142_{7/2} - 3540_{5/2}$	.0	--
10	5209.927	19188.78		$204_{3/2} - 3967_{5/2}$	−.01	--
1	5210.93	19185.1		$341_{9/2} - 5337_{9/2}$	.0	--
5H	5214.43	19172.2		$3919_{1/2} - 5836_{3/2}$	.0	--
5	5214.716	19171.16		$217_{2} - 4094_{7/2}$	+.03	--
2	5217.49	19161.0		$288_{7/2} - 4797_{5/2}$	.0	--
3	5222.124	19143.96		$244_{5/2} - 4356_{5/2}$	.00	--
				$280_{5/2} - 4717_{3/2}$	−.1	--
1	5222.733	19141.73		$341_{9/2} - 5353_{7/2}$	.0	--
				$304_{3/2} - 4966_{3/2}$	+.02	--
1	5223.022	19140.67		$224_{3/2} - 4155_{3/2}$	−.04	--
10	5224.786	19134.21		$285_{7/2} - 4766_{7/2}$	−.06	--
2h	5226.805	19126.82		$301_{1/2} - 4925_{3/2}$	+.02	--
1	5229.087	19118.47		$314_{3/2} - 5057_{3/2}$	−.1	--
1	5231.31	19110.3		$231_{5/2} - 4225_{3/2}$	+.03	--
20	5234.306	19099.41		$247_{7/2} - 4381_{7/2}$	+.03	--
10	5236.660	19090.82		$3899_{9/2} - 5806_{7/2}$	−.1	--
2	5243.52	19065.8		$194_{5/2} - 3852_{7/2}$	+.04	--
10	5244.334	19062.89		$304_{3/2} - 4957_{5/2}$	−.05	--
				$217_{7/2} - 4082_{5/2}$	+.03	--
30	5248.856	19046.46		$324_{5/2} - 5147_{5/2}$	.00	--
3	5250.085	19042.01		$338_{7/2} - 5285_{7/2}$	.0	--
3	5252.34	19033.8		$305_{11/2} - 4958_{9/2}$	.0	--
1h	5255.43	19022.7		$221_{9/2} - 4116_{7/2}$	.0	--
3	5260.62	19003.9		$3906_{5/2} - 5806_{7/2}$	−.1	7
(5)	5262.92	18995.6		$261_{3/2} - 4512_{5/2}$	−.07	--
4	5264.416	18990.17		$2363_{9/2} - 4259_{7/2}$	+.1	--
4000	5270.95	18966.6	(**.109**, .329, .549) **1.000**, 1.218, 1.436, 1.655.			
1000	5275.56	18950.1		$0_{3/2} - 1895_{5/2}$	.0	--
200	5278.245	18940.41		$164_{3/2} - 3529_{5/2}$	−.02	--
2	5279.102	18937.34		$306_{9/2} - 4958_{9/2}$	+.06	--
5	5284.581	18917.71		$338_{7/2} - 5274_{9/2}$	+.1	--
10	5287.92	18905.8		$278_{3/2} - 4673_{3/2}$	+.1	--
4	5292.278	18890.19		$224_{3/2} - 4151_{5/2}$	.00	--
5	5300.75	18860.0		$275_{9/2} - 4657_{9/2}$	+.1	--
3	5306.739	18838.72		$275_{9/2} - 4635_{7/2}$	+.04	--
6	5311.515	18821.78		$278_{3/2} - 4664_{5/2}$	+.01	--
30	5317.275	18801.39		$266_{5/2} - 4546_{7/2}$	−.01	--
1h	5318.76	18796.1		$271_{7/2} - 4593_{7/2}$	.0	--
2h	5319.23	18794.5		$324_{5/2} - 5122_{7/2}$	.0	--
40	5321.278	18787.25		$146_{5/2} - 3349_{3/2}$	−.02	--
				$221_{9/2} - 4094_{7/2}$	−.15	--
2	5321.534	18786.34		$338_{7/2} - 5261_{7/2}$	−.01	--
				$272_{9/2} - 4593_{7/2}$	+.1	--
2	5324.50	18775.9		$270_{13/2} - 4590_{11/2}$	.0	--
4	5325.00	18774.1		$138_{3/2} - 3259_{5/2}$	.0	--
200	5327.46	18765.5		$157_{5/2} - 3452_{7/2}$	.00	--
50	5331.896	18749.83		$324_{5/2} - 5118_{5/2}$	−.1	--
2h	5332.47	18747.8		$272_{9/2} - 4590_{11/2}$	+.1	--
20	5333.85	18743.0		$305_{11/2} - 4928_{11/2}$	.0	--
3	5338.63	18726.2		$304_{3/2} - 4925_{3/2}$	+.01	--
4	5339.416	18723.43		$3965_{9/2} - 5836_{9/2}$	+.2	--
3H	5342.37	18713.1		$280_{5/2} - 4673_{3/2}$	+.03	--
2	5345.221	18703.09		$231_{5/2} - 4184_{7/2}$	−.02	--
3	5349.245	18689.02		$247_{7/2} - 4341_{5/2}$	−.07	--
4	5350.45	18684.82		$311_{5/2} - 4986_{7/2}$	+.1	--
1h	5352.64	18677.2		$332_{5/2} - 5195_{7/2}$	.0	--
1	5353.73	18673.4		$341_{9/2} - 5285_{7/2}$	.0	--
1h	5356.65	18663.2		$333_{11/2} - 5194_{11/2}$	.00	--
2	5366.664	18628.37		$244_{5/2} - 4304_{5/2}$	−.02	--
30	5369.480	18618.60		$138_{3/2} - 3244_{1/2}$	+.01	--
30	5369.797	18617.50		$3906_{5/2} - 5766_{3/2}$	−.07	--
4	5374.720	18600.44				

TABLE 2. *Classified lines of* Re I—Continued

Int.	λ_{vac}	σ_{vac}	Zeeman effect	Transition	O–C	Notes	Int.	λ_{vac}	σ_{vac}	Zeeman effect	Transition	O–C	Notes
	A	*K*						*A*	*K*				
200	5377.10	18592.2		$173_{7/2}-35929_{9/2}$	.0	..	3	5778.343	17301.20		$29853_{/2}-47103_{/2}$	−.03	..
5	5378.163	18588.53		$261_{3/2}-44723_{/2}$	+.01	..	7	5782.58	17288.5		$26613_{/2}-43945_{/2}$	−.1	..
3	5379.707	18583.20		$204_{3/2}-39063_{/2}$	+.01	..	2	5783.01	17287.3		$30689_{/2}-47937_{/2}$	+.1	..
1h	5390.18	18547.1		$341_{9/2}-52749_{/2}$	+.1	..	7	5786.27	17277.5		$26113_{/2}-43415_{/2}$	.0	..
9	5390.50	18525.4		$306_{9/2}-49179_{/2}$	.0	..	20	5791.595	17261.61		$16413_{/2}-33583_{/2}$	.00	..
1	5409.52	18480.8		$319_{7/2}-50469_{/2}$	.0	..	2	5796.262	17247.71		$22413_{/2}-39773_{/2}$	+.02	..
2	5410.01	18479.1		$280_{5/2}-46503_{/2}$	.0	..	2	5805.77	17219.5		$21773_{/2}-38993_{/2}$	+.2	..
(1)	5416.26	18457.8		$194_{3/2}-37913_{/2}$	−.2	23	10	5806.97	17215.9		$20413_{/2}-37693_{/2}$	.0	..
5H	5417.78	18452.6		$3991_{11/2}-58369_{/2}$	+.1	..	4	5807.41	17214.6		$30689_{/2}-47851_{1/2}$	.0	..
(2)	5421.75	18439.1		$3259_{3/2}-51033_{/2}$	.0	23	8	5808.86	17210.3		$26113_{/2}-43343_{/2}$	.0	..
2	5423.29	18433.9		$324_{5/2}-50867_{/2}$	.0	..	4	5810.82	17204.5		$4116_{7/2}-58369_{/2}$	.0	..
4	5423.60	18432.8		$273'_{1/2}-45811_{/2}$	−.1	..	(1)	5810.96	17204.1		$29853_{/2}-47063_{/2}$	+.1	23
6	5423.81	18432.1		$273''_{1/2}-45811_{/2}$	.0	..	20	5815.92	17189.4		$17373_{/2}-34583_{/2}$	.0	..
30	5431.90	18404.6		$5965_{9/2}-58069_{/2}$	−.1	..	2	5818.28	17182.5		$33253_{/2}-50463_{/2}$	+.3	..
10	5437.03	18387.3		$224_{3/2}-40811_{/2}$	.0	..	1000	5834.31	17135.2	(.091, .273, .457, .642) .892, 1.075, 1.259, 1.442, 1.626†.	$11793_{/2}-28883_{/2}$	.0	..
3	5437.41	18386.0		$224_{1/2}-40803_{/2}$	.0	..							
2h	5443.31	18366.1		$332_{3/2}-51643_{/2}$	−.1	..							
15	5447.92	18350.5		$150_{7/2}-33403_{/2}$	.0	..							
4	5456.316	18322.29		$4094_{7/2}-59269_{/2}$	+.03	..	5	5835.52	17131.7		$24453_{/2}-41553_{/2}$	.0	..
2h	5458.92	18313.5		$278_{3/2}-46141_{/2}$	.0	..	20	5852.02	17083.4		$27173_{/2}-44223_{/2}$	−.1	..
30	5460.644	18307.77		$194_{3/2}-37767_{/2}$	+.01	..					$33311_{/2}-50409_{/2}$	.0	..
7	5465.43	18291.7		$288_{7/2}-47103_{/2}$	.0	..	3	5852.76	17081.2		$16413_{/2}-33493_{/2}$	.0	..
3	5467.54	18284.7		$266_{9/2}-44947_{/2}$	.0	..	3	5866.58	17041.0		$30113_{/2}-47183_{/2}$	−.3	..
				$278_{3/2}-46113_{/2}$	+.1	..					$26653_{/2}-43703_{/2}$	+.2	..
5	5481.003	18239.76		$194_{3/2}-37693_{/2}$	−.01	..	8	5868.05	17036.7		$22193_{/2}-39193_{11/2}$	.0	..
				$266_{9/2}-44903_{/2}$	+.04	..	2	5870.71	17029.0		$33253_{/2}-50313_{/2}$	−.1	..
3	5492.19	18202.6		$271_{7/2}-45343_{/2}$	+.2	..	1	5872.557	17023.63		$30693_{/2}-47663_{/2}$	−.05	..
2	5494.34	18195.5		$332_{3/2}-51473_{/2}$	.0	..	8	5899.25	16946.6		$30511_{/2}-47503_{/2}$	−.3	..
2	5495.69	18191.0		$271_{7/2}-45333_{/2}$	+.1	..	7	5903.99	16933.0		$29853_{/2}-46733_{/2}$	.0	..
1h	5499.79	18177.5		$338_{7/2}-52009_{/2}$	−.2	..	5	5909.99	16915.8		$28053_{/2}-44973_{/2}$	.0	..
5	5501.921	18170.42		$298_{5/2}-47973_{/2}$	−.02	..					$4145_{9/2}-58369_{/2}$	+.1	..
3	5505.60	18158.3		$231_{5/2}-41313_{/2}$	+.1	..	5	5911.14	16912.5		$26113_{/2}-43043_{/2}$	.0	..
2	5514.99	18127.4		$319_{7/2}-50113_{/2}$	+.1	..	4	5916.66	16896.7		$4116_{7/2}-58063_{/2}$	.0	..
4	5519.53	18112.5		$314_{3/2}-49573_{/2}$	.0	..	9	5919.86	16887.6		$24453_{/2}-41313_{/2}$	.0	..
15	5521.10	18107.3		$285_{7/2}-46643_{/2}$	.0	..	2h	5925.08	16872.7		$30113_{/2}-47003_{/2}$	−.1	..
2h	5521.83	18104.9		$4116_{7/2}-59269_{/2}$	.0	..	6	5927.38	16866.2		$27053_{/2}-43993_{11/2}$	.0	..
8	5523.40	18099.8		$273_{11/2}-45343_{/2}$	+.1	..	2h	5938.83	16833.7		$34193_{/2}-51023_{/2}$	.0	..
50	5532.676	18069.41		$217_{7/2}-39843_{/2}$	+.06	..	100	5943.24	16821.2		$15753_{/2}-32593_{/2}$	.0	..
1h	5534.35	18063.9		$311_{3/2}-49253_{/2}$	.0	..	2	5945.46	16814.9		$32453_{/2}-49253_{/2}$	.0	..
2h	5535.94	18058.8		$266_{9/2}-44723_{/2}$	+.1	..	2h	5947.57	16808.9		$27173_{/2}-43943_{/2}$	.0	..
2h	5545.15	18028.8		$324_{5/2}-50463_{/2}$	+.1	..	10	5950.21	16801.5		$28573_{/2}-45343_{/2}$	+.1	..
(1h)	5551.05	18009.6		$305_{11/2}-48561_{1/2}$	−.1	23	4	5954.308	16789.91		$28573_{/2}-45333_{/2}$	+.01	..
7	5557.20	17989.7		$278_{3/2}-46811_{/2}$	+.1	..	4	5956.10	16784.9		$31393_{/2}-48183_{/2}$	.0	..
100	5563.24	17970.1		$146_{3/2}-32593_{/2}$	−.1	..	5	5967.626	16752.44		$27311_{/2}-43991_{1/2}$	+.02	..
7	5564.12	17967.3		$285_{7/2}-46503_{/2}$	.0	..	20	5969.77	16746.4		$31153_{/2}-47953_{/2}$	−.1	..
30	5573.47	17937.2		$173_{7/2}-35263_{/2}$	+.1	..					$26653_{/2}-43403_{/2}$	.0	..
8	5577.69	17923.6		$194_{3/2}-37383_{/2}$	+.1	..	4	5972.58	16738.6		$24453_{/2}-41163_{/2}$	+.1	..
3	5578.38	17921.4		$272_{9/2}-45083_{1/2}$	+.1	..	6	5981.65	16713.2		$31153_{/2}-47893_{/2}$	+.1	..
2	5582.89	17906.9		$280_{5/2}-45933_{/2}$	.0	..	8	5982.67	16710.3		$27593_{/2}-44223_{/2}$	.0	..
30	5584.718	17901.03		$166_{9/2}-34523_{/2}$	+.06	..	7	5983.14	16709.0		$29853_{/2}-46503_{/2}$	.0	..
2	5592.68	17875.6		$324_{5/1}-50317_{/2}$	.0	..	8	5989.99	16689.9		$23153_{/2}-39873_{/2}$	.0	..
6	5594.856	17868.60		$298_{5/2}-47663_{/2}$	−.03	..					$28053_{/2}-44723_{/2}$	+.1	..
3	5661.92	17846.1		$280_{5/2}-45873_{/2}$	+.1	..	20	5995.73	16673.9		$27173_{/2}-43813_{/2}$	.0	..
2h	5604.15	17839.0		$273_{11/2}-45683_{11/2}$	+.2	..	2h	6021.83	16601.6		$30113_{/2}-46733_{/2}$	−.2	..
8	5607.21	17829.2		$275_{9/2}-45343_{/2}$	−.1	..	3	6026.53	16588.7		$24773_{/2}-41313_{/2}$	−.1	..
3	5607.41	17828.6		$244_{5/2}-42253_{/2}$	−.2	..	(1h)	6029.05	16581.8		$20413_{/2}-37063_{/2}$	−.1	23
3h	5608.803	17824.16		$338_{7/2}-51647_{/2}$	.00	..	2	6029.16	16581.5		$33253_{/2}-49863_{/2}$	−.1	..
3	5610.516	17818.72		$157_{5/2}-33583_{/2}$	+.02	..	3	6030.67	16577.3		$33873_{/2}-50493_{/2}$	−.1	..
2	5614.85	17805.0		$271_{7/2}-44943_{/2}$	.0	..	10	6039.67	16552.6		$29853_{/2}-46353_{/2}$	.0	..
4	5619.76	17789.4		$314_{3/2}-49253_{/2}$	.0	..	5	6051.19	16521.1		$24453_{/2}-40943_{/2}$	.0	..
1	5621.22	17784.8		$272_{9/2}-44943_{/2}$	.0	..	2h	6068.42	16474.2		$34523_{/2}-50993_{/2}$	+.3	..
8	5625.441	17771.44		$313_{9/2}-49179_{/2}$	−.02	..	2h	6081.57	16438.6		$31413_{/2}-47893_{/2}$	.0	..
3	5635.45	17739.9		$272_{9/2}-44903_{/2}$	+.1	..	2h	6097.20	16396.4		$24453_{/2}-40823_{/2}$	.0	..
8	5653.018	17684.75		$221_{9/2}-39843_{/2}$	+.04	..	60	6114.22	16350.8		$17213_{/2}-33583_{/2}$	.0	..
4	5658.68	17667.1		$231_{5/2}-40823_{/2}$	+.1	..	10	6125.47	16320.7		$27893_{/2}-44143_{/2}$	−.1	..
5	5662.83	17654.1		$231_{5/2}-40803_{/2}$	+.1	..	6	6132.98	16300.8		$27593_{/2}-43813_{/2}$	+.1	..
3	5664.69	17648.3		$301_{1/2}-47773_{/2}$	.0	..	100	6145.81	16266.7		$27173_{/2}-43403_{/2}$	.0	..
				$266_{9/2}-44303_{/2}$	.0	..	80	6146.82	16264.1		$16413_{/2}-32593_{/2}$	.0	..
3	5665.01	17647.3		$263_{11/2}-43991_{1/2}$	.0	..	6	6169.51	16204.3		$31413_{/2}-47653_{/2}$	+.2	..
100	5667.88	17638.4		$157_{5/2}-33403_{/2}$	+.1	..	3	6181.71	16172.3		$31153_{/2}-47353_{/2}$	.0	..
3	5671.04	17628.6		$313_{9/2}-49033_{/2}$	.0	..	15	6195.44	16136.4		$28873_{/2}-44943_{/2}$	+.1	..
3	5678.34	17605.9		$194_{3/2}-37663_{/2}$	+.1	..	3	6200.734	16122.66		$26113_{/2}-42253_{/2}$	.00	..
2h	5683.40	17590.2		$319_{7/2}-49573_{/2}$	+.1	..	20	6203.24	16116.1		$16413_{/2}-32443_{/2}$	.0	..
2	5684.31	17587.4		$332_{3/2}-50863_{/2}$	.0	..	50	6217.97	16078.0		$17373_{/2}-33403_{/2}$	+.1	..
2	5686.81	17579.7		$3340_{3/2}-50983_{/2}$	.0	..	4	6218.74	16076.0		$29853_{/2}-45873_{/2}$	.0	..
6	5689.75	17570.6		$261_{3/2}-43703_{/2}$	.0	..	60	6229.42	16048.4		$28853_{/2}-44913_{/2}$	.0	..
2	5692.46	17562.2		$314_{3/2}-49023_{/2}$	.0	..	80	6243.24	16012.9		$28883_{/2}-44913_{/2}$	.0	..
30	5711.426	17503.90		$224_{3/2}-39923_{/2}$	−.02	..	2	6252.08	15990.3		$21773_{/2}-37763_{/2}$	.0	..
5	5714.02	17495.9		$221_{9/2}-39659_{/2}$	−.1	..	5	6253.03	15987.8		$31973_{/2}-47973_{/2}$	.0	..
15	5716.950	17486.99		$266_{9/2}-44143_{/2}$	−.03	..	1	6254.96	15982.9		$30413_{/2}-46503_{/2}$	+.1	..
9	5725.626	17460.49		$324_{5/2}-49893_{/2}$	+.06	..	4	6265.07	15957.1		$(273'_{1/2}-43343_{/2}$	−.4	..
3	5727.90	17453.6		$341_{9/2}-51647_{/2}$	.0	..					$(273''_{1/2}-43343_{/2}$	+.4	..
1	5730.96	17444.2		$304_{3/2}-47973_{/2}$	.0	..	30	6271.37	15941.1		$28963_{/2}-44913_{/2}$	.0	..
5	5733.06	17437.9		$261_{3/2}-43563_{/2}$	+.1	..	3	6272.14	15939.1		$27593_{/2}-43453_{/2}$	+.1	..
5	5734.26	17434.2		$204_{3/2}-37913_{/2}$	+.1	..	30	6278.76	15922.3		$21773_{/2}-37693_{/2}$	−.1	..
2	5736.27	17428.1		$324_{5/2}-49863_{/2}$	.0	..	15	6286.41	15902.9		$27173_{/2}-43943_{/2}$	.0	..
2	5737.32	17424.9		$4184_{7/2}-59269_{/2}$	.0	..	6	6290.11	15893.6		$27593_{/2}-43403_{/2}$	.0	..
3H	5738.17	17422.3		$4094_{7/2}-58369_{/2}$	−.1	..	2	6298.35	15872.8		$44053_{/2}-59923_{/2}$	+.1	..
7	5739.445	17418.45		$244_{5/2}-41843_{/2}$	.00	..	10	6303.42	15860.0		$26113_{/2}-41993_{/2}$	.0	..
10	5740.32	17415.8		$247_{7/2}-42143_{/2}$	.0	..	2h	6306.19	15853.1		$33311_{/2}-49173_{/2}$	−.1	..
				$313_{9/2}-48783_{/2}$	−.2	..	400	6307.70	15849.3	(?) 1.876B.....	$28853_{/2}-44703_{/2}$	{+.1 −.5	28
2h	5749.86	17386.9		$275_{9/2}-44903_{/2}$	+.1	..	200	6307.91	15848.7				
200	5752.93	17377.6	(?) .752†	$115_{5/2}-28963_{/2}$	.0	19	800	6321.90	15813.7	(?) 1.408, 1.029, 1.650†	$28883_{/2}-44703_{/2}$	.0	..
3	5763.41	17346.0		$333_{11/2}-50963_{11/2}$	+.1	..							
1h	5773.32	17316.3		$204_{3/2}-37793_{/2}$	+.1	..	300	6350.64	15742.1		$28963_{/2}-44703_{/2}$	{+.3 −.3	28
				$115_{5/2}-28883_{/2}$	−.1	..	200	6350.87	15741.5				
300	5776.83	17305.7		$197_{1/2}-37063_{/2}$	.0	..	2	6362.69	15712.3		$31453_{/2}-47183_{/2}$	.0	..
1	5778.16	17301.8		$280_{5/2}-45333_{/2}$	+.1	..	3	6362.94	15711.7		$31493_{/2}-47173_{/2}$	+.2	..

TABLE 2. *Classified lines of* Re I—Continued

Int.	λ_{vac}	σ_{vac}	Zeeman effect	Transition	O-C	Notes
	A	*K*				
10	6373.47	15685.7		$301_{1/2} - 4581_{1/2}$	.0	--
15	6382.94	15662.4		$298_{5/2} - 4546_{7/2}$	−.1	--
20	6405.98	15606.1		$217_{7/2} - 3738_{5/2}$	+.1	--
(3)	6406.16	15605.7		$221_{9/2} - 3776_{7/2}$	+.1	23
20	6411.47	15592.7		$266_{5/2} - 4225_{3/2}$	−.1	--
2h	6416.13	15581.4		$278_{3/2} - 4341_{5/2}$	−.1	--
2h	6422.24	15566.6		$4570_{3/2} - 5926_{5/2}$	.0	--
3	6436.69	15531.6		$298_{5/2} - 4535_{5/2}$	−.1	--
8	6449.28	15501.3		$244_{3/2} - 3992_{3/2}$	−.1	--
5	6501.17	15377.58		$280_{5/2} - 4340_{7/2}$	+.03	--
7	6502.22	15375.10		$224_{3/2} - 3779_{1/2}$	−.02	--
80	6511.47	15353.27		$172_{1/2} - 3259_{3/2}$	−.06	--
20	6515.25	15344.36		$305_{11/2} - 4590_{11/2}$	+.02	--
7	6529.21	15311.56		$280_{3/2} - 4334_{3/2}$	+.03	--
10	6544.91	15274.82		$224_{3/2} - 3769_{3/2}$	−.01	--
8	6545.72	15272.93		$285_{7/2} - 4381_{7/2}$	+.05	--
4	6554.66	15252.10		$333_{11/2} - 4856_{11/2}$	+.04	--
10	6557.67	15245.11		$244_{5/2} - 3967_{5/2}$	−.01	--
70	6577.11	15200.04		$2885_{5/2} - 4405_{5/2}$	+.01	--
100	6592.52	15164.51		$2888_{7/2} - 4405_{5/2}$	+.02	--
250	6605.19	15135.43		$138_{3/2} - 2896_{3/2}$	.00	29
4	6612.53	15118.62		$319_{7/2} - 4710_{5/2}$	.00	--
100	6623.91	15092.65		$2896_{3/2} - 4405_{5/2}$	−.01	--
30	6637.25	15062.32		$194_{5/2} - 3452_{7/2}$	−.04	--
200	6652.39	15028.03		$138_{3/2} - 2885_{5/2}$	−.03	--
5	6658.74	15013.70		$280_{5/2} - 4304_{5/2}$	.00	--
20	6665.32	14998.89		$271_{7/2} - 4214_{9/2}$	−.04	--
8	6675.28	14976.51		$341_{9/2} - 4917_{9/2}$	+.02	--
20	6683.28	14958.57		$224_{3/2} - 3738_{5/2}$	−.01	--
7	6688.75	14946.34		$247_{7/2} - 3967_{5/2}$	+.04	--
10	6711.30	14896.13		$273_{11/2} - 4214_{9/2}$	−.05	--
2	6723.19	14869.77		$273'_{1/2} - 4225_{3/2}$	−.02	--
3h	6723.55	14868.98		$273''_{1/2} - 4225_{3/2}$	−.01	--
6	6724.98	14865.82		$285_{7/2} - 4340_{7/2}$	+.08	--
10	6761.19	14786.20		$204_{3/2} - 3526_{5/2}$	−.01	--
6	6799.59	14702.70		$271_{7/2} - 4184_{7/2}$	−.02	--
5	6801.66	14698.23		$306_{9/2} - 4534_{9/2}$	−.01	--
5	6805.35	14690.26	•	$261_{5/2} - 4082_{5/2}$ $311_{5/2} - 4587_{3/2}$	.00 .00	--
4	6811.37	14677.28		$261_{5/2} - 4080_{3/2}$	.00	--
300	6813.41	14672.88		$142_{7/2} - 2888_{7/2}$	+.02	--
2	6816.41	14666.43		$324_{3/2} - 4710_{5/2}$ $319_{7/2} - 4664_{5/2}$	−.04 .00	--
300	6829.90	14637.45	(.154, .460) .813, 1.111†.	$142_{7/2} - 2885_{5/2}$	+.13	--
3H	6835.35	14625.78		$275_{9/2} - 4214_{9/2}$	+.03	--
5	6844.06	14607.17		$273'_{1/2} - 4199_{1/2}$	+.01	--
5	6844.44	14606.36		$273''_{1/2} - 4199_{1/2}$	.00	--
8	6874.35	14542.81		$231_{5/2} - 3769_{5/2}$	−.04	--
3	6882.11	14526.41		$319_{7/2} - 4650_{5/2}$	.00	--
3	6963.70	14356.63		$314_{3/2} - 4581_{3/2}$	−.01	--
8	6967.67	14348.04		$298_{5/2} - 4474_{3/2}$	−.03	--
200	6971.53	14340.10		$146_{5/2} - 2896_{3/2}$	+.01	--
2	6976.67	14329.54		$275_{9/2} - 4184_{7/2}$	.00	--
20	6985.20	14312.02		$271_{7/2} - 4145_{9/2}$	−.03	--
150	7006.63	14268.26		$146_{5/2} - 2888_{7/2}$	.00	--
5	7012.56	14256.20		$4321_{1/2} - 5766_{3/2}$	−.12	--
200	7024.15	14232.66		$146_{5/2} - 2885_{5/2}$	−.06	--
(2)	7027.14	14226.61		$231_{5/2} - 3738_{5/2}$	+.01	23
7	7028.47	14223.92		$280_{5/2} - 4225_{3/2}$	+.05	--
10	7058.24	14163.92		$278_{3/2} - 4199_{1/2}$	+.01	--
6	7059.98	14160.43		$266_{5/2} - 4082_{5/2}$	+.03	--
3	7065.39	14149.59		$298_{5/2} - 4394_{5/2}$	−.01	--
10	7066.47	14147.43		$266_{5/2} - 4080_{3/2}$	+.01	--
(10)	7129.25	14022.85		$271_{7/2} - 4116_{7/2}$	+.07	30
(1)	7139.64	14002.45		$272_{9/2} - 4116_{7/2}$	−.11	23
10	7172.20	13938.87		$275_{9/2} - 4145_{9/2}$	.00	--
4	7198.25	13888.44		$333_{11/2} - 4799_{9/2}$	−.04	--
20	7228.03	13831.22		$197_{1/2} - 3358_{1/2}$	+.01	--
3	7233.90	13820.00		$332_{5/2} - 4710_{5/2}$	+.04	--
41	7237.26	13813.56		$280_{5/2} - 4184_{7/2}$	+.03	--
150	7246.49	13795.97		$150_{7/2} - 2885_{5/2}$	−.02	--
100	7246.89	13795.38		$261_{1/2} - 3992_{3/2}$	+.20	--
4	7263.86	13762.99		$221_{9/2} - 3592_{9/2}$	+.01	--
150	7273.84	13744.11		$2885_{5/2} - 4258_{7/2}$	+.02	--
300	7292.72	13708.52		$2888_{7/2} - 4258_{7/2}$	−.03	--
5	7307.55	13680.71		$271_{7/2} - 4082_{5/2}$	+.01	--
(4)	7316.1	13664.7		$305_{11/2} - 4429_{9/2}$	.0	31
(2)	7318.02	13661.13		$314_{3/2} - 4512_{3/2}$	−.06	31
7	7324.20	13649.60		$275_{9/2} - 4116_{7/2}$	.00	--
(1)	7346.88	13607.47		$298_{5/2} - 4340_{7/2}$	−.02	31
50	7352.04	13597.91		$285_{7/2} - 4214_{9/2}$	−.02	--
(2)	7362.12	13579.30		$306_{9/2} - 4422_{9/2}$	+.05	31
3	7382.67	13541.51		$298_{5/2} - 4334_{3/2}$	−.02	--
1	7384.07	13538.94		$261_{3/2} - 3975_{3/2}$	−.01	--
20	7386.35	13534.74		$338_{7/2} - 4735_{7/2}$	+.04	--
4	7390.71	13526.76		$280_{5/2} - 4155_{3/2}$	.00	--
2	7396.04	13517.02		$4414_{3/2} - 5766_{3/2}$	+.04	--
3h	7404.28	13501.98		$324_{5/2} - 4593_{7/2}$ $313_{9/2} - 4490_{7/2}$	−.06 +.13	--
20	7409.46	13492.54		$217_{7/2} - 3526_{5/2}$	.00	--
(2)	7413.41	13485.35		$278_{3/2} - 4131_{5/2}$	−.02	31
3	7416.44	13479.85		$319_{7/2} - 4546_{7/2}$	+.01	--
2	7431.93	13451.74		$332_{5/2} - 4673_{3/2}$	+.01	--
2	7437.79	13441.14		$324_{5/2} - 4587_{3/2}$	−.06	--
1	7442.75	13432.19		$275_{9/2} - 4094_{7/2}$	−.03	--
(1)	7446.97	13424.58		$273'_{1/2} - 4080_{3/2}$	+.13	31

Int.	λ_{vac}	σ_{vac}	Zeeman effect	Transition	O-C	Notes
	A	*K*				
4	7447.58	13423.48		$273''_{1/2} - 4080_{3/2}$ $304_{3/2} - 4394_{5/2}$ $332_{5/2} - 4664_{5/2}$	−.17 +.10 −.02	-- -- --
5	7478.63	13367.75		$270_{13/2} - 4049_{13/2}$	+.04	--
7	7481.15	13363.24		$319_{7/2} - 4534_{9/2}$	+.04	31
(1)	7482.62	13360.62		$306_{9/2} - 4399_{11/2}$	−.16	--
3	7488.12	13350.81		$319_{7/2} - 4533_{5/2}$	+.02	--
2	7489.10	13349.06		$244_{5/2} - 3776_{7/2}$	+.05	--
2	7494.02	13340.30		$4508_{11/2} - 5836_{9/2}$	+.02	--
10H	7524.48	13286.29		$280_{5/2} - 4131_{5/2}$	+.05	--
3	7526.49	13282.75		$266_{5/2} - 3992_{3/2}$	−.05	--
2	7536.40	13265.27		$314_{3/2} - 4472_{3/2}$	−.05	31
(1)	7539.73	13259.42		$273_{11/2} - 4049_{13/2}$	+.01	--
5	7545.39	13249.47		$298_{5/2} - 4304_{5/2}$	−.02	--
30	7548.72	13243.62		$301_{1/2} - 4534_{3/2}$	−.04	--
6	7567.80	13210.24		$157_{3/2} - 2896_{3/2}$	+.05	--
300	7578.73	13191.18		$266_{5/2} - 3984_{7/2}$	−.02	--
10	7583.26	13183.30		$304_{3/2} - 4370_{3/2}$	+.06	31
(2)	7587.66	13175.66		$194_{5/2} - 3259_{3/2}$ $280_{5/2} - 4116_{7/2}$	−.03 +.12	-- --
100	7611.89	13133.71		$311_{5/2} - 4430_{5/2}$	−.01	31
(3)	7618.32	13122.64		$157_{3/2} - 2888_{7/2}$	+.01	--
200	7620.25	13119.31		$157_{3/2} - 2885_{5/2}$	+.03	--
400	7640.94	13083.79		$333_{11/2} - 4637_{9/2}$	.00	31
7	7656.80	13056.68		$341_{9/2} - 4780_{9/2}$	−.07	--
3	7684.83	13009.06		$266_{5/2} - 3967_{5/2}$	−.03	--
10	7693.70	12994.06		$278_{3/2} - 4082_{5/2}$	−.12	--
30	7705.92	12973.46		$247_{7/2} - 3769_{5/2}$	+.02	--
2	7712.58	12962.26		$311_{5/2} - 4414_{3/2}$	−.11	--
(1)	7716.52	12955.64		$314_{3/2} - 4441_{1/2}$	−.07	31
30	7733.61	12927.01		$204_{3/2} - 3340_{5/2}$	+.01	--
(2)	7738.92	12918.14		$319_{7/2} - 4490_{7/2}$	−.02	31
5	7743.08	12911.20		$285_{7/2} - 4145_{9/2}$	+.15	--
(2)	7781.21	12847.93		$314_{3/2} - 4430_{5/2}$ $263_{13/2} - 3919_{11/2}$	−.20 +.15	31
7	7789.75	12833.85		$332_{5/2} - 4044_{7/2}$	.0	--
10	7789.96	12833.51		$197_{1/2} - 3259_{3/2}$	−.21	--
5	7794.67	12825.74		$338_{7/2} - 4664_{5/2}$	+.02	--
4	7801.05	12815.25		$304_{3/2} - 4334_{3/2}$	.00	--
10	7828.13	12770.93		$285_{7/2} - 4131_{5/2}$	+.04	--
10	7844.14	12744.86		$217_{7/2} - 3452_{7/2}$	+.01	--
100	7869.62	12703.59		$271_{7/2} - 3984_{7/2}$	−.03	--
3	7880.78	12685.60		$197_{1/2} - 3244_{1/2}$	−.10	--
20	7882.11	12683.46		$272_{9/2} - 3984_{7/2}$	+.06	--
9	7888.90	12672.55		$273_{11/2} - 3991_{11/2}$	+.04	--
40	7898.46	12657.21		$247_{7/2} - 3738_{5/2}$	+.02	--
400	7912.94	12634.04		$164_{3/2} - 2896_{3/2}$	.00	--
20	7970.87	12542.23		$273'_{1/2} - 3992_{3/2}$	−.12	--
30	7971.24	12541.65		$273''_{1/2} - 3992_{3/2}$	+.10	--
10	7979.03	12529.39		$271_{7/2} - 3967_{5/2}$ $338_{7/2} - 4635_{7/2}$	.00 +.06	--
300	7980.77	12526.66		$164_{3/2} - 2885_{5/2}$	−.01	--
4	8004.63	12489.33		$314_{3/2} - 4394_{5/2}$	−.03	--
4	8027.50	12453.74		$298_{5/2} - 4225_{3/2}$	−.07	--
10	8052.11	12415.68		$313_{9/2} - 4381_{7/2}$	−.03	--
30	8060.10	12403.37		$266_{5/2} - 3906_{5/2}$	−.12	--
15	8088.27	12360.19		$221_{9/2} - 3452_{7/2}$	−.02	--
(1)	8141.2	12279.8		$285_{7/2} - 4082_{5/2}$	+.1	31
6	8166.63	12241.58		$319_{7/2} - 4429_{9/2}$ $314_{3/2} - 4370_{3/2}$	−.01 .00	--
3	8224.31	12155.73		$311_{5/2} - 4334_{3/2}$	−.04	--
4	8246.93	12122.38		$301_{1/2} - 4225_{3/2}$	−.24	--
2	8253.24	12113.12		$231_{5/2} - 3526_{5/2}$	−.01	--
(4)	8254.0	12112.0		$3259_{3/2} - 4470_{5/2}$	+.3	31
(3)	8256.25	12108.71		$314_{3/2} - 4356_{5/2}$	−.03	31
5	8262.72	12099.22		$278_{3/2} - 3992_{3/2}$	+.12	--
(3)	8285.13	12066.50		$270_{13/2} - 3919_{11/2}$	−.10	31
20	8293.73	12053.98		$313_{9/2} - 4345_{9/2}$	−.02	--
20	8301.01	12043.41		$298_{5/2} - 4184_{7/2}$	−.06	--
(5)	8313.02	12026.02		$333_{11/2} - 4534_{9/2}$	+.02	31
3	8335.44	11993.67		$3899_{9/2} - 5098_{7/2}$	−.07	--
2	8354.00	11967.01		$239_{11/2} - 3592_{9/2}$ $319_{7/2} - 4394_{5/2}$	−.01 +.02	--
40	8357.58	11961.89		$204_{1/2} - 3244_{1/2}$	+.01	--
3	8403.58	11896.42		$280_{5/2} - 3992_{3/2}$	−.01	--
500	8417.13	11877.27		$117_{9/2} - 2363_{9/2}$	−.03	--
(2)	8430.87	11857.91		$311_{5/2} - 4304_{5/2}$	−.03	31
(4)	8433.90	11853.65		$271_{7/2} - 3899_{9/2}$	+.05	31
3	8503.35	11756.83		$298_{5/2} - 4155_{3/2}$	+.13	--
6	8507.73	11750.78		$273_{11/2} - 3899_{9/2}$	−.07	--
(2)	8513.44	11742.90		$341_{9/2} - 4593_{7/2}$	.00	31
(1)	8524.64	11727.48		$304_{3/2} - 4225_{3/2}$	−.11	31
500	8527.73	11723.23		$172_{1/2} - 2896_{3/2}$	−.02	--
(3)	8534.99	11713.26		$324_{5/2} - 4414_{3/2}$	−.05	31
2	8537.38	11709.97		$341_{9/2} - 4590_{11/2}$	−.01	--
(4)	8554.61	11686.39		$4637_{9/2} - 5806_{7/2}$	.00	31
(2)	8557.50	11682.45		$275_{9/2} - 3919_{11/2}$	+.02	31
15	8570.69	11664.47		$332_{5/2} - 4494_{7/2}$	.00	--
5	8588.50	11640.27		$280_{5/2} - 3967_{5/2}$	+.07	--
5	8593.60	11633.37		$217_{7/2} - 3540_{5/2}$	+.04	--
5H	8628.44	11586.39		$319_{7/2} - 4356_{5/2}$	+.02	--
7H	8630.60	11583.49		$314_{3/2} - 4304_{5/2}$	+.09	--
(3)	8633.10	11580.15		$305^{11}/_{2} - 4214_{9/2}$	.00	31
20	8643.59	11566.09		$261_{3/2} - 3769_{5/2}$	.00	--
20	8648.98	11558.87		$173_{7/2} - 2888_{7/2}$	−.03	--
40	8675.65	11523.35		$173_{7/2} - 2885_{5/2}$	−.01	--
10	8683.74	11512.60		$298_{5/2} - 4131_{5/2}$	−.04	--

TABLE 2. *Classified lines of* Re I—Continued

Int.	λ_{vac}	σ_{vac}	Zeeman effect	Transition	O–C	Notes	Int.	λ_{vac}	σ_{vac}	Zeeman effect	Transition	O–C	Notes
	A	K						A	K				
1	8686.94	11508.36		$338_{7/2} - 4533_{5/2}$	−.01	..	6	9749.66	10253.95		$231_{5/2} - 3340_{5/2}$	+.03	..
20	8697.25	11494.72		$306_{9/2} - 4214_{9/2}$	−.01	..	4	9752.08	10251.41		$275_{9/2} - 3776_{7/2}$	+.07	..
(2)	8715.7	11470.4		$319_{7/2} - 4345_{9/2}$	+.1	31	20	9762.65	10240.30		$271_{7/2} - 3738_{9/2}$	+.02	..
(6)	8721.64	11462.59		$3259_{3/2} - 4405_{5/2}$	+.01	31	9	9831.35	10168.75		$224_{3/2} - 3259_{3/2}$	−.05	..
3h	8750.44	11424.86		$319_{7/2} - 4340_{7/2}$	−.02	..	20	9842.65	10157.07		$319_{7/2} - 4214_{9/2}$	.00	..
30	8797.70	11363.48		$298_{9/2} - 4116_{7/2}$	−.05	..	15sd	9872.38	10126.48		$298_{9/2} - 3992_{7/2}$	+.11	..
3	8845.23	11302.42		$285_{7/2} - 3984_{7/2}$	−.20	..	1	9901.72	10096.48		$314_{3/2} - 4155_{5/2}$	+.02	..
3	8851.32	11294.64		$3340_{5/2} - 4470_{5/2}$	.00	..	5	9903.30	10094.87		$244_{5/2} - 3452_{7/2}$	+.02	..
1	8871.82	11268.54		$341_{9/2} - 4546_{7/2}$	−.02	..	4	9908.97	10089.09		$4094_{7/2} - 5104_{5/2}$	+.06	..
15	8882.95	11254.43		$266_{9/2} - 3791_{5/2}$	−.01	..	1	9937.8	10059.9		$332_{5/2} - 4334_{5/2}$	−.3	..
15	8886.58	11249.83		$261_{5/2} - 3738_{9/2}$	−.01	..	20	9943.70	10053.85		$313_{9/2} - 4145_{9/2}$	−.03	..
5	8927.28	11198.54		$306_{9/2} - 4184_{7/2}$	+.02	..	200	9949.90	10047.59		$4094_{7/2} - 5099_{9/2}$	−.03	..
7	8966.63	11149.40		$3984_{7/2} - 5099_{9/2}$	.00	..	3	9953.02	10044.44		$298_{9/2} - 3984_{7/2}$	+.07	..
				$341_{9/2} - 4534_{9/2}$	+.10	..	60	9955.45	10041.99		$4094_{7/2} - 5098_{7/2}$	+.05	..
4	8969.21	11146.19		$298_{9/2} - 4094_{7/2}$	+.04	..	2	9964.90	10032.47		$4405_{5/2} - 5408_{7/2}$	+.01	..
2	8971.14	11143.79		$3984_{7/2} - 5098_{7/2}$	+.09	..	1	9970.87	10026.46		$4094_{7/2} - 5097_{5/2}$	−.18	..
1	8983.55	11128.39		$3984_{7/2} - 5097_{5/2}$	−.03	..	4	9976.45	10020.85		$224_{3/2} - 3244_{1/2}$	+.07	..
				$285_{7/2} - 3967_{5/2}$	.00	..	7	10019.21	9978.09		$311_{9/2} - 4116_{7/2}$	+.26	..
2	8988.40	11122.39		$338_{7/2} - 4494_{7/2}$	−.07	..	5	10026.96	9970.38		$278_{9/2} - 3779_{1/2}$	+.08	..
1	8995.26	11113.91		$285_{7/2} - 3965_{9/2}$	+.05	..	2	10064.02	9933.66		$305_{11/2} - 4049_{13/2}$	+.23	..
				$3992_{5/2} - 5103_{3/2}$	+.08	..	1	10127.21	9871.68		$4116_{7/2} - 5104_{5/2}$	+.03	..
1	9003.24	11104.06		$266_{9/2} - 3776_{5/2}$	−.16	..	15	10128.78	9870.15		$298_{9/2} - 3967_{5/2}$	+.01	..
1	9018.9	11084.75		$4818_{7/2} - 5926_{5/2}$	+.16	..	2	10138.24	9860.94		$319_{7/2} - 4184_{7/2}$	+.08	..
3	9032.46	11068.14		$311_{5/2} - 4225_{3/2}$	+.03	..	1	10146.84	9852.59		$314_{3/2} - 4131_{5/2}$	+.19	..
3	9058.53	11036.28		$266_{9/2} - 3769_{5/2}$	+.05	..	100	10169.85	9830.29		$4116_{7/2} - 5099_{9/2}$	+.05	..
4	9059.85	11034.67		$280_{5/2} - 3906_{5/2}$	+.07	..	20	10175.68	9824.66		$4116_{7/2} - 5098_{7/2}$	+.10	..
5	9070.74	11021.43		$298_{9/2} - 4082_{5/2}$	−.02	..	1	10191.57	9809.35		$4116_{7/2} - 5097_{5/2}$	+.09	..
4	9081.45	11008.43		$298_{9/2} - 4080_{3/2}$	−.04	..	2	10201.86	9799.44		$4856_{11/2} - 5836_{9/2}$	+.17	..
2	9083.03	11006.52		$275_{9/2} - 3852_{7/2}$	+.09	..	20	10206.32	9795.16		$301_{1/2} - 3992_{3/2}$	−.02	..
				$261_{5/2} - 3706_{3/2}$	+.02	..	4	10238.26	9764.60		$313_{9/2} - 4116_{7/2}$	−.01	..
6	9144.86	10932.10		$4673_{3/2} - 5766_{1/2}$	+.05	..	1	10242.68	9760.39		$311_{5/2} - 4094_{7/2}$	−.06	..
2	9205.12	10860.53		$288_{7/2} - 3967_{5/2}$	−.12	..	5	10282.46	9722.63		$4131_{5/2} - 5104_{5/2}$	+.09	..
1	9220.40	10842.54		$244_{3/2} - 3526_{3/2}$	.00	..	4	10287.58	9717.80		$4131_{5/2} - 5103_{3/2}$	+.09	..
10	9250.02	10807.81		$306_{9/2} - 4145_{9/2}$	−.04	..	10	10332.55	9675.50		$4131_{5/2} - 5098_{7/2}$	+.05	..
4	9262.28	10793.51		$314_{3/2} - 4225_{3/2}$	−.06	..	1	10341.3	9667.4		$280_{5/2} - 3769_{5/2}$	+.1	..
15	9268.46	10786.32		$304_{3/2} - 4131_{5/2}$	−.10	..	4	10349.0	9660.16		$4131_{5/2} - 5097_{5/2}$	+.01	..
1	9298.07	10751.97		$341_{9/2} - 4494_{7/2}$	+.12	..	10	10464.25	9553.73		$278_{1/2} - 3738_{5/2}$	−.03	..
1	9307.72	10740.82		$313_{9/2} - 4214_{9/2}$	+.06	..	20	10556.54	9470.21		$319_{7/2} - 4145_{9/2}$	+.02	..
3	9325.90	10719.88		$266_{9/2} - 3738_{9/2}$	−.10	..	2	10593.74	9436.95		$231_{5/2} - 3259_{3/2}$	+.13	..
20	9363.13	10677.25		$301_{1/2} - 4080_{3/2}$	−.03	..	8	10599.31	9432.00		$194_{5/2} - 2888_{7/2}$	+.17	..
2	9370.87	10668.44		$332_{5/2} - 4394_{5/2}$	+.11	..	40	10618.45	9414.99		$142_{7/2} - 2363_{9/2}$	+.03	..
10	9380.24	10657.78		$311_{5/2} - 4184_{7/2}$	+.01	..	8	10625.57	9408.68		$324_{5/2} - 4184_{7/2}$	−.03	..
2	9391.12	10645.43		$3340_{5/2} - 4405_{5/2}$	−.05	..	100	10639.45	9396.40		$194_{5/2} - 2885_{5/2}$	+.11	..
15	9423.45	10608.90		$324_{5/2} - 4304_{5/2}$	+.02	..	10	10824.22	9236.01		$278_{1/2} - 3706_{3/2}$	+.01	..
3	9427.53	10604.31		$272_{9/2} - 3776_{7/2}$	+.01	..	10	10862.25	9203.67		$197_{1/2} - 2896_{3/2}$	+.03	..
30	9470.15	10556.59		$271_{7/2} - 3769_{5/2}$	+.06	..	1	10909.5	9163.8		$244_{3/2} - 3358_{1/2}$	+.1	..
1	9481.6	10543.85		$247_{7/2} - 3526_{5/2}$	+.13	..	1	10919.30	9155.59		$285_{7/2} - 3769_{5/2}$	+.06	..
8	9500.49	10522.88		$285_{7/2} - 3906_{5/2}$	+.09	..	2	10933.44	9143.74		$304_{3/2} - 3967_{5/2}$	−.18	..
3	9504.34	10518.62		$306_{9/2} - 4116_{7/2}$	+.04	..	3	10942.23	9136.40		$261_{5/2} - 3526_{3/2}$	+.03	..
6	9571.75	10444.54		$313_{9/2} - 4184_{7/2}$	−.01	..	2	11065.02	9035.02		$4470_{5/2} - 5373_{7/2}$	−.07	..
8	9581.12	10434.32		$231_{5/2} - 3358_{3/2}$	+.01	..					$5035_{7/2} - 5939_{9/2}$	−.04	..
1	9600.98	10412.75		$273''_{1/2} - 3779_{1/2}$	.00	..	1	11141.90	8972.67		$332_{5/2} - 4225_{3/2}$	+.13	..
3	9704.94	10301.20		$306_{9/2} - 4094_{7/2}$	.00	..	4	11309.97	8839.33		$285_{7/2} - 3738_{5/2}$	+.05	..
50	9710.52	10295.28		$304_{3/2} - 4082_{5/2}$	+.05	..	8	11383.70	8782.08		$271_{7/2} - 3592_{9/2}$	+.19	..
4	9722.76	10282.32		$304_{3/2} - 4080_{3/2}$	+.07	..	3	11453.12	8728.85		$324_{5/2} - 4116_{7/2}$	+.08	..
3	9748.60	10255.07		$288_{7/2} - 3906_{5/2}$	+.02	..	1	11615.8	8606.6		$266_{5/2} - 3526_{5/2}$	+.1	..

NOTES

1. Wavelength and intensity taken from R. Velasco, Anales real soc. espan. fis. y quim. Madrid **48**, 55 (1952).
2. From here (unless stated otherwise), all wavelengths and intensities have been taken from W. F. Meggers, J. Research NBS **49**, 187 (1952) RP2355; the intensities apply to the arc observations, and all details concerning line complexity due to hyperfine structure have been omitted.
3. Wavelength and intensity taken from MIT Wavelength Tables.
4. Observed only in spark by Meggers, but according to the MIT Wavelength Tables, the line belongs to the arc spectrum. The intensity given applies to the spark.
5. Enhanced in spark.
6. The indicated self-reversal is an apparent one. The analysis shows that actually a close doublet is formed by two different transitions.
7. Intensity from spark spectrum; not observed in the arc.
8. The wavelength given in the MIT Wavelength Tables fits appreciably better to the combination given (departure 0.3 K); the observed σ-component is in harmony with classification, the observed π-component is only badly accounted for.
9. Observed Zeeman effect in agreement only with second transition.
10. Observed π-pattern in disagreement with classification.
11. Observed σ-pattern in disagreement with classification.
12. σ-pattern perturbed.
13. Wavelength and intensity taken from spark observations made at the Zeeman Laboratory.
14. Probably there is a second line at this place.
15. The π-pattern and the strongest σ-component observed are in disagreement with classification.
16. Observed Zeeman effect in agreement with *both* transitions.
17. Paschen-Back interaction between levels *4080* and *4081*.
18. Paschen-Back interaction between levels *5034* and *5035*.
19. Observed Zeeman effect not consistent with classification.
20. Zeeman effect suggests that levels 273′ and 273″ are hyperfine components of the same level.
21. Paschen-Back interaction between levels *5103* and *5104*.
22. Observed Zeeman effect in agreement only with first transition.
23. Wavelength and intensity taken from W. F. Meggers, BS J. Research **6**, 1027 (1931) RP322.
24. In the MIT Wavelength Tables only one line is recorded with a wavelength intermediate between the two wavelengths given in Meggers' 1952 paper. The doubling is probably caused by hyperfine structure.
25. π-pattern in agreement with first combination. For the second combination no g-values are known.
26. Paschen-Back effect.
27. Apparent doubling caused by hyperfine structure; comp. note 24.
28. In the MIT Wavelength Tables, only one line is recorded here. The doubling is a common feature of the combinations of $4470_{5/2}$ ($= (5d^5\,6s\,7s)\ {}^6S_{5/2}$); see text.
29. Wavelength taken from Meggers' 1931 paper. The MIT Wavelength Tables also give a single line, whereas in Meggers' 1952 table two lines (with intensities 150 and 100) have been recorded which are situated at approximately equal distances from the calculated position. The doubling may be due to hyperfine structure.
30. Wavelength and intensity taken from the MIT Wavelength Tables. Meggers' 1931 table gives a single line also, whereas in his 1952 table a doublet is recorded, just as for 6605 A (see note 29).
31. Wavelength and intensity taken from W. F. Meggers, BS J. Research **10**, 757 (1933) RP564.

TABLE 3. *Unclassified* Re I *lines of intensity 50 or more*

Intensity	Wavelength	Intensity	Wavelength
	A		*A*
50r	2077. 280	100R	2344. 776
100R	2109. 22	50r	2365. 316
50	2187. 77	100r	2388. 569
50	2196. 72	50	2397. 31
50	2205. 15	100r	2404. 340
300r	2214. 58	60r	2406. 695
50	2226. 87	50r	2431. 538
50	2242. 66	100	2444. 09
50	2249. 51	50R	2611. 536
50	2253. 94	60	2722. 206
50	2271. 04	50	2982. 188
50	2285. 30	50	4251. 35
50	2290. 715	100	6751. 22

TABLE 4. *Electron configurations and spectral terms of* Re I

Config.	Desig.	*J*	Level	Interval	Obs. *g*	Config.	Desig.	*J*	Level	Interval	Obs. *g*
$5d^5\,6s^2$	$a\ ^6S$	$2\frac{1}{2}$	0. 00		1. 950	$5d^4\,6s^2(a\ ^5D)6p$	$z\ ^6D°$	$0\frac{1}{2}$	*32443. 61*	148. 02	
$5d^5\,6s^2$	$a\ ^4P$	$2\frac{1}{2}$	11583. 96	−2242. 16	1. 278			$1\frac{1}{2}$	*32591. 63*	817. 10	1. 762
		$1\frac{1}{2}$	13826. 12	−1339. 77	1. 485			$2\frac{1}{2}$	*33408. 73*	1111. 52	1. 500
		$0\frac{1}{2}$	15165. 89		2. 368			$3\frac{1}{2}$	*34520. 25*	1402. 77	1. 454
$5d^5(^5D)6s$	$a\ ^6D$	$4\frac{1}{2}$	11754. 52	−2462. 34	1. 545			$4\frac{1}{2}$	*35923. 02*		1. 440
		$3\frac{1}{2}$	14216. 86	−1553. 56	1. 567	$5d^5(^2G)6s$	$b\ ^3G°$	$2\frac{1}{2}$	33281. 65	542. 01	
		$2\frac{1}{2}$	15770. 42	−557. 09	1. 309			$3\frac{1}{2}$	33823. 66	370. 61	
		$1\frac{1}{2}$	16327. 51	−910. 79	1. 706			$4\frac{1}{2}$	34194. 27	−876. 70	
		$0\frac{1}{2}$	17238. 30		2. 521			$5\frac{1}{2}$	33317. 57		
$5d^5\,6s^2$	$a\ ^4G$	$2\frac{1}{2}$	14621. 46	436. 73	1. 151	$5d^4\,6s^2(^3D)6p$	$y\ ^6P°$	$1\frac{1}{2}$	*33589. 12*		2. 335
		$3\frac{1}{2}$	15058. 19	1561. 09	1. 153			$2\frac{1}{2}$			
		$4\frac{1}{2}$	16619. 28	−312. 13	1. 175			$3\frac{1}{2}$			
		$5\frac{1}{2}$	16307. 15		1. 242	$5d^5\,6s(a\ ^3S)6p$	$z\ ^4P°$	$2\frac{1}{2}$	*35267. 94*	−2647. 93	1. 385
$5d^5\,6s^2$	$a\ ^4D$	$3\frac{1}{2}$	17330. 82	−2127. 07	1. 255			$1\frac{1}{2}$	*37915. 87*	117. 92	1. 495
		$2\frac{1}{2}$	19457. 89	−1023. 84	1. 361			$0\frac{1}{2}$	*37797. 95*		2. 620
		$1\frac{1}{2}$	20481. 73	723. 82	1. 451	$5d^5\,6s(a\ ^3G)6p$	$z\ ^6G°$	$1\frac{1}{2}$	*37063. 65*	317. 76	0. 626
		$0\frac{1}{2}$	19757. 91		0. 983			$2\frac{1}{2}$	*37381. 41*	1139. 33	. 990
$5d^5\,6s(a\ ^7S)6p$	$z\ ^6P°$	$2\frac{1}{2}$	*18950. 1*	1497. 7	2. 274			$3\frac{1}{2}$	*38520. 74*	473. 99	1. 216
		$3\frac{1}{2}$	*20447. 8*	3184. 0	1. 926			$4\frac{1}{2}$	*38994. 73*	921. 66	1. 25
		$4\frac{1}{2}$	*23631. 82*		1. 768			$5\frac{1}{2}$	*39916. 39*	576. 95	1. 314
$5d^5\,6s^2$	$a\ ^2F$	$3\frac{1}{2}$	21775. 40	−2650. 00	1. 135			$6\frac{1}{2}$	*40493. 34*		1. 364
		$2\frac{1}{2}$	24425. 40		1. 067	$5d^4\,6s^2(a\ ^5D)6p$	$z\ ^6F°$	$0\frac{1}{2}$	*37381. 41*	2545. 34	
$5d^5\,6s^2$	$a\ ^2G$	$4\frac{1}{2}$	22160. 04	−2564. 18	1. 198			$1\frac{1}{2}$	*39926. 75*	−861. 83	0. 745
		$3\frac{1}{2}$	24724. 22		1. 03			$2\frac{1}{2}$	*39064. 92*	−1299. 27	1. 335
$5d^5\,6s^2$	$a\ ^2D$	$1\frac{1}{2}$	22422. 83	731. 98	0. 781			$3\frac{1}{2}$	*37765. 65*	1890. 34	4. 335
		$2\frac{1}{2}$	23154. 81		1. 189			$4\frac{1}{2}$	*39655. 99*	−459. 25	1. 444
$5d^5\,6s^2$	$a\ ^2I$	$5\frac{1}{2}$	23956. 00	2392. 96	0. 995			$5\frac{1}{2}$	*39196. 74*		1. 405
		$6\frac{1}{2}$	26348. 96		1. 100			$2\frac{1}{2}$	*37697. 66*		1. 219
$5d^5\,6s^2$	$a\ ^4F$	$1\frac{1}{2}$	26131. 57	1898. 75	0. 650			$2\frac{1}{2}$	*39670. 52*		1. 107
		$2\frac{1}{2}$	28030. 32	511. 81	1. 12	$5d^5\,6s(a\ ^3S)6p$	$x\ ^6P°$	$3\frac{1}{2}$	*39844. 75*	−3724. 61	1. 223
		$3\frac{1}{2}$	28542. 13	−1027. 82				$2\frac{1}{2}$	*43569. 36*	−132. 84	1. 504
		$4\frac{1}{2}$	27514. 31		1. 13			$1\frac{1}{2}$	*43702. 20*		1. 462
$5d^6(^3P)6s$	$b\ ^4P$	$2\frac{1}{2}$	26661. 43	−3865. 17	1. 32			$1\frac{1}{2}$	*40808. 85*		1. 351
		$1\frac{1}{2}$	30526. 60					$0\frac{1}{2}$	*40810. 17*		
		$0\frac{1}{2}$						$2\frac{1}{2}$	*40821. 83*		1. 126
$5d^6(^3H)6s$	$a\ ^4H$	$6\frac{1}{2}$	27130. 14	113. 74	1. 208	$5d^5\,6s(a\ ^3P)6p$	$y\ ^6D°$	$4\frac{1}{2}$			
		$5\frac{1}{2}$	27243. 88	82. 53	1. 18			$3\frac{1}{2}$	*40846. 53*	−366. 49	1. 534
		$4\frac{1}{2}$	27161. 35	1648. 52				$2\frac{1}{2}$	*41318. 02*	−244. 06	1. 278
		$3\frac{1}{2}$	28809. 87		0. 93			$1\frac{1}{2}$	*41557. 08*		1. 655
$5d^6(^3D)6s$	$b\ ^4D$	$3\frac{1}{2}$	27141. 13	−2659. 25	1. 34			$0\frac{1}{2}$			
		$2\frac{1}{2}$	29800. 38	1972. 73	1. 17			$3\frac{1}{2}$	*41163. 91*		1. 325
		$1\frac{1}{2}$	27827. 65	442. 85	0. 888			$4\frac{1}{2}$	*41453. 18*		1. 372
		$0\frac{1}{2}$	27384. 80		. 072			$3\frac{1}{2}$	*41843. 85*		1. 190
$5d^5\,6s(a\ ^7S)6p$	$z\ ^6P°$	$3\frac{1}{2}$	*28889. 72*	35. 54	1. 709	$5d^5\,6s(a\ ^3P)6p$	$z\ ^4D°$	$0\frac{1}{2}$	*41991. 56*	202. 63	0. 61
		$2\frac{1}{2}$	*28854. 18*	−107. 37	1. 871			$1\frac{1}{2}$	*42254. 19*	789. 83	1. 578
		$1\frac{1}{2}$	*28961. 55*		2. 333			$2\frac{1}{2}$	*43044. 02*	363. 85	1. 449
$5d^5\,6s^2$	$a\ ^2S$	$0\frac{1}{2}$	30131. 57					$3\frac{1}{2}$	*43407. 87*		1. 368
$5d^5\,6s^2$	$a\ ^2H$	$5\frac{1}{2}$	30559. 91	−839. 30	1. 07			$4\frac{1}{2}$	*42140. 06*		1. 249
		$4\frac{1}{2}$	31399. 30			$5d^5\,6s(a\ ^7S)7s$	$e\ ^8S$	$3\frac{1}{2}$	42598. 27		1. 957
$5d^6(^3F)6s$	$b\ ^4F$	$1\frac{1}{2}$	31460. 62	−274. 54	1. 17			$1\frac{1}{2}$	*43341. 85*		0. 975
		$2\frac{1}{2}$	31186. 08					$1\frac{1}{2}$	*43409. 11*		
		$3\frac{1}{2}$						$4\frac{1}{2}$	*43453. 90*		1. 336
		$4\frac{1}{2}$	30645. 33					$3\frac{1}{2}$	*43815. 01*		1. 348
$5d^5\,6s^2$	$b\ ^2F$	$3\frac{1}{2}$	31982. 99	−452. 15				$2\frac{1}{2}$	*43949. 98*		1. 385
		$2\frac{1}{2}$	32435. 14					$5\frac{1}{2}$	*43996. 30*		1. 26
								$2\frac{1}{2}$	44054. 21		
								$1\frac{1}{2}$	*44148. 45*		1. 573

TABLE 4. *Electron configurations and spectral terms of* Re I—Continued

Config.	Desig.	J	Level	Interval	Obs. g
		$4\frac{1}{2}$	*44324.58*		1.244
		$2\frac{1}{2}$	*44708.73*		1.223
	^6D	$0\frac{1}{2}$	*44416.33*		0.15
$5d^5\,6s(a\,^7S)7s$	$e\,^6S$	$2\frac{1}{2}$	44703.37		1.866
		$1\frac{1}{2}$	*44780.09*		1.330
		$3\frac{1}{2}$	*44901.15*		1.253
		$2\frac{1}{2}$	44902.60		
		$3\frac{1}{2}$	*44946.12*		0.905
$5d^5(^5D)6p$	$y\,^6F^\circ$	$5\frac{1}{2}$	*43082.63*		1.40
		$4\frac{1}{2}$	*43674.25*	−1291.62	1.341
		$3\frac{1}{2}$	*47932.55*	−1558.30	1.31
		$2\frac{1}{2}$	*49022.77*	−1090.22	1.495
		$1\frac{1}{2}$	*49667.95*	−644.48	1.27
		$0\frac{1}{2}$	*49859.53*	−192.28	0.410
		$1\frac{1}{2}$	*45121.81*		.674
		$2\frac{1}{2}$	*45332.03*		1.088
		$4\frac{1}{2}$	*45343.57*		1.131
		$3\frac{1}{2}$	*45462.83*		1.309
	$^4P^\circ$	$0\frac{1}{2}$	*45817.26*		2.197
		$1\frac{1}{2}$	*45876.34*		1.384
		$5\frac{1}{2}$	*45904.25*		1.175
		$3\frac{1}{2}$	*45937.18*		1.298
		$2\frac{1}{2}$	*46112.24*		1.405
		$0\frac{1}{2}$	*46141.11*		0.716
		$3\frac{1}{2}$	*46352.99*		1.271
		$2\frac{1}{2}$	*46509.40*		1.371
		$2\frac{1}{2}$	*46649.42*		1.334
		$1\frac{1}{2}$	*46733.38*		1.858
		$1\frac{1}{2}$	*47004.34*		1.285
		$2\frac{1}{2}$	*47101.61*		0.893
		$1\frac{1}{2}$	*47172.1*		
		$0\frac{1}{2}$	*47172.9*		2.215
		$4\frac{1}{2}$	*47205.73*		1.106
		$3\frac{1}{2}$	*47358.36*		1.151
		$6\frac{1}{2}$	*47506.79*		1.26
		$0\frac{1}{2}$	*47664.74*		1.50
		$3\frac{1}{2}$	*47669.01*		1.196
		$1\frac{1}{2}$	*47703.78*		1.443
		$1\frac{1}{2}$	*47779.91*		1.362
		$5\frac{1}{2}$	*47859.93*		1.20
		$2\frac{1}{2}$	*47899.22*		1.217
		$2\frac{1}{2}$	*47970.82*		1.169
		$3\frac{1}{2}$	*48184.20*		1.252
		$5\frac{1}{2}$	*48569.63*		1.27
		$3\frac{1}{2}$	*48786.35*		1.53
		$3\frac{1}{2}$	*48857.60*		1.24
		$3\frac{1}{2}$	*49027.85*		1.499
		$4\frac{1}{2}$	*49170.76*		1.135
		$1\frac{1}{2}$	*49250.02*		1.263
		$5\frac{1}{2}$	*49286.07*		1.075
		$2\frac{1}{2}$	*49549.96*		
		$2\frac{1}{2}$	*49573.11*		1.344
		$4\frac{1}{2}$	*49582.61*		1.058
		$3\frac{1}{2}$	*49863.22*		1.175
		$1\frac{1}{2}$	*49895.57*		1.989
		$2\frac{1}{2}$	*50110.28*		1.765
		$2\frac{1}{2}$	*50158.87*		1.422
		$4\frac{1}{2}$	*50196.94*		1.345
		$1\frac{1}{2}$	*50263.22*		1.234
		$3\frac{1}{2}$	*50310.70*		1.170
$5d^5\,6s(a\,^7S6)d$	$e\,^8D$	$1\frac{1}{2}$	*50332.60*		
		$2\frac{1}{2}$	*50340.62*	8.02	2.027
		$3\frac{1}{2}$	*50359.23*	18.61	1.820
		$4\frac{1}{2}$	*50395.72*	36.49	1.690
		$5\frac{1}{2}$	*50464.34*	68.62	1.629
		$4\frac{1}{2}$	*50401.01*		1.055
		$2\frac{1}{2}$	*50463.80*		1.144
		$1\frac{1}{2}$	*50571.02*		0.935
		$5\frac{1}{2}$	*50663.51*		1.220
		$3\frac{1}{2}$	*50869.00*		1.240
		$2\frac{1}{2}$	*50934.18*		1.385
		$2\frac{1}{2}$	*50973.17*		1.489
$5d^5\,6s(a\,^7S)6d$	$e\,^6D$	$4\frac{1}{2}$	*50994.15*		
		$3\frac{1}{2}$	*50988.47*	5.68	1.548
		$2\frac{1}{2}$	*51035.56*	−147.09	1.558
		$1\frac{1}{2}$	*51030.73*	4.83	1.546
		$0\frac{1}{2}$	*51049.87*	−19.14	
		$4\frac{1}{2}$	*51027.96*		
		$1\frac{1}{2}$	*51183.00*		1.456
		$4\frac{1}{2}$	*51193.49*		
		$3\frac{1}{2}$	*51229.64*		1.231
		$2\frac{1}{2}$	*51477.15*		0.97
		$4\frac{1}{2}$	*51486.29*		1.20
		$1\frac{1}{2}$	*51578.05*		0.92
		$2\frac{1}{2}$	*51590.08*		1.02
		$3\frac{1}{2}$	*51647.82*		1.139
		$1\frac{1}{2}$	*51874.43*		1.29
		$5\frac{1}{2}$	*51945.94*		

Config.	Desig.	J	Level	Interval	Obs. g
		$3\frac{1}{2}$	*51955.02*		1.200
		$4\frac{1}{2}$	*52001.37*		1.357
		$6\frac{1}{2}$	*52122.35*		1.17
		$2\frac{1}{2}$	*52218.11*		1.208
		$6\frac{1}{2}$	*52227.20*		
		$1\frac{1}{2}$	*52278.28*		1.422
		$3\frac{1}{2}$	*52373.12*		
		$0\frac{1}{2}$	*52469.45*		1.315
		$2\frac{1}{2}$	*52472.31*		
		$3\frac{1}{2}$	*52610.01*		
		$4\frac{1}{2}$	*52741.30*		
		$3\frac{1}{2}$	*52857.44*		1.30
		$2\frac{1}{2}$	*52881.34*		1.05
		$1\frac{1}{2}$	*52951.59*		1.14
		$1\frac{1}{2}$	*52954.46*		
		$2\frac{1}{2}$	*53058.74*		1.184
		$0\frac{1}{2}$	*53125.19*		1.145
		$0\frac{1}{2}$	*53288.28*		1.372
		$1\frac{1}{2}$	*53293.72*		1.323
		$4\frac{1}{2}$	*53320.95*		1.38
		$3\frac{1}{2}$	*53335.94*		1.290
		$4\frac{1}{2}$	*53379.35*		1.09
		$2\frac{1}{2}$	*53389.73*		1.19
$5d^5\,6s(a\,^7S)8s$	^8S	$3\frac{1}{2}$	53392.00		
		$5\frac{1}{2}$	*53467.57*		1.20
		$3\frac{1}{2}$	*53738.46*		1.203
		$1\frac{1}{2}$	*53842.53*		1.169
		$0\frac{1}{2}$	*53928.90*		1.113
		$5\frac{1}{2}$	*53948.73*		1.13
		$3\frac{1}{2}$	*54018.19*		0.723
		$3\frac{1}{2}$	*54086.69*		1.22
		$3\frac{1}{2}$	*54177.25*		1.270
		$2\frac{1}{2}$	*54208.18*		1.290
		$2\frac{1}{2}$	*54409.61*		1.069
		$1\frac{1}{2}$	*54467.40*		1.361
		$3\frac{1}{2}$	*54513.84*		
		$5\frac{1}{2}$	*54554.61*		
		$6\frac{1}{2}$	*54729.52*		
		$4\frac{1}{2}$	*54813.12*		1.185
		$2\frac{1}{2}$	*54823.02*		1.183
		$0\frac{1}{2}$	*54968.85*		1.314
		$5\frac{1}{2}$	*55223.85*		1.149
		$3\frac{1}{2}$	*55454.48*		1.17
		$6\frac{1}{2}$	*55776.51*		1.056
		$3\frac{1}{2}$	*55901.20*		1.22
		$1\frac{1}{2}$	*55902.01*		0.447
		$4\frac{1}{2}$	*55912.42*		1.06
		$4\frac{1}{2}$	*56307.97*		
		$4\frac{1}{2}$	*56411.22*		
		$6\frac{1}{2}$	*56523.41*		
		$0\frac{1}{2}$	*56451.87*		1.287
		$3\frac{1}{2}$	*56699.41*		1.25
		$2\frac{1}{2}$	*56822.75*		
		$1\frac{1}{2}$	*56866.66*		0.479
		$0\frac{1}{2}$	*57073.31*		.94
		$3\frac{1}{2}$	*57090.29*		
		$3\frac{1}{2}$	*57172.70*		1.19
		$4\frac{1}{2}$	*57280.86*		1.19
		$3\frac{1}{2}$	*57371.75*		
		$5\frac{1}{2}$	*57391.44*		1.30
		$6\frac{1}{2}$	*57452.83*		
		$2\frac{1}{2}$	*57524.31*		1.40
		$4\frac{1}{2}$	*57656.85*		1.19
$5d^4\,6s^2(a\,^5D)7s$	^6D	$0\frac{1}{2}$			
		$1\frac{1}{2}$	*57665.43*	1603.27	
		$2\frac{1}{2}$	*59268.70*	−1208.06	
		$3\frac{1}{2}$	*58060.64*	308.26	
		$4\frac{1}{2}$	*58368.90*		
		$1\frac{1}{2}$	*58050.58*		1.111
		$3\frac{1}{2}$	*58260.63*		1.43
		$4\frac{1}{2}$	*58279.31*		
		$2\frac{1}{2}$	*58332.42*		
		$1\frac{1}{2}$	*58442.51*		1.32
		$0\frac{1}{2}$	*58541.88*		
		$5\frac{1}{2}$	*58619.32*		1.165
		$1\frac{1}{2}$	*59127.30*		1.20
		$2\frac{1}{2}$	*59171.73*		
		$1\frac{1}{2}$	*59293.45*		
		$4\frac{1}{2}$	*59394.29*		
		$5\frac{1}{2}$	*59412.46*		1.15
		$3\frac{1}{2}$	*59784.67*		
		$3\frac{1}{2}$	*59926.91*		1.100
		$2\frac{1}{2}$	*60737.28*		
		$2\frac{1}{2}$	*60837.10*		1.22
		$5\frac{1}{2}$	*62142.97*		
		$3\frac{1}{2}$	*62350.13*		
		$3\frac{1}{2}$	*62493.51*		1.17
		$5\frac{1}{2}$	*63267.63*		1.135
$(^7S_3)$	***Limit***	.....	.....	**63530.**	
		$6\frac{1}{2}$	*63772.40*		
		$6\frac{1}{2}$	*63934.76*		1.07

WASHINGTON, January 23, 1957.

Journal of Research of the National Bureau of Standards Vol. 59, No. 5, November 1957 Research Paper 2805

An Apparatus for Measurement of Thermal Conductivity of Solids at Low Temperatures

Robert L. Powell, William M. Rogers, and Don O. Coffin

A description is given of an apparatus used for determining the thermal conductivities of solids in the temperature range 4° K to 300° K. The apparatus is especially suited to the determination of thermal conductivity over a large temperature interval, enabling coverage of the temperatures between the normal boiling points of liquefied gases. Illustrative results are given for an insulator, polytetrafluoroethylene, and for a high-conductivity commercial coalesced copper. The thermal conductivity of the insulator increases monotonically from 0.56 milliwatt per centimeter per degree K at 5° K, to 2.32 at 80° K. The thermal conductivity of the copper has a maximum of 24.9 watts per centimeter per degree K at 21° K, and a value of 8.15 at 5° K. The methods of data analysis and estimation of errors are given.

1. Introduction

Data on thermal conductivity are necessary for the selection of suitable construction materials, and the prediction of operating characteristics of low-temperature apparatus used in research and industry. In addition, accurate thermal conductivity values for pure metals and controlled alloys are important in the development and verification of theories of electronic transport phenomena in metals. The apparatus described in this paper is well suited to the measurement of thermal conductivity of metals and commercial alloys; it is also usable for poor conductors such as plastics and other dielectric solids.

2. Experimental Apparatus

2.1. General Description

The method of determining thermal conductivity by axial heat flow through a long cylindrical sample is used. A pictorial diagram of the apparatus is shown in figure 1. The apparatus is similar, in many respects, to some of those described in the review by Olsen and Rosenberg [5].

The cryostat consists of concentrically mounted sample, thermal shield, vacuum container, glass Dewar, Dewar support, and outside metal Dewar.

The sample rod is clamped to the heat sink at the top; the sample heater is attached to the bottom of this rod. The temperature distribution along the sample is measured by means of eight thermocouples attached to thermocouple holders positioned along the rod. Heat losses by gas convection and conduction are made negligible by evacuating the region surrounding the sample. Losses by radiation and conduction along the lead wires are reduced by enclosing the sample rod within a symmetric cylindrical thermal shield maintained at approximately the same temperature and axial gradient as the sample. Measurements of the temperature, thermal gradient,

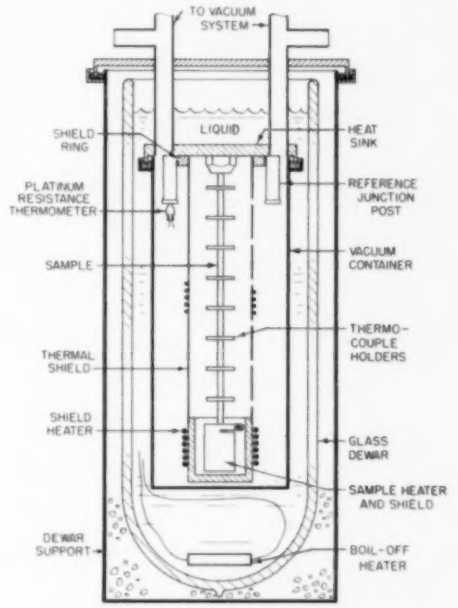

FIGURE 1. *Thermal conductivity apparatus.*

and power input to the sample, combined with data on the cross-sectional area, permit a calculation of the thermal conductivity of the sample based upon Fourier's equation for steady state, linear heat flow.

The heat sink is maintained at a constant low temperature by a refrigerant, usually a liquefied gas. This refrigerant, poured into the glass Dewar from a central fill tube, surrounds the heat sink and vacuum can. The glass Dewar is supported by a metal container that is, in turn, sealed to a top plate. For temperatures below 80° K in the internal apparatus, the Dewar support container is further surrounded by a metal Dewar containing liquid nitrogen, reducing heat conduction down into the colder refrigerant. The associated vacuum, electrical control, and measuring equipment are located on nearby racks and benches.

[1] Now at the Los Alamos Scientific Laboratory, Los Alamos, New Mexico.

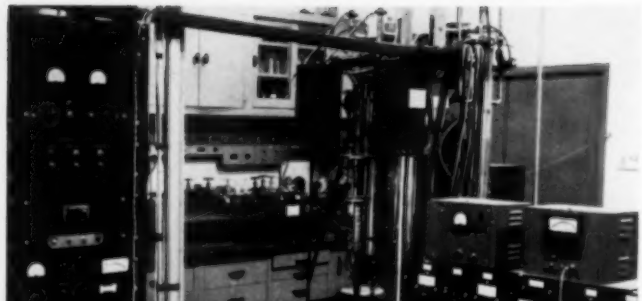

FIGURE 2. *Cryostat and associated equipment.*

Figure 2 is a photograph of this assembly. Two similar cryostats are used concurrently to increase the data output.

2.2. Sample Assembly

Metal and alloy sample rods are 0.367 cm in diameter and 23.2 cm long; plastic samples are 2.54 cm in diameter and 20.5 cm long. The metal and alloy rods are turned, then ground to the final diameter with a tolerance of 0.0005 cm. Because of their larger size, the plastics are turned with a tolerance of only 0.001 cm. When required, the sample is annealed after the last grinding operation. Then the thermocouple holders shown in figure 3 are attached, and the holders are placed on the sample with their centers 2.54 cm apart by means of gage blocks. The thermocouple holders have a thin interior edge that gives, essentially, line contact between the holder and the sample. The actual distances between flat surfaces on the holders are measured by a vernier height gage with an attached precision dial test-indicator. The accuracy is about 0.0005 cm. The average diameters of the sample are measured between the thermocouple holders to about the same accuracy.

The samples are attached to the heat sink by a clamping action for metals, or an internal tapered screw thread for plastics as is shown in figures 1 and 3. The details of the sample heaters are also included in figure 3. The heater for a metal sample is slipped onto the rod and clamped with a small screw. In order to improve the thermal contact, mercury is placed in the hole that surrounds the lower end of the metal sample. The heater for plastic samples is screwed on so that it presses against a large copper washer used to increase the heater-to-sample contact area. Both heater blocks made of copper are wrapped with No. 36 or 40 AWG constantan heater wire in a single layer held in place with G. E. 7031

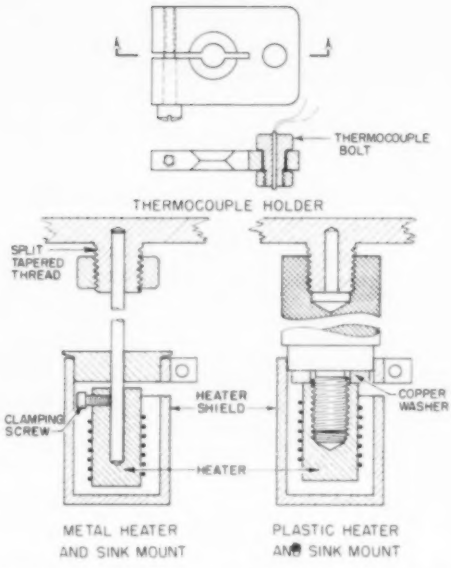

FIGURE 3. *Heaters and thermocouple holders.*

air-drying varnish. The sample heaters have a resistance ranging from 175 to 500 ohms for metals, and from 500 to 1,000 ohms for plastics. The power measuring circuits limit the current to a maximum of about 100 ma, and the voltage to a maximum of about 16 v. A small sample heater shield is attached to the sample by a split collet-and-screw clamp, so reducing radiation losses. These shields are covered on all exposed surfaces with aluminum foil to further reduce radiation.

2.3. Thermal Shielding, Tempering, and Controls

Several factors, such as gas conduction, radiation, and wire conduction, can lead to consistent errors in the experimental determinations of thermal conductivity. Heat losses by gas conduction or convection are reduced to an insignificant amount by baking out and evacuating the system to at least 10^{-5} mm of Hg while the system is at room temperature. Cooling of the system during experimental runs further reduces the residual gas pressure.

Heat losses by radiation and lead wire conduction are greatly reduced by surrounding the sample with a cylindrical thermal shield as shown in figure 1. The bottom, middle, and top of the shield are held at approximately the same temperature as the sample at the corresponding elevation. To provide a good thermal contact to the heat sink when the shield is bolted in place, the upper shield fastening ring is made of copper. The bottom of the shield is also made of copper to provide a nearly isothermal region surrounding the sample heater. The longer intermediate section of the shield is made of thin stainless steel to reduce the power input necessary to maintain any given temperature gradient. The shield is split in two, vertically, to allow rotation of the front half during the mounting and assembling of the sample.

The two halves are bolted together near the bottom, and a copper bar is soldered across the bottom to improve thermal contact. A mounted sample and the split shield are shown in figure 4.

Three heaters are wrapped on the shield to supply power necessary to maintain the proper thermal gradient. The main shield heater, wrapped back and forth across the bottom copper section, is made of 32 AWG constantan wire and has about 100 ohms resistance. The other two heaters at the midpoint and near the top, made of 45 AWG constantan, have about 300 ohms resistance. All three are kept in place with air-drying varnish. All wires connected to the sample pass through the shield and are cemented to it at areas close to the same temperature as that of their point of contact on the sample. These wires are 10 to 20 cm in length between the sample and shield.

The temperature difference between the sample heater and a horizontally opposed point on the lower copper section of the shield is measured with a gold-cobalt versus copper thermocouple. Potential differences of about 0.1 μv can be detected, corresponding to from 0.02° K at liquid helium temperatures, to 0.002° K at room temperature. Similar differential thermocouples are at midpoint and near the top.

The thermal electromotive forces developed across the middle and top differential thermocouples are measured with a d-c amplifier-galvanometer. To bring about thermal balance between the shield and sample, as indicated by null readings on the two upper differential thermocouples, the a-c voltages supplied to the heaters at the middle and top of the shield are adjusted manually. If the shield is hotter than the sample at either one of the two upper points, there is no way to obtain thermal balance. The lower, or main, differential thermocouple is the sensing device for a heater servomechanism. The approximately correct voltage for the bottom shield heater is adjusted manually by varying two autotransformers in series.

Heater and thermocouple wires are wrapped back and forth upwards on the shield for thermal tempering and then are wound on the posts attached to the heat sink. Two of the six cylindrical copper posts are shown in figure 1. The winding on the posts allows most of the heat conducted down the wires from above to be shorted to the liquid bath. One of the posts serves as a reference junction block for the eight measuring thermocouples; another is used to hold a platinum resistance thermometer that indicates the reference temperature. The others are used for thermal tempering only.

The heat sink and posts are machined from free-cutting leaded copper, assuring both good conductivity and machinability [6]. The vacuum chamber cylinder is soldered onto a lip of the heat sink with Rose's Alloy. Two thin stainless steel tubes serve as mechanical support for the internal apparatus, as exit tubes for the wires, and as pumping lines for evacuation of the inside chamber.

For measurements at liquid nitrogen, hydrogen, or helium temperatures, the entire apparatus is surrounded by liquid nitrogen in a large metal Dewar. To further reduce heat transfer to the internal apparatus, all the wires are again tied down thermally to a copper post inserted into the pumping line just above the top plate. The wires are brought out from the vacuum space through a hard wax seal. Near the top of the apparatus is a thermally insulated junction box where the various small wires from the cryostat are soldered to larger copper wires, usually 22 AWG, which lead to the control panel and measuring instruments.

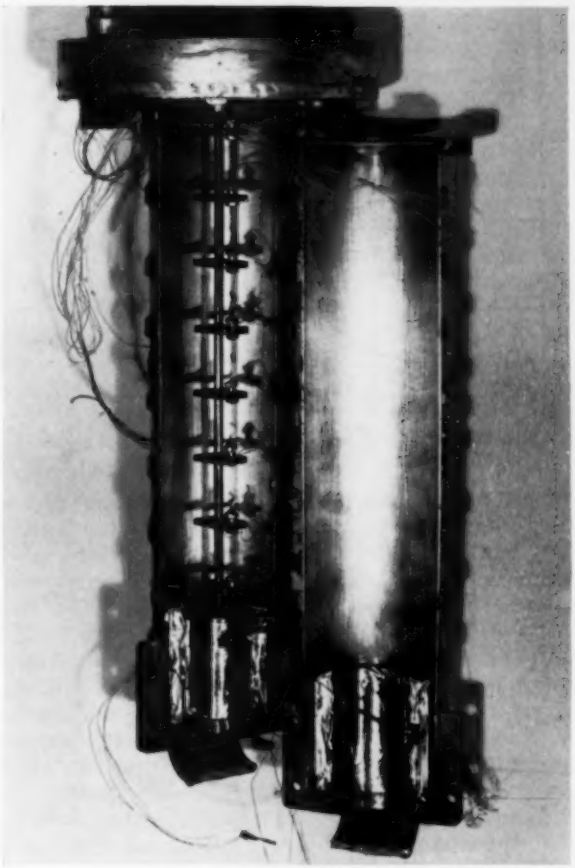

FIGURE 4. *Mounted sample.*

2.4. Measuring Apparatus

The reference junction temperature for the thermocouples is assumed to be the same as that of the thermometer post. The measuring thermometer is a strain-free capsule platinum resistor with an ice point resistance of about 25 ohms, which is embedded in one of the posts attached to the heat sink. The resistance of this thermometer, calibrated down to 12° K by the Temperature Measurements Section of the Bureau, is measured on a five-dial Mueller bridge. When actual readings are not being taken, this thermometer is switched to a resistance recorder. This switching allows a drift of the heat sink tem-

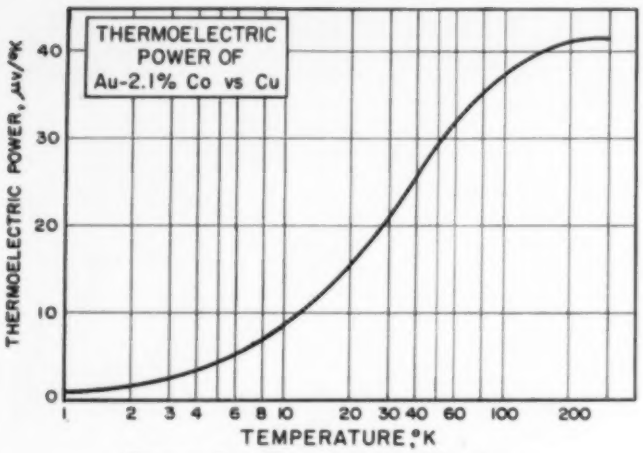

FIGURE 5. *Thermocouple calibration.*

perature to be observed without continual manual measurements. With liquid helium, the temperature of the heat sink is obtained from a reading of the barometric pressure by using the 1955 d compromise temperature scale [2].

Wire of 5-mil diameter, composed of gold with 2.1 atomic percent of cobalt, is used for the common element of the eight thermocouples [1]. The common reference junction is on one post of the heat sink. The external common lead and the separate wires going to each thermocouple junction on the sample are standard thermocouple copper. The thermocouple combination was calibrated in a separate apparatus. Different spools of gold-cobalt wire with the same nominal composition have been found to vary in sensitivity by about 5 to 10 percent. A graph of the sensitivity of the spool that was used is shown in figure 5. Each thermocouple junction has one separate external lead and is measured with reference to the common junction at the heat sink. The junctions are electrically insulated by epoxy resin from the thermocouple bolt and, therefore, from the holder, sample, and ground. The thermocouple leads are soldered to larger wires at the junction box. The voltages are read on a 5-dial Wenner potentiometer, usually to 0.01 μv.

A determination of the power to the sample heater is obtained by measuring the d-c voltage and current. Figure 6 shows the circuit diagram. The total current passes through a calibrated 1-ohm NBS—type resistor, R_c; the voltage developed across it is measured on a Rubicon type-B potentiometer. The effective current passes through the sample heater R_s and the lead resistances r_h. The currents range from several milliamperes to about 100. The voltage across the heater is divided across three calibrated resistors, arranged to give either 2 to 1 or 11 to 1 voltage division. Resistor R_3 is 10 K ohms; R_p is either 10 K ohms for 2 to 1 voltage divider ratio, or 1 K ohm for 11 to 1 ratio. The voltage, measured on the same potentiometer as the current, ranges from 1 to about 16 v. The four calibrated resistors are in an oil bath maintained at 25° C by a commercial mercury thermostat and infrared heating unit.

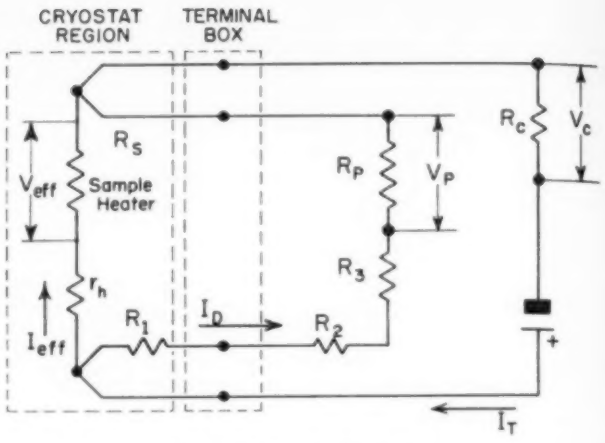

FIGURE 6. *Heater circuit.*

Galvanometer unbalance voltages from the bridge and two potentiometers are directed to a commercial d-c breaker amplifier rather than the more commonly used moving-coil galvanometers. The input selector switch to the amplifier can be set to any of the galvanometer terminals of the bridge or potentiometers, or to some of the differential thermocouples between the sample and shield. The high sensitivity and several-million-fold amplification of the breaker amplifier allow interpolation one figure beyond the last dial setting on either the Mueller bridge or the Wenner potentiometer. The signal from the amplifier is switched to a l-v, center zero, d-c voltmeter for precise readings, or to a slow-speed recorder for following temperature drifts or approach to equilibrium.

Standard low-level electric techniques have been used: that is, all wires are shielded; a special common ground wire is used; the bridges are on insulated ground plates; and all terminals, switches, batteries, and standard cells are thermally insulated.

2.5. Auxiliary Equipment

A photograph of the equipment is shown in figure 2. The vacuum control unit is behind the cryostat; the power panels and control are on the left. The sample space is evacuated through nominal 1-in. tubes by an oil diffusion pump. Between the system and the diffusion pump is a metal cold trap that can hold liquid nitrogen over a weekend without refilling. Between the diffusion pump and the rotary mechanical pump is a 2-liter reservoir that, with its valve to the mechanical pump closed, can normally hold the diffusion-pump output for 4 hr before the pressure builds up to 100 μ. In parallel with the cold trap, diffusion pump, and reservoir, is a bypass line for pumping the system down initially without breaking the vacuum in the cold trap or diffusion pump. The pressure in the sample system is measured with a commercial ion gage when it is below 1 μ, and with a thermocouple gage when above that. The pressure in the reservoir, that is, the back pressure of the diffusion pump, is measured on another thermo-

couple gage system that has shutoff relays controlling the diffusion pumps and ion gage. Whenever the back pressure goes above 100 μ, an alarm light turns on, and the power to the diffusion pump and ion gage turns off.

The liquid refrigerant can be either maintained at a reduced pressure by a high-capacity mechanical pump, or vented directly to an explosion-proof exhaust system. These vent lines are necessary to reduce the explosion danger during liquid hydrogen tests. The vapor space over the liquid is connected to a mercury manometer, permitting measurement of the vapor pressure of the bath.

The power panel supplies both a-c and d-c voltage to the heaters and electronic equipment. The d-c voltage is obtained from a large bank of nickel-cadmium batteries in a nearby room. The current through the main sample heater, which is adjusted by four variable decade resistors, is read preliminarily on a precision multirange milliammeter. The a-c power is obtained from a 110-v regulated power supply. Power to each of the shield heaters is controlled by two autotransformers in series. The a-c power supply also furnishes voltage to a millivolt recorder, breaker amplifier, and the main shield heater servomechanism.

2.6. Measurement Techniques

For each metal sample, the thermocouple holders are mounted in a temperature-controlled shop room, where the dimensions are also measured. After these preliminary measurements, the sample is mounted in the heat sink and the heaters and thermocouples are attached. The sample is not heated or soldered after assembly of the thermocouple holders, and it is subjected to as little mechanical strain as possible during insertion into the cryostat. After this assembly, the shield is closed and bolted; then the vacuum can is soldered into place with Rose's Alloy. The sample space and tubes are evacuated and baked out for several days, usually over a weekend. The liquid refrigerants are not placed into the glass Dewar until the pressure in the cryostat is down to at least 10^{-5} mm of Hg.

Experimental runs are usually begun at liquid helium temperatures, after precooling first with nitrogen, then with hydrogen; and then the runs are continued at the hydrogen triple point, hydrogen boiling point, nitrogen triple point, nitrogen boiling point, carbon dioxide sublimation point, and then ice point. Normally, about six series of measurements at various temperature gradients are made in each temperature range. Two sets of measurements are made for each gradient to insure against reading errors or lack of steady state. The over-all temperature differences across the sample vary from 1° K to a sufficiently large temperature necessary to overlap readings in the next higher temperature range. The approach to steady-state conditions is observed by amplifying the unbalance emf from the Wenner potentiometer with the input switch set for the lowest thermocouple. The amplified signal is switched to the millivolt recorder, and, when this thermocouple emf no longer drifts with time, precise measurements of the voltage, current, and temperatures are begun. Measurements are also made at each sink temperature with no power input and with the normal vacuum space filled with helium exchange gas at a pressure of several hundred microns. Because the apparatus should be isothermal under these conditions, these readings give the "zero" corrections for the thermocouples. These corrections are attributed primarily to inhomogeneous emf's and are assumed to be constant for a particular sink temperature.

Subsidiary measurements are made afterwards on a short section of the sample. They include mounting and polishing of the metal for photomicrographs of grain structure, measurement of hardness, measurement of density, and spectrographic or chemical analyses.

3. Analyses of Data

3.1. Basic Calculations

The fundamental equation of heat flow is utilized in its differential form:

$$\dot{Q}=-\lambda A\frac{dT}{dx}$$

where $\dot{Q}$ is the heat flux, λ is the thermal conductivity, and A the cross-sectional area. Because $\dot{Q}$ and A are essentially constants of the sample for each run,

$$\lambda=\frac{d(-\dot{Q}x/A)}{dT}.$$

Because we do not measure the temperature directly, but rather the thermocouple voltage E, we rearrange the equation to

$$\lambda=\frac{d(-\dot{Q}x/A)}{dE}\frac{dE}{dT}$$

where dE/dT is the thermoelectric power of the thermocouple at the given voltage E and for the given reference temperature.

Several corrections to a straightforward calculation of the heat power of the sample heater are necessary. The various components of the power circuit are shown in figure 6. Basically, the power is the product of the voltage and current through the sample heater. The effective current through the heater is given by

$$I_{eff}=I_T-I_D,$$

where I_T is the total current and I_D is the current through the divider circuit. The total current is given by the measured voltage V_C across the standard resistor divided by its resistance R_C. Similarly, the divider current is given by the measured divider voltage V_P divided by the resistance of the particular resistor R_P. The effective current is then

$$I_{eff}=\frac{V_C}{R_C}-\frac{V_P}{R_P}.$$

The effective voltage is

$$V_{eff}=\rho V_P-r_h I_{eff},$$

where $r_h I_{eff}$ is the temperature-dependent voltage developed across the heater leads between the shield and the sample, and ρ is the voltage divider ratio. The ratio is given by

$$\rho=\frac{R_1+R_2+R_3+R_P}{R_P},$$

where R_1 and R_2 are lead resistances (R_1 is temperature dependent), R_3 is a standard 10 K ohm resistor, and R_P is either 1 K ohm or 10 K ohm.

The cross section and distances along the sample are measured at room temperature. These dimensions are corrected for thermal contraction at each sink temperature range whenever thermal expansion data are available. A preliminary plot is made of $\dot{Q}x/A$ against E to check for points that are considered to have too large a deviation.

For the acceptable runs, the $\dot{Q}x/A$ and E are tabulated, and the values are processed by an IBM 650 digital computer. The program fits the $\dot{Q}x/A$ data by a least squares method to polynomials to the first, second, third, and fourth degree in E. Generally speaking, the first-degree polynomials give the best results for small temperature gradients, and the fourth-degree polynomials give the best for the large gradients. The computer is then programed to take the derivative of each of the polynomials, and then to multiply by the thermoelectric power of the thermocouples at each temperature. The final result is the thermal conductivity at 1-deg intervals based upon each of the above polynomials.

Thermal conductivities as a function of temperature for each run are then plotted on a large scale graph. Average or best curves are drawn through the many points for each range, and the various ranges are connected smoothly to give the complete graph.

3.2. Estimation of Errors

Three main sources of error appear in the apparatus described here: (1) Calibration of the thermocouples, (2) placement of the thermocouple holders, and (3) thermal contact resistance between the thermocouple and the sample. The first can be improved by a more complete and accurate thermocouple calibration. A new series of thermocouple calibrations to improve the range and accuracy of the data has been started in thermometry calibration apparatus. The second source of error has been practically eliminated because of better control of the dimensions and placement of the holders. The third source of error can be reduced by increasing the length of the thermocouple lead wire between the shield and the sample, and by obtaining better contact between the thermocouple bolt and its holder.

Even after improvement, the first and third will probably remain the main sources of error. The thermocouple measurements can be improved, but appreciable errors will still come from chemical inhomogeneities, mechanical strains, uncertainty in calibration, reduced sensitivity at the lowest temperatures, and thermal emf in the external circuitry. The thermocouple error is estimated to be less than 1 percent over most of the temperature range. This error will be systematic and cannot be estimated or eliminated by statistical methods. The error caused by thermal contact resistance can be estimated by deliberately holding the thermal shield hotter or colder than the sample.

Except for gas conduction and radiation at high temperatures, the other sources of error have been reduced to an insignificant amount, considering the larger errors mentioned above. Errors in the cross-sectional measurements are probably about 0.2 percent; inaccuracy in locating the actual contact point between the thermocouple holder and sample is about the same. Errors due to radiation below 100° K and conduction along lead wires were calculated to be below 0.1 percent. To check these radiation losses at higher temperatures, several trial runs with different gradients were made at the ice point. Apparently, for metals, an error of about 1 to 2 percent exists in the readings at that temperature as disclosed by a systematic dependence of the apparent conductivity on the gradient. Several runs were made with a residual helium gas pressure of approximately 1×10^{-5} mm Hg within the system. These runs differed by about 3 percent for most temperature ranges.

Experimental runs in each temperature range have been analyzed for internal consistency. The deviations from an average curve are usually less than 1 percent in the liquid helium and hydrogen ranges, and less than ½ percent at liquid nitrogen temperatures and above. These inconsistencies are apparently due to the combined result of the various errors mentioned above, the one exception being thermocouple calibration error, which is systematic. The inaccuracies increase if the sample has either a very high or a very low conductivity. The range of usable sample diameters is not as great as the variation in conductivity; therefore, at both extremes of conductivity, optimum measuring conditions cannot be obtained. Recent measurements on a very pure copper sample that had a conductivity maximum over 100 w/cm °K gave inconsistencies of about 5 percent between 4° K and 60° K. Measurements on very low conductivity alloys or plastics have about this same inaccuracy, and, in addition, are usually not reliable above 100° K because of the increasing significance of radiation exchange between the sample and shield.

Many control experiments have been carried out to test the self-consistency of the apparatus. Many of the runs overlap in temperature range. For example, some of the runs were carried out with the heat sink at 4° K and the bottom of the sample

around 25° K, thus overlapping runs made with the sink at 19.7° K. The conductivity curves from the lower ranges fit smoothly with the curves at the higher temperatures. Apparent conductivities from runs with different thermal gradients on the sample usually agree within the scatter normally characteristic of a single run. Various runs with different size samples and holders gave consistent results.

4. Results

4.1. Polytetrafluoroethylene

The graph of thermal conductivity of this plastic is given in figure 7. The estimated inaccuracy of the results is about 10 percent. The sample was extruded and had a density of 2.218 g/cm^3. Thermal contraction was calculated by using the data of Quinn, et al. [7] for the higher temperatures, and the data of Head and Laquer [3] for the low temperatures [4].

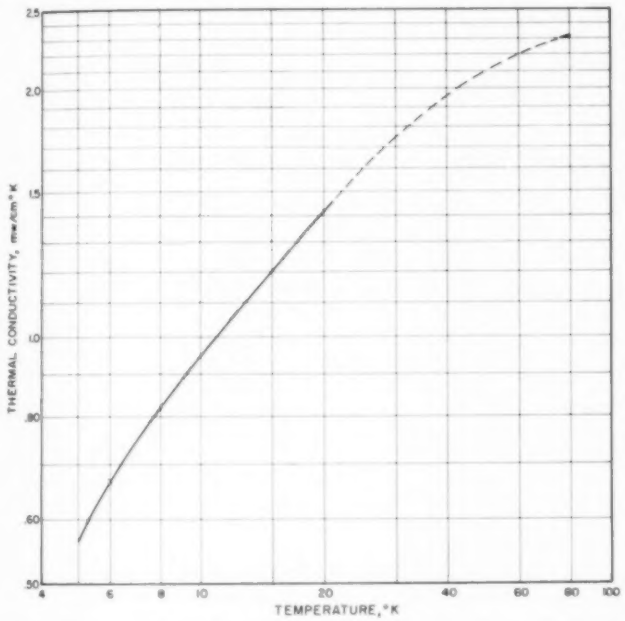

FIGURE 7. *Thermal conductivity of polytetrafluoroethylene.*
(The dashed lines indicate interpolated regions.)

4.2. Coalesced Copper

The graph of the thermal conductivity of this high-purity commercial copper is given in figure 8. The estimated inaccuracy of these results ranges from 2 to 5 percent. The sample had a mill specification giving the impurities by weight as 13 ppm O_2; 8 ppm Pb; 7 ppm Ni; less than 5 ppm each of Fe, As, and Sb; 2 ppm Sn; less than 1 ppm Te and Ag; and less than 0.5 ppm Bi. The sample was annealed 4 hr at 400° C, cooled slowly to 200° C, and then kept at 200° C for 8 hr. During the entire heating cycle, the sample was kept in a flowing helium atmosphere. The density of the sample was 8.90 g/cm^3, and its hardness on the Vickers diamond point system with a 10 kg weight was 54.1 in the longitudinal section, and 48.8 in the transverse.

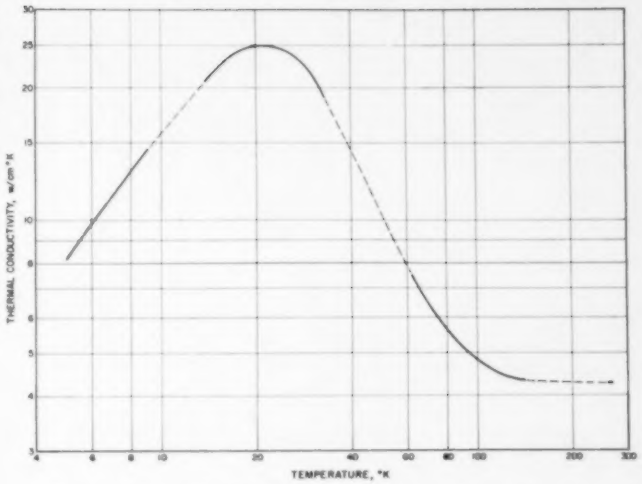

FIGURE 8. *Thermal conductivity of coalesced copper.*
(The dashed lines indicate interpolated regions.)

The authors thank R. J. Corruccini, W. B. Hanson, and R. B. Scott for advice and assistance during the progress of this project, and G. A. Yates of the Phelps Dodge Copper Products Corp. for the generous supply of samples and fabrication information.

5. References

[1] G. Borelius, W. H. Keesom, C. H. Johansson, and J. O. Linde, Commun. Phys. Lab. Univ. Leiden, No. 206b.
[2] J. R. Clement, liquid helium vapor pressure—temperature scale. Distributed by the Naval Research Laboratory as an informal report (1955).
[3] E. L. Head and H. L. Laquer, Low temperature thermal expansion of various materials, Available from Office of Technical Services, AEC D–3706.
[4] Richard K. Kirby, J. Research NBS **57,** 91 (1956). Received after completion of the data analysis.
[5] J. L. Olsen and H. M. Rosenberg, Adv. Physics **2,** 28 (1953).
[6] R. L. Powell and D. O. Coffin, Rev. Sci. Inst. **26,** 516 (1955).
[7] F. A. Quinn, D. E. Roberts, and R. N. Work, J. Appl. Phys. **22,** 1085 (1951).

BOULDER, COLO., December 8, 1956.

U. S. GOVERNMENT PRINTING OFFICE: 1957

THE NATIONAL BUREAU OF STANDARDS

The scope of activities of the National Bureau of Standards at its headquarters in Washington, D. C., and its major field laboratories in Boulder, Colorado, is suggested in the following listing of the divisions and sections engaged in technical work. In general, each section carries out specialized research, development, and engineering in the field indicated by its title. A brief description of the activities, and of the resultant publications, appears on the inside of the front cover.

WASHINGTON, D. C.

Electricity and Electronics. Resistance and Reactance. Electron Devices. Electrical Instruments. Magnetic Measurements. Dielectrics. Engineering Electronics. Electronic Instrumentation. Electrochemistry.

Optics and Metrology. Photometry and Colorimetry. Optical Instruments. Photographic Technology. Length. Engineering Metrology.

Heat. Temperature Physics. Thermodynamics. Cryogenic Physics. Rheology. Engine Fuels. Free Radicals Research.

Atomic and Radiation Physics. Spectroscopy. Radiometry. Mass Spectrometry. Solid State Physics. Electron Physics. Atomic Physics. Neutron Physics. Nuclear Physics. Radioactivity. X-rays. Betatron. Nucleonic Instrumentation. Radiological Equipment. AEC Radiation Instruments.

Chemistry. Organic Coatings. Surface Chemistry. Organic Chemistry. Analytical Chemistry. Inorganic Chemistry. Electrodeposition. Molecular Structures and Properties of Gases. Physical Chemistry. Thermochemistry. Spectrochemistry. Pure Substances.

Mechanics. Sound. Mechanical Instruments. Fluid Mechanics. Engineering Mechanics. Mass and Scale. Capacity, Density, and Fluid Meters. Combustion Controls.

Organic and Fibrous Materials. Rubber. Textiles. Paper. Leather. Testing and Specifications. Polymer Structure. Plastics. Dental Research.

Metallurgy. Thermal Metallurgy. Chemical Metallurgy. Mechanical Metallurgy. Corrosion. Metal Physics.

Mineral Products. Engineering Ceramics. Glass. Refractories. Enameled Metals. Concreting Materials. Constitution and Microstructure.

Building Technology. Structural Engineering. Fire Protection. Air Conditioning, Heating, and Refrigeration. Floor, Roof, and Wall Coverings. Codes and Specifications. Heat Transfer.

Applied Mathematics. Numerical Analysis. Computation. Statistical Engineering. Mathematical Physics.

Data Processing Systems. SEAC Engineering Group. Components and Techniques. Digital Circuitry. Digital Systems. Analog Systems. Application Engineering.

• Office of Basic Instrumentation.

• Office of Weights and Measures.

BOULDER, COLORADO

Cryogenic Engineering. Cryogenic Equipment. Cryogenic Processes. Properties of Materials. Gas Liquefaction.

Radio Propagation Physics. Upper Atmosphere Research. Ionospheric Research. Regular Propagation Services. Sun-Earth Relationships.

Radio Propagation Engineering. Data Reduction Instrumentation. Modulation Systems. Navigation Systems. Radio Noise. Tropospheric Measurements. Tropospheric Analysis. Radio Systems Application Engineering.

Radio Standards. High Frequency Electrical Standards. Radio Broadcast Service. High Frequency Impedance Standards. Calibration Center. Microwave Physics. Microwave Circuit Standards.

Recent Publications of the National Bureau of Standards

Journal of Research of the National Bureau of Standards, Volume 59, No. 3, September 1957 (RP2783 to RP2791 incl.). 60 cents. Annual subscription $4.00.

Technical News Bulletin, Volume 41, No. 9, September 1957. 10 cents. Annual subscription $1.00.

Basic Radio Propagation Predictions for December 1957. Three months in advance. CRPL-D 157. Issued September 1957. 10 cents. Annual subscription $1.00.

Building Materials and Structures Reports

BMS149. Combustible contents in buildings. 20 cents.

Available from the Superintendent of Documents, U. S. Government Printing Office, Washington 25, D. C. (foreign postage, one-fourth additional).

UNIVERSITY OF MICHIGAN
GENERAL LIBRARY
DOCUMENTS DIVISION
1276 ANN ARBOR MICH

UNITED STATES
GOVERNMENT PRINTING OFFICE
DIVISION OF PUBLIC DOCUMENTS
WASHINGTON 25, D. C.

OFFICIAL BUSINESS

PENALTY FOR PRIVATE USE TO AVOID PAYMENT OF POSTAGE, $300 (GPO)

Journal of Research of the National Bureau of Standards Vol. 59, No. 5 November 1957

Contents

		Page
A determination of the gamma-ray emission of radium. Frank H. Attix and Victor H. Ritz.	RP2801	293
Radiation from slots on dielectric-clad and corrugated cylinders. James R. Wait and Alyce M. Conda.	RP2802	307
Infrared emission spectrum of methane at 3.3 microns. Earle K. Plyler and Lamdin R. Blaine.	RP2803	317
Term analysis of the first spectrum of rhenium (Re I). P. F. A. Klinkenberg, W. F. Meggers, R. Velasco, and M. A. Catalán.	RP2804	319
An apparatus for measurement of thermal conductivity of solids at low temperatures. Robert L. Powell, William M. Rogers, and Don O. Coffin.	RP2805	349

[A list of recent NBS publications is given on page 3 of the cover.]

For sale by the Superintendent of Documents, U. S. Government Printing Office, Washington 25, D. C. Price 60 cents (single copy). Subscription price: $4.00 a year; $1.25 additional for foreign mailing.

UNITED STATES GOVERNMENT PRINTING OFFICE, WASHINGTON : 1957